AD-A135 945 EROSION CONTROL OF SCOUR DURING CONSTRUCTION REPORT 4 1/3
STABILITY OF UNDERL..(U) ARMY ENGINEER WATERWAYS
EXPERIMENT STATION VICKSBURG MS HYDRA..
UNCLASSIFIED L Z HALES ET AL. JUN 83 WES/TR/HL-80-3-4 F/G 8/3 NL

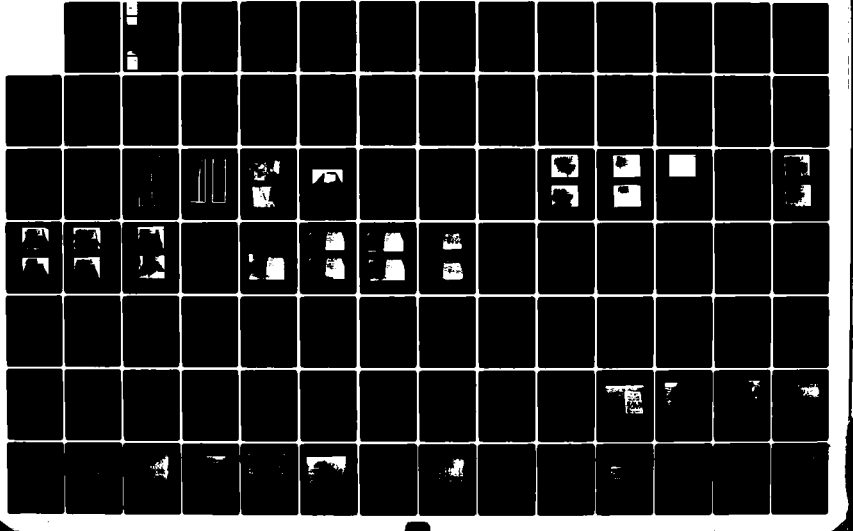

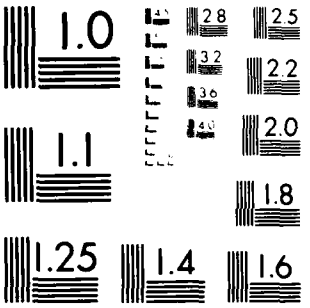

US Army Corps of Engineers

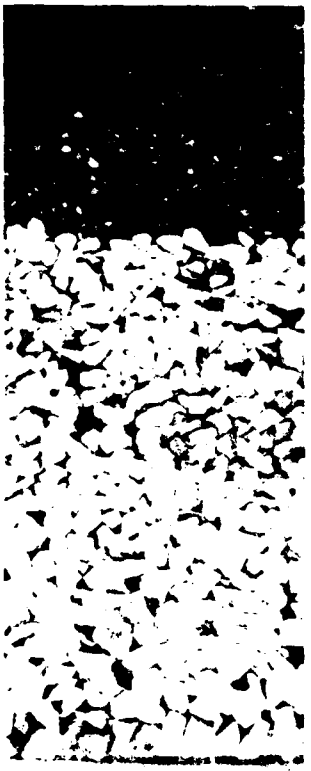

HYDRAULICS LABORATORY

TECHNICAL REPORT HL-80-3

12

EROSION CONTROL OF SCOUR DURING CONSTRUCTION

Report 4

STABILITY OF UNDERLAYER MATERIAL PLACED IN ADVANCE OF CONSTRUCTION TO PREVENT SCOUR

Hydraulic Model Investigation

by

Lyndell Z. Hales, James R. Houston

Hydraulics Laboratory
U. S. Army Engineer Waterways Experiment Station
P. O. Box 631, Vicksburg, Miss. 39180

June 1983
Report 4 of a Series

Prepared for Office, Chief of Engineers, U. S. Army
Washington, D. C. 20314

Destroy this report when no longer needed. Do not return it to the originator.

The findings in this report are not to be construed as an official Department of the Army position unless so designated by other authorized documents.

The contents of this report are not to be used for advertising, publication, or promotional purposes. Citation of trade names does not constitute an official endorsement or approval of the use of such commercial products.

The covers of U. S. Army Engineer Waterways Experiment Station (WES) engineering and scientific reports have been redesigned. Each WES Laboratory and support organization will have its own distinctive color imprinted on white coverstock. This standardizes WES publications and enhances their professional appearance.

Unclassified

SECURITY CLASSIFICATION OF THIS PAGE *(When Data Entered)*

REPORT DOCUMENTATION PAGE

READ INSTRUCTIONS BEFORE COMPLETING FORM

1. REPORT NUMBER Technical Report HL-80-3	2. GOVT ACCESSION NO. AD A155 795
3. RECIPIENT'S CATALOG NUMBER	
4. TITLE *(and Subtitle)* EROSION CONTROL OF SCOUR DURING CONSTRUCTION; Report 4, STABILITY OF UNDERLAYER MATERIAL PLACED IN ADVANCE OF CONSTRUCTION TO PREVENT SCOUR; Hydraulic Model Investigation	5. TYPE OF REPORT & PERIOD COVERED Report 4 of a series
	6. PERFORMING ORG. REPORT NUMBER
7. AUTHOR(s) Lyndell Z. Hales James R. Houston	8. CONTRACT OR GRANT NUMBER(s)
9. PERFORMING ORGANIZATION NAME AND ADDRESS U. S. Army Engineer Waterways Experiment Station Hydraulics Laboratory P. O. Box 631, Vicksburg, Miss. 39180	10. PROGRAM ELEMENT, PROJECT, TASK AREA & WORK UNIT NUMBERS
11. CONTROLLING OFFICE NAME AND ADDRESS Office, Chief of Engineers, U. S. Army Washington, D. C. 20314	12. REPORT DATE June 1983
	13. NUMBER OF PAGES 207
14. MONITORING AGENCY NAME & ADDRESS *(If different from Controlling Office)*	15. SECURITY CLASS. *(of this report)* Unclassified
	15a. DECLASSIFICATION/DOWNGRADING SCHEDULE

16. DISTRIBUTION STATEMENT *(of this Report)*

Approved for public release; distribution unlimited.

17. DISTRIBUTION STATEMENT *(of the abstract entered in Block 20, if different from Report)*

18. SUPPLEMENTARY NOTES

Available from National Technical Information Service, 5285 Port Royal Road, Springfield, Va. 22161

19. KEY WORDS *(Continue on reverse side if necessary and identify by block number)*

Coastal structures
Erosion control
Hydraulic models
Scour
Water waves

20. ABSTRACT *(Continue on reverse side if necessary and identify by block number)*

When major rubble-mound stone structures such as breakwaters, jetties, or groins are constructed in the coastal zone, they alter the existing current and wave conditions that normally exist at a particular location. Waves breaking on such structures under construction may cause bottom material to be suspended and transported from the region, resulting in scour holes that must be filled with construction material. This may result in substantial cost overruns. To minimize potential cost increases due to scour during nearshore construction, a foundation blanket of underlayer material can be placed some distance ahead of the construction of the upper portions of the structure. The stability of such an underlayer material section will depend on the size of the material used in the layer, the extent of the section, and the incoming wave climate.

(Continued)

DD FORM 1 JAN 73 1473 EDITION OF 1 NOV 65 IS OBSOLETE

Unclassified

SECURITY CLASSIFICATION OF THIS PAGE *(When Data Entered)*

20. ABSTRACT (Continued).

The purpose of this study was to determine the stability during construction of such an underlayer material section, which also serves as the foundation blanket for rubble-mound structures constructed on a movable bottom. A simple beach profile consisting of straight, uniform contours parallel with the shoreline was physically modeled on a 1V-on-25H slope in a 6-ft-wide wave flume. A major stone structure was assumed to be under construction perpendicular to the shoreline and thus perpendicular to the uniform parallel contours. A two-dimensional section of this stone structure was modeled (16-to-1 linear scale ratio) along the major axis of the structure. The waves which produced the most severe movement of the underlayer section (scour) were those with characteristics that caused breaking with plunging to occur directly at the toe of the rubble-mound structure. Seven uniform material sizes were used to construct three different lengths of underlayer material sections (3-, 5-, and 7-ft model dimensions; 48-, 80-, and 112-ft prototype dimensions, respectively). These 21 different underlayer sections were subjected to breaking waves with periods of 2-, 3-, 4-, and 5-sec model time (8-, 12-, 16-, and 20-sec prototype time, respectively). These 168 total tests were performed with an underlayer material section thickness of 2.0 ft prototype, which is a typically representative value presently being utilized under prototype conditions.

It was determined that the average best-fit line separating stable from unstable regions for all of the experimental data of this physical model investigation generated a stability number, N_s:

$$N_s = \frac{\omega_r^{1/3} H_b}{(S_r - 1) W_{UL}^{1/3}} = 28.5 \left(\frac{L}{\lambda}\right)^{2/3} \tag{22}$$

From this expression can be deduced the weight, W_{UL}, of a representative stone comprising an underlayer material section for this average best-fit relationship:

$$W_{UL} = \frac{\omega_r H_b^3}{23{,}150 (S_r - 1)^3 \left(\frac{L}{\lambda}\right)^2} \tag{23}$$

Because of experimental scatter in some of the data points, some tests were found to exceed the values of stone weight, W_{UL}, indicated by Equation 23. In order to ensure that all the experimental data fall within the stability region described by a stability number, a conservative stability number was developed which included all the experimental data used to generate the representative stone weight, W_{UL}, of the underlayer section. The expression for this conservative stability number, N_s, is:

$$N_s = \frac{\omega_r^{1/3} H_b}{(S_r - 1) W_{UL}^{1/3}} = 17.5 \left(\frac{L}{\lambda}\right)^{2/3} \tag{24}$$

with the corresponding conservative expression for the weight, W_{UL}, of the representative stone comprising such an underlayer section:

$$W_{UL} = \frac{\omega_r H_b^3}{5{,}360 (S_r - 1)^3 \left(\frac{L}{\lambda}\right)^2} \tag{25}$$

PREFACE

The study reported herein was authorized as a part of the Civil Works Research and Development Program by the Office, Chief of Engineers (OCE), U. S. Army. This particular work unit, Erosion Control of Scour During Construction, is part of the Improvement of Operations and Maintenance Techniques (IOMT) Program. Mr. James L. Gottesman was the OCE Technical Monitor for the IOMT Program during preparation and publication of this report.

This study was conducted during the period 1 October 1981 through 30 September 1982 by personnel of the Hydraulics Laboratory of the U. S. Army Engineer Waterways Experiment Station (WES) under the general supervision of Messrs. H. B. Simmons, Chief of the Hydraulics Laboratory; F. A. Herrmann, Jr., Assistant Chief of the Hydraulics Laboratory; R. A. Sager, Chief of the Estuaries Division and IOMT Program Manager; Dr. R. W. Whalin and Mr. C. E. Chatham, former and acting Chiefs of the Wave Dynamics Division, respectively; Mr. D. D. Davidson, Chief of the Wave Research Branch; and Dr. J. R. Houston, Research Hydraulic Engineer and Principal Investigator for the Erosion Control of Scour During Construction work unit. The hydraulic model tests described herein were performed by Mr. Cornelius Lewis, Civil Engineering Technician, and Mr. Glenn Pierce, Student Aid, under the supervision of Dr. L. Z. Hales, Research Hydraulic Engineer. Mr. R. D. Carver, Research Hydraulic Engineer, and Mr. Dennis Markle, Research Hydraulic Engineer, assisted with physical model design and test program planning. Drs. Houston and Hales performed the data analysis, and Dr. Hales prepared this report.

Commanders and Directors of WES during the conduct of this investigation and the preparation and publication of this report were COL Nelson P. Conover, CE, and COL Tilford C. Creel, CE. Technical Director was Mr. F. R. Brown.

A-1

CONTENTS

CONVERSION FACTORS, U. S. CUSTOMARY TO METRIC (SI) UNITS OF MEASUREMENT

U. S. customary units of measurement used in this report can be converted to metric (SI) units as follows:

Multiply	By	To Obtain
feet	0.3048	metres
feet per second	0.3048	metres per second
gallons per minute	3.785412	cubic decimetres per minute
inches	25.4	millimetres
pounds (force) per square inch	6894.757	pascals
pounds (mass)	0.4535924	kilograms
pounds (mass) per cubic foot	16.01846	kilograms per cubic metre
pounds (mass) per square foot	4.882428	kilograms per square metre
square feet	0.09290304	square metres
tons (2,000 lb, mass)	907.1847	kilograms

EROSION CONTROL OF SCOUR DURING CONSTRUCTION

STABILITY OF UNDERLAYER MATERIAL PLACED IN ADVANCE OF CONSTRUCTION TO PREVENT SCOUR

Hydraulic Model Investigation

PART I: INTRODUCTION

Statement of the Problem

1. When major stone structures such as jetties or breakwaters are erected in the coastal zone, they alter the existing tidal, wave-induced, or wind-driven currents. Waves breaking on such structures under construction may cause bottom material to be suspended and transported from the region by these currents. This removal of material is often not compensated for by an influx of additional material, and the result is a scour hole that usually develops in the near vicinity of the toe of the partially completed structure. Any such scour area must be filled with nonerodible material (sufficiently stable to withstand the environmental forces to which it will be subjected) to allow construction to continue and to ensure stability of the structure. Scour problems may result in additional quantities of material being required during construction in the nearshore zone and thus may lead to substantial cost overruns. Such cost overruns attributable to scour problems have been documented by Hales (1980).

2. For many years it has been realized that rubble-mound structures such as breakwaters, jetties, and groins should be placed on an underlayer for foundation purposes where the bottom soil conditions are unfavorable. Quinn (1961), discussing the design and construction of ports and marine structures, noted that:

> ....A rock-mound breakwater will withstand a considerable amount of settlement as the nature of its construction permits internal adjustment to take place without affecting its overall strength. The amount of settlement should be estimated and allowed for in determining the height to which the breakwater is to be constructed; otherwise the top may eventually have to be raised....Whenever a rock-mound breakwater is to be constructed on a soft bottom it is important first to place a layer of rock over the bottom for a width considerably wider than the base of the breakwater. The

> purpose of this is not only to distribute the load over a wider base but also to prevent shear failure and erosion of the underlying soil at the toe of the rock mound....

The Office, Chief of Engineers (1963), in providing guidance for the design of breakwaters and jetties to field offices, elaborates on the fact that:

> ....Wave forces acting against a breakwater have been found to attack the natural bottom and the foundations of the structures, even at depths usually supposed to be little affected by such forces. Where a natural bottom exists which might be subjected to excessive scour, the structure can be protected by use of a blanket mat. Each area will be somewhat different, but a blanket consisting of a well-graded mixture of quarry-run stone varying in size from a few pounds up to several hundred pounds weight, and having a thickness of only a few feet, will suffice for many conditions....

3. Likewise, scour and erosion of foundation material around major structures during construction in the nearshore zone are well-known and continuing problems. Over the years, those responsible for the integrity of such structures have developed construction techniques to minimize quantity and cost overruns. Because of varying wave and current conditions from one locality to another, those techniques that are optimum for one location may not be applicable to another region. While in most cases these procedures are regional in nature, it is generally accepted that most major stone structures require a foundation blanket as a bearing surface to support the mass of the structure above, and to serve as scour protection during the actual construction. The thickness and design features of this blanket of underlayer material vary with location, but have historically been on the order of 2 to 5 ft* thick and have extended on either side of the structure from 5 to 25 ft beyond the toe. This foundation blanket of underlayer bedding material also has been placed along the axis of the structure ahead of the core construction for varying distances to prevent scouring which could potentially undermine the working section. Currently, this is the most widely used construction practice to reduce scour problems that occur during construction in the nearshore zone.

---

* A table of factors for converting U. S. customary units of measurement to metric (SI) units is presented on page 3.

Purpose of the Study

4. The purpose of this study was to develop equations or design curves that for given expected wave conditions would provide design guidance on characteristics of the underlayer material (stone size and length of blanket) placed in advance of construction that ensure its stability during construction. Presently, there is no guidance, and consequently, expensive trial-and-error actions must be used whenever a structure is constructed. In some instances, construction cost may be much greater than necessary since the material is larger than that required or placed farther in advance of construction than is necessary. In other cases, the material may be smaller than that required or the spatial extent of its placement ahead of construction inadequate, and scour problems may develop and increase costs. Proper design guidance minimizes costs and ensures stability of the material placed in advance of construction (and thus stability of the sand bottom).

PART II: PHYSICAL MODEL DESIGN

General Considerations

5. A rubble structure is composed of several layers of random-shaped and random-placed stones, protected with a cover layer of selected armor units of either quarrystones or specially shaped concrete units. Armor units in the cover layer may be placed in an orderly manner to obtain good wedging or interlocking action between individual units, or they may be placed at random. Wave action against such a rubble structure will often scour the natural bottom and the foundation of the structure, even at depths usually considered unaffected by such action. A foundation bedding of underlayer material should be used to protect the structure from undermining except: (a) where depths are many times greater than the maximum wave height, or (b) where the bottom is a hard, durable material such as bedrock. When large quarrystones are placed directly on a sand foundation at depths where waves and currents act on the bottom, the rubble will settle into the sand until it reaches the depth below which the sand will not be disturbed. Large amounts of material may be required to allow for this loss during construction.

Design Wave Selection

6. The choice of the design wave height depends on whether the structure is subjected to the attack of nonbreaking, breaking, or broken waves, and on the geometrical and porosity characteristics of the structure. The type of wave action experienced by a structure may vary with position along the structure and with water level and time at a given structure section. For these reasons, wave conditions should be determined at various points along a structure and for various water levels. Critical wave conditions that result in maximum forces on structures such as groins, breakwaters, or jetties may be found at a location other than the seaward end of the structure.

7. If breaking in shallow water does not limit wave height, a nonbreaking wave condition exists. For nonbreaking waves, the design height is selected from a statistical height distribution. The selected design height depends on whether the structure is defined as rigid, semirigid, or flexible. For flexible structures, such as rubble-mound structures, the design height is

usually taken as the yearly significant wave height, H_s* (U. S. Army CERC 1977), where H_s is the average of the highest one-third of waves in a storm. Waves higher than H_s impinging on flexible structures for short durations of time seldom create serious damage although some stone may be displaced (rehabilitation is relatively easy to perform).

8. Damage to rubble-mound structures is usually progressive, and an extended period of destructive wave action is required before a structure ceases to provide protection. It is therefore necessary in selecting a design wave to consider both frequency of occurrence of damaging waves and economics of construction and maintenance. While hurricanes occasionally (although infrequently) occur along the Atlantic and Gulf coasts of the United States, it may be uneconomical to build a structure that could withstand hurricane conditions; hence H_s is a reasonable design wave height. On the North Pacific coast of the United States, the weather pattern is more uniform, and severe storms are likely to occur each year. The use of H_s as a design wave height under these conditions could result in extensive annual damage and frequent maintenance because of the higher frequency and duration of waves greater than H_s in the spectrum. Here, a higher design wave of about H_{10} may be advisable. (H_{10} is the average of the highest 10 percent of the waves, whereas H_s is the average of the highest 33 percent of the waves at a given location.) The distribution of significant wave heights, H_s, from coastal wave gages (except for the North Pacific) is shown in Figure 1. The selected design wave is used to determine the weight, W, of the cover layer of armor units as:

$$W = \frac{\omega_r H^3}{K_D (S_r - 1)^3 \cot \theta} \tag{1}$$

where

W = weight of an individual armor unit in the primary cover layer, lb

ω_r = unit weight of rock, lb/ft^3

H = design wave height at the structure, ft

---

* For convenience, symbols are listed and defined in the Notation (Appendix C).

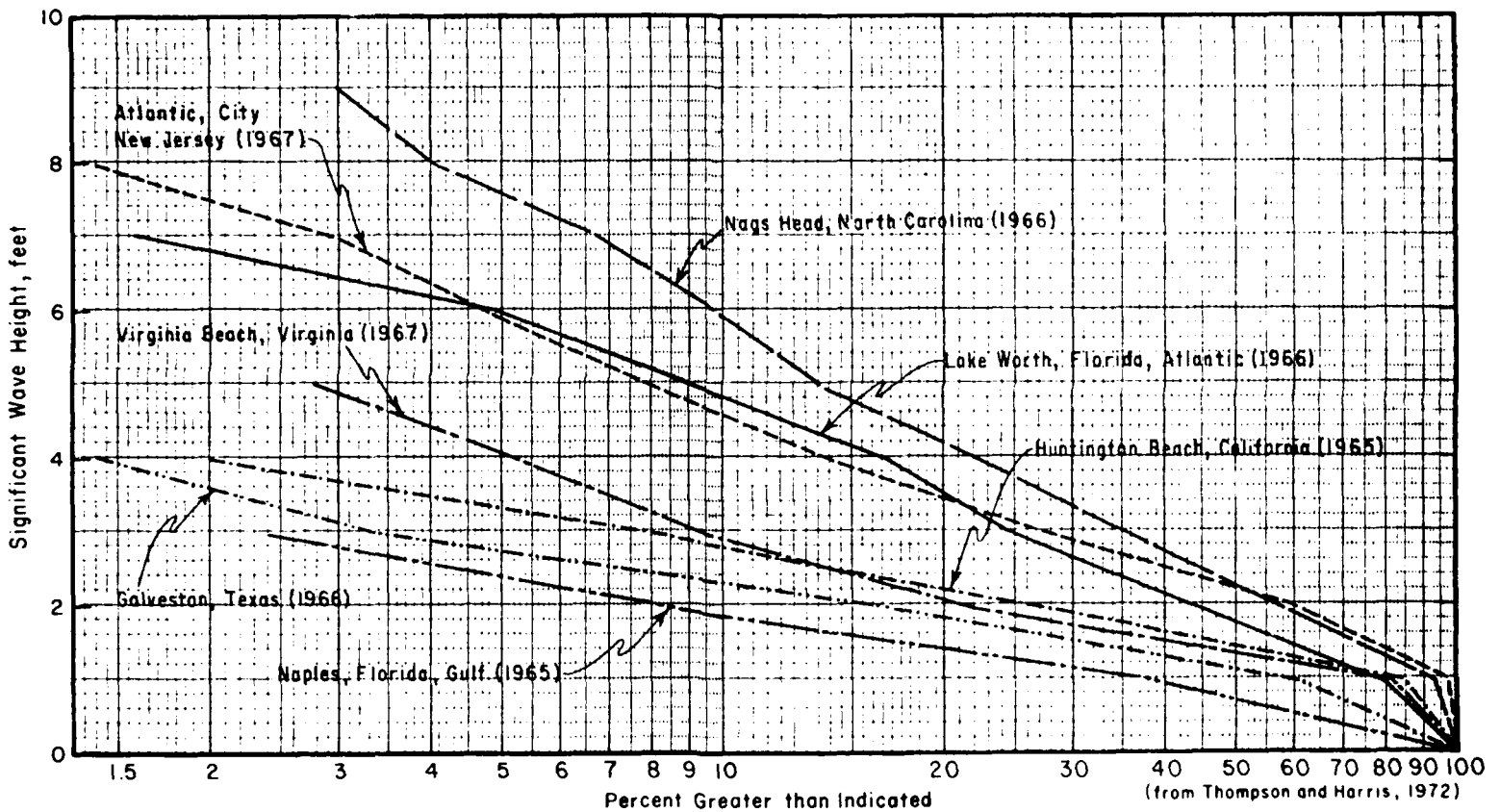

Figure 1. Distribution of significant wave heights, H_s, from coastal wave gages (after CERC 1977)

K_D = stability coefficient that varies primarily with the shape of the armor units, roughness of the armor unit surface, sharpness of edges, and degree of interlocking obtained in placement, dimensionless

S_r = specific gravity of armor unit relative to the water at the structure ($S_r = \omega_r/\omega_w$), dimensionless

ω_w = unit weight of water, lb/ft^3 (fresh water = 62.4 lb/ft^3, seawater = 64.0 lb/ft^3)

θ = angle of structure slope measured from horizontal, deg

The experimental facilities utilized in this study could produce a range of breaking wave heights up to a maximum of 1.8 ft. By considering a prototype-to-model linear scale ratio of 16 to 1, the maximum prototype wave height that could be tested was 28.8 ft. For rough, angular, quarrystone armor units of two layers thickness placed randomly, a suggested K_D value for no-damage criteria and minor overtopping is 3.5. The core and bedding layer for a rubble-mound section with breaking wave conditions and moderate overtopping may consist of material that varies from W/200 to W/4,000 . These data indicate that the dimension of the model core material should be $d_{50} = 0.50$ in. A material mix for this purpose was formulated to this specification.

Structure Cross Section

9. A rubble structure is normally comprised of a bedding layer and a core of quarry-run stone covered by one or more layers of larger stone, and an exterior layer(s) of large quarrystone or concrete armor units. Typical rubble-mound cross sections for nonbreaking and breaking waves are shown in Figures 2 and 3, respectively. The right-hand column of the tables in these figures gives the rock-size gradation of each layer as a percentage of the average layer rock size given in the left-hand column.

10. The thickness of the cover and the number of armor units required can be determined from CERC (1977) as:

$$r = nk_\Delta \left(\frac{W}{\omega_r}\right)^{1/3} \qquad (2)$$

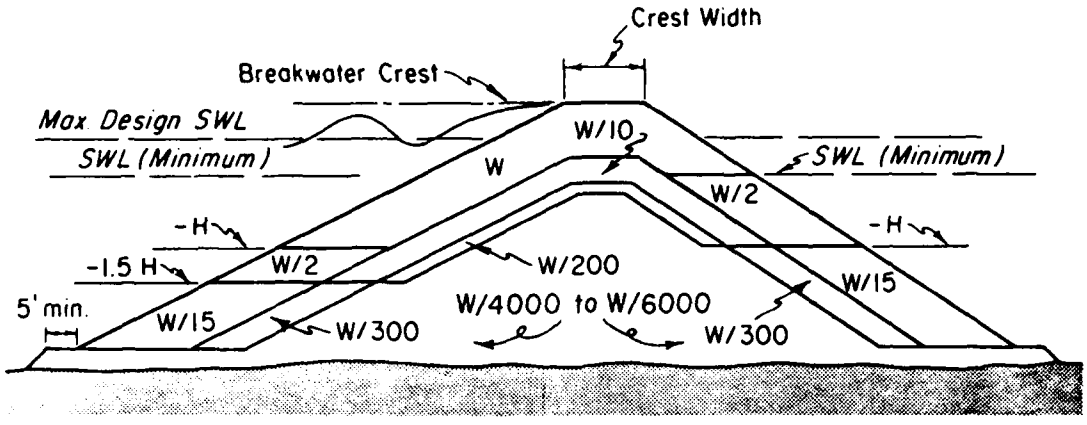

Idealized Multilayer Section

Rock Size	Layer	Rock Size Gradation (%)
W	Primary Cover Layer	125 to 75
W/2 and W/15	Secondary Cover Layer	125 to 75
W/10 and W/300	First Underlayer*	130 to 70
W/200	Second Underlayer	150 to 50
W/4000–W/6000	Core and Bedding Layer	170 to 30

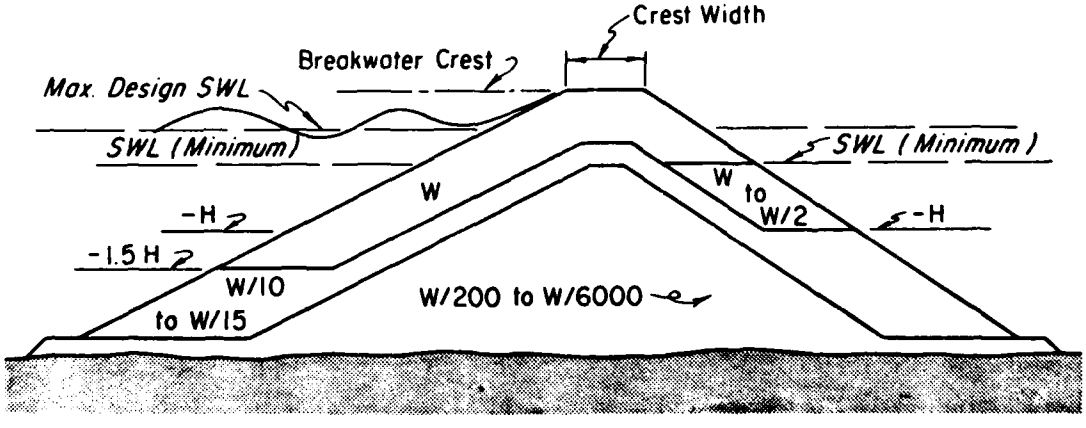

Recommended Three-layer Section

Figure 2. Rubble-mound section for nonbreaking wave conditions with zero to moderate overtopping conditions (after CERC 1977)

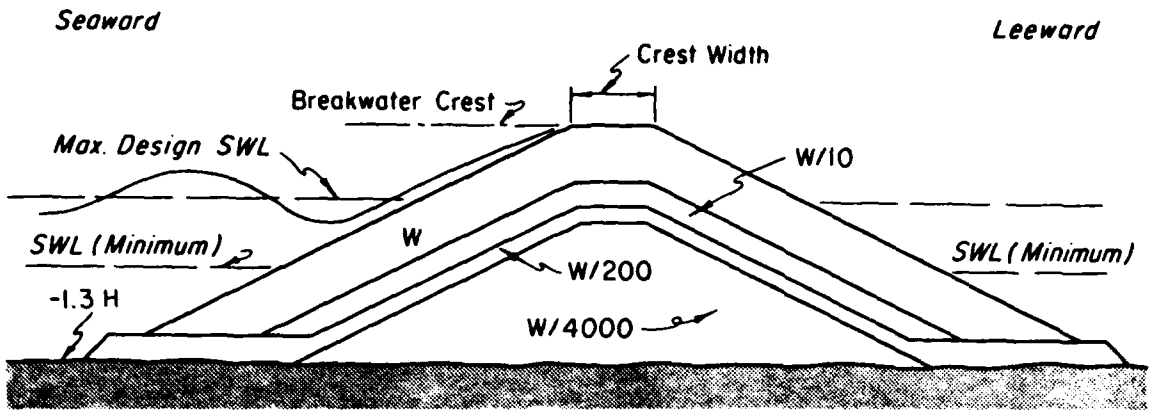

Idealized Multilayer Section

Rock Size	Layer	Rock Size Gradation (%)
W	Primary Cover Layer	125 to 75
W/10	First Underlayer*	130 to 70
W/200	Second Underlayer	150 to 50
W/4000	Core and Bedding Layer	170 to 30

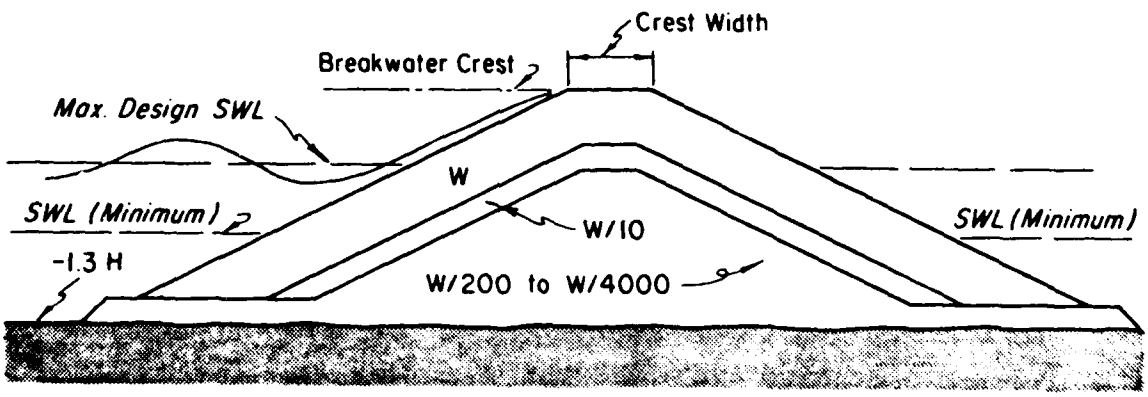

Recommended Three-layer Section

Figure 3. Rubble-mound section for breaking wave conditions with moderate overtopping (after CERC 1977)

where

r = average layer thickness, ft

n = number of quarrystone or concrete armor units in thickness comprising the cover layer, dimensionless

k_Δ = layer coefficient obtained from Table 1, dimensionless

W = weight of individual armor units, lb

ω_r = unit weight of armor unit, lb/ft^3

Table 1

Layer Coefficient and Porosity for Various Armor Units

Armor Unit	n	Placement	Layer Coefficient k_Δ	Porosity (P) percent
Quarrystone (smooth)	2	Random	1.02	38
Quarrystone (rough)	2	Random	1.15	37
Quarrystone (rough)	>3	Random	1.10	40
Cube (modified)	2	Random	1.10	47
Tetrapod	2	Random	1.04	50
Quadripod	2	Random	0.95	49
Hexapod	2	Random	1.15	47
Tribar	2	Random	1.02	54
Dolos	2	Random	1.00	63
Tribar	1	Uniform	1.13	47
Quarrystone	Graded	Random	--	37

The placing density is given by

$$N_r = Ank_\Delta \left(1 - \frac{P}{100}\right) \left(\frac{\omega_r}{W}\right)^{2/3} \quad (3)$$

where

N_r = required number of individual armor units for a given surface area, dimensionless

A = surface area, ft^2

P = average porosity of the cover layer obtained from Table 1, percent

The values of k_Δ and P, presented in Table 1, have been determined from experimental studies.

Primary cover layer

11. The stability of armor units is related to the design wave height, H, and other parameters according to the stability formula, Equation 1, which is based on the results of extensive small-scale model testing and some preliminary verification by large-scale model testing. Suggested values of K_D for use in determining armor unit weight are presented in Table 2. Equation 1 is intended for conditions where the crest of the structure is high enough to prevent major overtopping.

Underlayers and bedding layer

12. The first underlayer (directly beneath the primary armor units) should have a minimum thickness of two quarrystones ($n = 2$), and these should weigh about 1/10 the weight of the overlying armor units (W/10). This applies where: (a) cover layer and first underlayer are both quarrystones, or (b) first underlayer is quarrystone and the cover layer is concrete armor units with a stability coefficient $K_D \leq 12$. When the cover layer is of armor units with $K_D \leq 20$, the first underlayer quarrystone should weigh about W/5, or 1/5 the weight of the overlying armor units. The second underlayer for this part of the structure should have a minimum equivalent thickness of two quarrystones; these should weigh about 1/20 the weight of overlying quarrystones (W/200). The first underlayer for that part below $-1.5H$ should have a minimum of two thicknesses of quarrystone; these should weigh about 1/20 the overlying secondary armor unit (W/300). The second underlayer for that part below $-1.5H$, and the core and bedding layer material, can be as light as W/6,000, or quarry-run stone.

Scale Effects

13. If rubble-mound structures are modeled geometrically similar to their prototype structures, there is relatively more wave reflection from the model structures and relatively less wave transmission through the model structures, compared with the prototype, unless the model scale is large enough to ensure that the motion is fully turbulent in the model. Scale effects for both wave reflection and transmission can be reduced by using model quarrystone sizes in the protective cover layers and core material (and foundation bedding underlayer material) larger than those determined by the linear scale of the model:

Table 2

Suggested K_D Values for Use in Determining Armor Unit Weight

Armor Units	n*	Placement	No-Damage Criteria and Minor Overtopping: Structure Trunk K_D** Breaking Wave	Structure Trunk K_D** Nonbreaking Wave	Structure Head K_D Breaking Wave	Structure Head K_D Nonbreaking Wave	Slope cot θ
Quarrystone							
Smooth rounded	2	Random	2.1	2.4	1.7	1.9	1.5 to 3.0
Smooth rounded	>3	Random	2.8	3.2	2.1	2.3	†
Rough angular	1	Random††	††	2.9	††	2.3	†
Rough angular	2	Random	3.5	4.0	2.9	3.2	1.5
					2.5	2.8	2.0
					2.0	2.3	3.0
Rough angular	>3	Random	3.9	4.5	3.7	4.2	†
Rough angular	2	Special‡	4.8	5.5	3.5	4.5	†
Tetrapod and quadripod	2	Random	7.2	8.3	5.9	6.6	1.5
					5.5	6.1	2.0
					4.0	4.4	3.0
Tribar	2	Random	9.0	10.4	8.3	9.0	1.5
					7.8	8.5	2.0
					7.0	7.7	3.0
Dolos	2	Random	22.0	25.0	15.0	16.5	2.0‡‡
					13.5	15.0	3.0
Modified cube	2	Random	6.8	7.8	--	5.0	†
Hexapod	2	Random	8.2	9.5	5.0	7.0	†
Tribar	1	Uniform	12.0	15.0	7.5	9.5	†
Quarrystone (K_{RR})							
Graded angular	--	Random	2.2	2.5			

* n is the number of units comprising the thickness of the armor layer.

** Applicable to slopes ranging from 1V on 1.5H to 1V on 5H.

† Until more information is available on the variation of K_D value with slope, the use of K_D should be limited to slopes ranging from 1V on 1.5H to 1V on 3H. Some armor units tested on a structure head indicate a K_D-slope dependence.

†† The use of single layer of quarrystone armor units subject to breaking waves is not recommended, and only under special conditions for nonbreaking waves. When it is used, the stone should be carefully placed.

‡ Special placement with long axis of stone placed perpendicular to structure face.

‡‡ Stability of dolosse on slopes steeper than 1V on 2H should be substantiated by site-specific model tests.

$$\frac{D_m}{D_p} = K\left(\frac{L_m}{L_p}\right) \tag{4}$$

where

D_m = model effective stone dimension, ft

D_p = prototype effective stone dimension, ft

K = coefficient greater than 1, dimensionless

L_m = model representative length, ft

L_p = prototype representative length, ft

The value of K for the armor units in the protective cover layer, the characteristics of which determine the reflection coefficient for a rubble-mound structure, is not the same value of K for the core and bedding material, which determines to a large extent the wave transmission characteristics of the breakwater or jetty. This is especially true if the crest of the core material section is high relative to the total height of the structure.

LeMéhauté method

14. Approximate values of K for wave transmission can be obtained from a nomograph of LeMéhauté (1965) (Figure 4) based on analytical considerations and available experimental data. The variables of this figure are defined as follows:

$\Delta H/\Delta L$ = gradient of the head loss through the voids in the core material part of the structure section, dimensionless

ΔH = height of the incident wave, ft

ΔL = average width of the core material section, ft

D_p = effective quarrystone dimensions of the prototype core material, cm, and is taken to be the 10 percent smaller than quarrystone from the core material gradation curve

P_p = porosity of the prototype core material, dimensionless

P_m = porosity of the model material, dimensionless

D_m = effective dimension of the model core material, cm

LeMéhauté assumed that the gradation curves of the core material in the model and prototype are the same, or $P_m = P_p$.

Keulegan method

15. Keulegan (1973) gave the following equations for wave transmission through model and prototype rubble-mound structures with core material of various porosities:

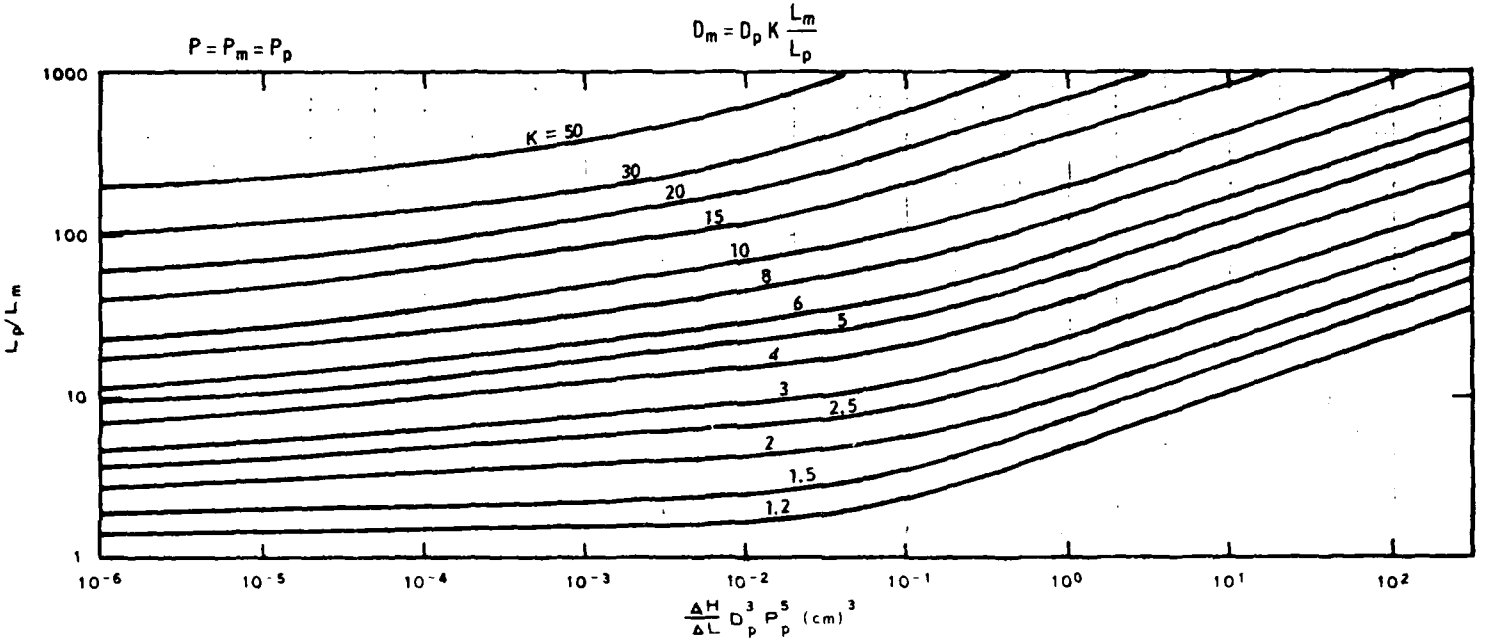

Figure 4. Method of the LeMéhauté for similitude of permeability of core material for rubble structures (after LeMéhauté 1965)

$$\left(\frac{a_i}{a_t}\right)^{2/3} = 1 + \left[M\left(\frac{a_i}{d}\right)^{2/3}\left(\frac{W_s}{\lambda}\right)\right] \qquad \text{model} \qquad (5)$$

$$M = C_m\left(\frac{\nu T}{d_m \lambda}\right)^{1/3}\left(\frac{\lambda}{d_m}\right)\left(\frac{gdT^2}{\lambda^2}\right)^{4/3} \qquad \text{model} \qquad (6)$$

$$\frac{a_i}{a_t} = 1 + \left[M\left(\frac{a_i}{d}\right)\left(\frac{W_s}{\lambda}\right)\right] \qquad \text{prototype} \qquad (7)$$

$$M = C_p\left(\frac{\lambda}{d_p}\right)\left(\frac{gdT^2}{\lambda^2}\right)^{4/3} \qquad \text{prototype} \qquad (8)$$

where

a_i = amplitude of incident wave, ft

a_t = amplitude of transmitted wave, ft

M = Keulegan rubble-mound parameter

d = undisturbed water depth, ft

W_s = structure width, ft

λ = wavelength, ft

ν = fluid kinematic viscosity, ft^2/sec

T = wave period, sec

d_m = model size of rocks, ft

g = gravitational constant, 32.174 ft/sec^2

d_p = prototype size of rocks, ft

C_m, C_p = numerical multiplier for M, functionally related to porosity according to Table 3, dimensionless

The procedure to determine what rock size in the model will assure similarity in the wave transmission is as follows: using prototype values of λ, T, d_p, and d in Equations 7 and 8, the prototype ratio a_i/a_t is obtained from Equation 8. This prototype value is also required to be the same in the model for similarity; hence the ratio a_i/a_t obtained from Equation 8 is inserted into Equations 5 and 6 to determine the model rock size, d_m, of the model core material and foundation bedding underlayer.

Table 3

Numerical Multiplier for Keulegan Method

Porosity, P	Numerical Multiplier in M	
	Model, C_m	Prototype, C_p
0.50	10.5	1.51
0.46	14.7	2.11
0.45	16.1	2.31
0.40	25.7	3.70
0.35	43.8	6.29
0.30	81.2	11.65

Comparison of LeMéhauté and Keulegan methods

16. The methods of LeMéhauté and Keulegan for the determination of K have been compared by Hudson et al. (1979) for a scale ratio of 1:100 and are presented in Table 4. The water depths, wave dimensions, and quarrystone sizes used represent the ranges of these variables commonly found in prototype structures. Keulegan's equations and Table 4 show that the porosity and size

Table 4

Comparison of LeMéhauté and Keulegan Methods

d ft	T sec	H ft	D_p ft	K_L*	K_K*	$\frac{K_L}{K_K}$
15	5	7.5	0.25	6.0	4.6	1.30
15	5	7.5	0.75	3.5	2.7	1.30
15	10	7.5	0.25	6.0	4.2	1.43
15	10	7.5	0.75	3.5	2.5	1.40
30	10	15.0	0.25	5.5	4.0	1.38
30	10	15.0	0.75	3.0	2.3	1.31
30	15	15.0	0.25	5.5	3.9	1.41
30	15	15.0	0.75	3.0	2.3	1.31
45	15	25.0	0.25	5.0	3.7	1.35
45	15	25.0	0.75	2.7	2.2	1.23
45	20	25.0	0.25	5.0	3.6	1.39
45	20	25.0	0.75	2.7	2.2	1.23

* Subscripts L and K refer to LeMéhauté and Keulegan, respectively; 1:100-scale comparison after Hudson et al. (1979).

of the core material quarrystone have an appreciable effect on the wave transmission coefficient, a_i/a_t. Thus it is important that accurate values of these variables are obtained for the core material used in the prototype structures. Keulegan's equations also show that adjustments can be made in both the ratios of P_m/P_p and D_m/D_p to obtain practical solutions to the problem of minimizing scale effects in wave transmission through rubble-mound structures. Generally, the problems of obtaining dynamic similarity for wave transmission through such structures should be the subject for future analysis and experimentation. However, until the results of such studies become available, scale effects can be reduced appreciably by LeMéhauté's (1965) nomograph and Keulegan's (1973) equations and by the proper selection of linear scales. The most accurate of the two methods is unknown at present; therefore it is recommended by Hudson et al. (1979) that the value of K used in the model design should be the average of the two methods, or:

$$K = \frac{K_L + K_K}{2} \tag{9}$$

17. Supplemental comparisons were made for prototype values analogous to this study of wave height = 28.8 ft, wave period = 16 sec, and rubble-mound material with a porosity, P, of 0.46, and prototype-to-model scale ratio of 16 to 1. Keulegan's method indicated that model material greater than d_{50} = 0.52 in. would cause no appreciable scale effects. This value compared favorably with the d_{50} = 0.50 in. mix which had been prepared for this study from other available material distributions.

Wave Dissipation Inside Porous Structures

18. In actual prototype situations and laboratory model studies, the dissipation of wave energy inside a porous rubble-mound structure will be partly due to turbulence and partly due to viscous forces. Keulegan (1973) deduced an expression for the amplitude, a, of a wave at any location, x, within a porous structure as:

$$a = a_i e^{-\alpha k x} \tag{10}$$

with

$$\alpha = \frac{P\lambda^2}{4\pi\kappa dT} \tag{11}$$

where

a_i = initial wave amplitude at the entering face of structure, ft
e = base of system of natural logarithms, 2.71828, dimensionless
α = Keulegan dissipation coefficient, dimensionless
k = wave number, $2\pi/\lambda$, 1/ft
P = porosity of rock structure, dimensionless
λ = wavelength, ft
π = 3.14159, dimensionless
κ = coefficient of permeability, ft/sec
d = undisturbed water depth, ft
T = wave period, sec

The coefficient of permeability, κ , used in Equation 11 is the engineer's or Darcy's coefficient. It is defined as the discharge velocity through unit area under unit hydraulic gradient. From theoretical considerations, it can be shown that permeability can be expected to vary with the squares of the diameters of pore spaces and with the squares of the diameters of the rock material.

Physical Model Parameters

19. It is apparent from Figures 2 and 3 that the material comprising the core of a rubble-mound breakwater or jetty can vary over a large range of values without affecting the structural integrity of the system. Considering the range of model breaking wave heights up to 1.8 ft, the maximum prototype breaking wave height which could be tested under a representative linear scale ratio of 16 to 1 is 28.8 ft. From Figure 3 and Equation 1, the prototype core material corresponding to this wave height could vary over a range of values from 15 to 1,500 lb. The structure is not intended to transmit wave energy; hence the model structure specifications need not be overly restrictive in adhering to scaled prototype rock size gradation as the bulk of the material is

placed for structure volume filler substance. Because of the orientation of the model structure for these specific test purposes, it is necessary however to ensure that a sufficient section of structure is being modeled to preclude any transmitted wave energy along the major axis to the rear of the section (in this case, through the structure).

20. The minimum weight stone existing in the prototype structure (15 lb) can be effectively represented as a cube of side length 5.4 in. Based on LeMéhauté and Keulegan scaling relations, a 50 percent increase in the model linear scale will preclude significant scale effects. This indicates a model core material with a representative dimension of 8.0 in. prototype (0.5 in. model) and a 16-to-1 linear scale ratio will satisfactorily comprise the core of the model structure. A composite material mix with a 50 percent finer by weight of 0.5 in. was formul ' (d_{50} = 0.5 in. model = 8.0 in. prototype = 50 lb prototype). The gradation curve for this composite material mix is shown in Figure 5.

21. The physical model was operated under the assumption that waves would approach directly perpendicular to the offshore contours and would thus propagate along the major axis of the structure. A two-dimensional section of structure was placed in the wave basin with a length sufficient to ensure that wave energy would not penetrate through the structure and be reflected from the rear of the basin. It was desired that the wave energy which penetrated the scale-model core of the structure be effectively dissipated internally within the structure. Keulegan's (1973) expressions for wave dissipation inside porous structures (Equations 10 and 11) indicated that any section of structure in excess of 10 ft would dissipate over 99 percent of the wave energy approaching the structure (i.e., essentially no fluid motion would be detected within the structure at a distance of 10 ft from the incident face). The model structure was placed on a nearshore beach slope of 1V on 25H, which was considered typically representative of many coastal zones. This also provided a shoaling region whereby the waves of various periods could be forced to break directly at the toe of the structure, as this had been determined to be the situation of most severe condition.

Experimental Facilities

Wave flume

22. This experimental study was conducted in a two-dimensional wave

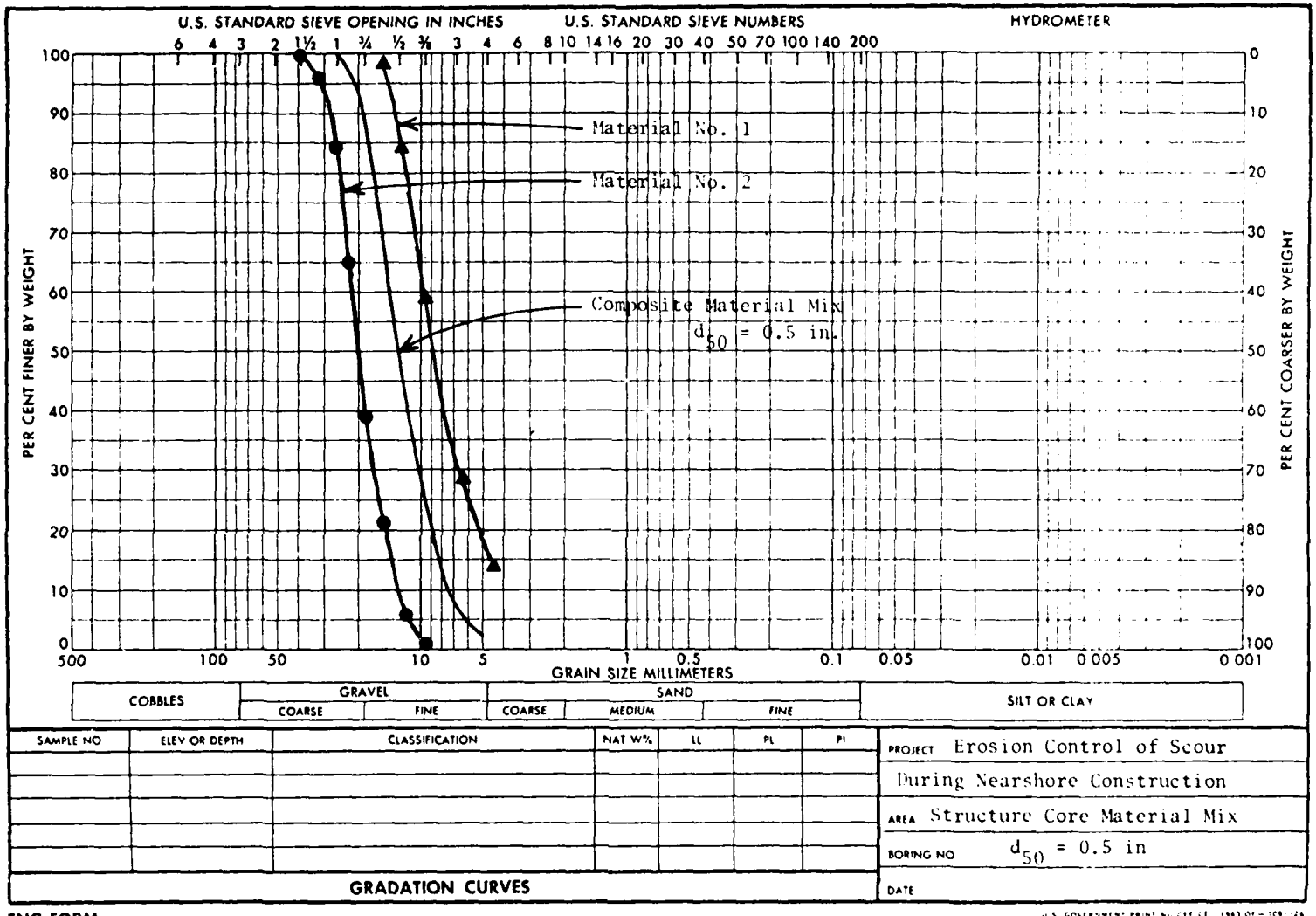

Figure 5. Gradation curve of composite mix for physical model structure

flume 120 ft long by 6 ft wide by 6 ft deep (Figures 6 and 7). The concrete flume was modified by the installation of a beach with a slope of 1V on 25H to simulate representative prototype conditions, and to facilitate the breaking wave phenomenon under investigation. The model structure was placed on the concrete slope at the end of the flume.

Wave generator

23. A dual channel irregular wave generation system had previously been installed in the wave flume and was used to generate the monochromatic waves utilized in this study. The wave generator consisted of: (a) a rotational actuator assembly with a 6-in. stroke and a dynamic force of 2,500-lb tension or 7,000-lb compression; (b) a translational actuator assembly with a 26-in. stroke and a dynamic force of 2,500-lb tension or 7,000-lb compression; (c) a hydraulic power supply system providing 10 gpm at 3,000 psi; (d) a wave-board system providing both translation and rotation capabilities, either individually or simultaneously; and (e) an electronic console system providing variable controllers and accelerometer conditioners. The wave generator equipment can be programmed with both analog and digitally generated random data; therefore the equipment will reproduce waves that vary from cycle to cycle in both amplitude and period. The wave-board motion does not vary in amplitude from the programmed value more than ±5 percent over a range of amplitude from 10 to 80 percent of maximum motion. Wave period does not vary by more than ±1 percent.

24. Automated Data Acquisition and Control Systems (ADACS) have been designed and built at the U. S. Army Engineer Waterways Experiment Station (WES) for the purpose of collecting wave data and controlling operations of hydraulic wave models. The computer hardware configuration for each system consists of a minicomputer with 32k 16-bit words of memory, a magnetic tape controller with two 9-track tape drives, one moving head disc controller with one removable platter and one nonremovable platter, an interval timer (1 μsec), an analog-to-digital 12-bit converter featuring 64 analog (±10 volts) inputs and a 45 kHz multiplexer, a teletype unit, 96 sense/control lines, and one matrix electrostatic printer/plotter. One of the ADACS is shown in Figure 8, and is connected to the dual channel irregular wave generation system. The irregular wave generator translational and rotational actuators are shown connected to the wave board in Figure 9, and the 6-ft-wide wave flume and wave-board portion of the wave generation system is shown in Figure 10.

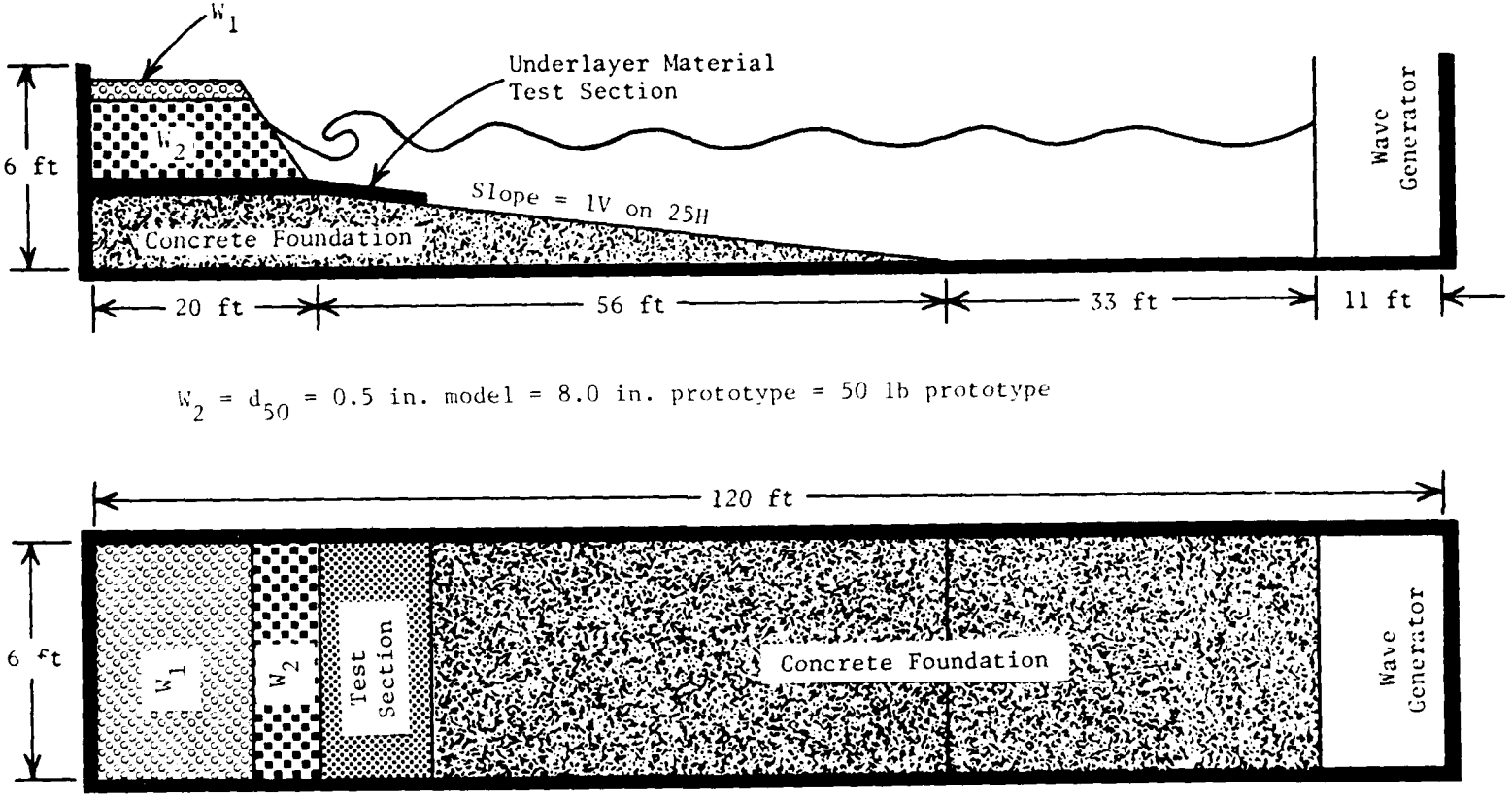

Figure 6. Two-dimensional wave flume

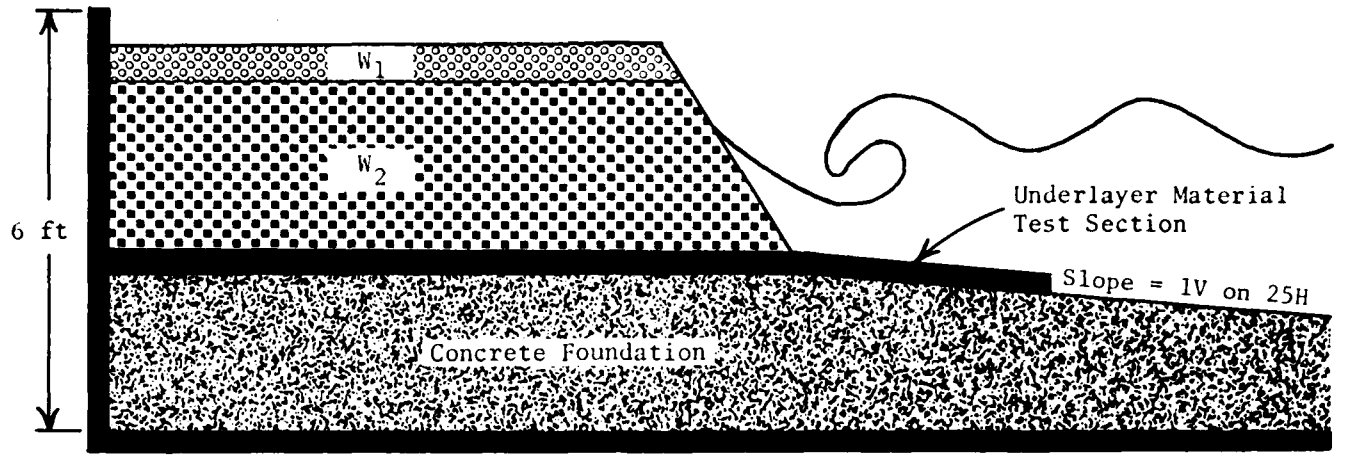

$W_2 = d_{50}$ = 0.5 in. model = 8.0 in. prototype = 50 lb prototype

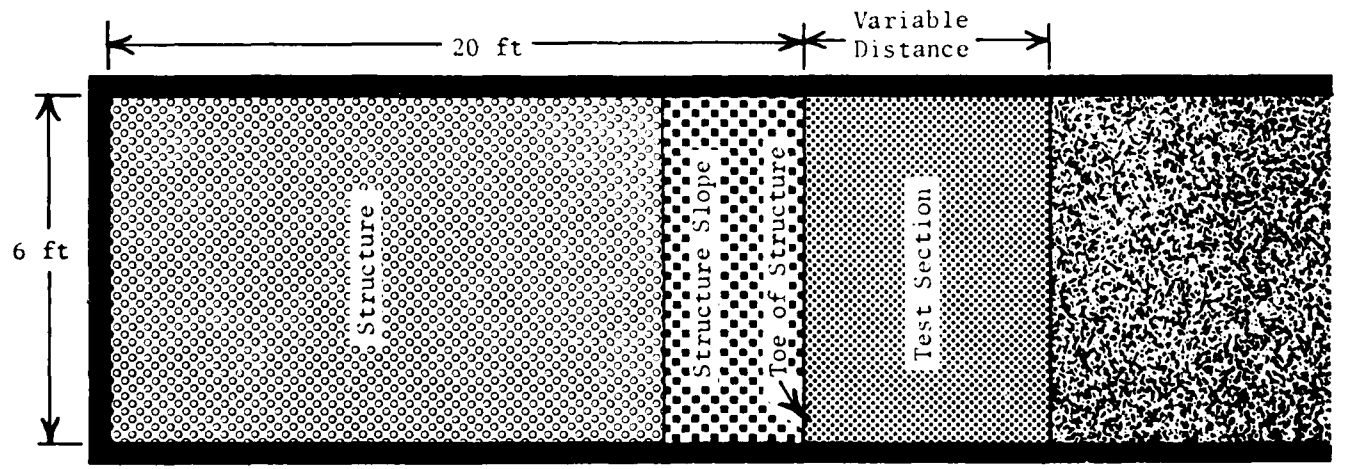

Figure 7. Details of model structure and test section in two-dimensional wave flume

Figure 8. Automated Data Acquisition and Control System (ADACS) connected to dual channel irregular wave generation system

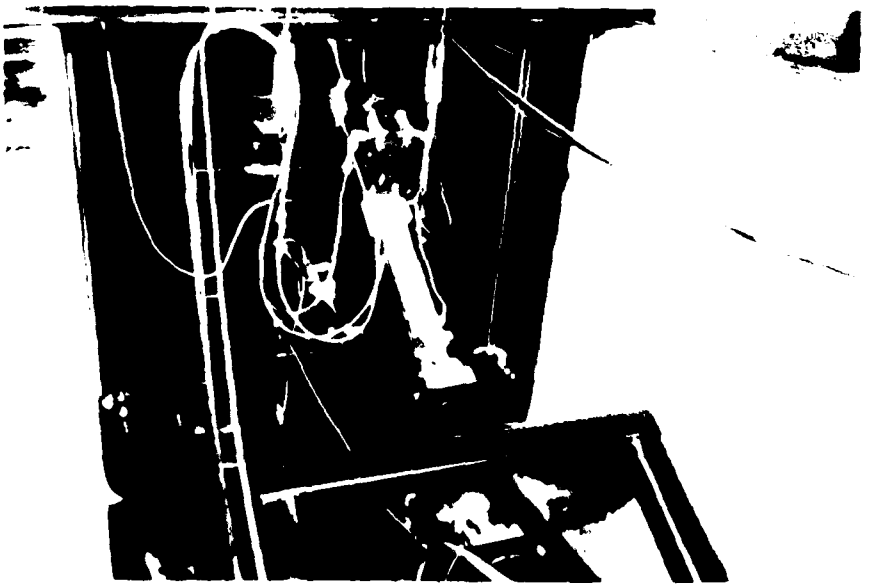

Figure 9. Irregular wave generator translational and rotational actuators connected to wave board

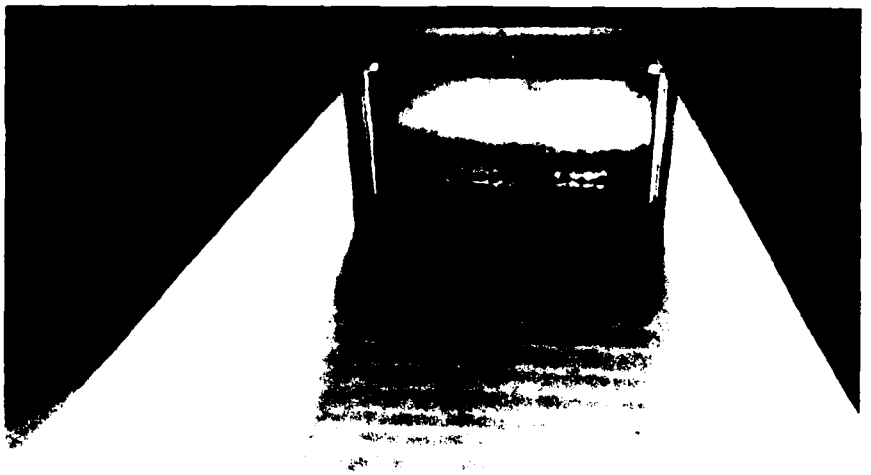

Figure 10. Wave flume and 6-ft-wide wave board used in experimental study

PART III: TEST PROGRAM DEVELOPMENT

Background

25. Naheer (1977, 1979, 1980) developed an empirical relationship to describe the conditions under which a rock embedded in the upper layer of a bed of similar rocks will start to move during passage of solitary waves. Rock (specific gravity 2.68) of two different diameters was tested (5.44 and 7.70 mm), and coal (specific gravity 1.28) of two different diameters (8.00 and 11.10 mm) also was investigated. The amount of motion of these four materials was measured in a wave flume and found to depend on a dimensionless shear stress similar to the Shields parameter. The dimensionless shear stress was defined as the ratio of the hydrodynamic shear force exerted on the bed to the submerged weight of the particles. Extrapolation of the curve passing through the experimental data to the point of zero motion yields the value of the dimensionless shear for which incipient motion occurs. Theoretical considerations were used to evaluate the shear stress under the waves, and the dimensionless shear was then transformed such that incipient motion could be described in terms of measurable quantities, i.e., the density and diameter of the particle, the density and depth of the water, and the wave height. Wave period has no meaning for solitary waves. The relationship between these quantities was expressed as:

$$\tau_{max} = \frac{K_F \left(\frac{H}{d}\right)^2 \left(\frac{d_b}{d}\right)^{-0.37}}{2\left(\frac{\rho_s}{\rho_w} - 1\right)\left[1 + \left(\frac{H}{d}\right)\right]} \tag{12}$$

where

τ_{max} = maximum shear stress on the particle, lb/ft^2

K_F = friction coefficient, lb/ft^2

H = wave height, ft

d = still-water depth, ft

d_b = diameter of bed particle, ft

ρ_s = density of particle, $lb\text{-}sec^2/ft^4$

ρ_w = density of water, $lb\text{-}sec^2/ft^4$

The empirical relationship for the friction coefficient, K_F , is presented in Figure 11. This coefficient was found to be independent of Reynolds number.

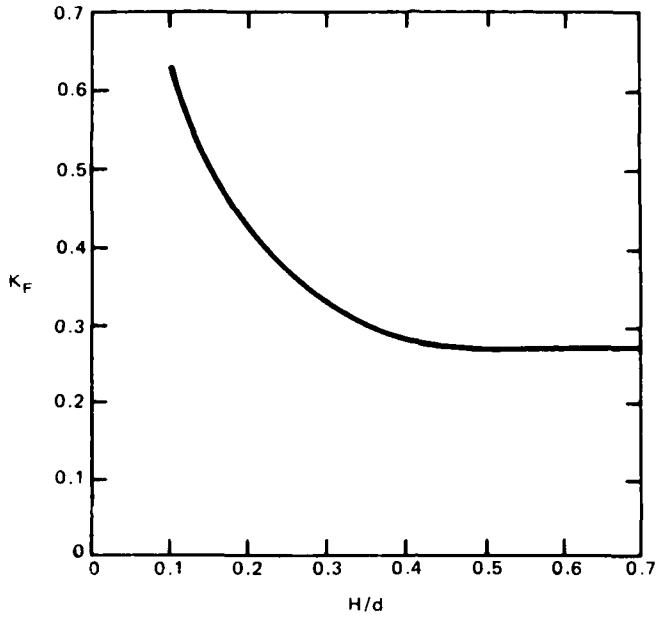

Figure 11. Empirical relationship between K_F and H/d (after Naheer 1979)

26. The empirical relationships for incipient motion developed by Naheer (1977) with a scaled model in a laboratory are of limited use from a practical engineering aspect. In order to estimate local shear stresses exerted on a rough bottom under waves, it is necessary to study the development of the rough turbulent boundary layer under these waves. The stresses estimated with the aid of the mean resistance coefficient which was developed from considerations of energy dissipation may not represent the actual stresses exerted on the bed. Naheer (1977) noted that a slight rocking motion of a few particles in the bed is insignificant from a practical engineering standpoint. Such a motion does not endanger the bed and does not reduce the protection of a rock armoring underlayer section. Naheer (1977) recommended that a future, larger scale study be concentrated on the conditions under which the entire bed changes from a stable to an unstable condition. His observations of motion of particles of arbitrary shape resulted in a large error when used to determine the size of the rock required for incipient motion under breaking waves. Since that error was partly due to the extrapolation of

the data from observed motion to the point of zero motion, Naheer (1977) recommended that a study should be performed of the case where the particles are in a state of incipient motion under breaking waves.

Preliminary 1V-on-30H Bottom-Slope Tests

27. An existing 5-ft-wide, two-dimensional wave flume with a 1V-on-30H bottom slope was used initially to test a limited range of wave conditions in order to develop a test program for investigating the effects of various wave parameters and underlayer material characteristics on resulting scour near major rubble-mound structures. The range of parameter variations to be used in the experimental investigation was established in this preliminary evaluation. Based on Froudian scaling relationships (gravity being the restoring function for recurring surface water waves), model materials were obtained and a structure representing a prototype was constructed in the 5-ft-wide flume. The face of the core material was stabilized with model armor stone to prevent the various underlayer materials from becoming mixed with the core stone near the toe of the structure. It was determined that the most severe wave condition (that situation producing the most movement of underlayer material) existed when the waves were permitted to break and plunge directly at the toe of the structure. Various combinations of parameters were considered and are discussed subsequently.

Effect of underlayer length and number of waves

28. The first series of preliminary tests was conducted to obtain information regarding the number of waves (duration of test required for material movement compared with length of representative prototype storms), and to determine if the length of the underlayer section was a pertinent variable for evaluation. Typical results of these tests (qualitatively) are presented in Figures 12-16 and show that for a constant size material (crushed stone passing a 1/2-in. screen but being retained on a 3/8-in. screen), a longer underlayer section tends to preclude initial movement of underlayer material. Waves plunging at or about the toe of the structure and material section tend to displace the underlayer material toward the major structure. While these tests were performed with a 2-ft-thick prototype layer on a nonmovable bottom, indications are that the movement of the underlayer material toward the structure

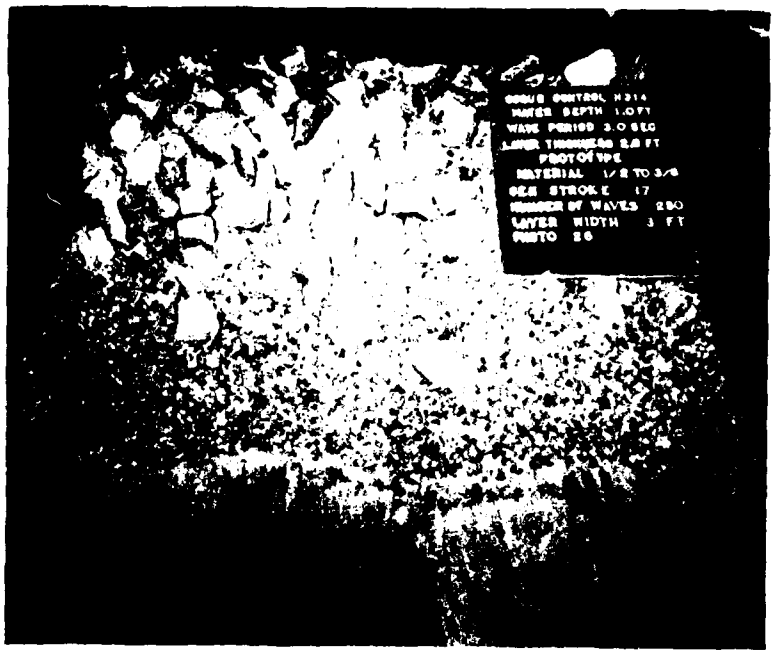

Figure 12. Preliminary 1V-on-30H bottom-slope tests; water depth 1.00 ft, wave period 3.00 sec, layer thickness 2 ft prototype, layer extent 48 ft prototype, underlayer material size 20 to 50 lb prototype (W_{UL} = 35 lb prototype), number of waves 250

Figure 13. Preliminary 1V-on-30H bottom-slope tests; water depth 1.00 ft, wave period 3.00 sec, layer thickness 2 ft prototype, layer extent 64 ft prototype, underlayer material size 20 to 50 lb prototype (W_{UL} = 35 lb prototype), number of waves 250

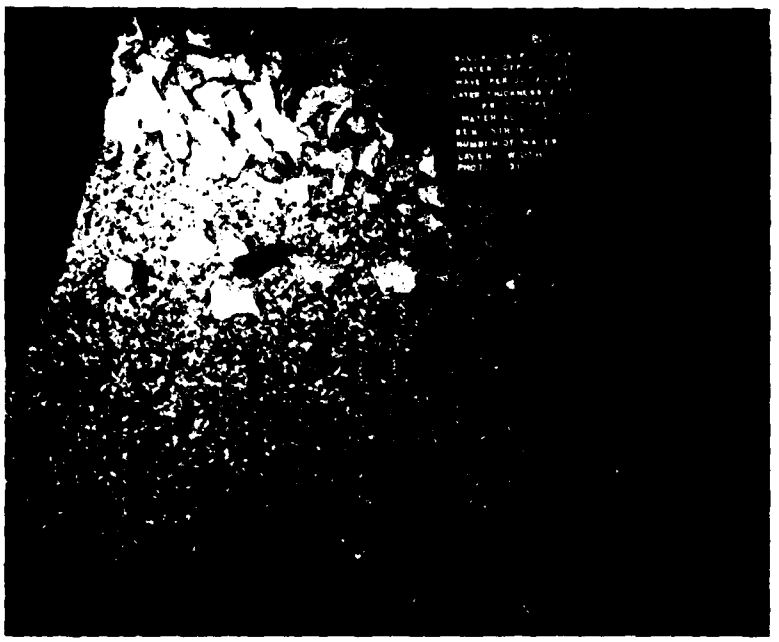

Figure 14. Preliminary 1V-on-30H bottom-slope tests; water depth 1.00 ft, wave period 3.00 sec, layer thickness 2 ft prototype, layer extent 80 ft prototype, underlayer material size 20 to 50 lb prototype (W_{UL} = 35 lb prototype), number of waves 640

Figure 15. Preliminary 1V-on-30H bottom-slope tests; water depth 1.00 ft, wave period 3.00 sec, layer thickness 2 ft prototype, layer extent 96 ft prototype, underlayer material size 20 to 50 lb prototype (W_{UL} = 35 lb prototype), number of waves 500

Figure 16. Preliminary 1V-on-30H bottom-slope tests; water depth 1.00 ft, wave period 3.00 sec, layer thickness 2 ft prototype, layer extent 304 ft prototype, underlayer material size 20 to 50 lb prototype (W_{UL} = 35 lb prototype), number of waves 1,000

would allow development of a scour area at a location seaward of the major structure.

29. When the length of the underlayer material section was extended seaward of the plunging wave effect, movement of the underlayer material decreased, even when the number of waves was significantly increased (comparison of Figures 12-15). One thousand waves produced no discernible scour area when the section was extended to a length of 304 ft prototype (Figure 16), and when the test wave had a 12-sec prototype period.

Effect of underlayer material size

30. It is well documented that for nonbreaking waves and constant wave height, the stability of a rubble-mound structure is dependent upon the size of the armor stone protecting the structure. To extend this relationship from a major stone structure to the underlayer material section, all parameters were held constant and three different size underlayer stone materials were tested: (a) passing a 1/2-in. screen but being retained on a 3/8-in. screen (W_{UL} = 35 lb prototype); (b) passing a 5/8-in. screen but being retained on a 1/2-in. screen (W_{UL} = 72 lb prototype); and (c) passing a 3/4-in. screen but

being retained on a 7/8-in. screen (W_{UL} = 212 lb prototype). Comparisons of these test results are presented in Figures 12, 17, and 18, respectively. These tests indicated that the material size must be increased significantly to provide stability of the underlayer material section with a 48-ft prototype extent.

Effect of wave period

31. Wave period appears to affect the movement of underlayer material at constant water depth. Figures 19 and 20 show that for the same number of waves, and with a longer underlayer section, the longer period wave induces a significantly greater degree of material movement than does the shorter period wave. However, this apparent period effect may actually be the result of an increase in wave height with increasing period (required to maintain wave breaking at the same location in the model). The change in wave height is inherent with the wave period change and may produce an apparent period effect that does not actually exist.

32. Additional tests were performed at a water depth of 0.50 ft (the first tests had been conducted in 1.00 ft of water) to further investigate the apparent period effect. Results of these tests are shown qualitatively in Figures 21-24 for a constant size material subjected to three wave periods (with the same extent of underlayer material section). It was found that the 2-sec wave produced no discernible material movement for a large number of waves. An increase in wave period to 3 sec (with an accompanying increase in wave height) caused the initiation of a scour region near the toe of the major structure. A further increase in wave period to 4 sec caused the displacement of the entire 48-ft prototype section to the toe of the major structure. Obviously, a significant scour hole would have developed in a movable-bed model. When the 48-ft prototype section was extended to 96 ft prototype (for the same 4-sec wave period), the scour region shown in Figure 24 developed, indicating that it is only necessary to stabilize a finite region ahead of the construction of a major stone structure. The optimization of the location and extent of this finite region is dependent on the incident wave climate and the material available for stabilization.

Test Program

33. Based on the results of the preliminary 1V-on-30H bottom-slope

Figure 17. Preliminary 1V-on-30H bottom-slope tests; water depth 1.00 ft, wave period 3.00 sec, layer thickness 2 ft prototype, layer extent 48 ft prototype, underlayer material size 50 to 95 lb prototype (W_{50} = 72 lb prototype), number of waves 250

Figure 18. Preliminary 1V-on-30H bottom-slope tests; water depth 1.00 ft, wave period 3.00 sec, layer thickness 2 ft prototype, layer extent 48 ft prototype, underlayer material size 165 to 260 lb prototype (W_{50} = 212 lb prototype), number of waves 250

Figure 19. Preliminary 1V-on-30H bottom-slope tests; water depth 1.00 ft, wave period 2.00 sec, layer thickness 2 ft prototype, layer extent 48 ft prototype, underlayer material size 165 to 260 lb prototype (W_{UL} = 212 lb prototype), number of waves 510

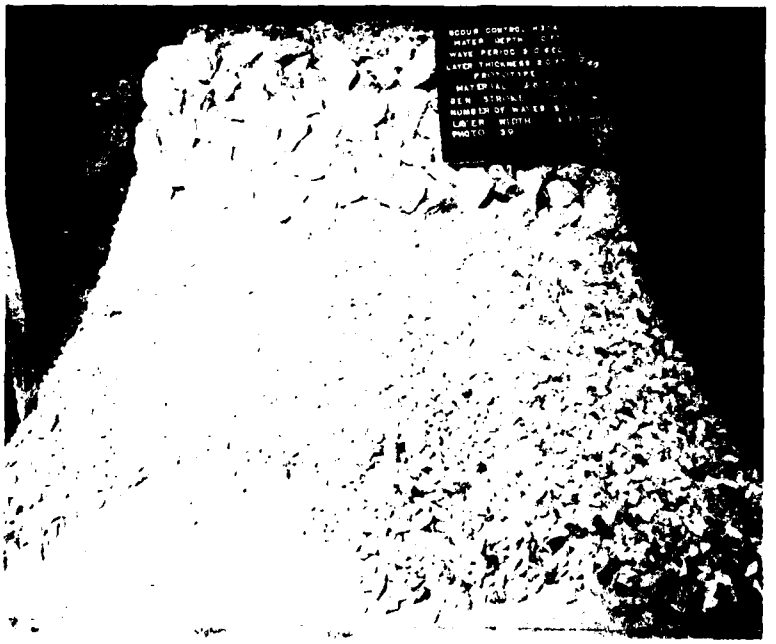

Figure 20. Preliminary 1V-on-30H bottom-slope tests; water depth 1.00 ft, wave period 3.00 sec, layer thickness 2 ft prototype, layer extent 64 ft prototype, underlayer material size 165 to 260 lb prototype (W_{UL} = 212 lb prototype), number of waves 500

Figure 21. Preliminary IV-on-30H bottom-slope tests; water depth 0.50 ft, wave period 2.00 sec, layer thickness 2 ft prototype, layer extent 48 ft prototype, underlayer material size 20 to 50 lb prototype (W_{UL} = 35 lb prototype), number of waves 510

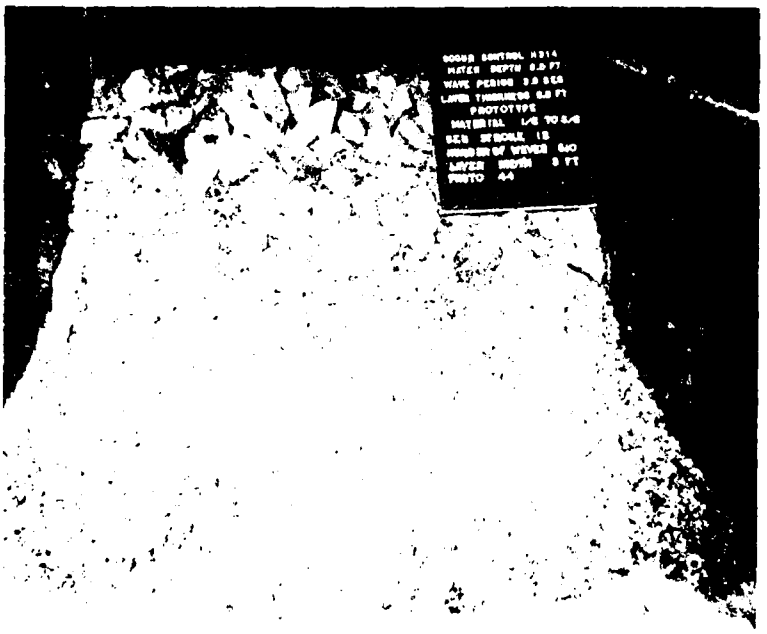

Figure 22. Preliminary IV-on-30H bottom-slope tests; water depth 0.50 ft, wave period 3.00 sec, layer thickness 2 ft prototype, layer extent 48 ft prototype, underlayer material size 20 to 50 lb prototype (W_{UL} = 35 lb prototype), number of waves 510

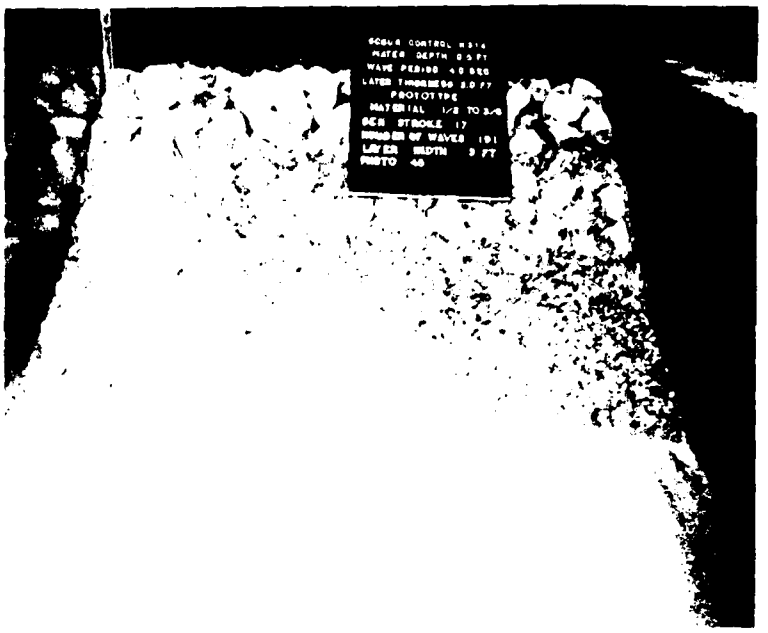

Figure 23. Preliminary 1V-on-30H bottom-slope tests; water depth 0.50 ft, wave period 4.00 sec, layer thickness 2 ft prototype, layer extent 48 ft prototype, underlayer material size 20 to 50 lb prototype (W_{UL} = 35 lb prototype), number of waves 191

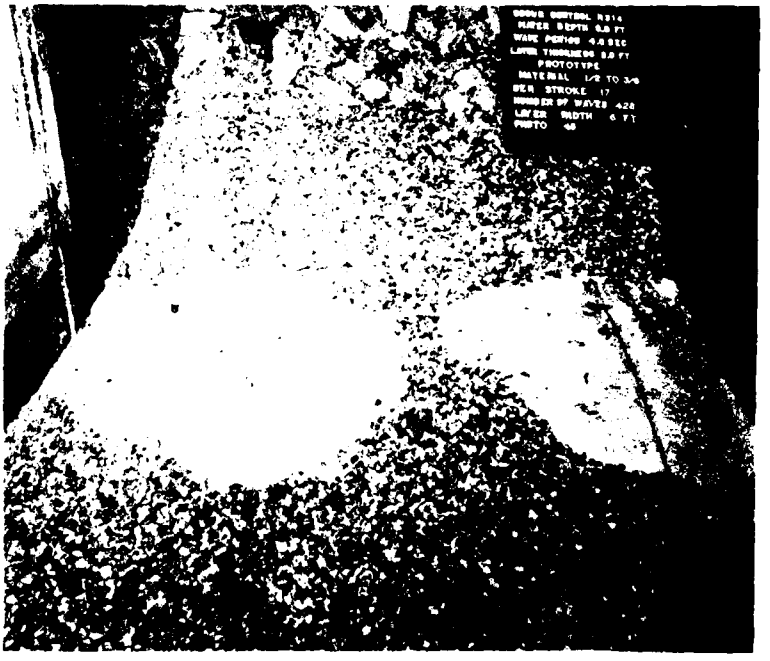

Figure 24. Preliminary 1V-on-30H bottom-slope tests; water depth 0.50 ft, wave period [illegible]0 sec, layer thickness 2 ft prototype, layer extent 96 ft prototype, underlayer material size 20 to 50 lb prototype, (W_{UL} = 35 lb prototype), number of waves 428

tests, it was determined that the stability of the underlayer material section is functionally related to the size of the material comprising the stabilization layer and to certain parameters of the incoming wave climate. These wave characteristics may consist of the wave period T, plunging breaker wave height H_b, still-water depth d, wave celerity C, and wavelength λ. It was also determined that the most severe scour condition resulted from a breaking wave which plunged directly at the toe of the major stone structure. Certain of these wave parameters may not be completely independent, i.e., the breaking wave height at the toe of the structure may depend on the water depth and wave period.

$$\text{Stability} = (W_{UL}, H_b, T, C, g, d, L, \lambda, \omega_r, \omega_w) \qquad (13)$$

where

W_{UL} = weight of representative stone in the underlayer section, lb

H_b = maximum breaker wave height when wave plunges at structure toe, ft

T = wave period, sec

C = wave celerity, ft/sec

g = gravitational constant, 32.174 ft/sec^2

d = still-water depth, ft

L = width of underlayer structure section, ft

λ = wavelength, ft

ω_r = unit weight of underlayer material, lb/ft^3

ω_w = unit weight of water, lb/ft^3

The functional relationship of Equation 13 remains to be determined by physical model tests.

Underlayer material

34. The size of quarry-run stone and the routine requirements of rubble-mound stone construction provide an indication of the size of stone material that can be reasonably feasible to obtain for utilization as underlayer material. Based on a Froudian scaling, and a 16-to-1 linear scale ratio between prototype dimensions and model size, seven material sizes were selected for investigation (Table 5). These seven materials are shown in Figures 25-31. To investigate the effect of underlayer material extent on the scour phenomena, three different lengths of underlayer section were tested (3 ft, 5 ft, and 7 ft model, or 48 ft, 80 ft, and 112 ft prototype, respectively). The remaining

Table 5

Underlayer Test Section Materials

Material	Model Dimension Retained Screen Size in.	Model Dimension Passing Screen Size in.	Prototype Weight Retained lb	Prototype Weight Passing lb	Prototype Weight lb	Prototype Size in.
1	3/8	1/2	20	50	35	7
2	1/2	5/8	50	95	72	9
3	5/8	3/4	95	165	130	11
4	3/4	7/8	165	260	212	13
5	7/8	1	260	390	325	15
6	1	1-1/4	390	765	577	18
7	1-1/4	1-1/2	765	1,320	1,042	22

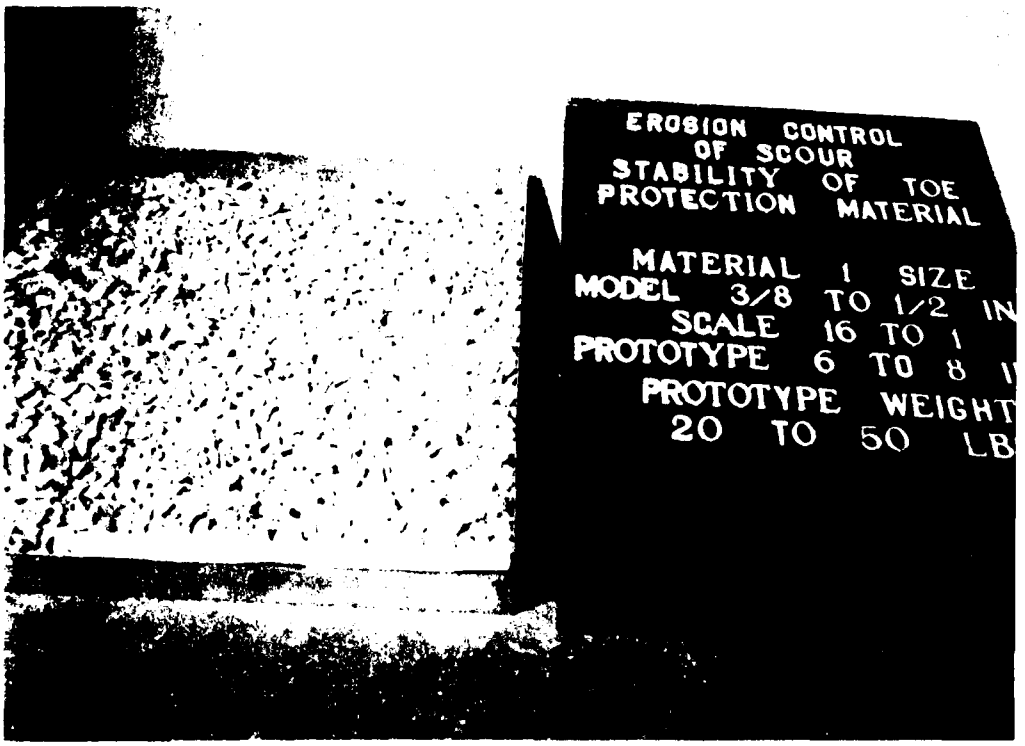

Figure 25. Underlayer test material 1, passing 1/2 in. and retained 3/8 in. model, 20 to 50 lb prototype (W_{UL} = 35 lb prototype), 7-in. prototype size

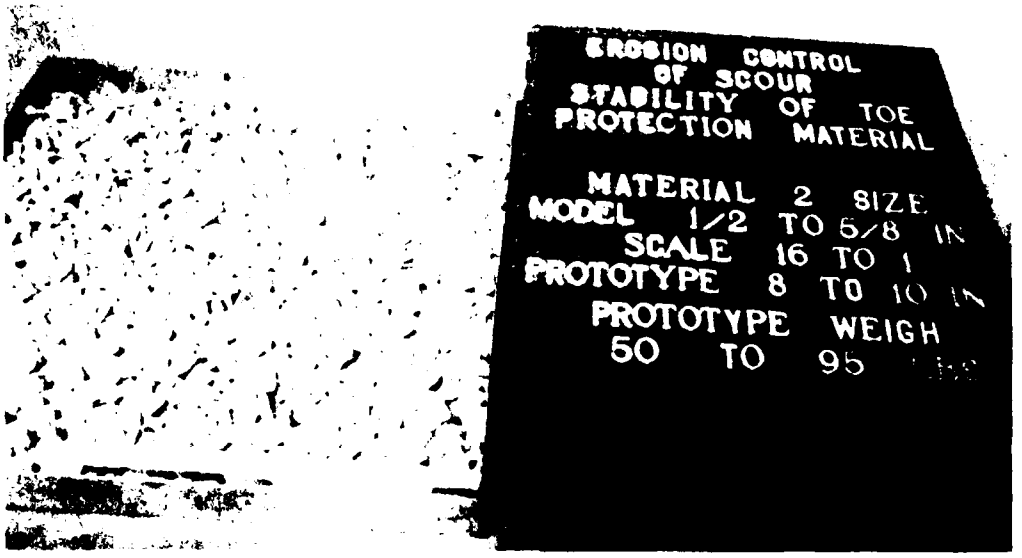

Figure 26. Underlayer test material 2, passing 5/8 in. and retained 1/2 in. model, 50 to 95 lb prototype (W_{UL} = 72 lb prototype), 9-in. prototype size

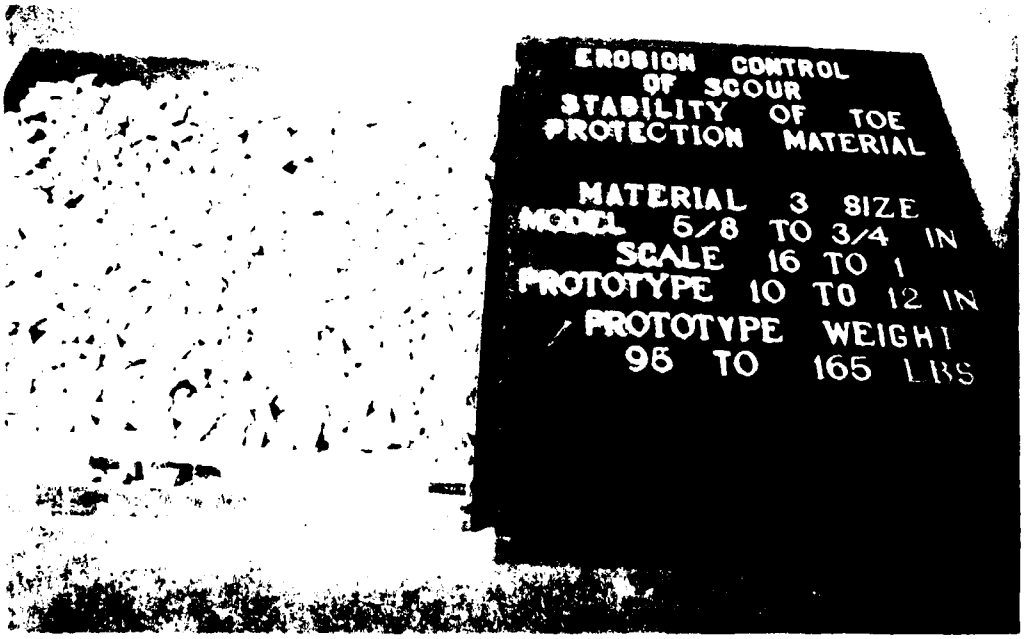

Figure 27. Underlayer test material 3, passing 3/4 in. and retained 5/8 in. model, 95 to 165 lb prototype (W_{UL} = 130 lb prototype), 11-in. prototype size

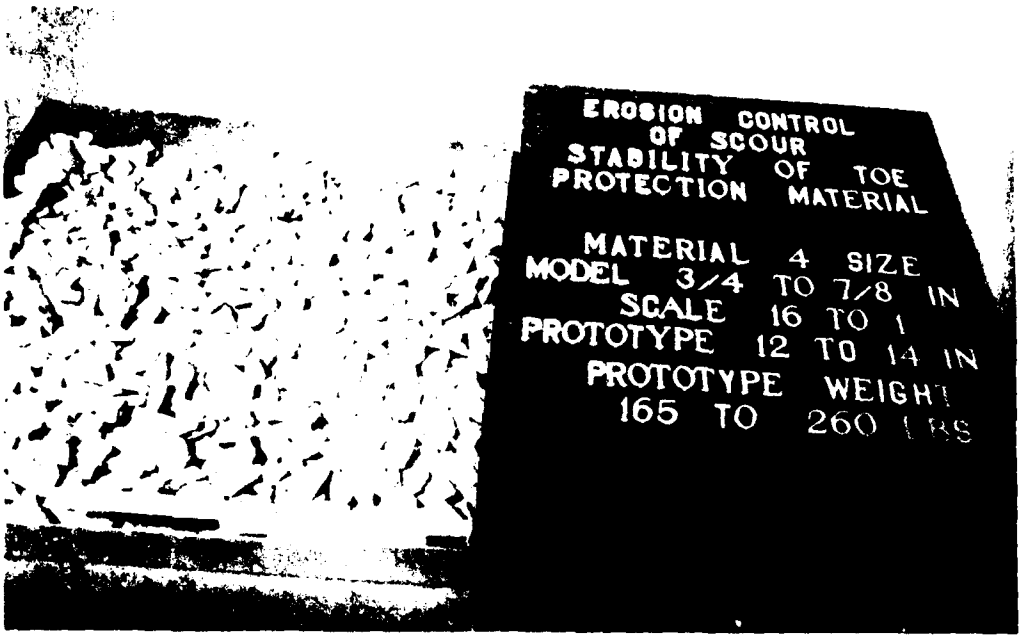

Figure 28. Underlayer test material 4, passing 7/8 in. and retained 3/4 in. model, 165 to 260 lb prototype (W_{UL} = 212 lb prototype), 13-in. prototype size

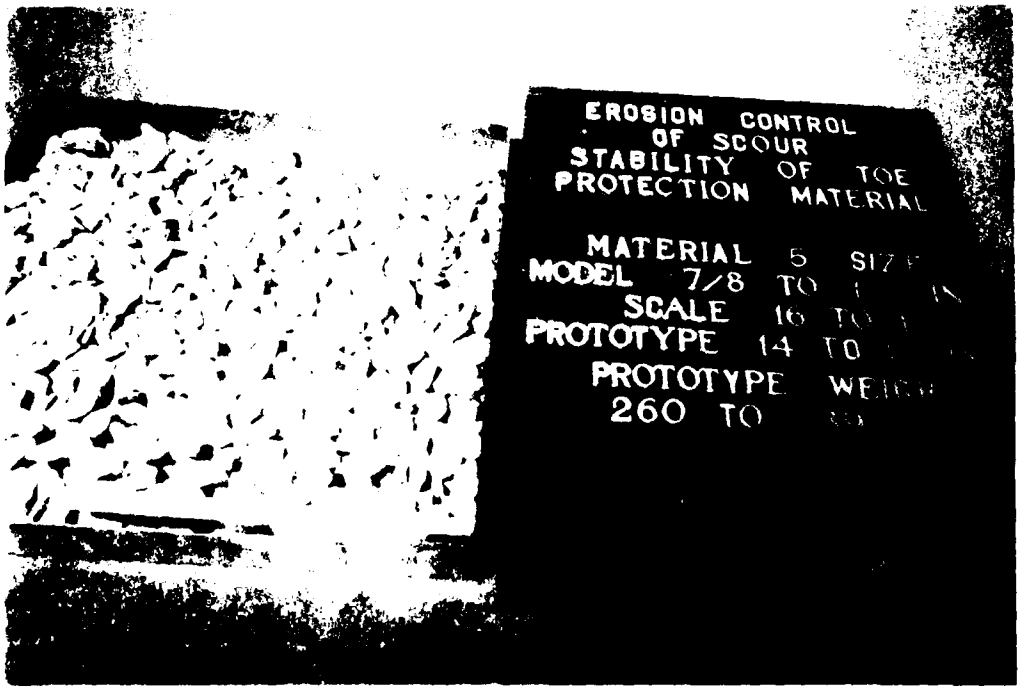

Figure 29. Underlayer test material 5, passing 1 in. and retained 7/8 in. model, 260 to 390 lb prototype (W_{UL} = 325 lb prototype), 15-in. prototype size

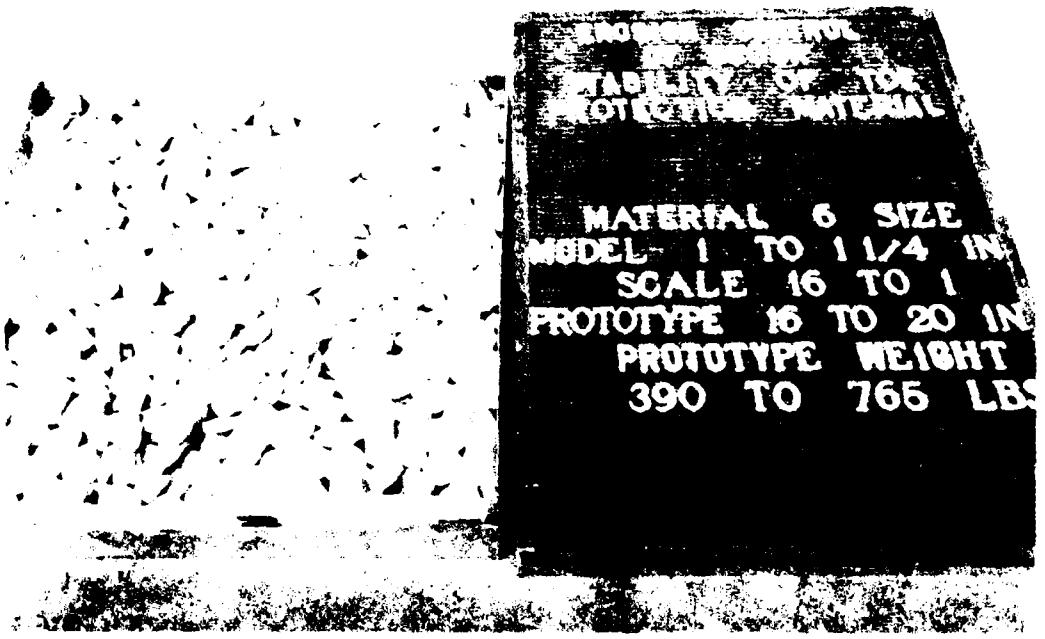

Figure 30. Underlayer test material 6, passing 1-1/4 in. and retained 1 in. model, 390 to 765 lb prototype (W_{UL} = 577 lb prototype), 18-in. prototype size

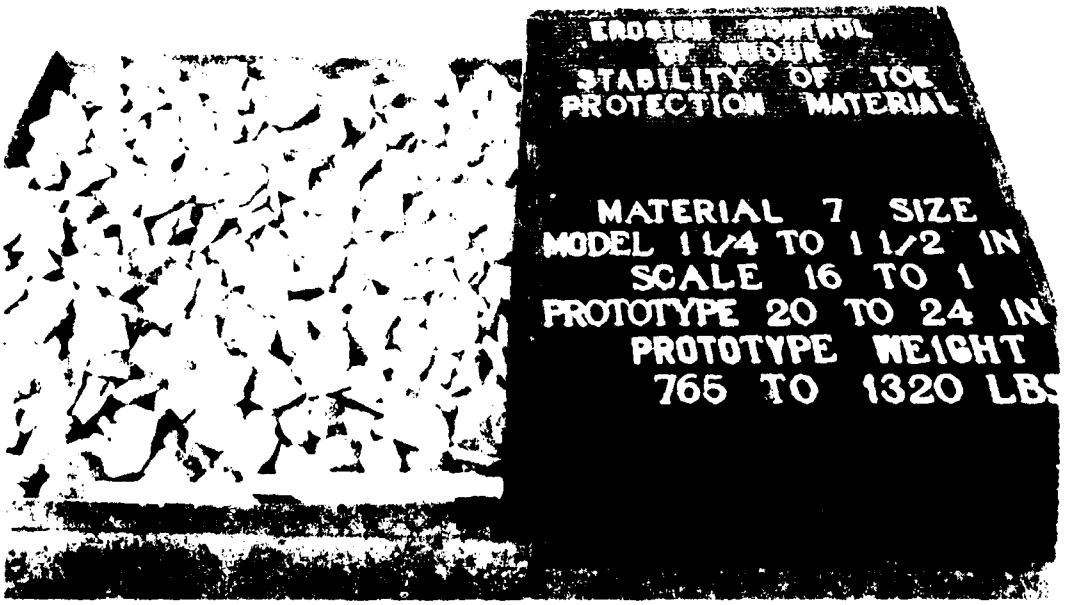

Figure 31. Underlayer test material 7, passing 1-1/2 in. and retained 1-1/4 in. model, 765 to 1,320 lb prototype (W_{UL} = 1,042 lb prototype), 22-in. prototype size

pertinent variables of Equation 13 are related to the water depth and wave climate.

Wave characteristics

35. Because breaking waves are being evaluated (with plunging occurring directly at the toe of the major stone structure), the breaking wave height, H_b , should be directly related to the water depth, d . Hence more than one water depth should be tested to isolate any scale effects. Also, a range of wave periods is necessary to determine the inherent relationship between wave period, T , and breaking wave height. Model wave periods of 2, 3, 4, and 5 sec were selected to be generated in water depths of 0.50 and 1.00 ft. The wave generation system was capable of producing breaking waves under these conditions on the 1V-on-25H slope that was selected for the tests. The breaking wave heights were determined along the center line of the flume by the ADACS system (Table 6). The wave generator was operated as a sinusoidally moving wave maker, and the shallow-water waves broke down into a primary and one or more secondary waves. The primary and secondary waves traveled at different speeds (depending on their individual wave heights), and the resulting water surface exhibited secondary waves, depending on the distance from the wave generator. The fact that the breaking wave heights for the 5-sec waves of Table 6 were determined by the ADACS system to be less than the breaking wave heights for the 4-sec waves is attributed to this secondary wave phenomenon.

Table 6

Model Wave Characteristics

Water Depth, d ft	Wave Period, T sec	Maximum Breaker Wave Height, H_b ft
0.50	2	0.65
0.50	3	0.70
0.50	4	0.80
0.50	5	0.68
1.00	2	1.09
1.00	3	1.11
1.00	4	1.45
1.00	5	1.12

Flume slope

36. A 1V-on-25H slope was molded in a 6-ft-wide wave flume using fixed-bed concrete materials. This slope fit into the geometry of the existing 6-ft-wide wave flume satisfactorily, and would provide the required characteristics necessary to induce breaking of all waves desired to be tested in this program. This bottom slope of 1V-on-25H is typical of many prototype conditions.

Experimental test conditions

37. Two water depths (0.50 and 1.00 ft) and four wave periods (2, 3, 4, and 5 sec) were tested. These eight combinations of wave periods and water depths were evaluated using three different widths of underlayer section (3, 5, and 7 ft). Each of these three different widths of underlayer sections was constructed of seven separate gradations of material, ranging from that which passed a 1/2-in. screen to that which passed a 1-1/2-in. screen (prototype size range of 7 to 22 in., with the average weight of each material being 35, 72, 130, 212, 325, 577, and 1,042 lb, prototype). These combinations of material sizes, underlayer structure width, water depth, and wave periods resulted in 168 separate tests.

PART IV: DATA ANALYSIS

38. The stability of the major rubble-mound structures has been investigated quite thoroughly from both an analytical and experimental standpoint. Even though the importance of the underlayer foundation blanket for scour prevention during construction has been recognized, the stability of this underlayer material has been given only empirical rule-of-thumb design considerations. Because of the many similarities that exist between a rubble-mound structure and the underlayer material on which it is placed, it is desirable to perform an analysis of the stability during construction of the underlayer material along analogous lines to those which have been developed for rubble-mound structures.

Stability of Rubble-Mound Structures

39. The classic analysis of the stability of the armor units which protect a rubble-mound structure from excessive damage due to wave attack was presented by Iribarren Cavanilles (1938), and has come to be known as the Iribarren formula:

$$W_R = \frac{K_B H_B^3 S_{cr}}{(\cos \theta - \sin \theta)^3 (S_{cr} - 1)^3} \tag{14}$$

where

W_R = weight of individual cap rock, kg

K_B = 15 and 19 for breakwaters constructed of natural rock fill and artificial blocks, respectively, kg/m^3

H_B = height of wave which breaks on the structure, m

S_{cr} = specific weight of cap rock, metric tons/m^3

θ = angle, measured from horizontal, of the sea-side slope, deg

This expression, in the form of Equation 14, is not dimensionally homogeneous, and the coefficient, K_B, is not dimensionless. These limitations restrict the equation from being universally applicable in its present form.

40. In 1951 a comprehensive investigation of rubble-mound breakwaters was begun at the WES for the Office, Chief of Engineers (OCE). These studies have been discussed by Hudson (1957, 1958, 1961, 1974, 1975), and Hudson and

Jackson (1953). In 1951, it was assumed that the Iribarren formula could be used to correlate test data and that it could be made sufficiently accurate for use in designing full-scale rubble-mound breakwaters, if sufficient test data were available to evaluate the experimental coefficient, K_B. Early tests in this investigation showed that the friction coefficient in Iribarren's formula, as measured by the tangent of the angle of repose, varied appreciably with the shape of armor units and with the method used to place these units in the cover layer. These results led to the realization that the experimental coefficient, K_B, could not be determined accurately from small-scale breakwater stability tests unless accurate comparative values of the friction coefficient could be obtained for the different shapes of armor units. This realization was made more acute by the fact that Irribarren's force diagram, from which his basic stability equation was derived, is predicated on the assumption that the friction between armor units, specifically that component of the friction force parallel to the breakwater slope, is the primary force that resists the forces of wave action and determines the stability of the armor units. Based on the results of the tests to determine friction coefficients, correlation of test data by the use of Iribarren's formula was abandoned, and a new stability equation, similar to the Iribarren formula but capable of more general application, was derived by Hudson (1957).

41. A dimensionless parameter, designated the stability number, N_s, was developed by Hudson (1957) as:

$$N_s = \frac{\omega_r^{1/3} H}{(S_r - 1) W^{1/3}} \tag{15}$$

where

ω_r = unit weight of the rock

H = design wave height

W = weight of an individual armor stone

When damage was allowed to occur to the breakwater (by use of wave heights greater than the design wave height), the geometry of the structure, the motion of the water particles, and the resulting forces on the breakwater differed from those resulting from tests in which the no-damage criterion was used. Thus a damage parameter, D, defined as the percentage of armor units

displaced from the cover layer by wave action, was included by Hudson (1957).

42. For breakwater sections investigated in the first phase of the testing program, in which the armor units were rocks simulating rounded and smooth quarry stones placed randomly, it was found that:

$$N_s = \frac{\omega_r^{1/3} H}{(S_r - 1)^{1/3}} = f(\theta \ , \ H/\lambda \ , \ d/\lambda \ , \ D) \qquad (16)$$

In the second phase of the testing program, the armor units used were patterned after the tetrapod, and the rubble mound was protected by two or more layers of armor units placed over one or two quarrystone underlayers. For these tests, it was determined that:

$$N_s = \frac{\omega_r^{1/3} H}{(S_r - 1) W^{1/3}} = f(\theta \ , \ H/\lambda \ , \ d/\lambda \ , \ r) \qquad (17)$$

Here r is the thickness of the cover layer.

43. Data obtained from stability test of quarrystone and tetrapod shaped armor units for the no-damage criteria are shown in Figure 32 in the form of log-log plots, with the stability number, N_s, as the ordinate, cot θ as the abscissa, and the shape of the armor unit as the parameter. Analysis by Hudson (1957) of the test data indicated that for the conditions tested, the effects of the variables H/λ and d/λ on the stability of armor units are of second order in importance when compared with the effects of breakwater slope, θ, and the shape of the armor units, D or r (no period effect could be ascertained from these data).

44. A formula for determining the weight of armor units necessary to ensure stability of rubble-mound breakwaters of the types tested, and in relatively deep water, can be obtained from the equation of the approximate best-fit lines of Figure 32. The lines AB and MN were drawn through the data points with a best-fit slope of 1/3. The equation of this straight line on log-log paper is of the form $y = ax^b$, where a is the y-intercept at $x = 1$, and b is the slope of the line. The equation of lines AB and MN therefore is:

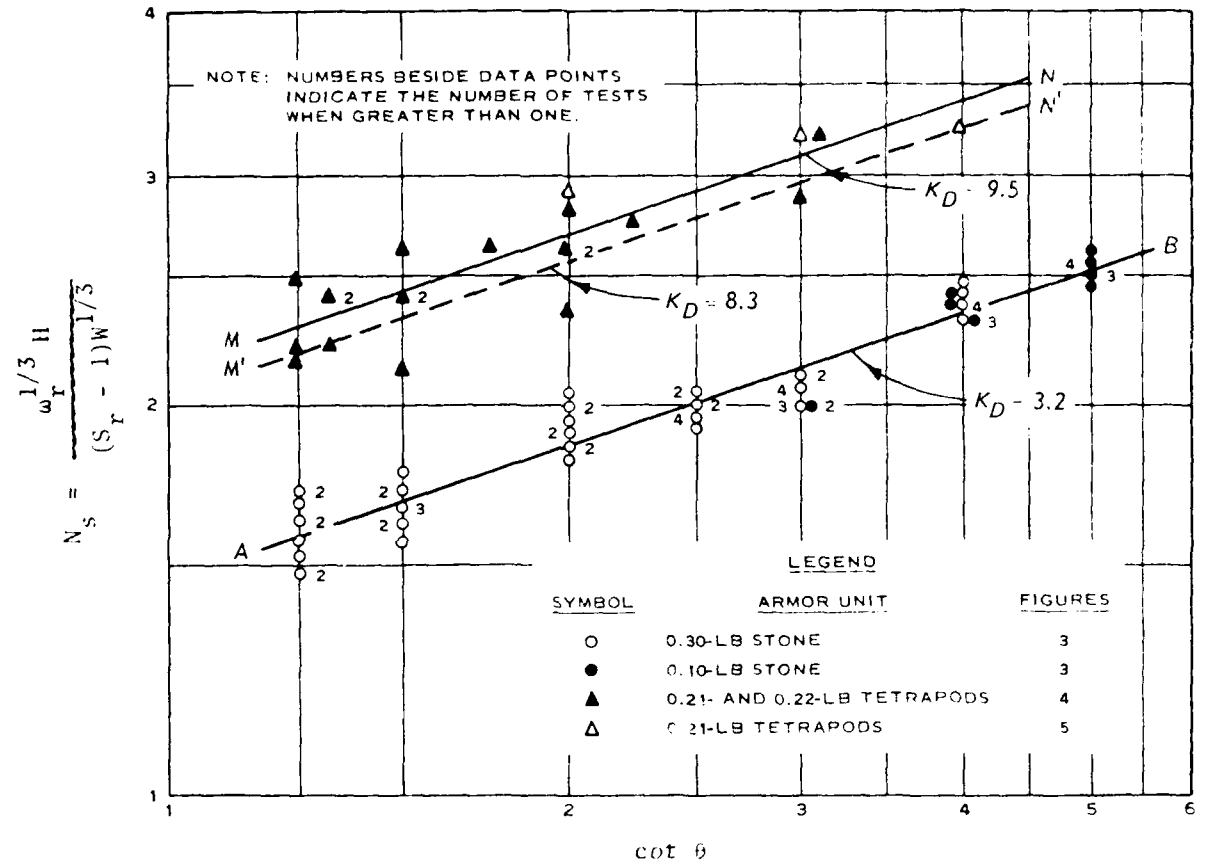

Figure 32. Stability of quarrystone and tetrapod armor units, N_s, as a function of Δ and θ for no-damage and no-overtopping criteria (after Hudson 1957)

$$N_s = \frac{\omega_r^{1/3} H}{(S_r - 1) W^{1/3}} = a\ (\cot \theta)^{1/3} \qquad (18)$$

for which, if $a^3 = K_D$:

$$W = \frac{\omega_r H^3}{K_D (S_r - 1)^3 \cot \theta} \qquad (1\ bis)$$

Equation 1 has been applied with apparent success to many model-prototype studies under varying conditions of wave climate and local topography, i.e., Davidson (1971, 1978), Carver (1976, 1980), and Carver and Davidson (1977).

45. In recent years, other investigators have become concerned that there may indeed be a period dependency effect on the stability of armor units of rubble-mound structures. Whillock and Price (1976) reported that during an investigation for the design of dolosse for the High Island Breakwater in Hong Kong, various slopes of breakwater were subjected to waves of different periods. Having selected a wave period, the wave height was increased until failure occurred. A definite influence of wave period, T , was observed by these researchers. As the wave period increased, the wave tended to surge onto the protective layer rather than break. This set up high velocities over the surface layer. It was suspected from observations of many tests that although dolosse were very stable to plunging breakers acting normal to the slope, their weakness lies in their inability to resist the drag caused by this surface flow.

46. Bruun and Gunbak (1976), and Bruun (1979), found a "phase difference" to be the dominant factor in the relation between waves and structure geometry. They defined this period effect "phase difference" as the ratio of the runup time to the wave period, T . Sollitt and DeBok (1976) found that for a given value of wave steepness and depth, the short-period waves always produced less absolute runup. For a given wave period, T , shallower water produced more runup relative to the depth, and this was reflected in more damage to the structure armor stone.

47. Hannoura and McCorquodale (1979) conducted experimental studies of waves breaking on rubble-mound structures and of the instantaneous pressure distribution due to the wave impact. They believed they observed an effect of period as a result of these studies. Gravesen, Jensen, and Sorensen

(unpublished manuscript) have conducted numerous stability tests at the Danish Hydraulic Institute. They report that the stability coefficient, K_D, in Hudson's Equation 1, is proportional to the characteristic wave steepness, H/λ, with the wavelength, λ, being a function of both water depth, d, and wave period, T.

Stability of Underlayer Material

Test conditions

48. The experimental study performed in this investigation was conducted in a 6-ft-wide, 6-ft-deep, and 120-ft-long wave flume. A portion of the flume length was occupied by the wave generator and model (16-to-1 scale) of the rubble-mound structure (breakwater, jetty, groin, etc.). The model structure was assumed to be oriented in a manner such that the incoming surface gravity waves were propagating directly onto the long axis of the structure, as construction proceeded seaward from the coastline. Because of the finite length of wave flume remaining (89 ft), it was necessary to generate the test waves in a burst of finite duration, to then cease wave generation, and to allow the water surface to become still before generating another burst of waves. This method prevented reflected wave energy from returning to the wave generator and being rereflected with the newly generated waves back toward the structure (thus distorting the initial wave calibration).

49. The duration of an actual burst of generated waves varied, depending on the period of the wave and the water depth. The duration consisted of the time necessary for a generated wave to travel from the wave generator to the model structure and return to the wave generator. This time increment was about 30 to 45 sec; however, the amount of time necessary to allow the water surface to become still before the next burst of waves was generated was approximately 5 min. Only 6 to 12 waves could be generated in a burst (depending on the travel time of 2-, 3-, 4-, and 5-sec waves in 0.50 and 1.00 ft of water depth). Hence a significant portion of the model operation time was spent in quieting the water surface. A longer flume would have permitted more waves to be generated in a burst, thus reducing the amount of time required to perform this experimental physical model investigation.

50. Typical representative examples of the tests which were conducted are shown photographically in Appendix A, at the conclusion of a particular

test. A minimum number of at least 500 individual waves were generated at each of the sections of underlayer material tested. If significant movement of material occurred prior to this number of waves being generated, then testing of a particular material and wave combination may have been terminated, as it could be concluded that this particular combination of parameters produced an unstable condition. Occasionally, the number of waves in a test would be continued to gain additional information for supplemental purposes. Model operator sketches of the movement of underlayer material after N number of waves during a test is shown in Appendix B. (The last sketch of the figures of Appendix B should correspond to the appropriate photograph of Appendix A.)

51. Preliminary tests used for the development of this experimental test program had indicated that the greatest amount of underlayer material movement would be produced by breaking waves which plunge directly onto the toe of the rubble-mound structure. For a given wave period, T , higher waves would break seaward of this location and the reduced wave energy would not cause as much material movement. Lower waves at this period would break on the structure, and the effects would be less noticeable on the underlayer material. Hence, in the testing operation, it was necessary to set the desired wave period and then adjust the stroke of the wave generator to produce a wave that would break at the desired location (the position of most severe wave effects).

52. The majority of the failures occurred as material moved from the seaward edge of the underlayer section toward the base of the rubble-mound structure. The temporal movement was functionally related to the wave characteristics (wave height, H_b , and/or wave period, T), and to the size of the material being tested. For some tests that utilized an underlayer section which was relatively long when compared with the water depth, d , or wave height, H_b , the instability would be reflected as a failure section at some location other than the toe of the underlayer section. This implies that if all sections could be extended far enough seaward, the instability would appear as a scour hole development through the underlayer section, and the stability then becomes also a function of the layer thickness. (All tests in this study were conducted with a layer test section thickness of 2 ft prototype.) It is impractical to extend an underlayer section for an infinite distance seaward; hence the optimization of material size, W_{UL} , and layer

extent, L, with wave characteristics is necessary for efficient construction methods. The 168 tests performed in this study are presented in Table 7.

Data display

53. A review of the pertinent variables involved indicates that the stability of an underlayer section (for fixed underlayer thickness) may be expressed as some functional relationship between nine basic parameters:

$$f(\omega_w , \omega_r , W_{UL} , H_b , T , g , d , L , \lambda) = 0 \qquad (19)$$

All symbols have been defined previously, and $S_r = \omega_r/\omega_w$. A layer of 2-ft-thick prototype underlayer material was utilized throughout these tests; hence the dependency on thickness was not evaluated in this study. Since it was desired to display these data in a manner similar to that of Hudson (1957) for the armor slope stability of rubble-mound structures, the stability number, N_s, can again be expressed as Equation 15 and becomes functionally related to two other fully independent dimensionless terms:

$$N_s = \frac{\omega_r^{1/3} H_b}{(S_r - 1) W_{UL}^{1/3}} = f\left[\frac{L}{d} , \left(\frac{d}{g}\right)^{1/2} \frac{1}{T}\right] = f\left(\frac{L}{d} , \frac{d}{\lambda}\right) \qquad (20)$$

Since shallow-water waves were used, $\lambda = T(gd)^{1/2}$, and the angle of the breakwater seaward slope with the horizontal, θ, becomes meaningless for the underlayer material section of this analysis.

54. For constant values of the parameter L/d, the data of Table 7 are displayed in Figures 33-38 as N_s versus d/λ, where L is the extent of the underlayer section, and λ is the wavelength. While the data are fairly limited for each individual value of L/d, it does appear reasonable to separate the regions of stability from the unstable regions by a straight line on these log-log plots. While the precise slope of such a straight line cannot be determined, it appears that the same line slope could equally well be fit to each of these figures, except for Figure 38, which is inconclusive.

55. The data of Table 7 are again displayed in Figures 39-46 as N_s versus L/d, for constant values of the parameter d/λ. Here again, the data are fairly limited for each individual value of d/λ; however, the regions of stability may be separated from the unstable regions adequately with

Table 7

Test Conditions, Underlayer Material and Wave Characteristics

Still-Water Depth d, ft	Wave Period T, sec	Maximum Breaker Wave Height H_b, ft	Wave-length λ, ft	Underlayer Material Extent L, ft	L/λ	Average Model Stone Weight W_{UL}, lb	$\omega_r^{1/3} H_b / (S_r - 1) W_{UL}^{1/3}$	Stable, S or Unstable, U
0.5	2	0.65	8.02	3	0.37	0.0085	11.05	S
0.5	2	0.65	8.02	3	0.37	0.0175	8.68	S
0.5	2	0.65	8.02	3	0.37	0.0315	7.14	S
0.5	2	0.65	8.02	3	0.37	0.0520	6.05	S
0.5	2	0.65	8.02	3	0.37	0.0795	5.25	S
0.5	2	0.65	8.02	3	0.37	0.1405	4.34	S
0.5	2	0.65	8.02	3	0.37	0.2540	3.56	S
0.5	2	0.65	8.02	5	0.62	0.0085	11.05	S
0.5	2	0.65	8.02	5	0.62	0.0175	8.68	S
0.5	2	0.65	8.02	5	0.62	0.0315	7.14	S
0.5	2	0.65	8.02	5	0.62	0.0520	6.05	S
0.5	2	0.65	8.02	5	0.62	0.0795	5.25	S
0.5	2	0.65	8.02	5	0.62	0.1405	4.34	S
0.5	2	0.65	8.02	5	0.62	0.2540	3.56	S
0.5	2	0.65	8.02	7	0.87	0.0085	11.05	S
0.5	2	0.65	8.02	7	0.87	0.0175	8.68	S
0.5	2	0.65	8.02	7	0.87	0.0315	7.14	S
0.5	2	0.65	8.02	7	0.87	0.0520	6.05	S
0.5	2	0.65	8.02	7	0.87	0.0795	5.25	S
0.5	2	0.65	8.02	7	0.87	0.1405	4.34	S
0.5	2	0.65	8.02	7	0.87	0.2540	3.56	S
0.5	3	0.70	12.04	3	0.25	0.0085	11.91	S
0.5	3	0.70	12.04	3	0.25	0.0175	9.34	S
0.5	3	0.70	12.04	3	0.25	0.0315	7.69	S
0.5	3	0.70	12.04	3	0.25	0.0520	6.51	S
0.5	3	0.70	12.04	3	0.25	0.0795	5.65	S
0.5	3	0.70	12.04	3	0.25	0.1405	4.67	S
0.5	3	0.70	12.04	3	0.25	0.2540	3.84	S
0.5	3	0.70	12.04	5	0.42	0.0085	11.91	S
0.5	3	0.70	12.04	5	0.42	0.0175	9.34	S
0.5	3	0.70	12.04	5	0.42	0.0315	7.69	S
0.5	3	0.70	12.04	5	0.42	0.0520	6.51	S
0.5	3	0.70	12.04	5	0.42	0.0795	5.65	S
0.5	3	0.70	12.04	5	0.42	0.1405	4.67	S
0.5	3	0.70	12.04	5	0.42	0.2540	3.84	S
0.5	3	0.70	12.04	7	0.58	0.0085	11.91	S
0.5	3	0.70	12.04	7	0.58	0.0175	9.34	S
0.5	3	0.70	12.04	7	0.58	0.0315	7.69	S
0.5	3	0.70	12.04	7	0.58	0.0520	6.51	S
0.5	3	0.70	12.04	7	0.58	0.0795	5.65	S
0.5	3	0.70	12.04	7	0.58	0.1405	4.67	S
0.5	3	0.70	12.04	7	0.58	0.2540	3.84	S
0.5	4	0.80	16.05	3	0.19	0.0085	13.61	U
0.5	4	0.80	16.05	3	0.19	0.0175	10.68	U
0.5	4	0.80	16.05	3	0.19	0.0315	8.78	U
0.5	4	0.80	16.05	3	0.19	0.0520	7.44	S
0.5	4	0.80	16.05	3	0.19	0.0795	6.46	S
0.5	4	0.80	16.05	3	0.19	0.1405	5.34	S
0.5	4	0.80	16.05	3	0.19	0.2540	4.39	S
0.5	4	0.80	16.05	5	0.31	0.0085	13.61	U
0.5	4	0.80	16.05	5	0.31	0.0175	10.68	U
0.5	4	0.80	16.05	5	0.31	0.0315	8.78	S
0.5	4	0.80	16.05	5	0.31	0.0520	7.44	S
0.5	4	0.80	16.05	5	0.31	0.0795	6.46	S
0.5	4	0.80	16.05	5	0.31	0.1405	5.34	S
0.5	4	0.80	16.05	5	0.31	0.2540	4.39	S
0.5	4	0.80	16.05	7	0.44	0.0085	13.61	S
0.5	4	0.80	16.05	7	0.44	0.0175	10.68	S
0.5	4	0.80	16.05	7	0.44	0.0315	8.78	S
0.5	4	0.80	16.05	7	0.44	0.0520	7.44	S
0.5	4	0.80	16.05	7	0.44	0.0795	6.46	S
0.5	4	0.80	16.05	7	0.44	0.1405	5.34	S
0.5	4	0.80	16.05	7	0.44	0.2540	4.39	S

(Continued)

Table 7 (Continued)

Still-Water Depth d, ft	Wave Period T, sec	Maximum Breaker Wave Height H_b, ft	Wavelength λ, ft	Underlayer Material Extent L, ft	$\frac{L}{\lambda}$	Average Model Stone Weight W_{UL}, lb	$\frac{\omega_r^{1/3} H_b}{(S_r - 1) W_{UL}^{1/3}}$	Stable, S or Unstable, U
0.5	5	0.68	20.06	3	0.15	0.0085	11.57	U
0.5	5	0.68	20.06	3	0.15	0.0175	9.08	S
0.5	5	0.68	20.06	3	0.15	0.0315	7.47	S
0.5	5	0.68	20.06	3	0.15	0.0520	6.33	S
0.5	5	0.68	20.06	3	0.15	0.0795	5.49	S
0.5	5	0.68	20.06	3	0.15	0.1405	4.54	S
0.5	5	0.68	20.06	3	0.15	0.2540	3.73	S
0.5	5	0.68	20.06	5	0.25	0.0085	11.57	U
0.5	5	0.68	20.06	5	0.25	0.0175	9.08	S
0.5	5	0.68	20.06	5	0.25	0.0315	7.47	S
0.5	5	0.68	20.06	5	0.25	0.0520	6.33	S
0.5	5	0.68	20.06	5	0.25	0.0795	5.49	S
0.5	5	0.68	20.06	5	0.25	0.1405	4.54	S
0.5	5	0.68	20.06	5	0.25	0.2540	3.73	S
0.5	5	0.68	20.06	7	0.35	0.0085	11.57	S
0.5	5	0.68	20.06	7	0.35	0.0175	9.08	S
0.5	5	0.68	20.06	7	0.35	0.0315	7.47	S
0.5	5	0.68	20.06	7	0.35	0.0520	6.33	S
0.5	5	0.68	20.06	7	0.35	0.0795	5.49	S
0.5	5	0.68	20.06	7	0.35	0.1405	4.54	S
0.5	5	0.68	20.06	7	0.35	0.2540	3.73	S
1.0	2	1.09	11.35	3	0.26	0.0085	18.54	U
1.0	2	1.09	11.35	3	0.26	0.0175	14.55	U
1.0	2	1.09	11.35	3	0.26	0.0315	11.97	S
1.0	2	1.09	11.35	3	0.26	0.0520	10.14	S
1.0	2	1.09	11.35	3	0.26	0.0795	8.80	S
1.0	2	1.09	11.35	3	0.26	0.1405	7.27	S
1.0	2	1.09	11.35	3	0.26	0.2540	5.98	S
1.0	2	1.09	11.35	5	0.44	0.0085	18.54	U
1.0	2	1.09	11.35	5	0.44	0.0175	14.55	S
1.0	2	1.09	11.35	5	0.44	0.0315	11.97	S
1.0	2	1.09	11.35	5	0.44	0.0520	10.14	S
1.0	2	1.09	11.35	5	0.44	0.0795	8.80	S
1.0	2	1.09	11.35	5	0.44	0.1405	7.27	S
1.0	2	1.09	11.35	5	0.44	0.2540	5.98	S
1.0	2	1.09	11.35	7	0.62	0.0085	18.54	S
1.0	2	1.09	11.35	7	0.62	0.0175	14.55	S
1.0	2	1.09	11.35	7	0.62	0.0315	11.97	S
1.0	2	1.09	11.35	7	0.62	0.0520	10.14	S
1.0	2	1.09	11.35	7	0.62	0.0795	8.80	S
1.0	2	1.09	11.35	7	0.62	0.1405	7.27	S
1.0	2	1.09	11.35	7	0.62	0.2540	5.98	S
1.0	3	1.11	17.02	3	0.18	0.0085	18.88	U
1.0	3	1.11	17.02	3	0.18	0.0175	14.81	U
1.0	3	1.11	17.02	3	0.18	0.0315	12.19	U
1.0	3	1.11	17.02	3	0.18	0.0520	10.33	U
1.0	3	1.11	17.02	3	0.18	0.0795	8.96	S
1.0	3	1.11	17.02	3	0.18	0.1405	7.41	S
1.0	3	1.11	17.02	3	0.18	0.2540	6.08	S
1.0	3	1.11	17.02	5	0.29	0.0085	18.88	U
1.0	3	1.11	17.02	5	0.29	0.0175	14.81	U
1.0	3	1.11	17.02	5	0.29	0.0315	12.19	S
1.0	3	1.11	17.02	5	0.29	0.0520	10.33	S
1.0	3	1.11	17.02	5	0.29	0.0795	8.96	S
1.0	3	1.11	17.02	5	0.29	0.1405	7.41	S
1.0	3	1.11	17.02	5	0.29	0.2540	6.08	S
1.0	3	1.11	17.02	7	0.41	0.0085	18.88	S
1.0	3	1.11	17.02	7	0.41	0.0175	14.81	S
1.0	3	1.11	17.02	7	0.41	0.0315	12.19	S
1.0	3	1.11	17.02	7	0.41	0.0520	10.33	S
1.0	3	1.11	17.02	7	0.41	0.0795	8.96	S
1.0	3	1.11	17.02	7	0.41	0.1405	7.41	S
1.0	3	1.11	17.02	7	0.41	0.2540	6.08	S

(Continued)

Table 7 (Concluded)

Still-Water Depth d, ft	Wave Period T, sec	Maximum Breaker Wave Height H_b, ft	Wavelength λ, ft	Underlayer Material Extent L, ft	$\frac{L}{\lambda}$	Average Model Stone Weight W_{UL}, lb	$\frac{\omega_r^{1/3} H_b}{(S_r - 1) W_{UL}^{1/3}}$	Stable, S or Unstable, U
1.0	4	1.45	22.70	3	0.13	0.0085	24.66	U
1.0	4	1.45	22.70	3	0.13	0.0175	19.35	U
1.0	4	1.45	22.70	3	0.13	0.0315	15.92	U
1.0	4	1.45	22.70	3	0.13	0.0520	13.49	U
1.0	4	1.45	22.70	3	0.13	0.0795	11.70	U
1.0	4	1.45	22.70	3	0.13	0.1405	9.68	U
1.0	4	1.45	22.70	3	0.13	0.2540	7.95	U
1.0	4	1.45	22.70	5	0.22	0.0085	24.66	U
1.0	4	1.45	22.70	5	0.22	0.0175	19.35	U
1.0	4	1.45	22.70	5	0.22	0.0315	15.92	U
1.0	4	1.45	22.70	5	0.22	0.0520	13.49	U
1.0	4	1.45	22.70	5	0.22	0.0795	11.70	U
1.0	4	1.45	22.70	5	0.22	0.1405	9.68	U
1.0	4	1.45	22.70	5	0.22	0.2540	7.95	U
1.0	4	1.45	22.70	7	0.31	0.0085	24.66	U
1.0	4	1.45	22.70	7	0.31	0.0175	19.35	U
1.0	4	1.45	22.70	7	0.31	0.0315	15.92	U
1.0	4	1.45	22.70	7	0.31	0.0520	13.49	U
1.0	4	1.45	22.70	7	0.31	0.0795	11.70	U
1.0	4	1.45	22.70	7	0.31	0.1405	9.68	U
1.0	4	1.45	22.70	7	0.31	0.2540	7.95	S
1.0	5	1.12	28.37	3	0.11	0.0085	19.05	U
1.0	5	1.12	28.37	3	0.11	0.0175	14.95	U
1.0	5	1.12	28.37	3	0.11	0.0315	12.30	U
1.0	5	1.12	28.37	3	0.11	0.0520	10.42	U
1.0	5	1.12	28.37	3	0.11	0.0795	9.04	U
1.0	5	1.12	28.37	3	0.11	0.1405	7.47	U
1.0	5	1.12	28.37	3	0.11	0.2540	6.14	S
1.0	5	1.12	28.37	5	0.18	0.0085	19.05	U
1.0	5	1.12	28.37	5	0.18	0.0175	14.95	U
1.0	5	1.12	28.37	5	0.18	0.0315	12.30	U
1.0	5	1.12	28.37	5	0.18	0.0520	10.42	U
1.0	5	1.12	28.37	5	0.18	0.0795	9.04	U
1.0	5	1.12	28.37	5	0.18	0.1405	7.47	S
1.0	5	1.12	28.37	5	0.18	0.2540	6.14	S
1.0	5	1.12	28.37	7	0.25	0.0085	19.05	U
1.0	5	1.12	28.37	7	0.25	0.0175	14.95	U
1.0	5	1.12	28.37	7	0.25	0.0315	12.30	U
1.0	5	1.12	28.37	7	0.25	0.0520	10.42	S
1.0	5	1.12	28.37	7	0.25	0.0795	9.04	S
1.0	5	1.12	28.37	7	0.25	0.1405	7.47	S
1.0	5	1.12	28.37	7	0.25	0.2540	6.14	S

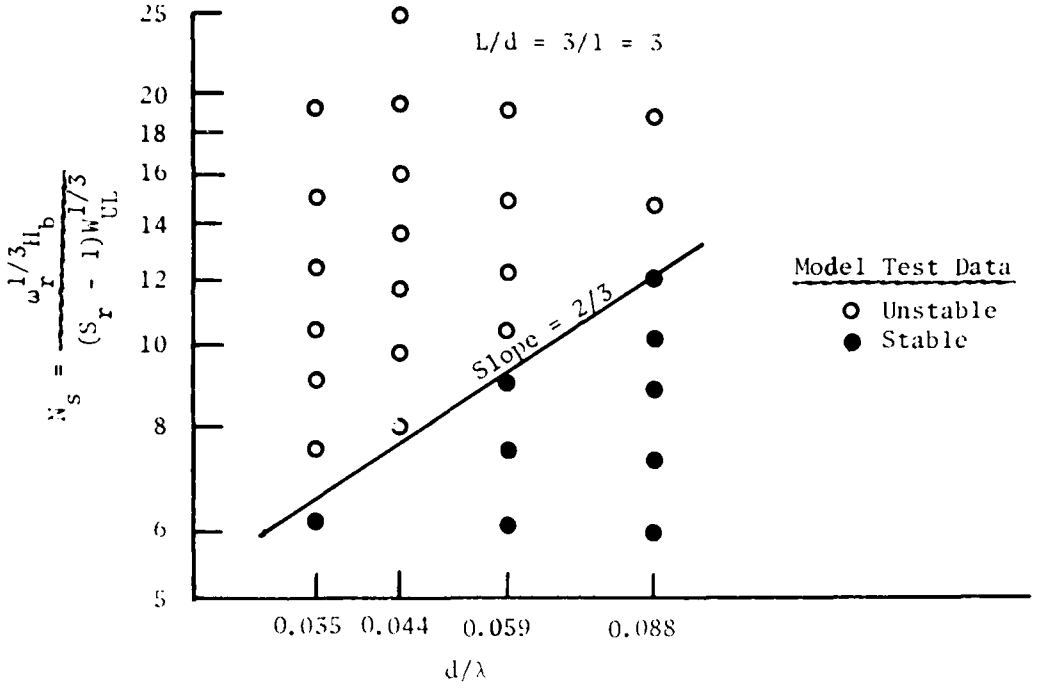

Figure 33. Stability number, N_s, versus the relative water depth, d/λ, for a 3-ft extent of model underlayer section (L/d = 3)

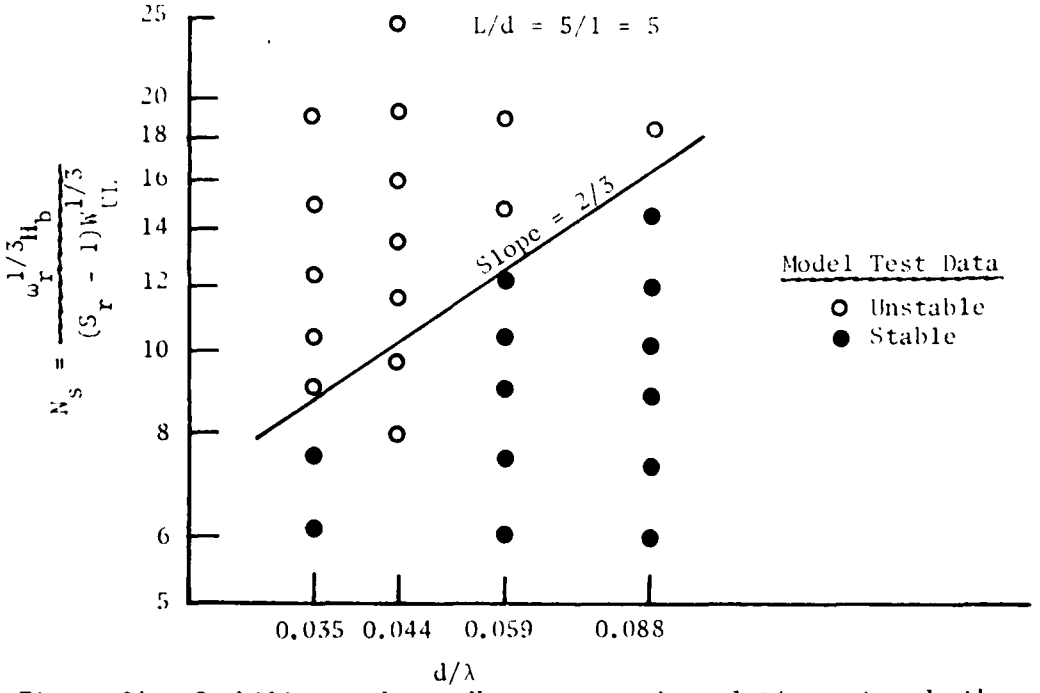

Figure 34. Stability number, N_s, versus the relative water depth, d/λ, for a 5-ft extent of model underlayer section (L/d = 5)

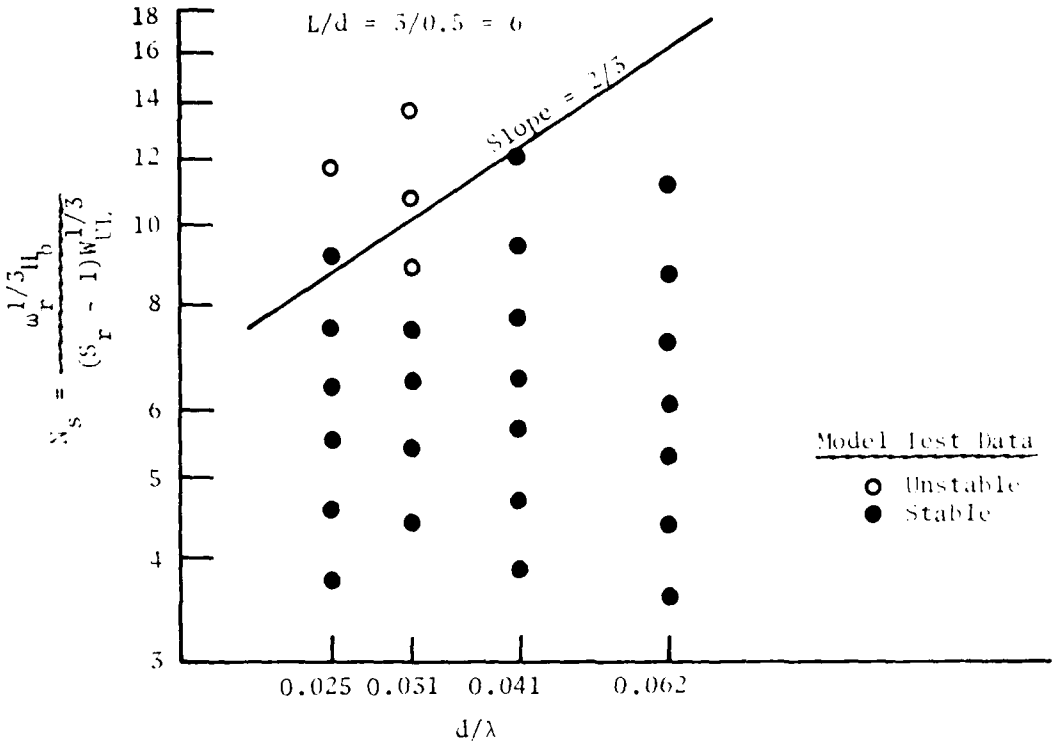

Figure 35. Stability number, N_s, versus the relative water depth, d/λ, for a 3-ft extent of model underlayer section (L/d = 6)

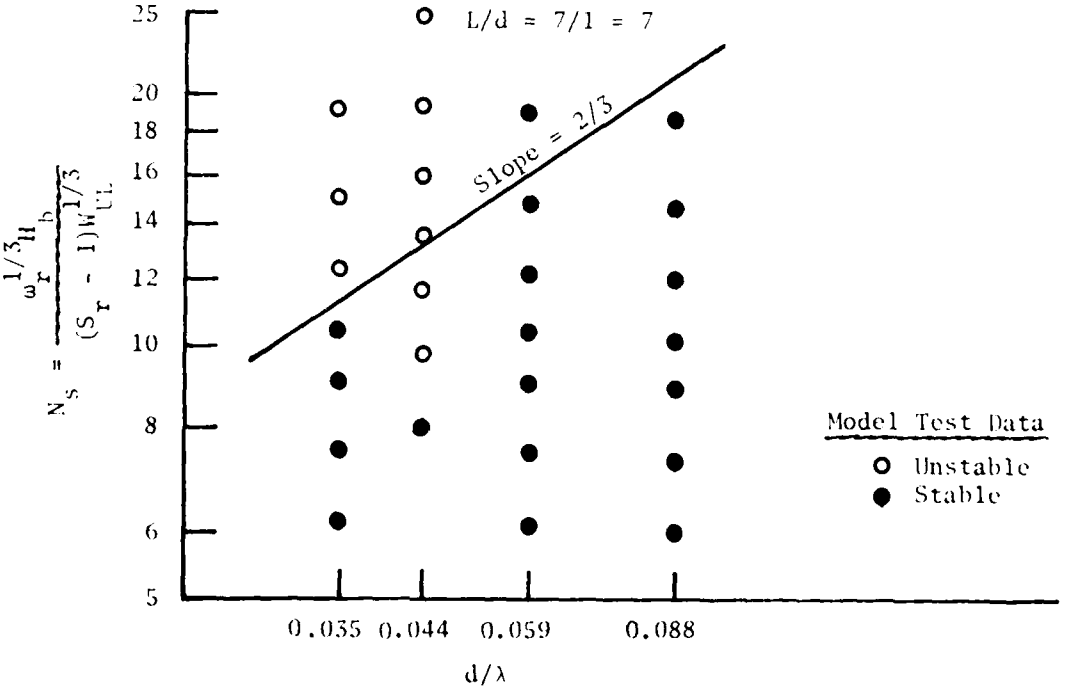

Figure 36. Stability number, N_s, versus the relative water depth, d/λ, for a 7-ft extent of model underlayer section (L/d = 7)

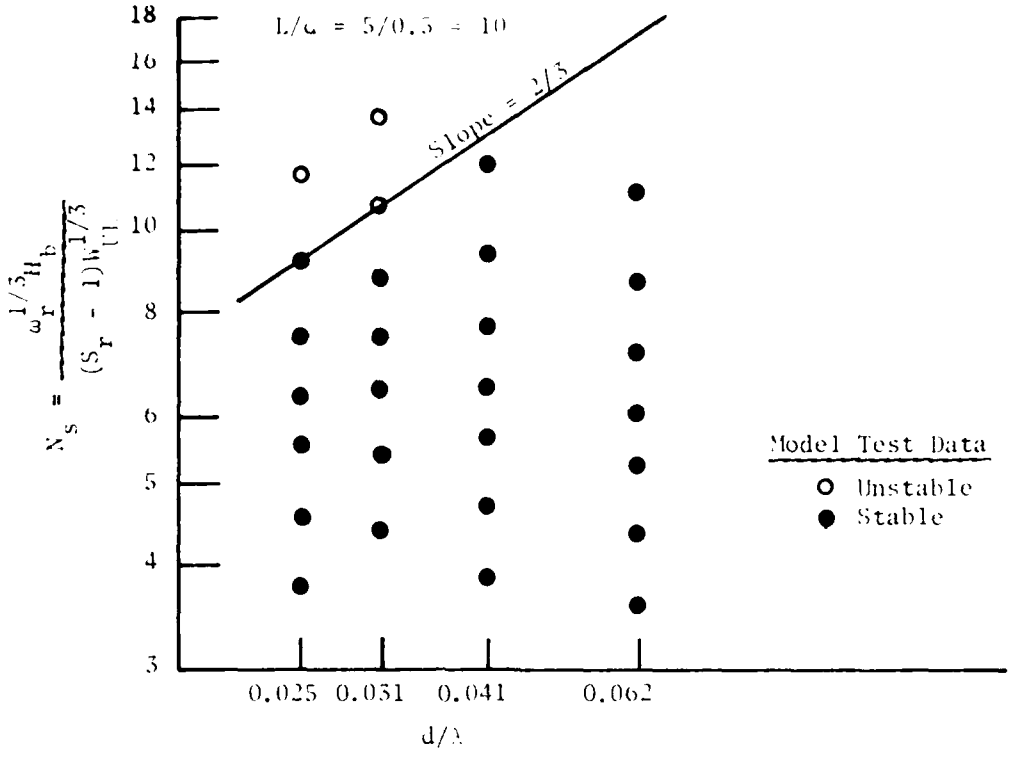

Figure 37. Stability number, N_s, versus the relative water depth, d/λ, for a 5-ft extent of model underlayer section (L/d = 10)

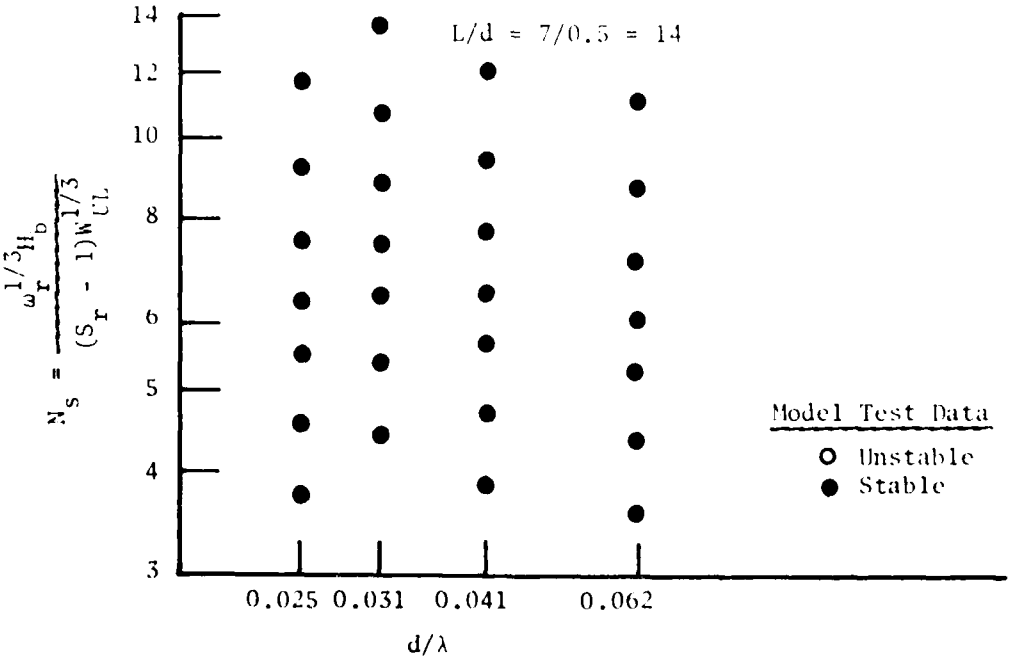

Figure 38. Stability number, N_s, versus the relative water depth, d/λ, for a 7-ft extent of model underlayer section (L/d = 14)

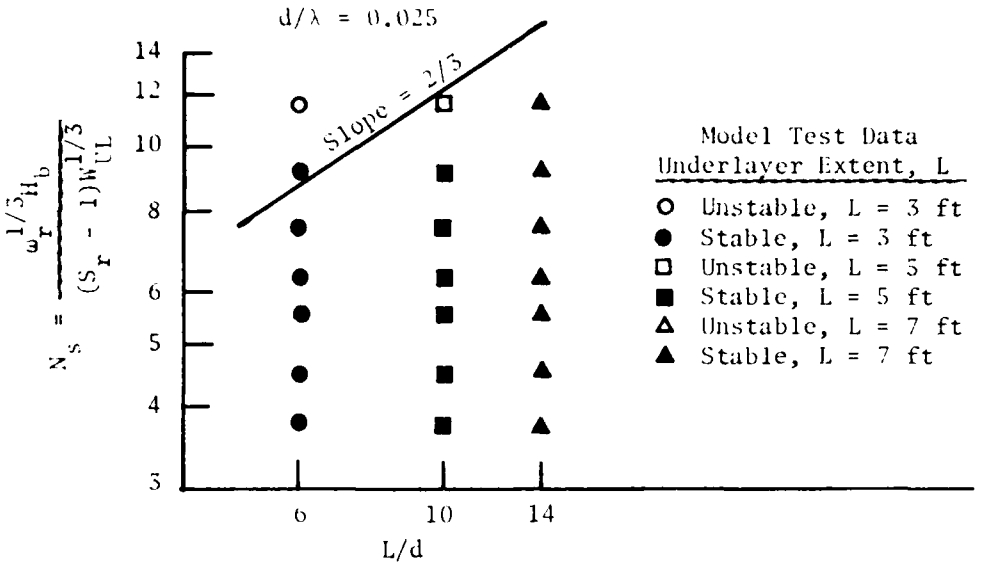

Figure 39. Stability number, N_s, versus the structure parameter, L/d, for relative water depth d/λ = 0.025

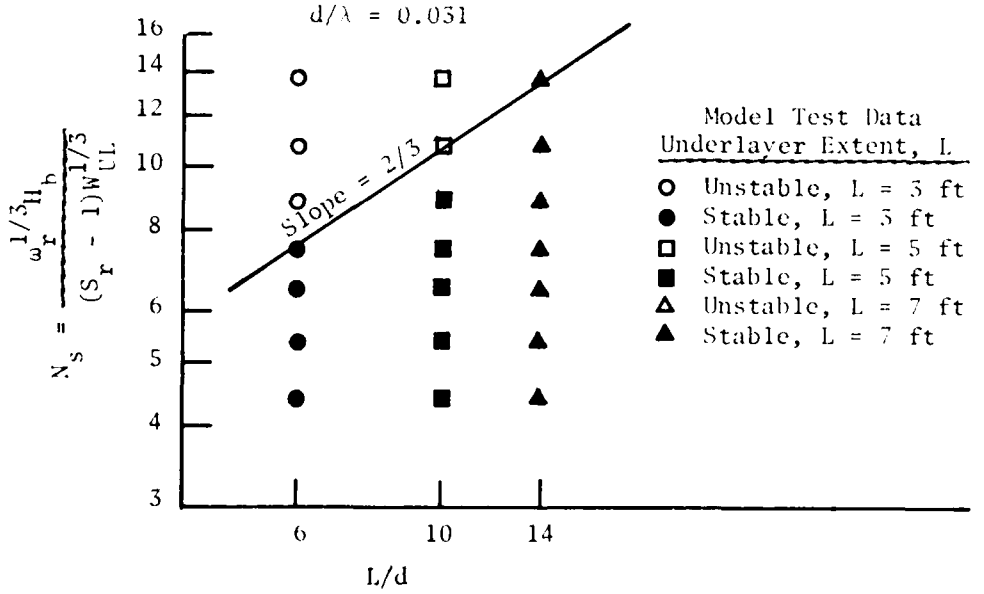

Figure 40. Stability number, N_s, versus the structure parameter, L/d, for relative water depth, d/λ = 0.031

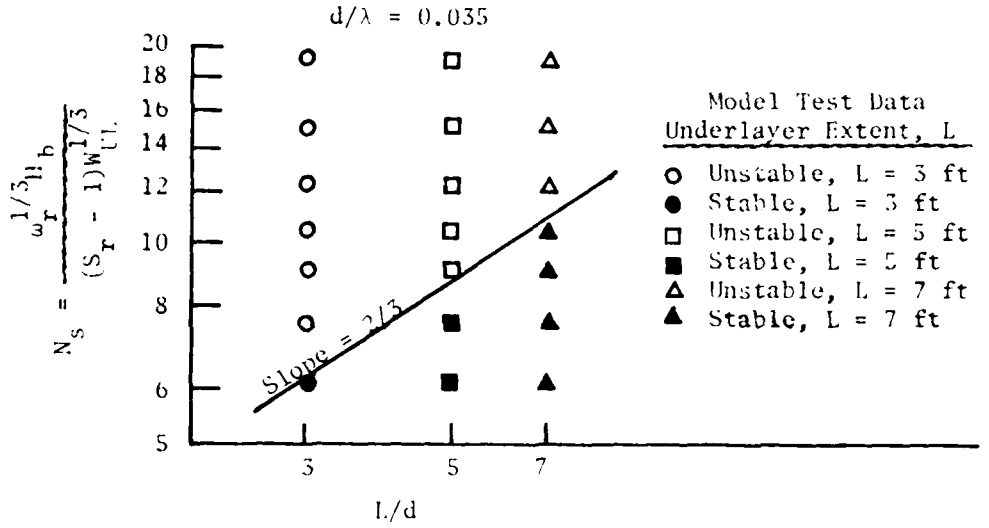

Figure 41. Stability number, N_s, versus the structure parameter, L/d, for relative water depth, d/λ = 0.035

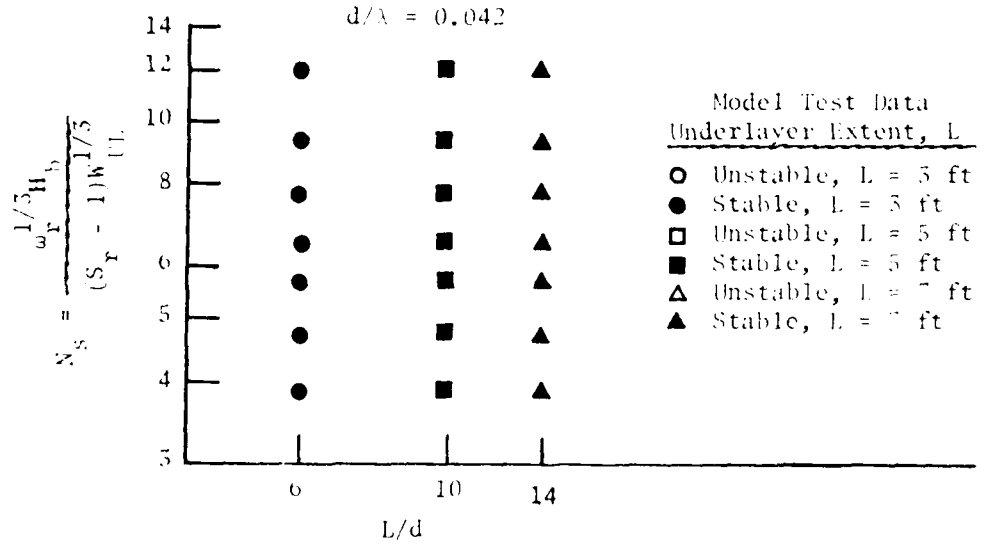

Figure 42. Stability number, N_s, versus the structure parameter, L/d, for relative water depth, d/λ = 0.042

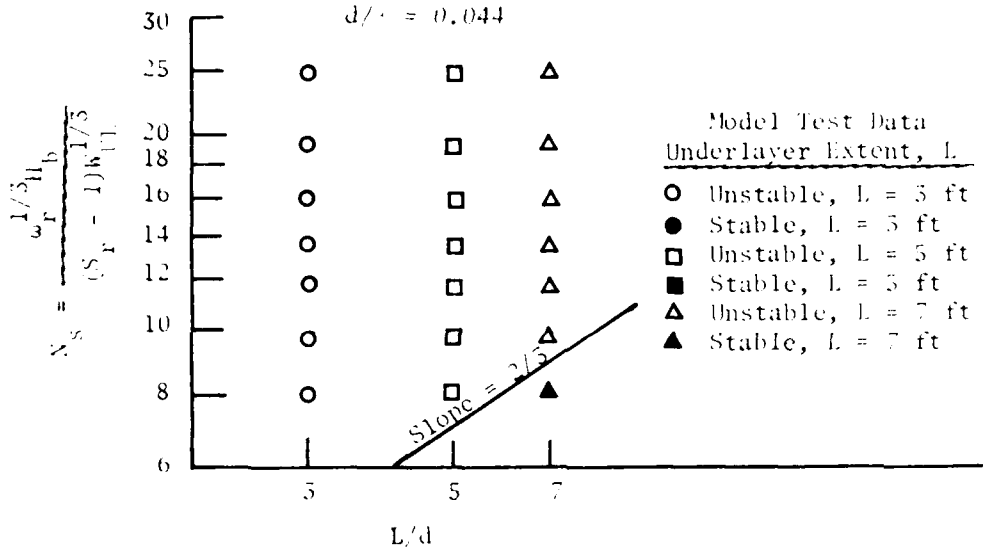

Figure 43. Stability number, N_s, versus the structure parameter, L/d, for relative water depth, d/λ = 0.044

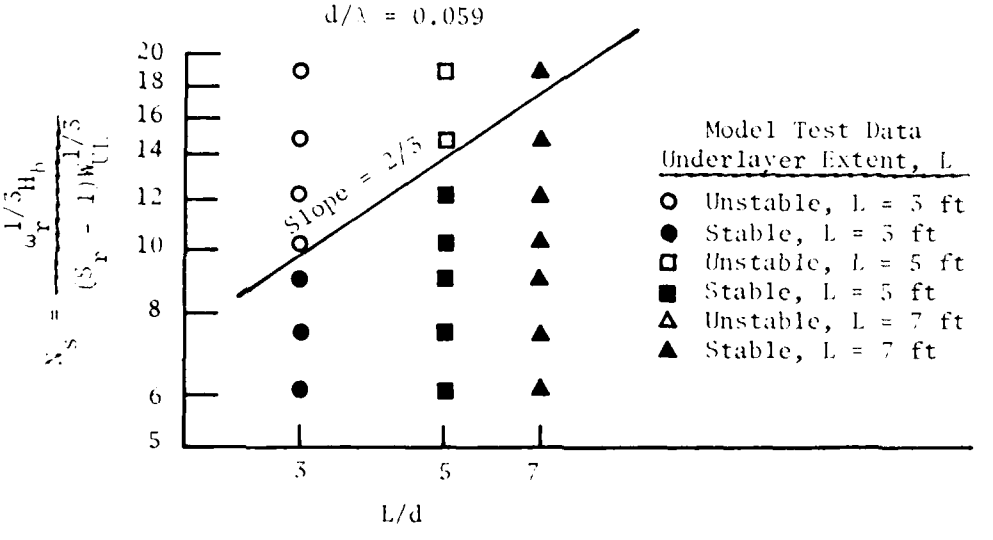

Figure 44. Stability number, N_s, versus the structure parameter, L/d, for relative water depth, d/λ = 0.059

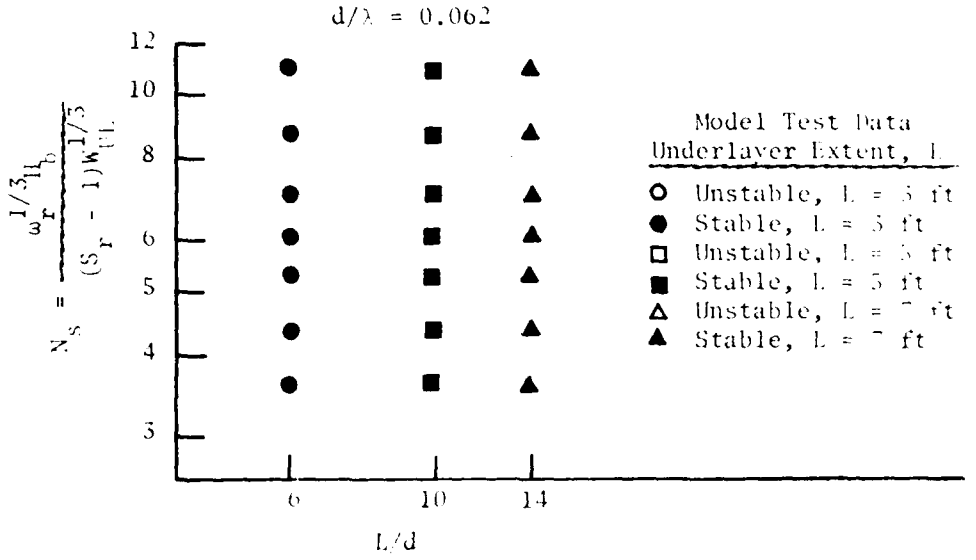

Figure 45. Stability number, N_s, versus the structure parameter, L/d, for relative water depth, d/λ = 0.062

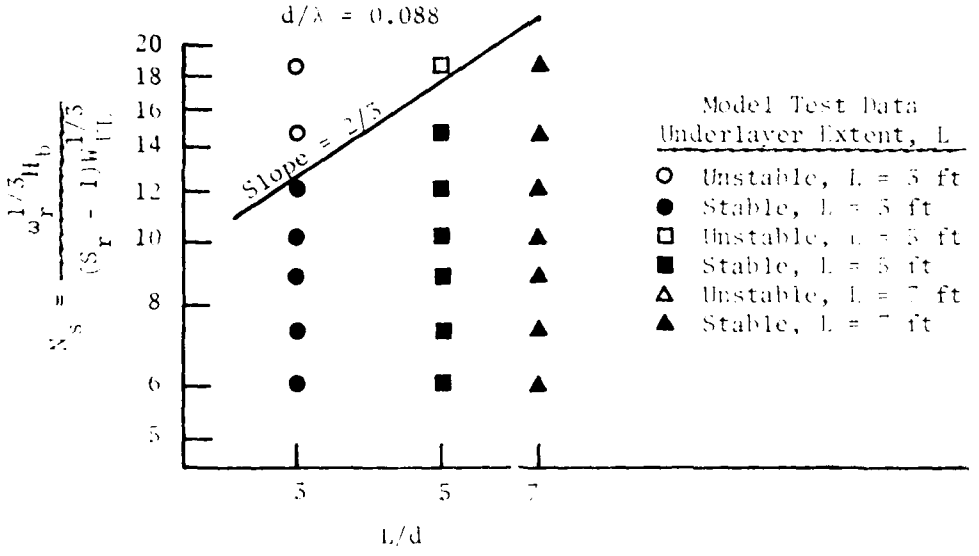

Figure 46. Stability number, N_s, versus the structure parameter, L/d, for relative water depth, d/λ = 0.088

a straight line on these log-log plots (except for Figures 42 and 45, which are inconclusive). Again, the precise slope of such a straight line cannot be precisely ascertained; however, it appears the same slope can be equally as well fit to data sets of Figures 33-38 as to data sets of Figures 39-46.

56. If indeed the same slope line can be fit to the data of constant values of L/d as can be fit to the data of constant values of d/λ, then the regions of stability can be separated from the unstable regions on a display which plots the stability number, N_s, of Equation 20, versus the relative underlayer section length, L/λ :

$$N_s = \frac{\omega_r^{1/3} H_b}{(S_r - 1) W_{UL}^{1/3}} = f\left(\frac{L}{\lambda}\right) \tag{21}$$

The precise functional representation can be determined from Figure 47. The average best-fit line slope on this log-log plot which separates the regions of stability from the unstable regions is determined to have a value of 2/3. While some scatter was found to exist in the experimental data, this value of 2/3 can be satisfactorily fit to the data of Figures 33-46. The average best-fit line generated a stability number:

$$N_s = \frac{\omega_r^{1/3} H_b}{(S_r - 1) W_{UL}^{1/3}} = 28.5\left(\frac{L}{\lambda}\right)^{2/3} \tag{22}$$

from which the weight, W_{UL}, of a representative stone in the underlayer material section is:

$$W_{UL} = \frac{\omega_r H_b^3}{23{,}150(S_r - 1)^3\left(\frac{L}{\lambda}\right)^2} \tag{23}$$

57. Because of experimental scatter in a few of the data points of Figure 47, the average best-fit line (Equation 22) lies above some of the test results. This implies that on the average Equation 22 describes the stability of an underlayer material section; however, some tests were found to exceed the

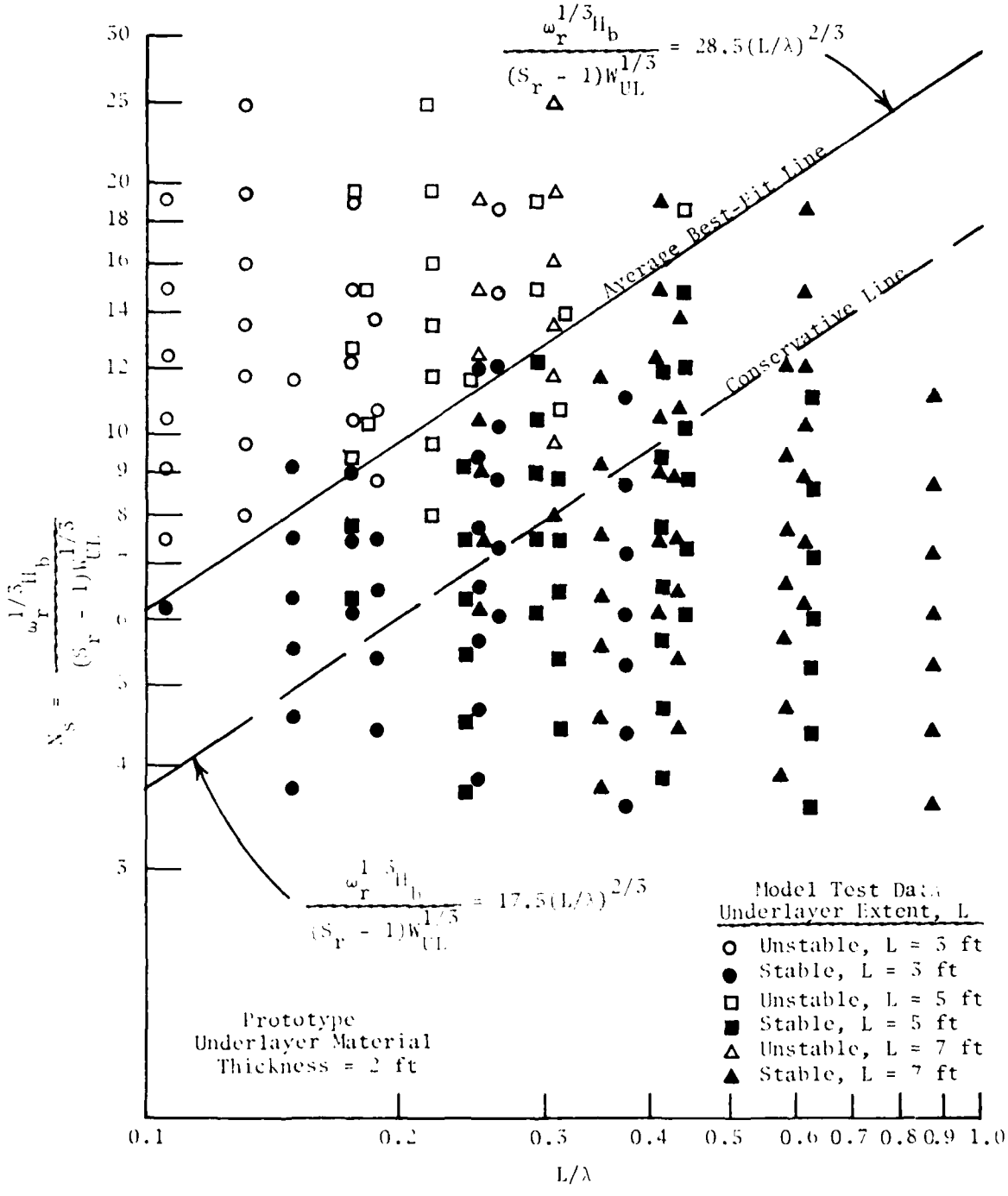

Figure 47. Stability number, N_s, versus the relative underlayer section length, L/λ, showing the average best-fit line to all the experimental data, and the conservative line enveloping all unstable conditions tested

values of stone weight indicated by this expression and by Equation 23. In order to ensure that all the experimental data fall within the stability region described by a stability number, a conservative stability number should be established which will include all the experimental data used to generate the representative stone weight size, W_{UL}, in the underlayer section. Such a conservative line should remain parallel on the log-log plot of Figure 47 with the average best-fit line, but be displaced until it passes through the data point of known stability that lies adjacent to a companion test which proved to be unstable. That is, for a relative underlayer section length, $L/\lambda = 0.31$, the experimental test which produced a stability number, $N_s = 7.95$, was stable. The most nearly adjacent test in this family of experiments at the same value of $L/\lambda = 0.31$ was unstable and produced a stability number of $N_s = 9.68$. (These are the data which are displaced lower on Figure 47 from the average best-fit line.) Hence the conservative curve should pass through point $L/\lambda = 0.31$, $N_s = 7.95$, as this was a value of known stability from the experimental test results. The expression of this conservative line, in terms of stability number, N_s, is:

$$N_s = \frac{\omega_r^{1/3} H_b}{(S_r - 1) W_{UL}^{1/3}} = 17.5\left(\frac{L}{\lambda}\right)^{2/3} \tag{24}$$

For this conservative expression, the weight, W_{UL}, of a representative stone comprising such an underlayer material section can be developed as:

$$W_{UL} = \frac{\omega_r H_b^3}{5{,}360(S_r - 1)^3\left(\frac{L}{\lambda}\right)^2} \tag{25}$$

The test material used to develop these conservative expressions was sorted, passing one gradation screen and being retained by the next size screen. Furthermore, the size of the material used in a test was defined as the midpoint between these two screen sizes.

PART V: SUMMARY AND CONCLUSIONS

Summary

58. When major rubble-mound stone structures such as breakwaters, jetties, or groins are constructed in the coastal zone, they alter the existing current and wave conditions that normally exist at a particular location. Waves breaking on such structures under construction may cause bottom material to be suspended and transported from the region, resulting in scour holes that must be filled with construction material. This may result in substantial cost overruns. To minimize potential cost increases due to scour during nearshore construction, a foundation blanket of underlayer material can be placed some distance ahead of the construction of the upper portions of the structure. The stability of such an underlayer material section will depend on the size of the material used in the layer, the extent of the section, and the incoming wave climate.

59. The purpose of this study was to determine the stability during construction of such an underlayer material section, which also serves as the foundation blanket for rubble-mound structures constructed on a movable bottom. A simple beach profile consisting of straight, uniform contours parallel with the shoreline was physically modeled on a 1V-on-25H slope in a 6-ft-wide wave flume. A major stone structure was assumed to be under construction perpendicular to the shoreline and thus perpendicular to the uniform parallel contours. A two-dimensional section of this stone structure was modeled (16-to-1 linear scale ratio) along the major axis of the structure. The waves which produced the most severe movement of the underlayer section (scour) were those with characteristics that caused breaking with plunging to occur directly at the toe of the rubble-mound structure. Seven uniform material sizes were used to construct three different lengths of underlayer material sections (3-, 5-, and 7-ft model dimensions; 48-, 80-, and 112-ft prototype dimensions, respectively). These 21 different underlayer sections were subjected to breaking waves with periods of 2-, 3-, 4-, and 5-sec model time (8-, 12-, 16-, and 20-sec prototype time, respectively). The characteristics of these 168 individual tests are presented in Table 7. All tests were performed with an underlayer material section thickness of 2.0 ft prototype, which is a typically representative value presently being utilized under prototype conditions.

Conclusions

60. The stability of an underlayer material section is analogous to the stability of the armor layer of a rubble-mound structure, with the exception that the slope of the seaward face, θ , of such a structure vanishes from this problem and thus is not a pertinent variable. Hence the objective of the experimental study was to determine which of those combinations of underlayer material sizes and wave characteristics would result in a stable condition. The majority of the failures (unstable conditions) occurred as material moved from the seaward edge of the underlayer section toward the base of the rubble-mound structure. This temporal movement was functionally related to the wave characteristics (breaking wave height, H_b , and/or wave period, T), and to the size of the material being tested, W_{UL} . For some tests that utilized an underlayer section which was relatively long when compared with the water depth, d , or breaking wave height, H_b , the instability would be reflected as a failure section at some location other than the toe of the underlayer section. This implies that if all sections could be extended far enough seaward, the instability would appear as a scour hole development through the underlayer section (the instability becomes a function of layer thickness). Since it is impractical to extend an underlayer section for an infinite distance seaward, the optimization of material size, W_{UL} , and layer extent, L , with wave characteristics of breaking height, H_b , and length, λ , is necessary for efficient construction.

61. The stability of an underlayer section may be expressed as some functional relationship between nine basic parameters:

$$f(\omega_w , \omega_r , W_{UL} , H_b , T , g , d , L , \lambda) = 0 \qquad (19 \text{ bis})$$

The effect of thickness of the underlayer material section was not investigated in these tests. Since it was desired to display these experimental data in a manner similar to that of Hudson (1957) for the armor slope stability of rubble-mound structures, the stability number, N_s , can be developed and is functionally related to two other fully independent dimensionless terms:

$$N_s = \frac{\omega_r^{1/3} H_b}{(S_r - 1) W_{UL}^{1/3}} = f\left[\frac{L}{d} , \left(\frac{d}{g}\right)^{1/2} \frac{1}{T}\right] = f\left(\frac{L}{d} , \frac{d}{\lambda}\right) \qquad \text{(20 bis)}$$

62. It was determined that for constant values of the structure parameter, L/d, a straight line could be fit to a display of the stability number, N_s, versus relative water depth, d/λ. Furthermore, a straight line of the same slope could be fit to a display of the stability number, N_s, versus the structure parameter, L/d, for constant values of relative water depth, d/λ, when all data are displayed on log-log plots. This implies that if the same slope line can be fit to data of constant values of L/d as it can be fit to data of constant values of d/λ, then the stability number, N_s, of Equation 20 is simply a function of only one other dimensionless parameter, that being the relative underlayer section length, L/λ.

$$N_s = \frac{\omega_r^{1/3} H_b}{(S_r - 1) W_{UL}^{1/3}} = f\left(\frac{L}{\lambda}\right) \qquad \text{(21 bis)}$$

This functional relationship can be determined by separating the regions of stability from the unstable regions on a display that plots the stability number, N_s, versus the relative underlayer section length, L/λ (Figure 47).

63. The average best-fit line separating stable from unstable regions for all of the experimental data of this physical model investigation generated a stability number, N_s:

$$N_s = \frac{\omega_r^{1/3} H_b}{(S_r - 1) W_{UL}^{1/3}} = 28.5\left(\frac{L}{\lambda}\right)^{2/3} \qquad \text{(22 bis)}$$

From this expression can be deduced the weight, W_{UL}, of a representative stone comprising an underlayer material section for this average best-fit line:

$$W_{UL} = \frac{\omega_r H_b^3}{23{,}150(S_r - 1)^3\left(\frac{L}{\lambda}\right)^2} \qquad (23 \text{ bis})$$

64. Because of experimental scatter in some of the data points, some tests were found to exceed the values of stone weight, W_{UL}, indicated by Equation 23. In order to ensure that all the experimental data fall within the stability region described by a stability number, a conservative stability number was developed which included all the experimental data used to generate the representative stone weight, W_{UL}, of the underlayer section. The expression for this conservative stability number, N_s, is:

$$N_s = \frac{\omega_r^{1/3} H_b}{(S_r - 1)W_{UL}^{1/3}} = 17.5\left(\frac{L}{\lambda}\right)^{2/3} \qquad (24 \text{ bis})$$

with the corresponding conservative expression for the weight, W_{UL}, of the representative stone comprising such an underlayer material section:

$$W_{UL} = \frac{\omega_r H_b^3}{5{,}360(S_r - 1)^3\left(\frac{L}{\lambda}\right)^2} \qquad (25 \text{ bis})$$

Equation 25 is the recommended equation for determining the weight, W_{UL}, of rock that will remain stable during construction for given wave conditions. Since these data were obtained from the most severe wave conditions (waves that break and plunge directly at the toe of the structure), the application of these results to less-severe wave climates will indicate a stone size requirement larger than necessary. Hence Equation 25 is additionally conservative.

REFERENCES

Bruun, P. 1979 (Sep). "Breakwater Design, Design of Mound Breakwaters, Proceedings, Civil Engineering in the Oceans IV, San Francisco, Calif., Vol 1, pp 344-366.

Bruun, P., and Gunbak, A. R. 1976 (Jul). "New Design Principles for Rubble Mound Structures," Proceedings, Fifteenth Coastal Engineering Conference, Honolulu, Hawaii, Vol III, pp 2429-2473.

Carver, R. D. 1976 (Apr). "Stability of Rubble-Mound Breakwater, Lahaina Harbor, Hawaii; Hydraulic Model Investigation," Miscellaneous Paper H-76-8, U. S. Army Engineer Waterways Experiment Station, CE, Vicksburg, Miss.

_____. 1980 (Jan). "Effects of First Underlayer Weight on the Stability of Stone-Armored Rubble-Mound Breakwater Trunks Subjected to Nonbreaking Waves with No Overtopping; Hydraulic Model Investigation," Technical Report HL-80-1, U. S. Army Engineer Waterways Experiment Station, CE, Vicksburg, Miss.

Carver, R. D., and Davidson, D. D. 1977 (Nov). "Dolos Armor Units Used on Rubble-Mound Breakwater Trunks Subjected to Nonbreaking Waves with No Overtopping," Technical Report H-77-19, U. S. Army Engineer Waterways Experiment Station, CE, Vicksburg, Miss.

Cavanilles, R. I. 1938 (Jul). "A Formula for the Calculation of Rock-Fill Dykes," TR-He-116-295, University of California, Berkeley, Calif.

Davidson, D. D. 1971 (Nov). "Proposed Jetty-Head Repair Sections, Humboldt Bay, California; Hydraulic Model Investigation," Technical Report H-71-8, U. S. Army Engineer Waterways Experiment Station, CE, Vicksburg, Miss.

_____. 1978 (Jan). "Stability Tests of Nawiliwili Breakwater Repair," Miscellaneous Paper H-78-4, U. S. Army Engineer Waterways Experiment Station, CE, Vicksburg, Miss.

Gravesen, H., Jensen, O. J., and Sorensen, T. "Stability of Rubble Mound Breakwaters II" (unpublished), Danish Hydraulic Institute and Technical University of Denmark.

Hales, L. Z. 1980 (Mar). "Erosion Control of Scour During Construction; Present Design and Construction Practice," Technical Report HL-80-3, Report 1, U. S. Army Engineer Waterways Experiment Station, CE, Vicksburg, Miss.

Hannoura, A. A., and McCorquodale, J. A. 1979 (Sep). "Environmental Wave Forces on Rubble-Mound Breakwaters," Proceedings, Civil Engineering in the Oceans IV, San Francisco, Calif., Vol 1, pp 367-379.

Hudson, R. Y. 1957 (Jun). "Laboratory Investigation of Rubble-Mound Breakwaters," Proceedings, American Society of Civil Engineers.

_____. 1958 (Jul). "Design of Quarry-Stone Cover Layers for Rubble-Mound Breakwaters," Research Report No. 2-2, U. S. Army Engineer Waterways Experiment Station, CE, Vicksburg, Miss.

_____. 1961 (Sep). "Wave Forces on Rubble-Mound Breakwaters and Jetties," Miscellaneous Paper No. 2-453, U. S. Army Engineer Waterways Experiment Station, CE, Vicksburg, Miss.

Hudson, R. Y., ed. 1974 (Jan). "Concrete Armor Units for Protection Against Wave Attack; Report of Ad Hoc Committee on Artificial Armor Units for Coastal Structures," Miscellaneous Paper H-74-2, U. S. Army Engineer Waterways Experiment Station, CE, Vicksburg, Miss.

Hudson, R. Y. 1975 (Jun). "Reliability of Rubble-Mound Breakwater Stability Models," Miscellaneous Paper H-75-5, U. S. Army Engineer Waterways Experiment Station, CE, Vicksburg, Miss.

Hudson, R. Y., and Jackson, R. A. 1953 (Jun). "Stability of Rubble-Mound Breakwaters; Hydraulic Model Investigation," Technical Memorandum No. 2-365, U. S. Army Engineer Waterways Experiment Station, CE, Vicksburg, Miss.

Hudson, R. Y., et al. 1979 (May). "Coastal Hydraulic Models," Special Report No. 5, U. S. Army Coastal Engineering Research Center, Fort Belvoir, Va.

Keulegan, G. H. 1973 (Feb). "Wave Transmission Through Rock Structures; Hydraulic Model Investigation," Research Report H-73-1, U. S. Army Engineer Waterways Experiment Station, CE, Vicksburg, Miss.

LeMéhauté, B. 1965 (Jun). "Wave Absorbers in Harbors," Contract Report No. 2-122, U. S. Army Engineer Waterways Experiment Station, CE, Vicksburg, Miss.

Naheer, E. 1977 (Jan). "Stability of Bottom Armoring Under the Attack of Solitary Waves," Report No. KH-R-34, California Institute of Technology, Pasadena, Calif.

_____. 1979. "Incipient Motion of Arbitrary Shape Particles Under Solitary Waves," Coastal Engineering, Vol 2, pp 277-296.

_____. 1980. "Incipient Motion of Discrete Spheres Under Solitary Waves," Coastal Engineering, Vol 3, pp 297-315.

Office, Chief of Engineers. 1963 (Apr). "Design of Breakwaters and Jetties," Washington, D. C.

Quinn, A. F. 1961. Design and Construction of Ports and Marine Structures, McGraw-Hill, New York.

Sollitt, C. K., and DeBok, D. H. 1976 (Jul). "Large Scale Model Tests of Placed Stone Breakwaters," Proceedings, Fifteenth Coastal Engineering Conference, Honolulu, Hawaii, Vol III, pp 2572-2588.

Thompson, E. F., and Harris, D. L. 1972 (May). "A Wave Climatology for U. S. Coastal Waterways," Proceedings, Offshore Technology Conference, Dallas, Tex., pp 675-688.

U. S. Army Coastal Engineering Research Center. 1977. Shore Protection Manual, Fort Belvoir, Va.

Whillock, A. F., and Price, W. A. 1976 (Jul). "Armour Blocks as Slope Protection," Proceedings, Fifteenth Coastal Engineering Conference, Honolulu, Hawaii, Vol III, pp 2564-2571.

APPENDIX A: TEST CONDITIONS

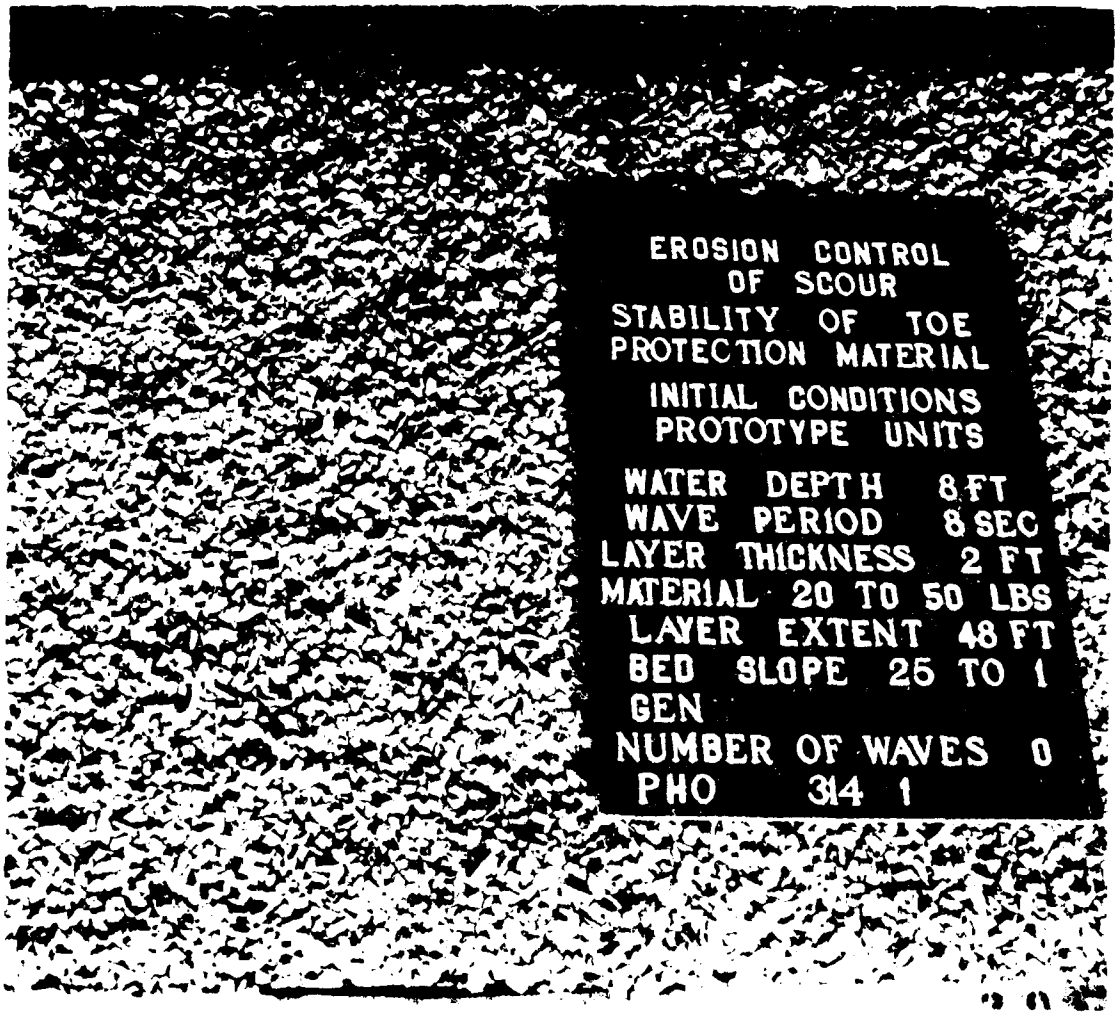

Photo A1. Material 20 to 50 lb prototype (WUL = 35 lb prototype); initial layer extent, 3.0 ft model = 48 ft prototype; number of waves 0; bed slope 1V on 25H; layer thickness 2 ft prototype

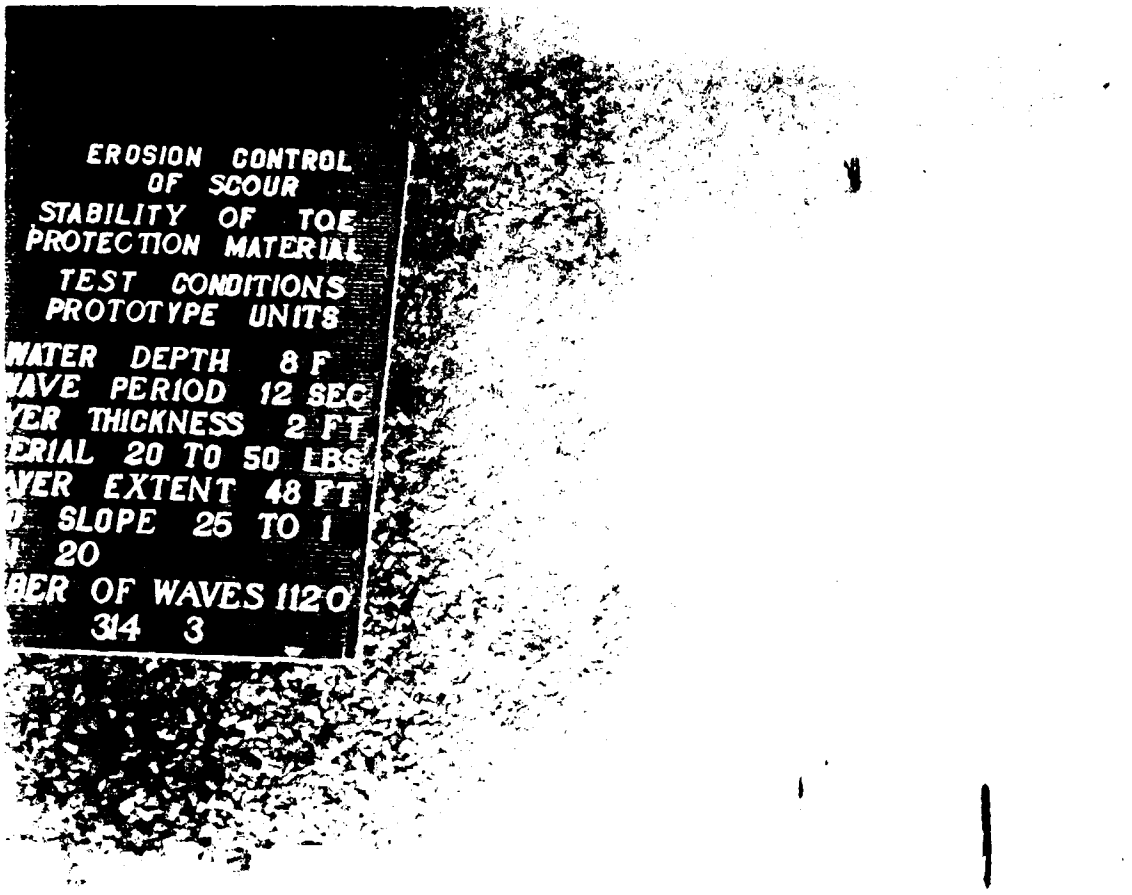

Photo A2. Material 20 to 50 lb prototype (W_{UL} = 35 lb prototype); initial layer extent, 3.0 ft model = 28 ft prototype; number of waves 1,120; bed slope 1V on 25H; layer thickness 2 ft prototype; water depth 8 ft prototype; wave period 12 sec prototype; maximum wave height 11.2 ft prototype

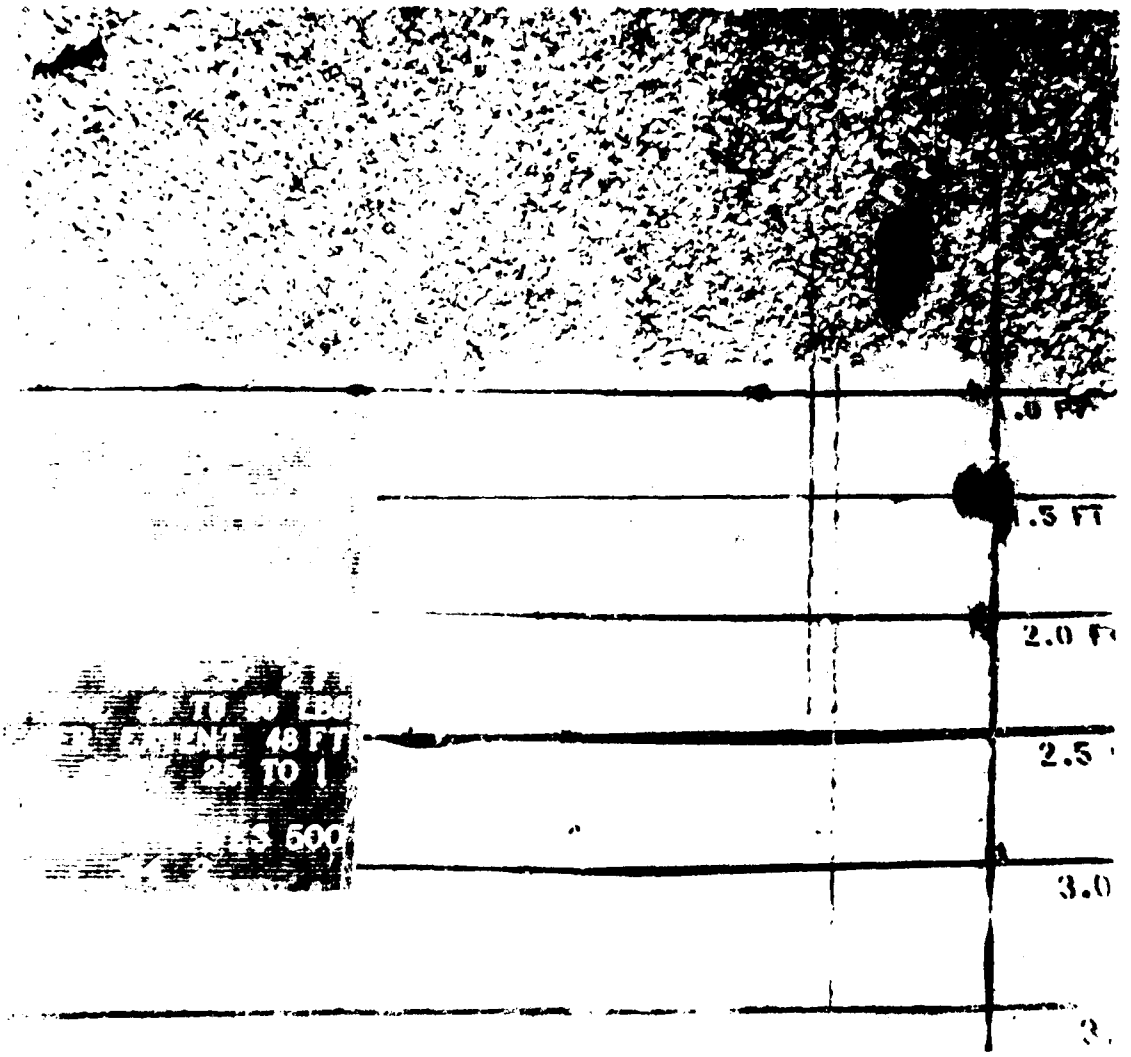

Photo A3. Material 20 to 50 lb prototype (W_{UL} = 35 lb prototype); initial layer extent, 3.0 ft model = 48 ft prototype; number of waves 500; bed slope 1V on 25H; layer thickness 2 ft prototype; water depth 8 ft prototype; wave period 16 sec prototype; maximum wave height 12.8 ft prototype

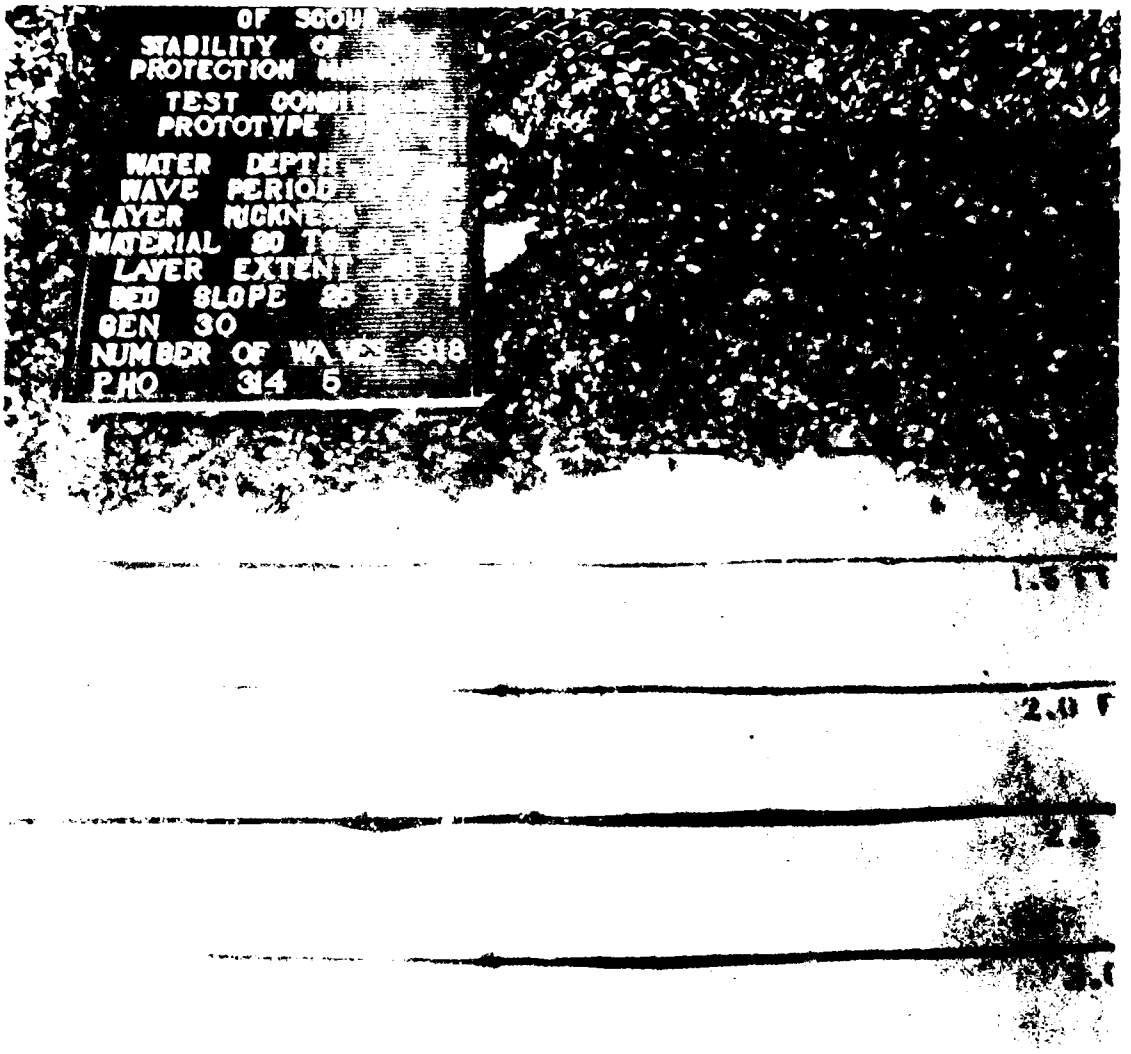

Photo A4. Material 20 to 50 lb prototype (W_{UL} = 35 lb prototype); initial layer extent, 3.0 ft model = 48 ft prototype; number of waves 318; bed slope 1V on 25H; layer thickness 2 ft prototype; water depth 8 ft prototype; wave period 20 sec prototype; maximum wave height 10.9 ft prototype

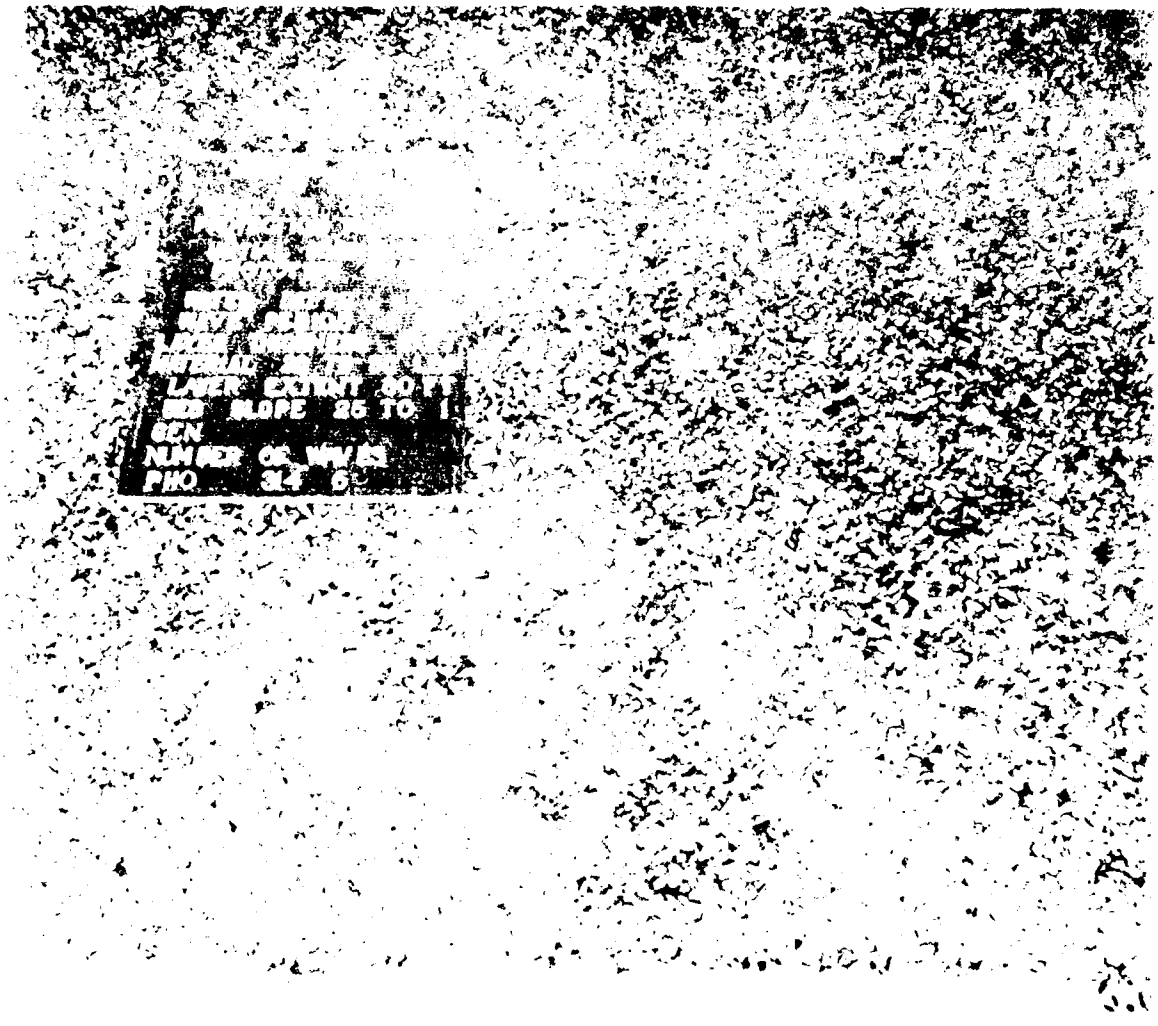

Photo A5. Material 20 to 50 lb prototype (W_{50} = 35 lb prototype); initial layer extent, 5.0 ft model = 80 ft prototype; number of waves 0; bed slope 1V on 25H; layer thickness 2 ft prototype

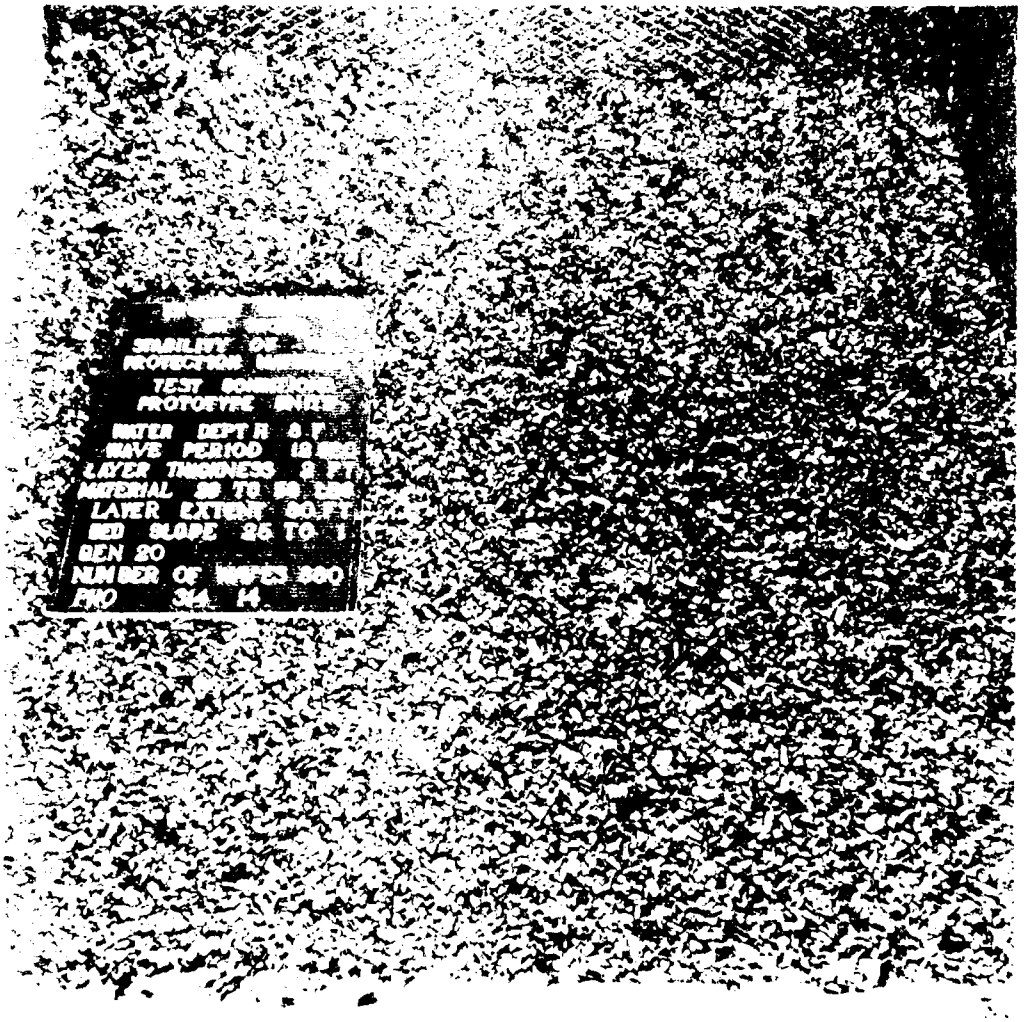

Photo A6. Material 20 to 50 lb prototype (WUL = 35 lb prototype); initial layer extent, 5.0 ft model = 80 ft prototype; number of waves 880; bed slope IV on 25H; layer thickness 2 ft prototype; water depth 8 ft prototype; wave period 12 sec prototype; maximum wave height 11.2 ft prototype

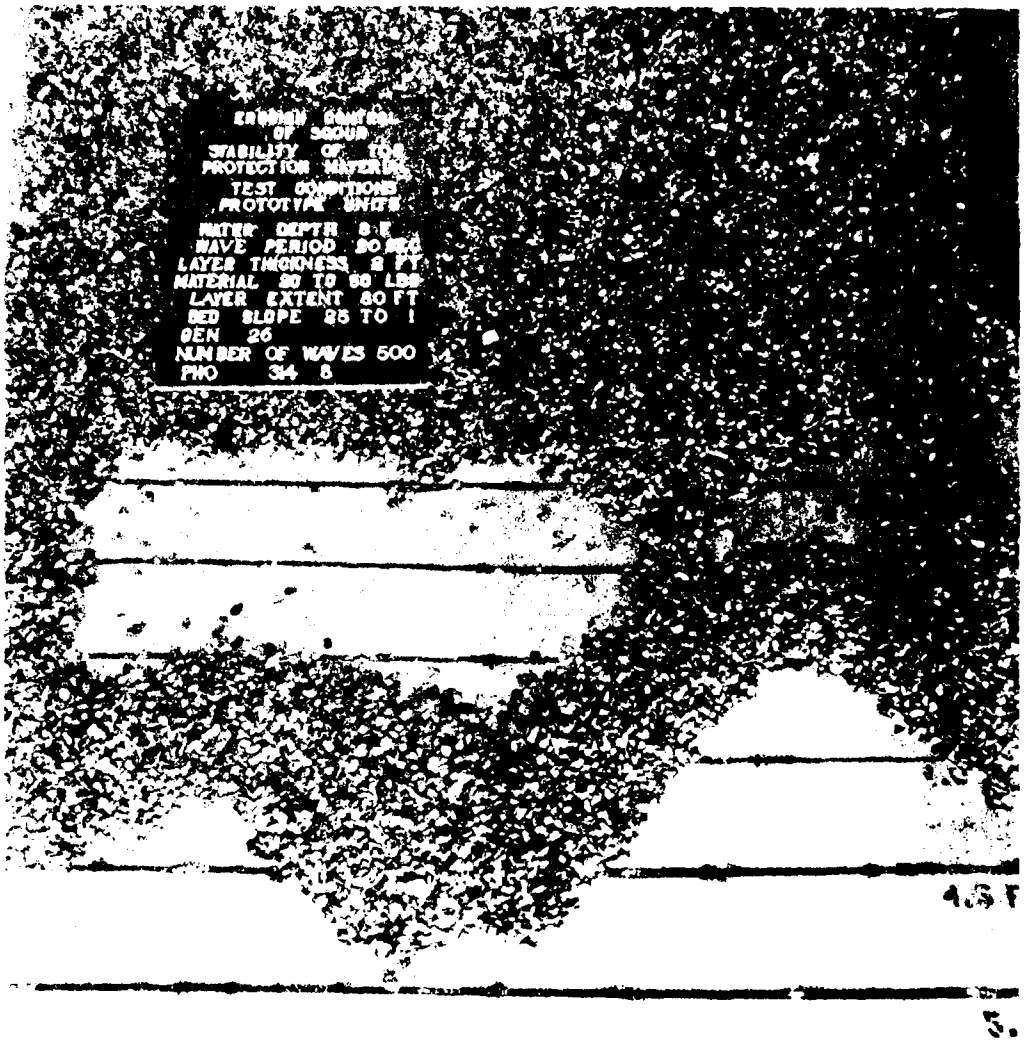

Photo A7. Material 20 to 50 lb prototype (W_{UL} = 35 lb prototype); initial layer extent, 5.0 ft model = 80 ft prototype; number of waves 500; bed slope 1V on 25H; layer thickness 2 ft prototype; water depth 8 ft prototype; wave period 16 sec prototype; maximum wave height 12.8 ft prototype

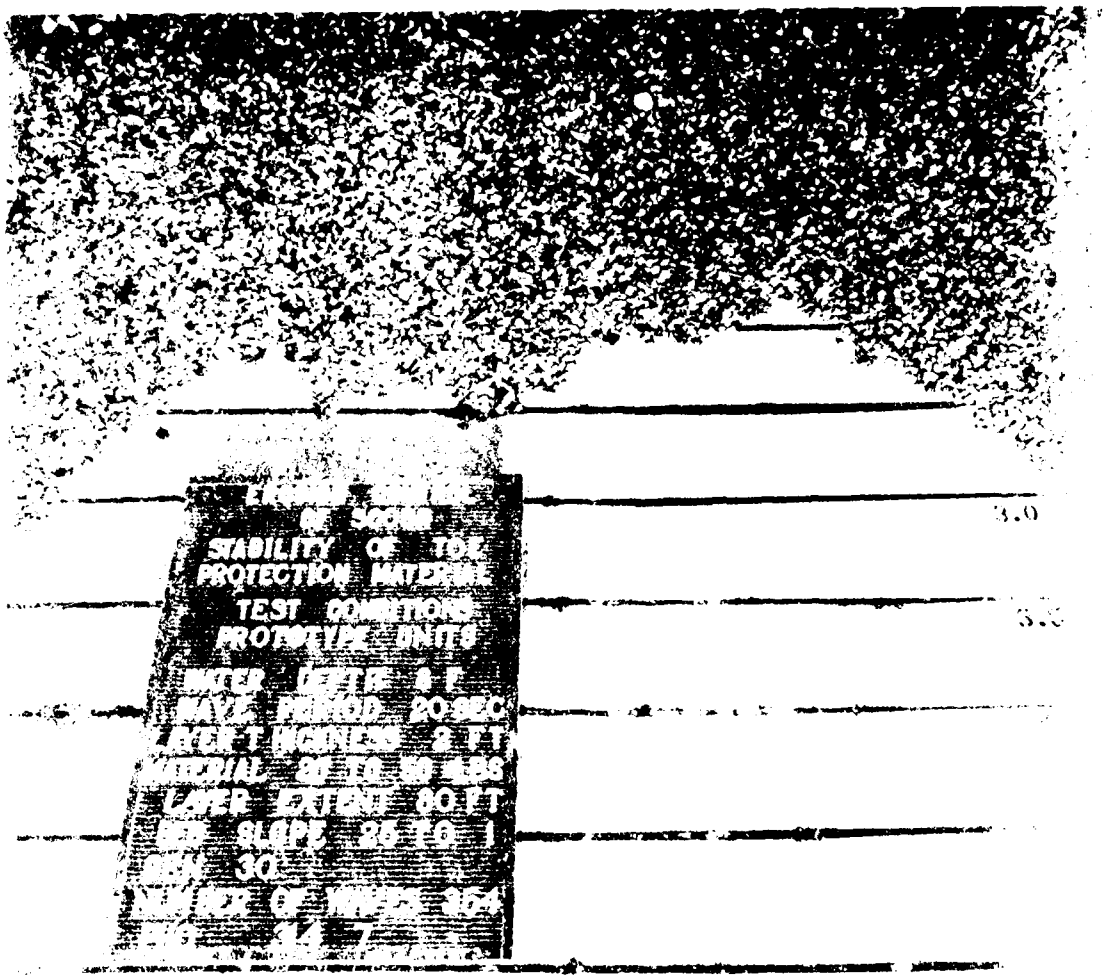

Photo A8. Material 20 to 50 lb prototype (W_{UL} = 35 lb prototype); initial layer extent, 5.0 ft model = 80 ft prototype; number of waves 354; bed slope 1V on 25H; layer thickness 2 ft prototype; water depth 8 ft prototype; wave period 20 sec prototype; maximum wave height 10.9 ft prototype

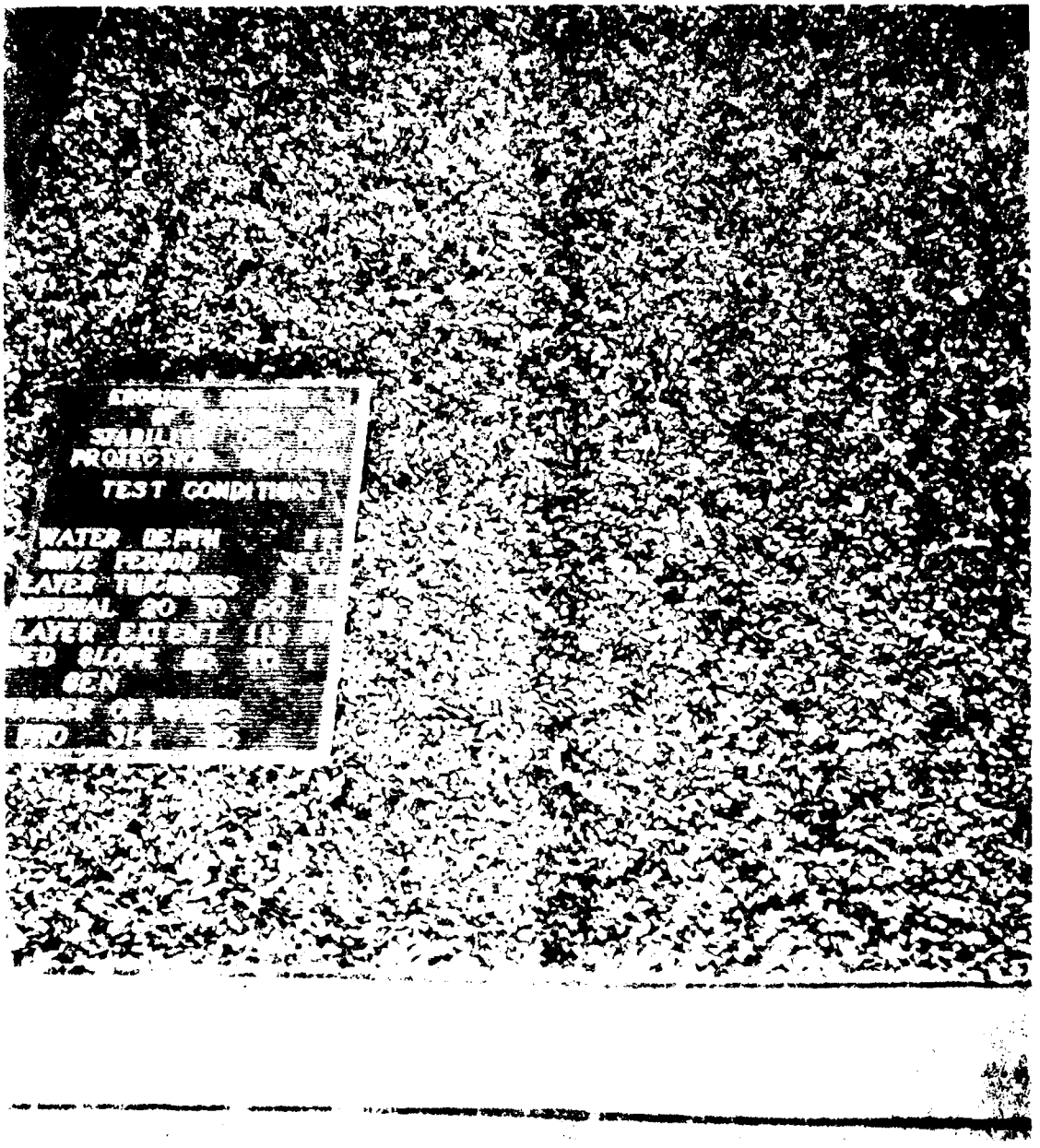

Photo A9. Material 20 to 50 lb prototype (WUL = 35 lb prototype); initial layer extent, 7.0 ft model = 112 ft prototype; number of waves 0; bed slope 1V on 25H; layer thickness 2 ft prototype

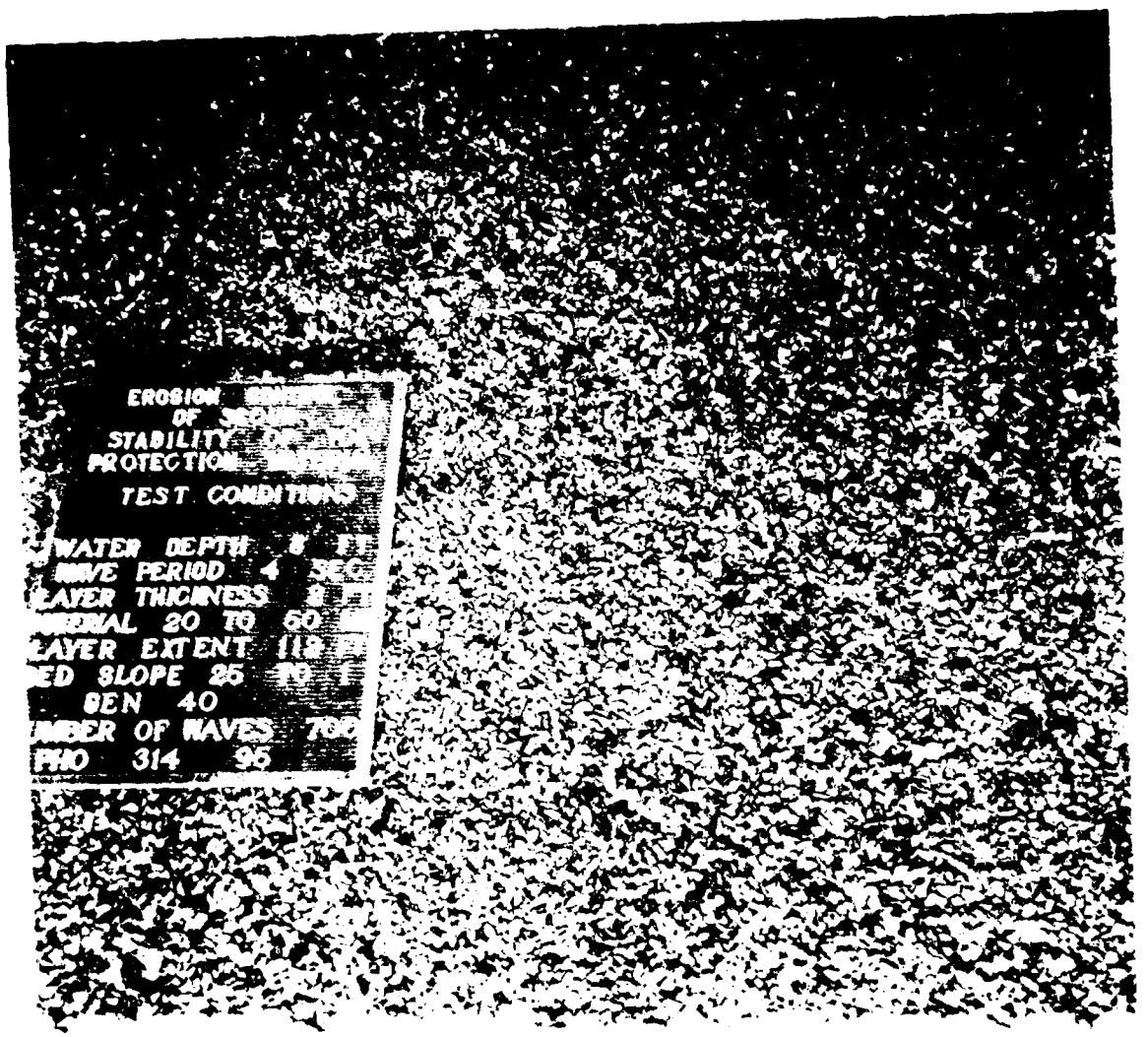

Photo A10. Material 20 to 50 lb prototype (WUL = 35 lb prototype); initial layer extent, 7.0 ft model = 112 ft prototype; number of waves 700; bed slope 1V on 25H; layer thickness 2 ft prototype; water depth 8 ft prototype; wave period 16 sec prototype; maximum wave height 12.8 ft prototype

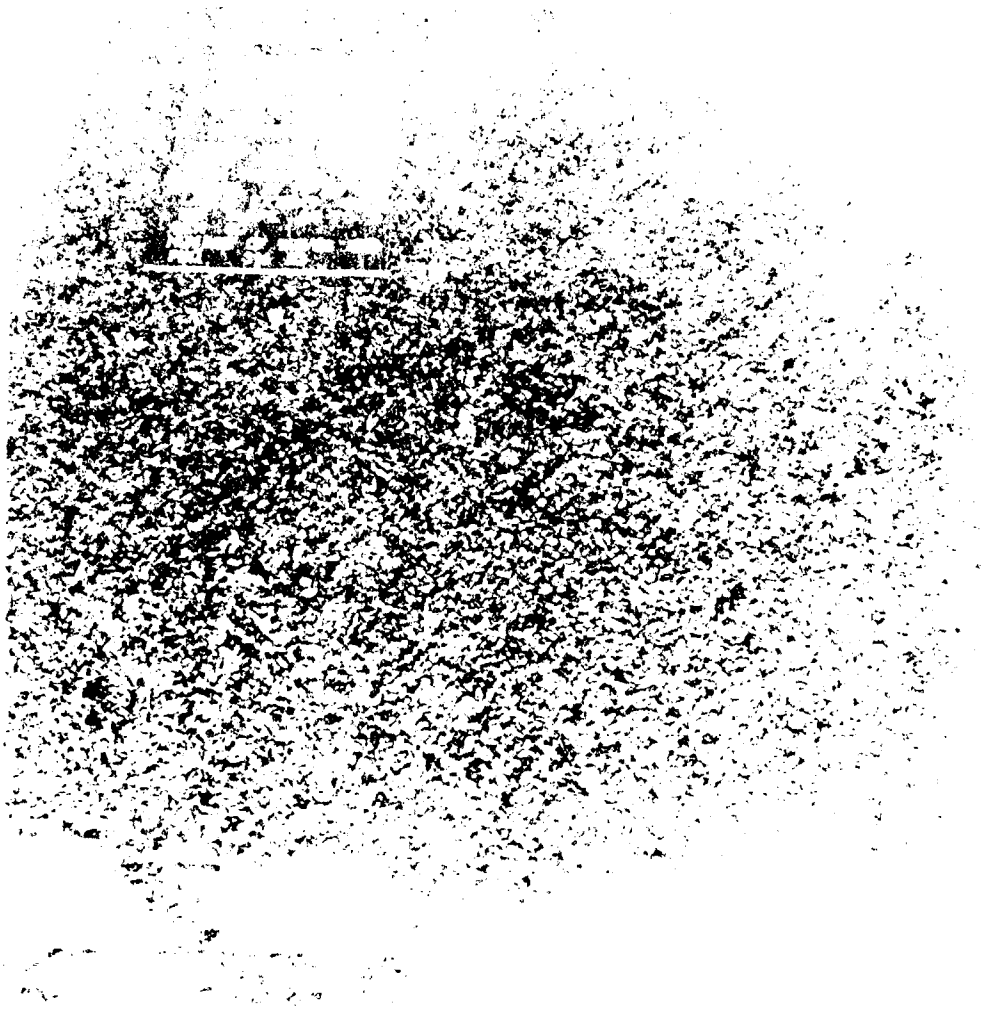

Photo A11. Material 20 to 50 lb prototype (W_{UL} = 35 lb prototype); initial layer extent, 7.0 ft model = 112 ft prototype; number of waves 500; bed slope 1V on 25H; layer thickness 2 ft prototype; water depth 8 ft prototype; wave period 20 sec prototype; maximum wave height 10.9 ft prototype

Photo A12. Material 20 to 50 lb prototype (W_{UL} = 35 lb prototype); initial layer extent, 3.0 ft model = 48 ft prototype; number of waves 1,026; bed slope IV on 25H; layer thickness 2 ft prototype; water depth 16 ft prototype; wave period 8 sec prototype; maximum wave height 17.4 ft prototype

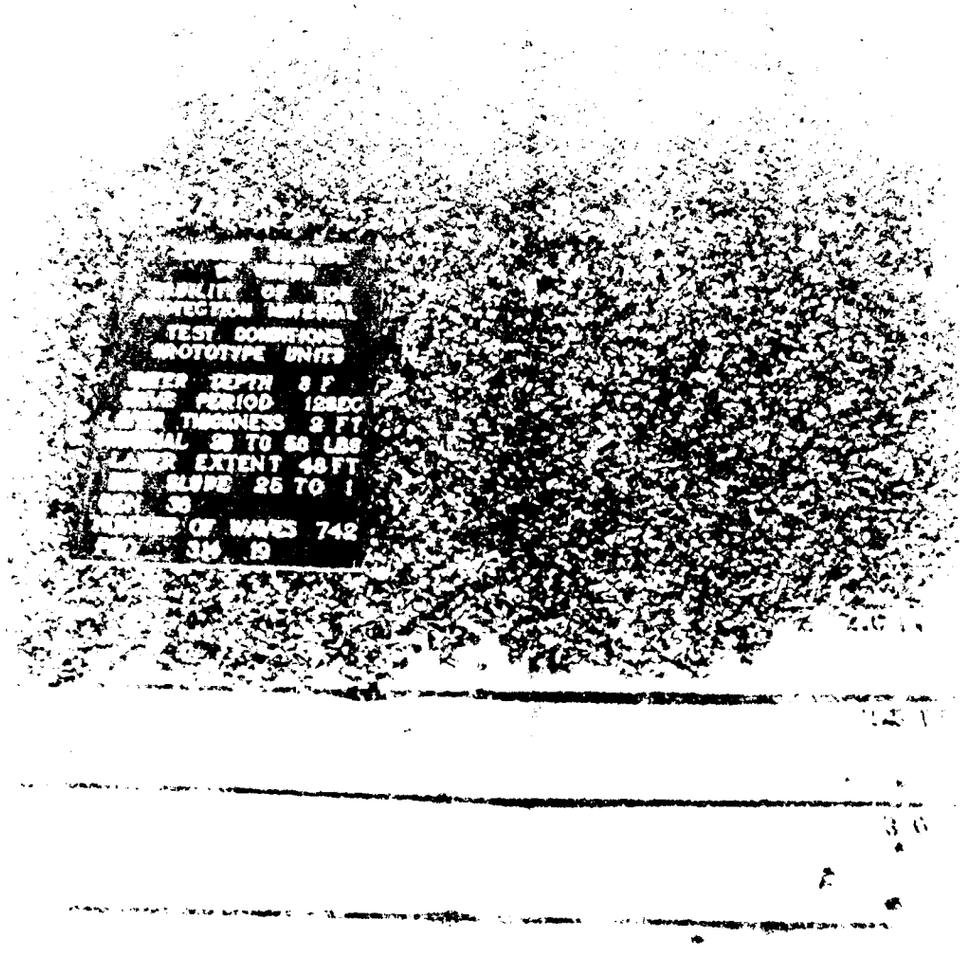

Photo A13. Material 20 to 50 lb prototype (W_{50} = 35 lb prototype); initial layer extent, 3.0 ft model = 48 ft prototype; number of waves 742; bed slope 1V on 25H; layer thickness 2 ft prototype; water depth 16 ft prototype; wave period 12 sec prototype; maximum wave height 17.8 ft prototype

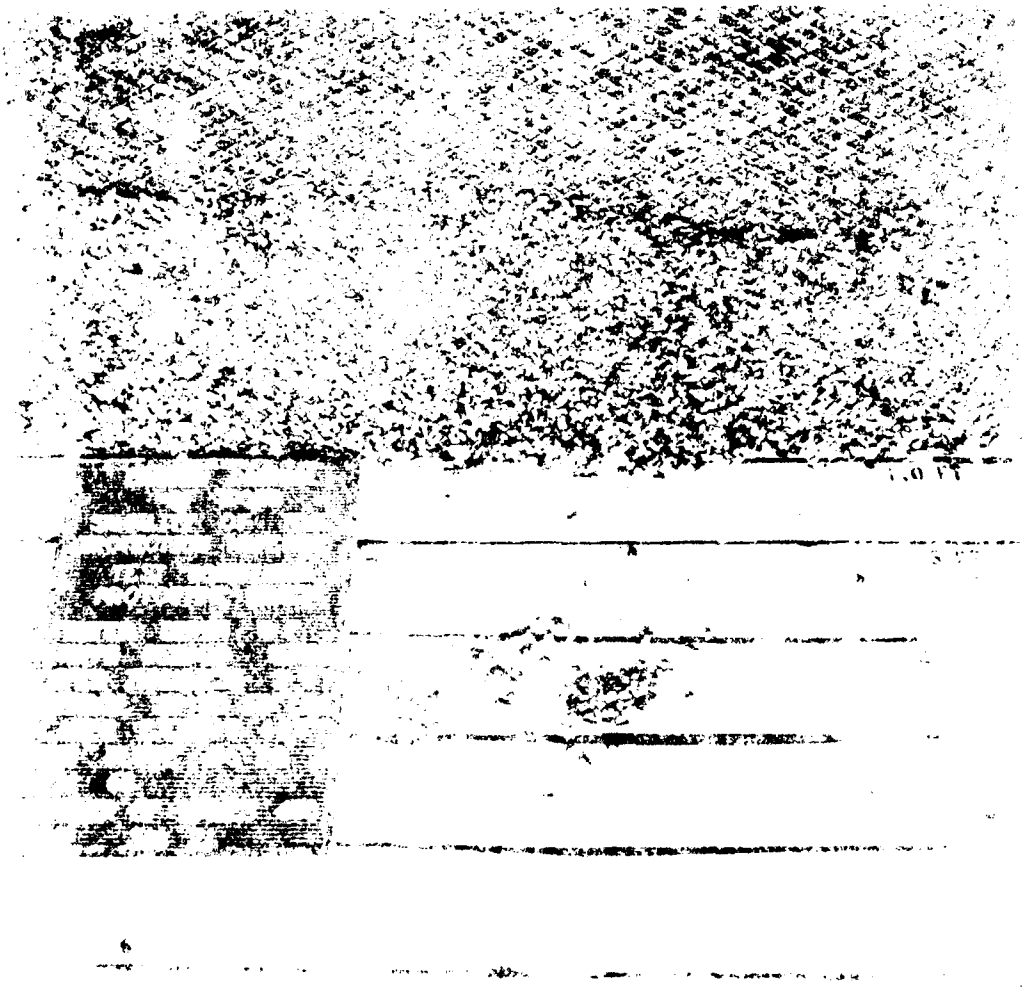

Photo A14. Material 20 to 50 lb prototype (W_{UL} = 35 lb prototype); initial layer extent, 3.0 ft model = 48 ft prototype; number of waves 488; bed slope 1V on 25H; layer thickness 2 ft prototype; water depth 16 ft prototype; wave period 16 sec prototype; maximum wave height 23.2 ft prototype

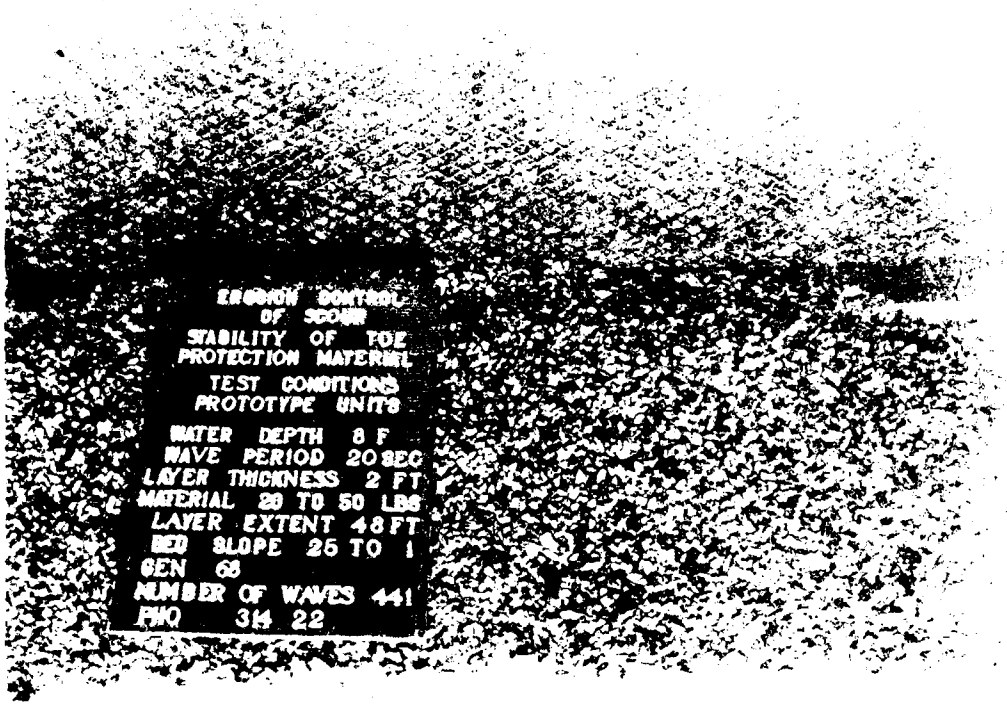

Photo A15. Material 20 to 50 lb prototype (W_{UL} = 35 lb prototype); initial layer extent, 3.0 ft model = 48 ft prototype; number of waves 441; bed slope 1V on 25H; layer thickness 2 ft prototype; water depth 16 ft prototype; wave period 20 sec prototype; maximum wave height 17.9 ft prototype

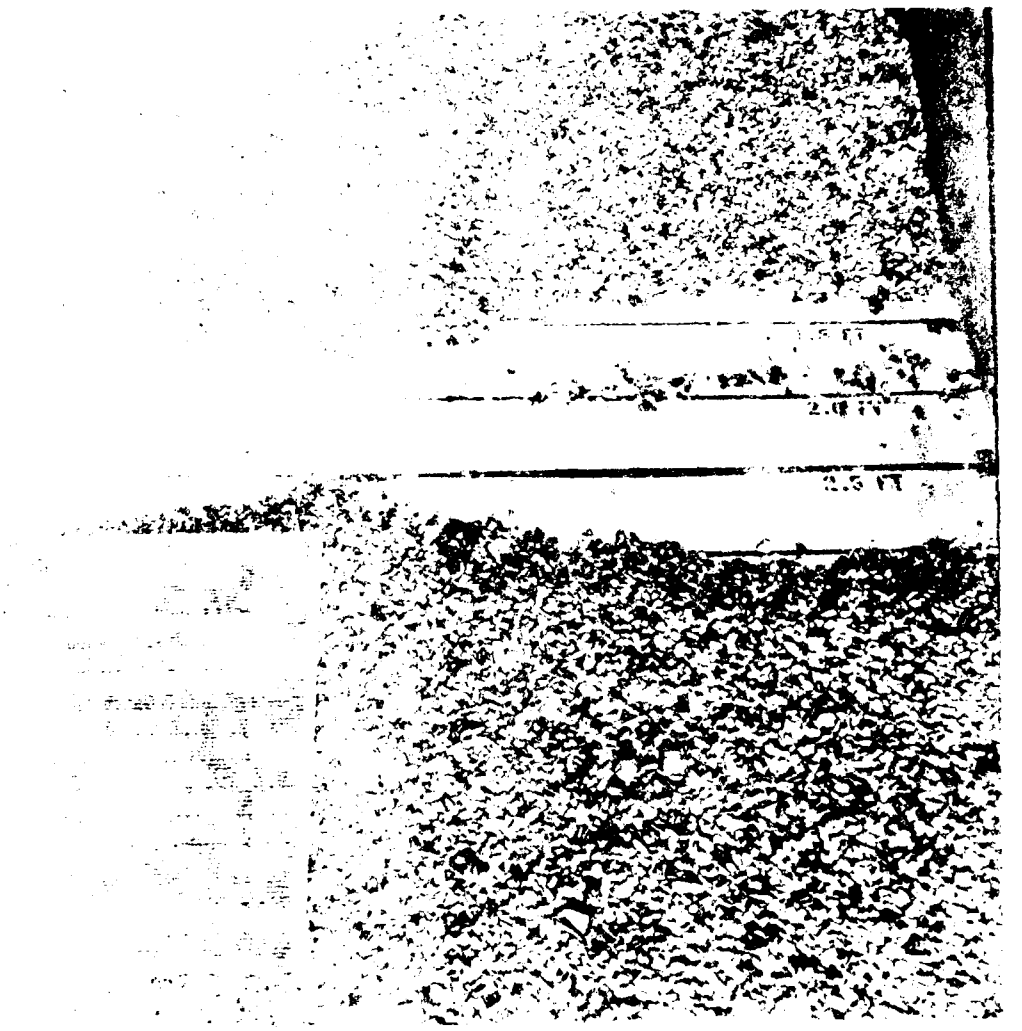

Photo A16. Material 20 to 50 lb prototype (W_{50} = 35 lb prototype); initial layer extent, 5.0 ft model = 50 ft prototype; number of waves 840; bed slope 1V on 25H; layer thickness 2 ft prototype; water depth 16 ft prototype; wave period 8 sec prototype; maximum wave height 17.4 prototype

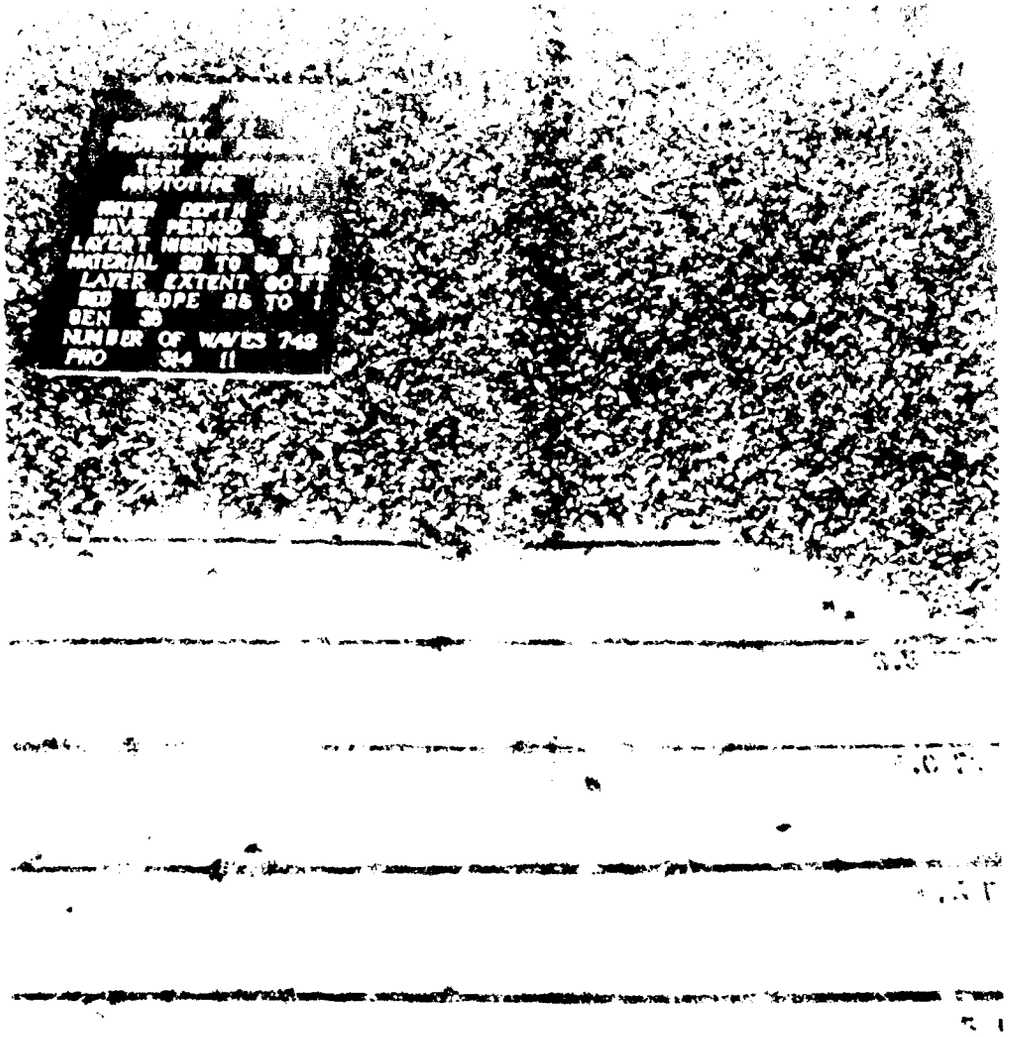

Photo A17. Material 20 to 50 lb prototype (W_{UL} = 35 lb prototype); initial layer extent, 4.0 ft model = 80 ft prototype; number of waves 742; bed slope 1V on 25H; layer thickness 2 ft prototype; water depth 16 ft prototype; wave period 12 sec prototype; maximum wave height 17.8 ft prototype

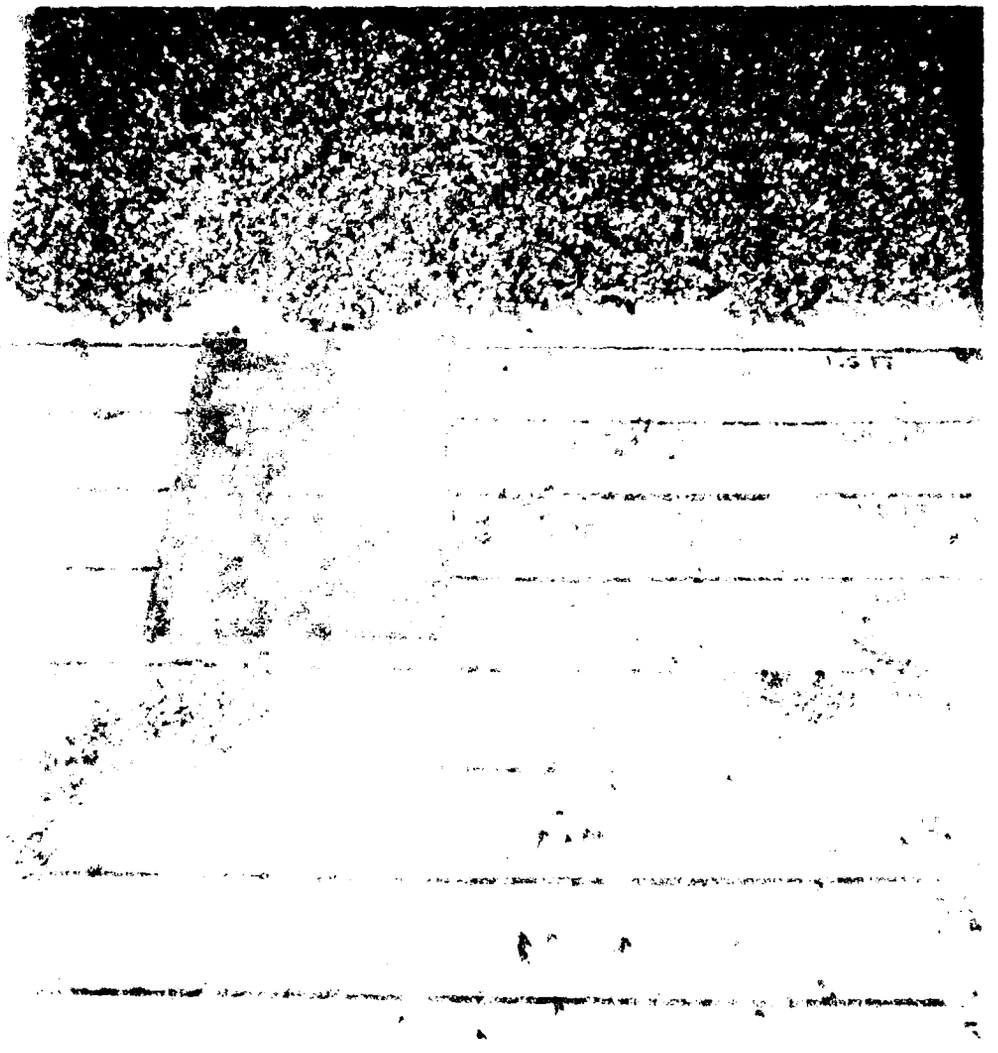

Photo A18. Material 20 to 50 lb prototype (W_{50} = 35 lb prototype); initial layer extent, 5.0 ft model = 80 ft prototype; number of waves 315; bed slope 1V on 25H; layer thickness 2 ft prototype; water depth 16 ft prototype; wave period 16 sec prototype; maximum wave height 23.2 ft prototype

AD-A135 945 EROSION CONTROL OF SCOUR DURING CONSTRUCTION REPORT 4 STABILITY OF UNDERL..(U) ARMY ENGINEER WATERWAYS EXPERIMENT STATION VICKSBURG MS HYDRA.. 2/3

UNCLASSIFIED L Z HALES ET AL. JUN 83 WES/TR/HL-80-3-4 F/G 8/3 NL

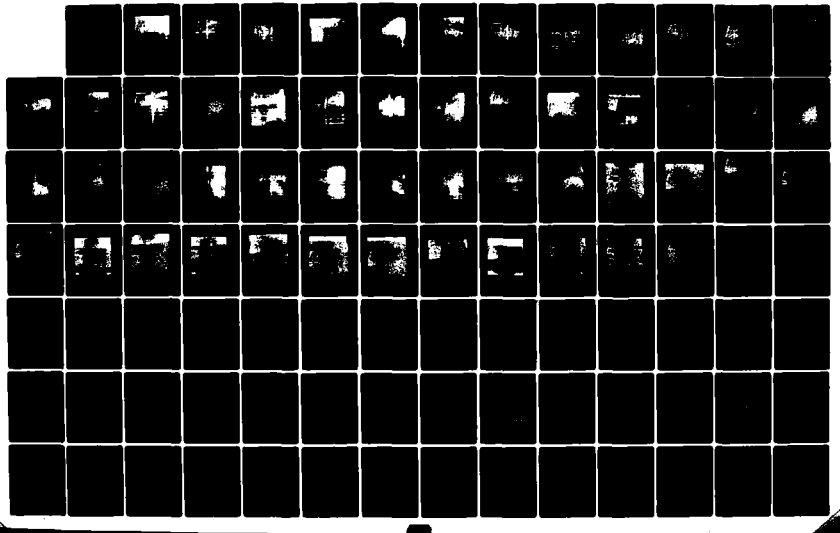

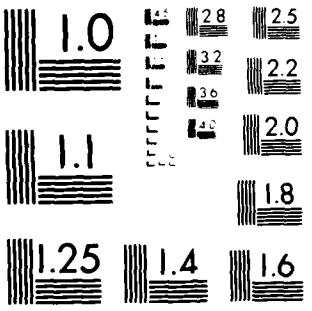

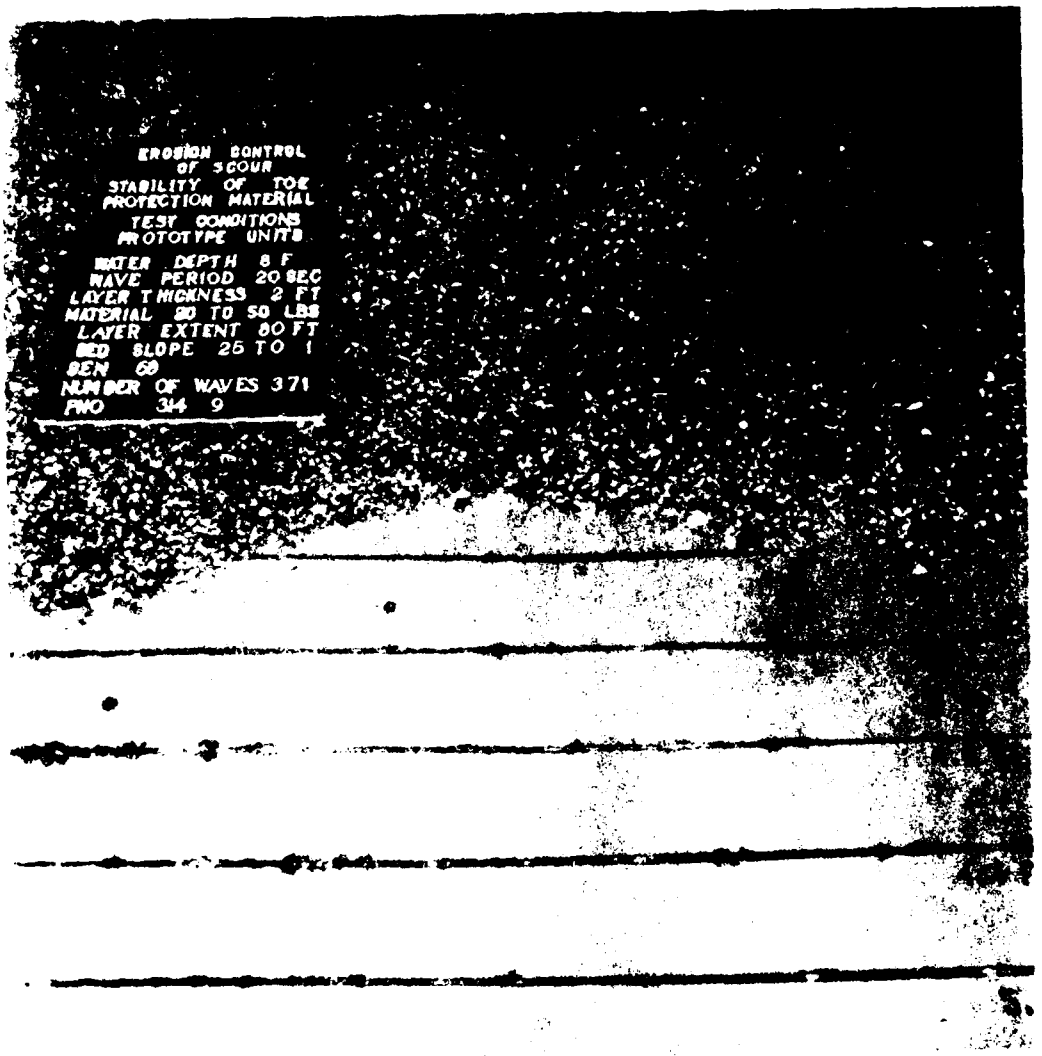

Photo A19. Material 20 to 50 lb prototype (W_{UL} = 35 lb prototype); initial layer extent, 5.0 ft model = 80 ft prototype; number of waves 371; bed slope 1V on 25H; layer thickness 2 ft prototype; water depth 16 ft prototype; wave period 20 sec prototype; maximum wave height 17.9 ft prototype

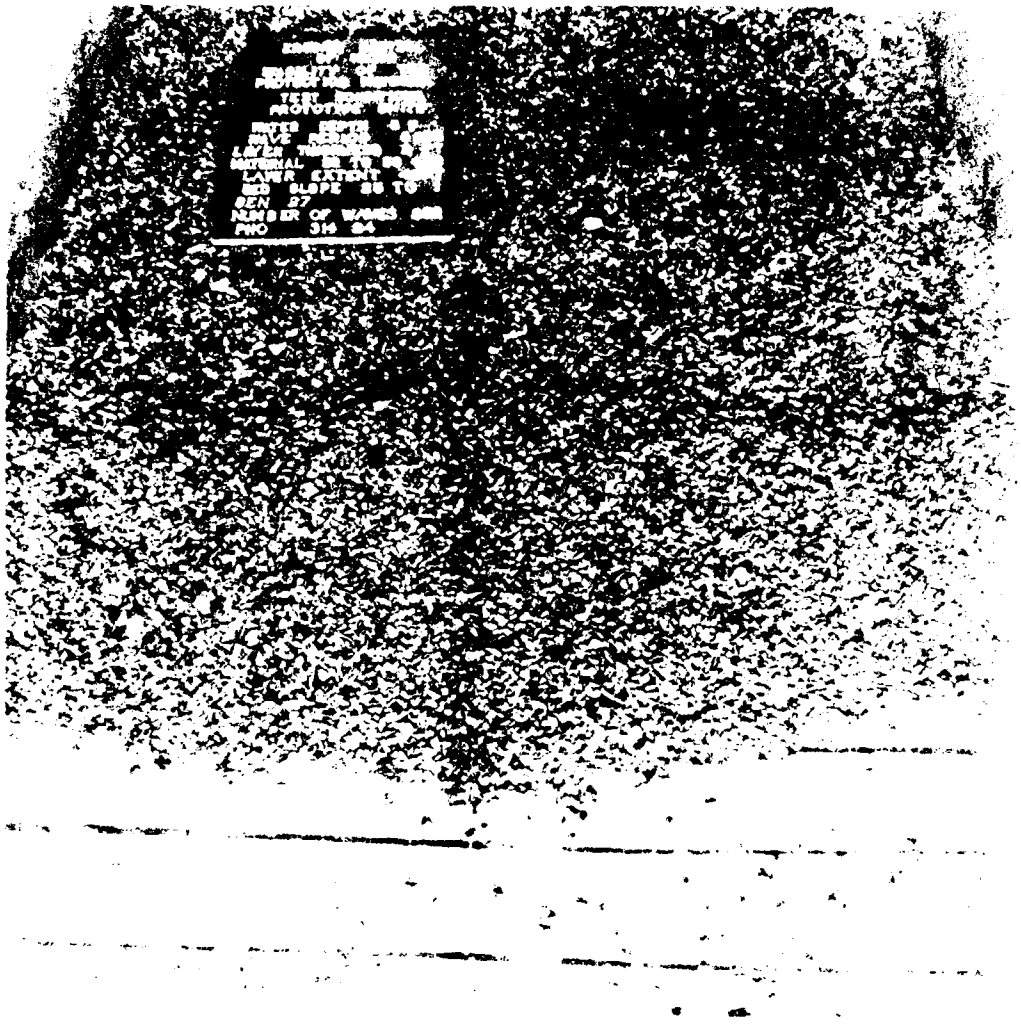

Photo A20. Material 20 to 50 lb prototype (WUL = 35 lb prototype); initial layer extent, 7.0 ft model = 112 ft prototype; number of waves 352; bed slope 1V on 25H; layer thickness 2 ft prototype; water depth 16 ft prototype; wave period 8 sec prototype; maximum wave height 17.4 ft prototype

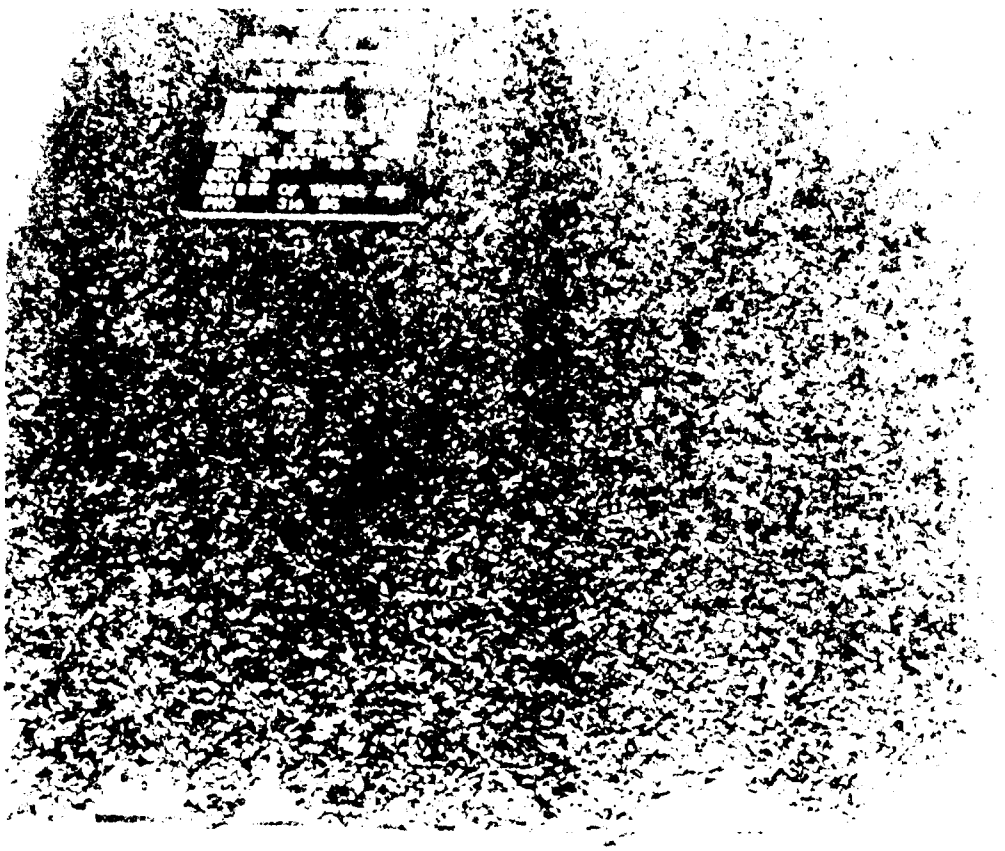

Photo A21. Material 20 to 50 lb prototype (WUL = 35 lb prototype); initial layer extent, 7.0 ft model = 112 ft prototype; number of waves 868; bed slope 1V on 25H; layer thickness 2 ft prototype; water depth 16 ft prototype; wave period 12 sec prototype; maximum wave height 17.8 prototype

Photo A22. Material 20 to 50 lb prototype (WUL = 35 lb prototype); initial layer extent, 7.0 ft model = 112 ft prototype; number of waves 420; bed slope 1V on 25H; layer thickness 2 ft prototype; water depth 16 ft prototype; wave period 16 sec prototype; maximum wave height 23.2 ft prototype

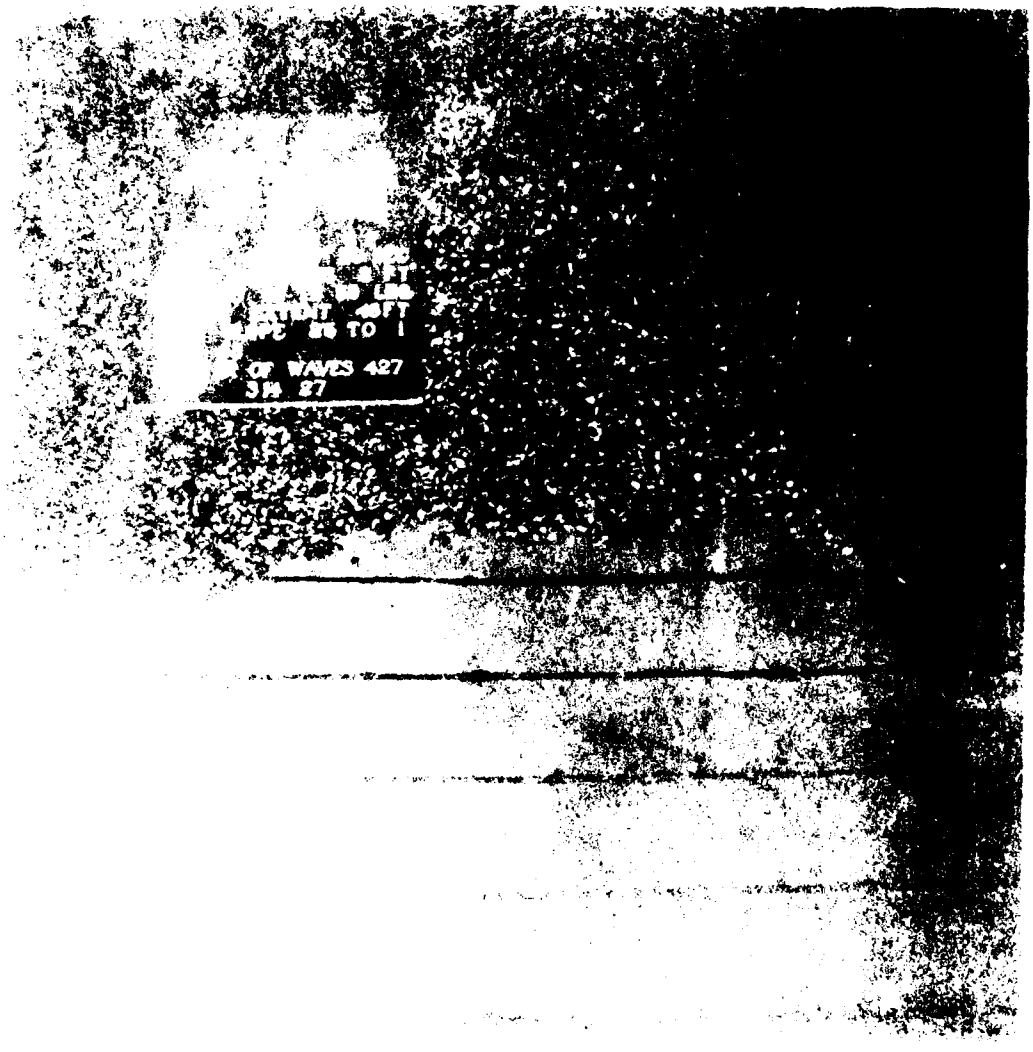

Photo A23. Material 20 to 50 lb prototype (WUL = 35 lb prototype); initial layer extent, 7.0 ft model = 112 ft prototype; number of waves 427; bed slope 1V on 25H; layer thickness 2 ft prototype; water depth 16 ft prototype; wave period 20 sec prototype; maximum wave height 17.9 ft prototype

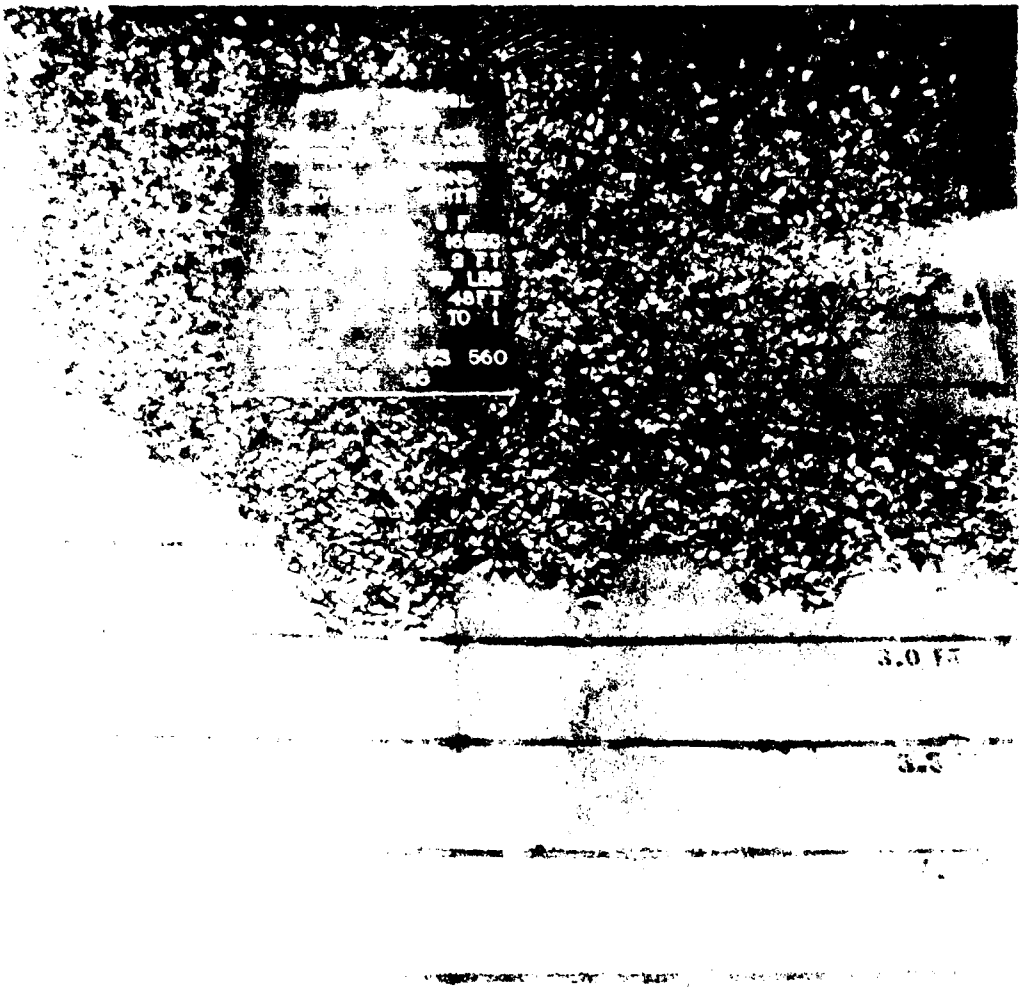

Photo A24. Material 50 to 95 lb prototype (WUL = 72 lb prototype); initial layer extent, 3.0 ft model = 48 ft prototype; number of waves 560; bed slope 1V on 25H; layer thickness 2 ft prototype; water depth 8 ft prototype; wave period 16 sec prototype; maximum wave height 12.8 ft prototype

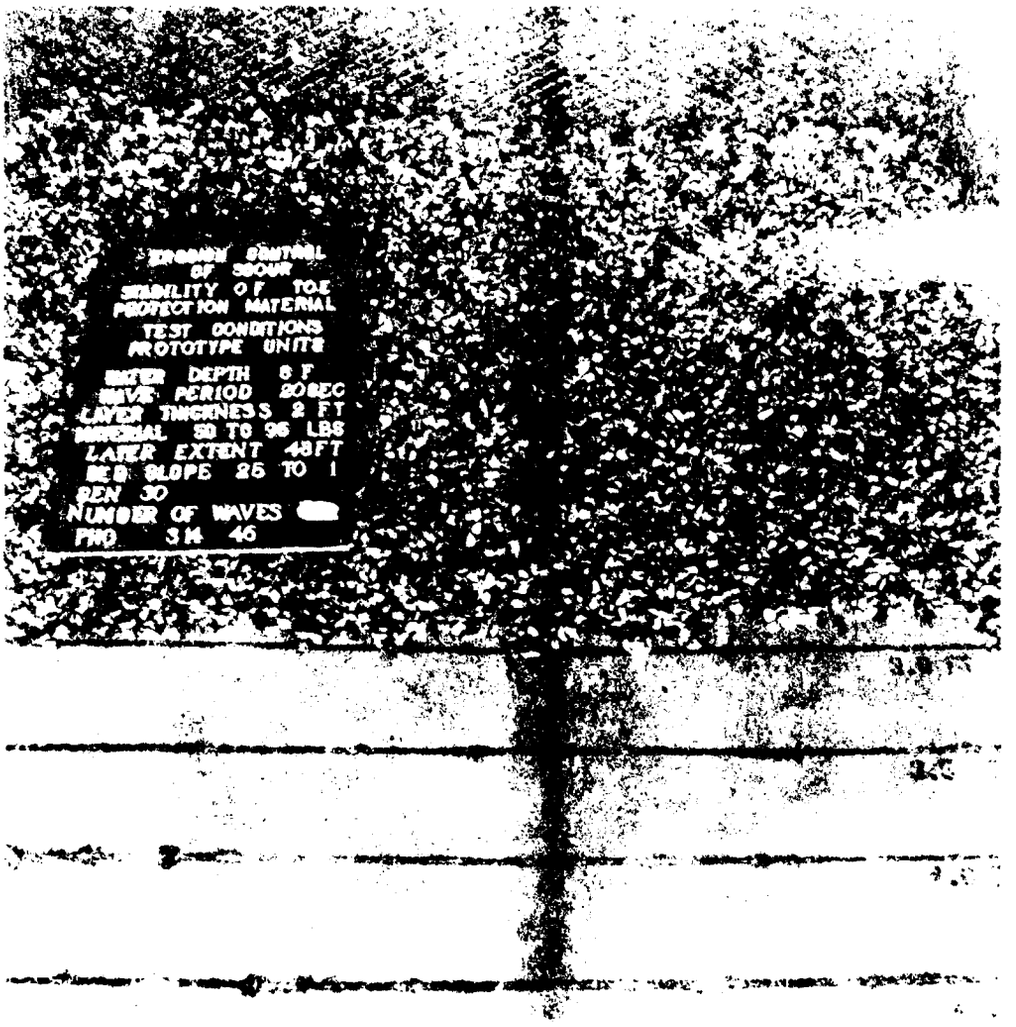

Photo A25. Material 50 to 95 lb prototype (WUL = 72 lb prototype); initial layer extent, 3.0 ft model = 48 ft prototype; number of waves 500; bed slope 1V on 25H; layer thickness 2 ft prototype; water depth 8 ft prototype; wave period 20 sec prototype; maximum wave height 10.9 ft prototype

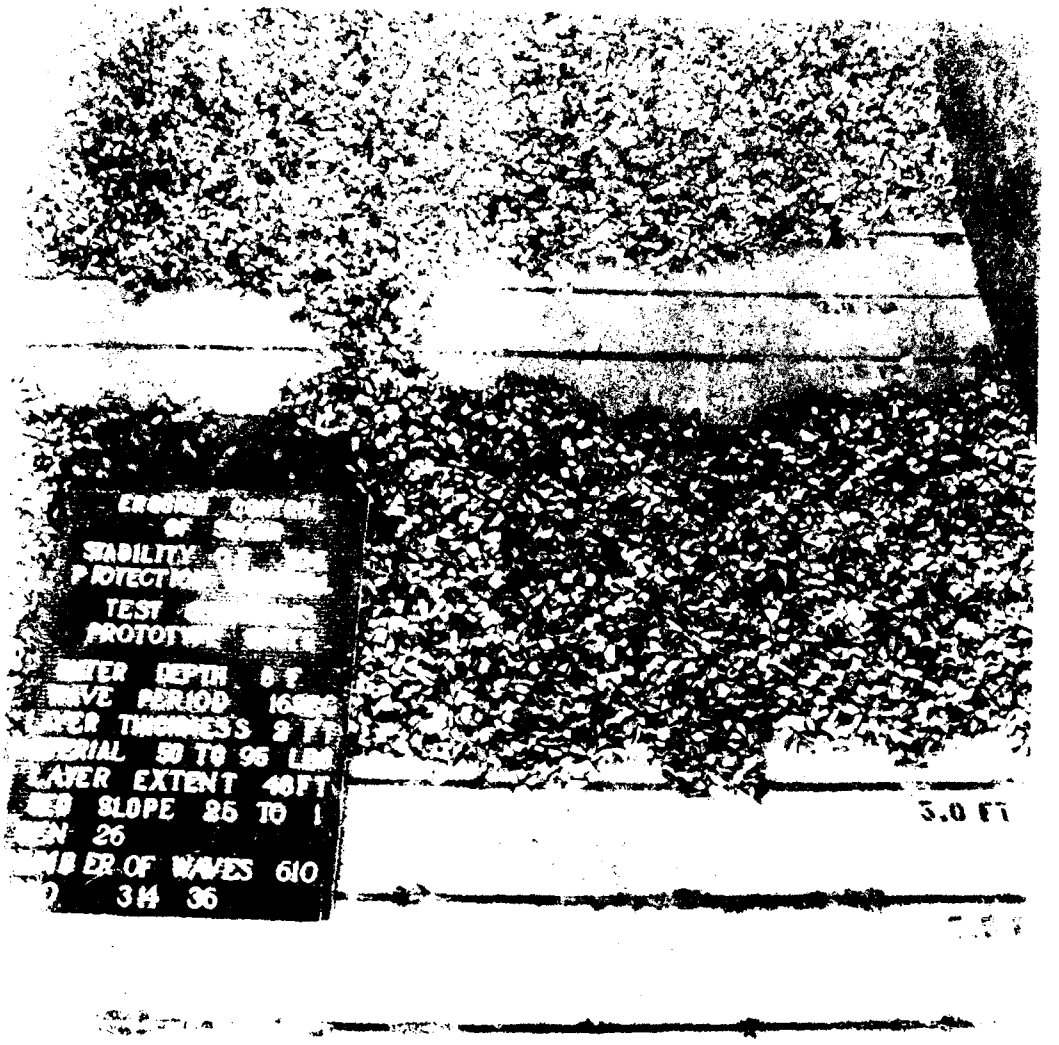

Photo A26. Material 50 to 95 lb prototype (WUL = 72 lb prototype); initial layer extent, 5.0 ft model = 80 ft prototype; number of waves 610; bed slope 1V on 25H; layer thickness 2 ft prototype; water depth 8 ft prototype; wave period 16 sec prototype; maximum wave height 12.8 ft prototype

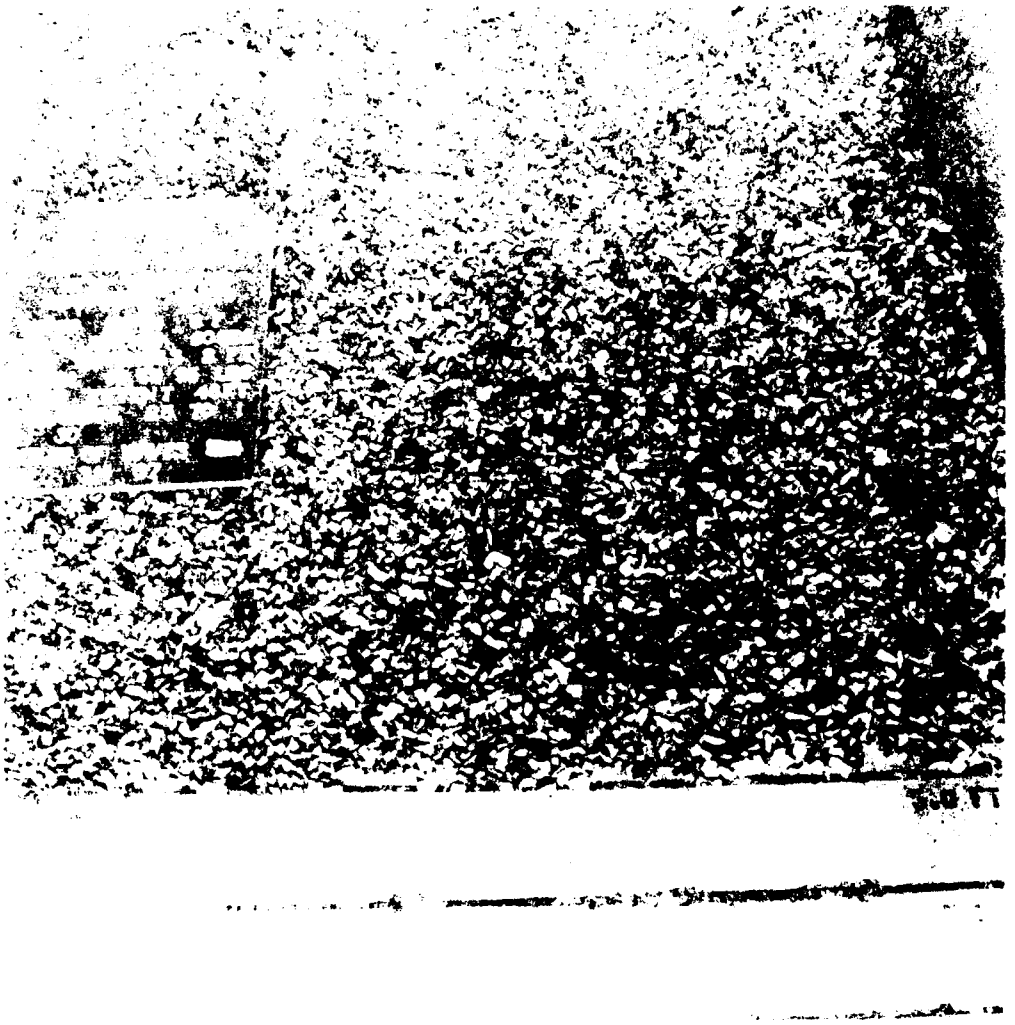

Photo A27. Material 50 to 95 lb prototype (WUL = 72 lb prototype); initial layer extent, 5.0 ft model = 80 ft prototype; number of waves 500; bed slope 1V on 25H; layer thickness 2 ft prototype; water depth 8 ft prototype; wave period 20 sec prototype; maximum wave height 30.9 ft prototype

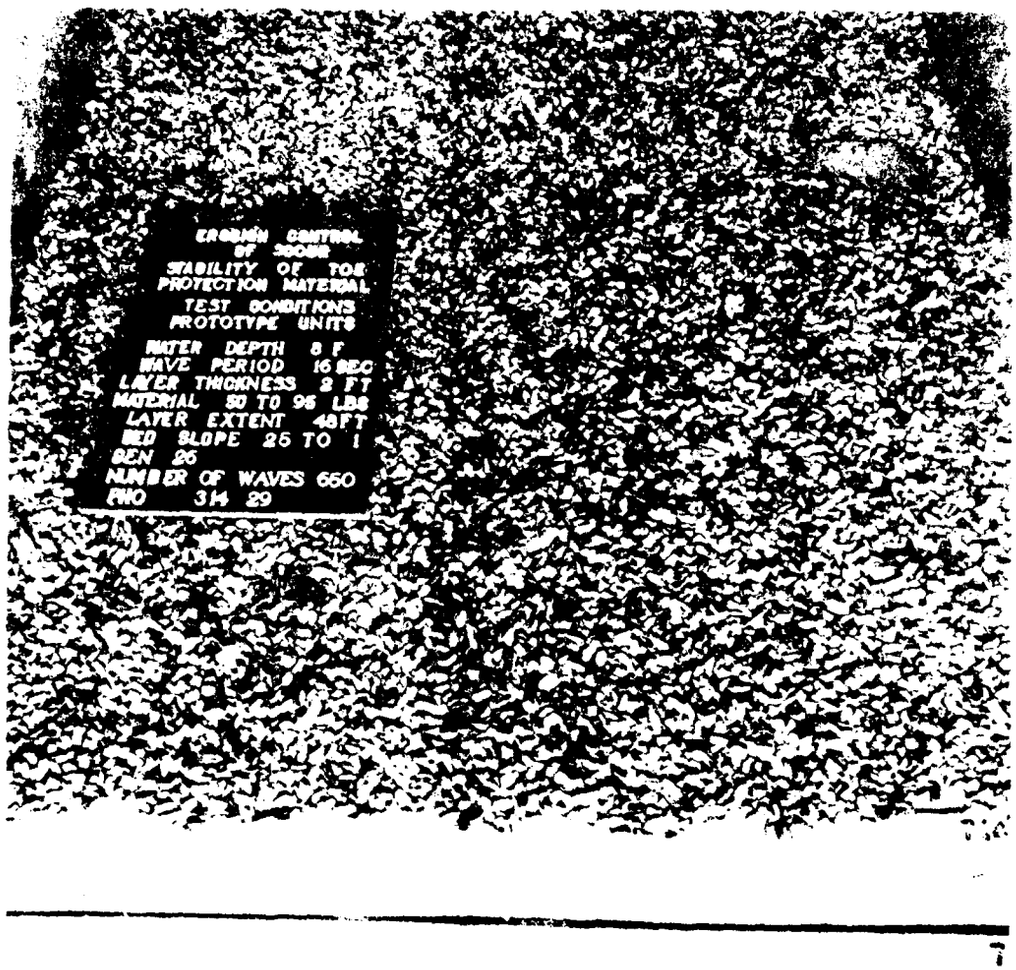

Photo A28. Material 50 to 95 lb prototype (WUL = 72 lb prototype); initial layer extent, 7.0 ft model = 112 ft prototype; number of waves 650; bed slope 1V on 25H; layer thickness 2 ft prototype; water depth 8 ft prototype; wave period 16 sec prototype; maximum wave height 12.8 ft prototype

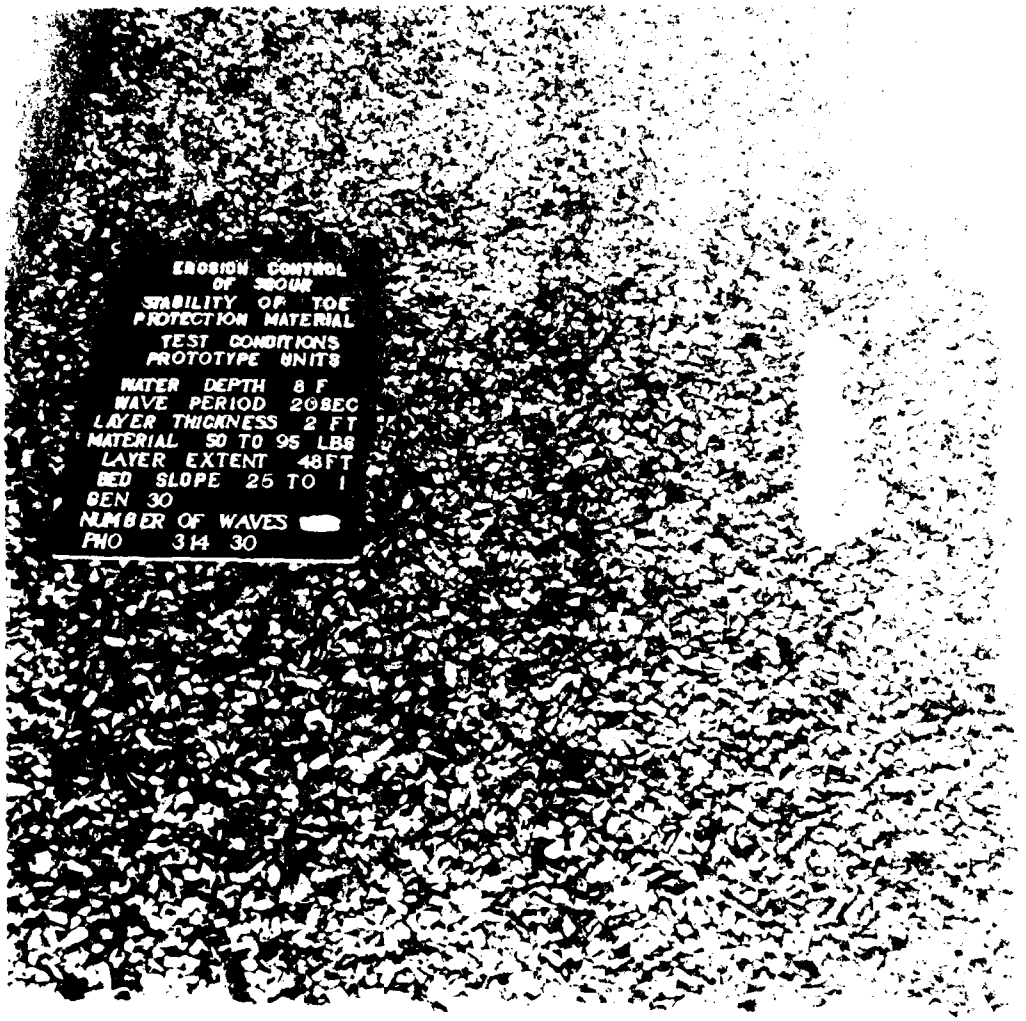

Photo A29. Material 50 to 95 lb prototype (WUL = 72 lb prototype); initial layer extent, 7.0 ft model = 112 ft prototype; number of waves 500; bed slope 1V on 25H; layer thickness 2 ft prototype; water depth 8 ft prototype; wave period 20 sec prototype; maximum wave height 10.9 ft prototype

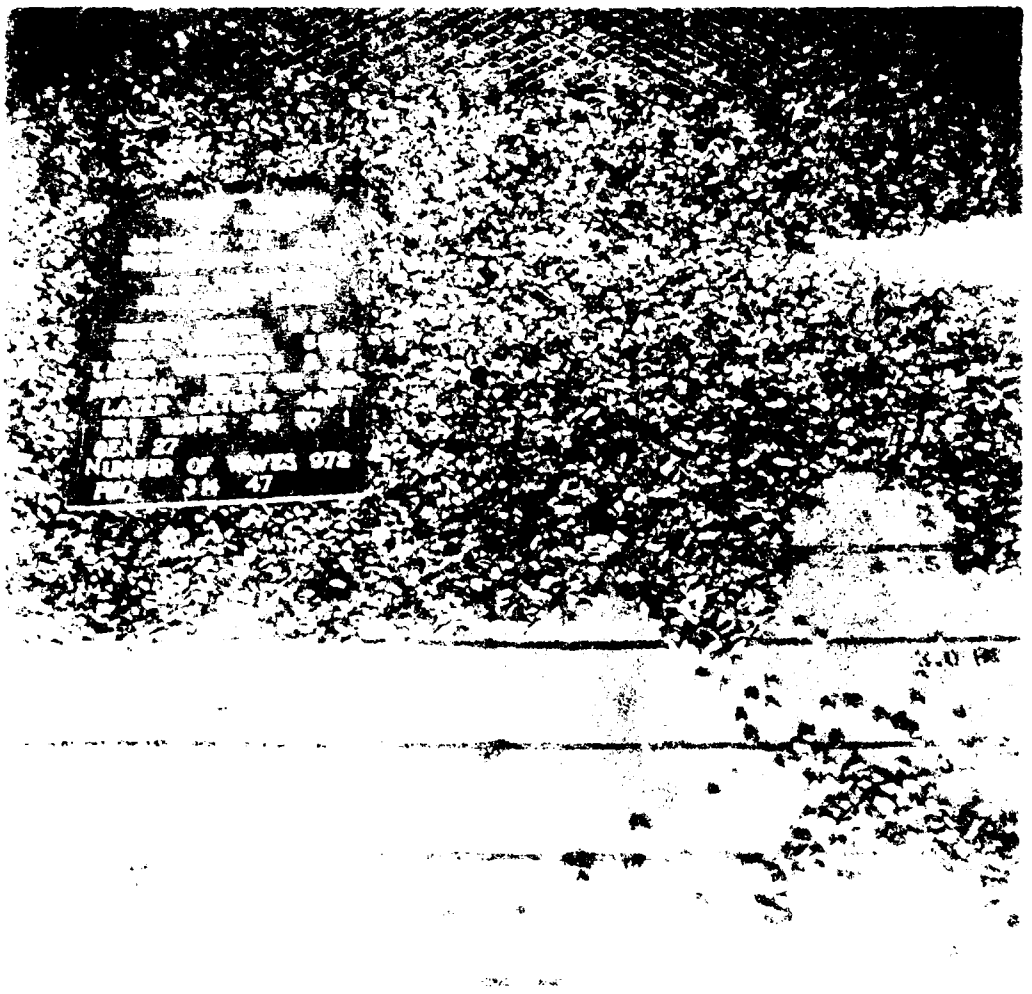

Photo A30. Material 50 to 95 lb prototype (WUL = 72 lb prototype); initial layer extent, 3.0 ft model = 48 ft prototype; number of waves 972; bed slope 1V on 25H; layer thickness 2 ft prototype; water depth 16 ft prototype; wave period 8 sec prototype; maximum wave height 17.4 ft prototype

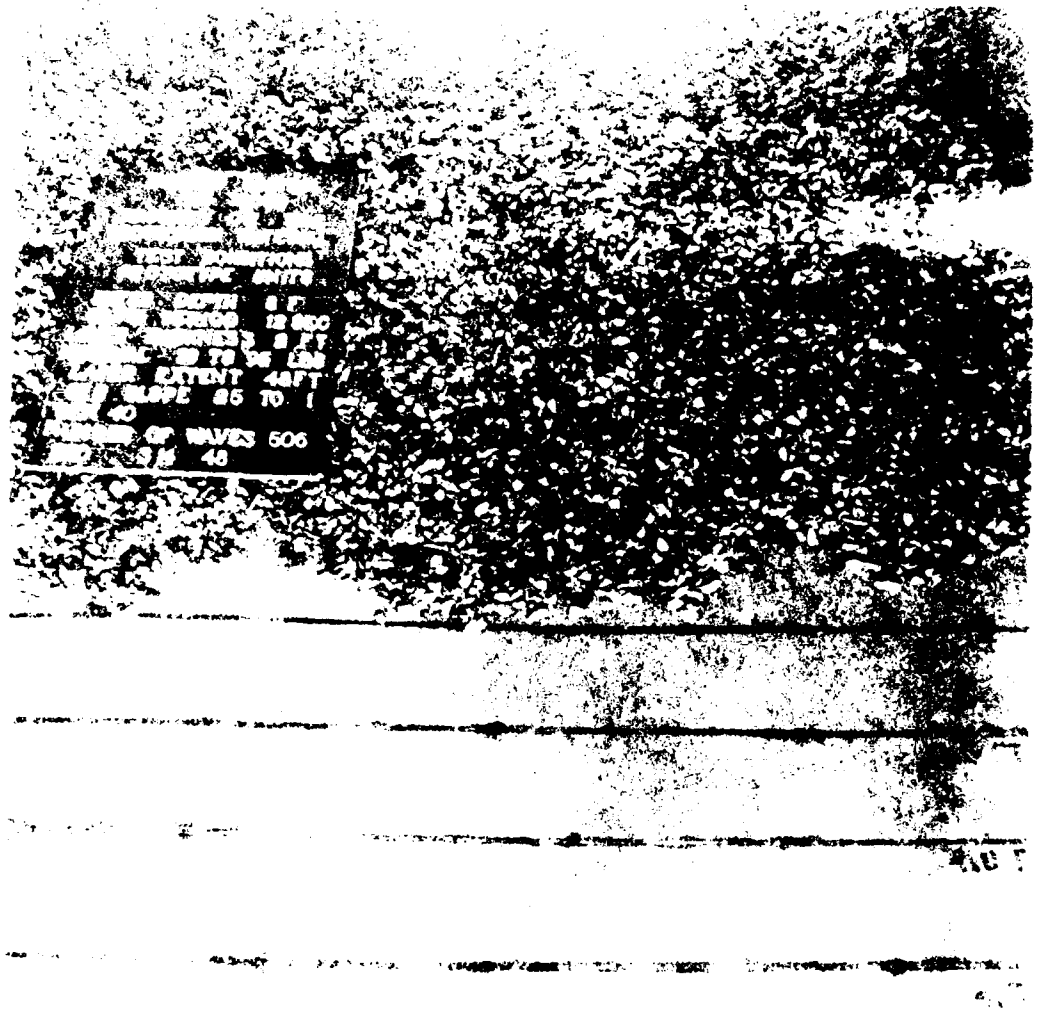

Photo A31. Material 50 to 95 lb prototype (WUL = 72 lb prototype); initial layer extent, 3.0 ft model = 48 ft prototype; number of waves 506; bed slope 1V on 25H; layer thickness 2 ft prototype; water depth 16 ft prototype; wave period 12 sec prototype; maximum wave height 17.8 ft prototype

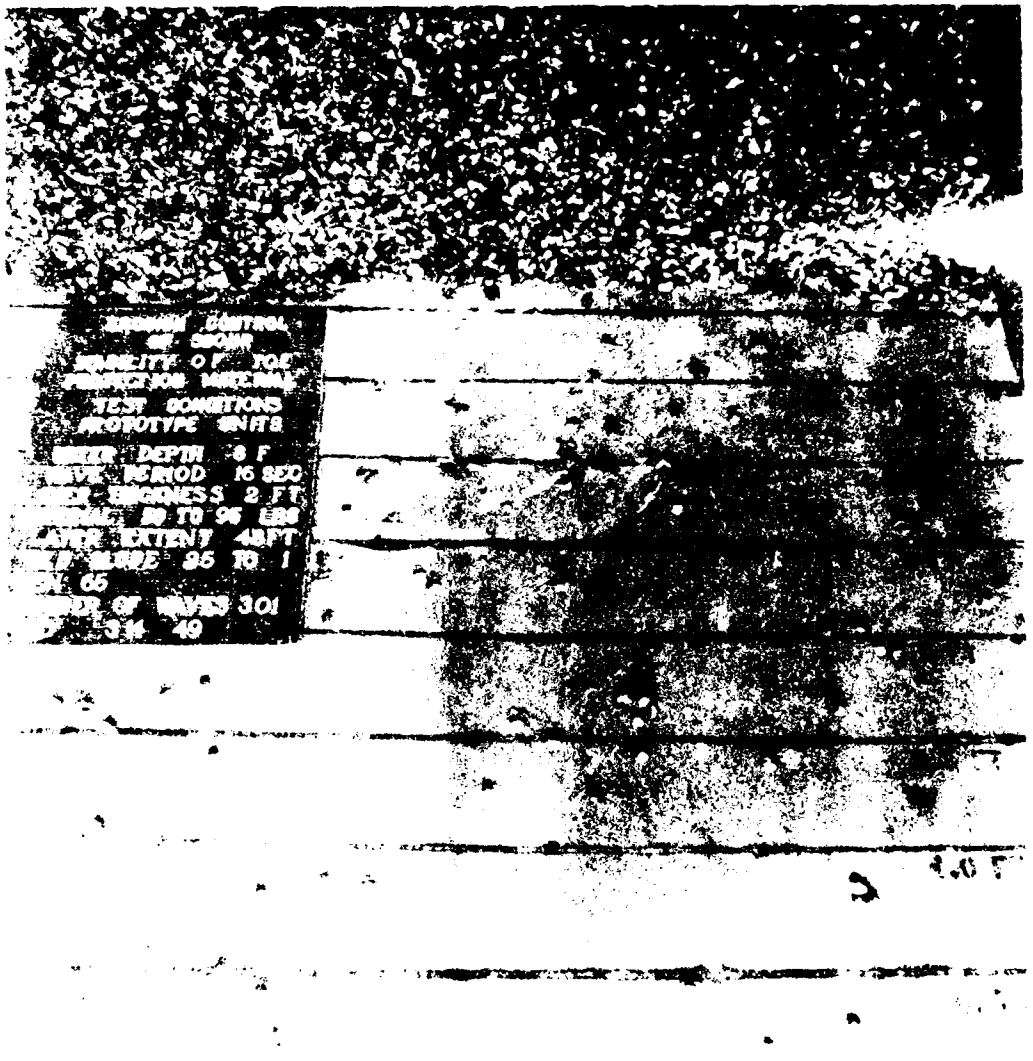

Photo A32. Material 50 to 95 lb prototype (WUL = 72 lb prototype); initial layer extent, 3.0 ft model = 48 ft prototype; number of waves 301; bed slope 1V on 25H; layer thickness 2 ft prototype; water depth 16 ft prototype; wave period 16 sec prototype; maximum wave height 23.2 ft prototype

Photo A33. Material 50 to 95 lb prototype (WUL = 72 lb prototype); initial layer extent, 3.0 ft model = 48 ft prototype; number of waves 455; bed slope 1V on 25H; layer thickness 2 ft prototype; water depth 16 ft prototype; wave period 20 sec prototype; maximum wave height 17.9 ft prototype

Photo A34. Material 50 to 95 lb prototype (WUL = 72 lb prototype); initial layer extent, 5.0 ft model = 80 ft prototype; number of waves 682; bed slope 1V on 25H; layer thickness 2 ft prototype; water depth 16 ft prototype; wave period 12 sec prototype maximum wave height 17.8 ft prototype

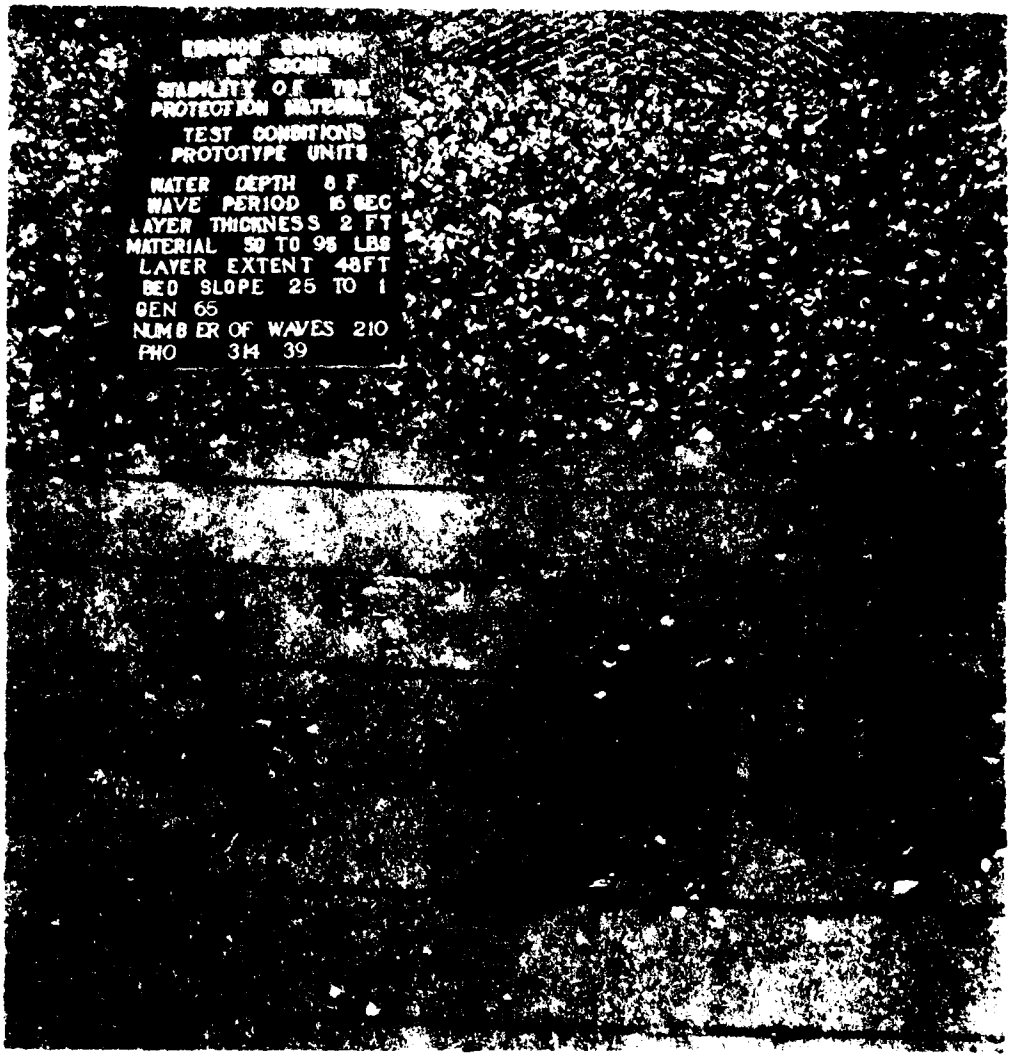

Photo A35. Material 50 to 95 lb prototype (WUL = 72 lb prototype); initial layer extent, 5.0 ft model = 80 ft prototype; number of waves 210; bed slope 1V on 25H; layer thickness 2 ft prototype; water depth 16 ft prototype; wave period 16 sec prototype; maximum wave height 23.2 ft prototype

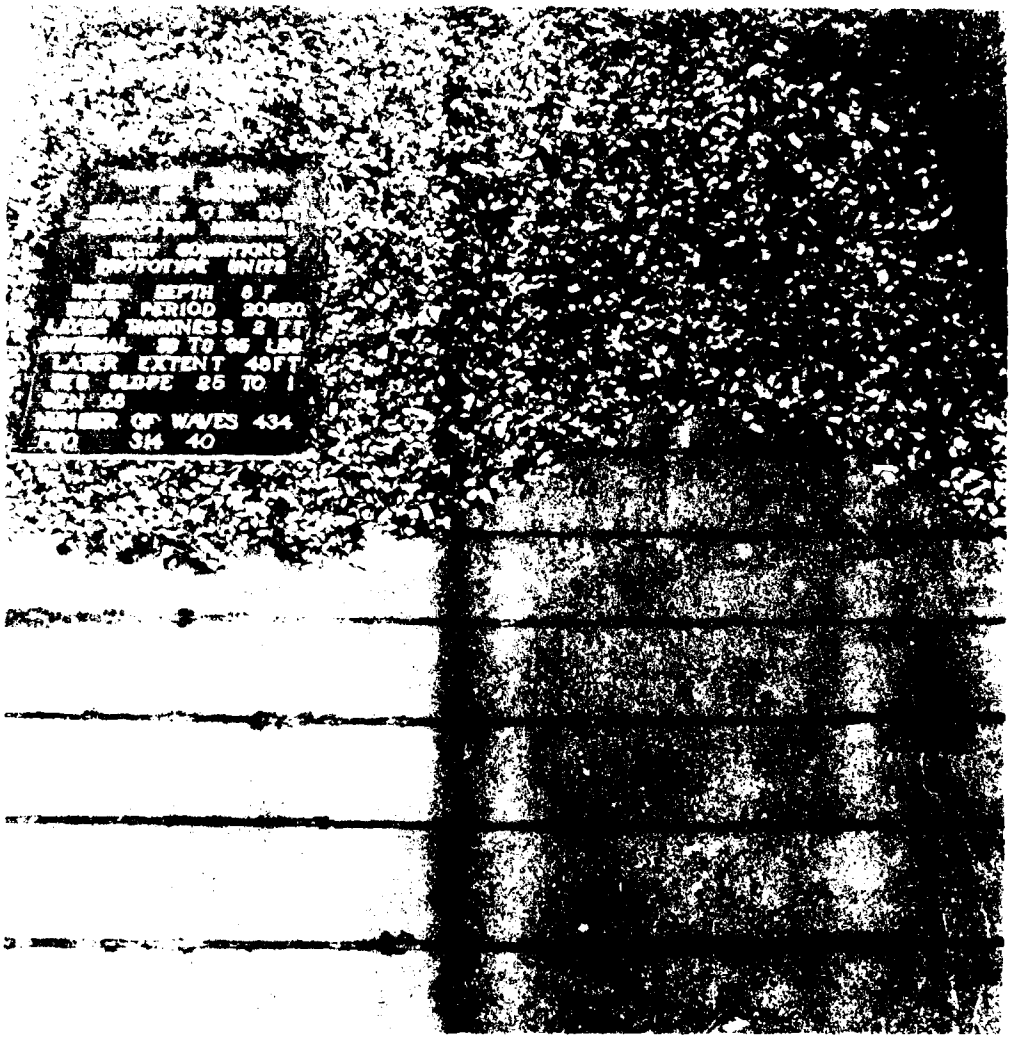

Photo A36. Material 50 to 95 lb prototype (WUL = 72 lb prototype); initial layer extent, 5.0 ft model = 80 ft prototype; number of waves 434; bed slope 1V on 25H; layer thickness 2 ft prototype; water depth 16 ft prototype; wave period 20 sec prototype; maximum wave height 17.9 ft prototype

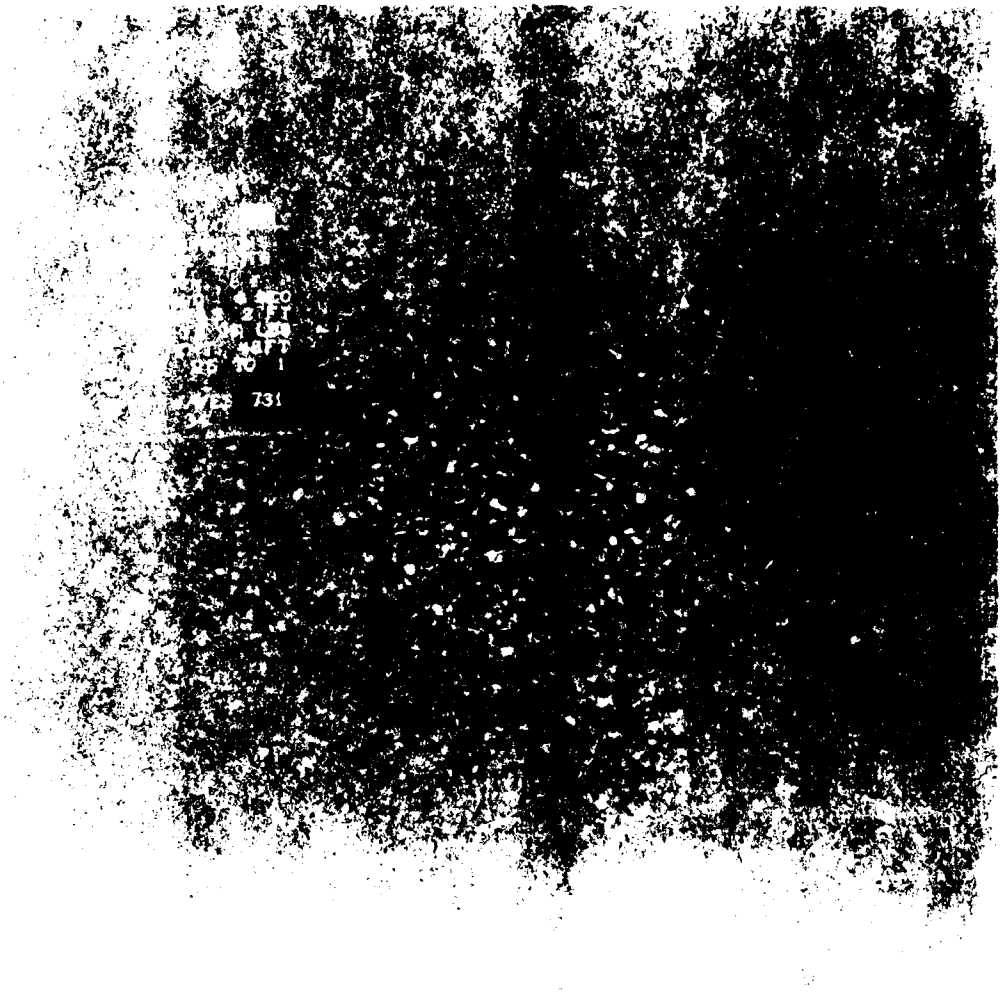

Photo A37. Material 50 to 95 lb prototype (WUL = 72 lb prototype); initial layer extent, 7.0 ft model = 112 ft prototype; number of waves 731; bed slope 1V on 25H; layer thickness 2 ft prototype; water depth 16 ft prototype; wave period 8 sec prototype; maximum wave height 17.4 ft prototype

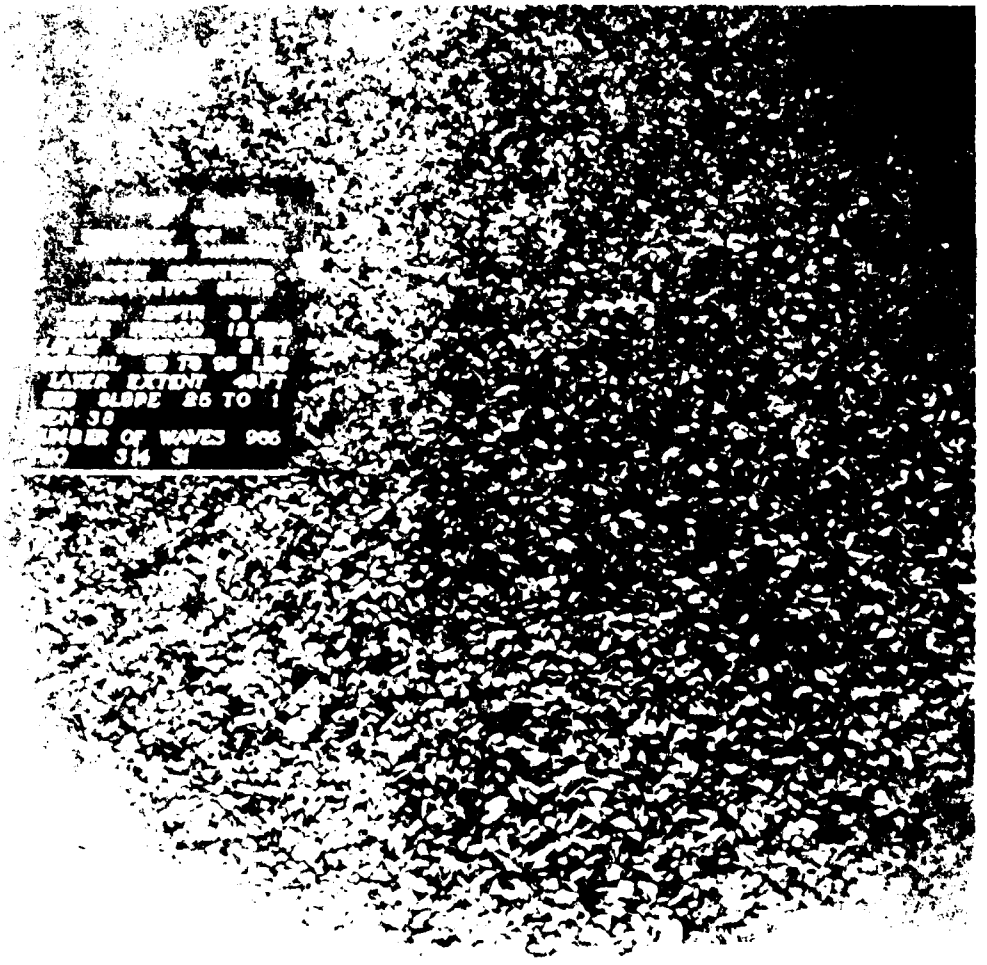

Photo A38. Material 50 to 95 lb prototype (WUL = 72 lb prototype); initial layer extent, 7.0 ft model = 112 ft prototype; number of waves 966; bed slope 1V on 25H; layer thickness 2 ft prototype; water depth 16 ft prototype; wave period 12 sec prototype; maximum wave height 17.8 ft prototype

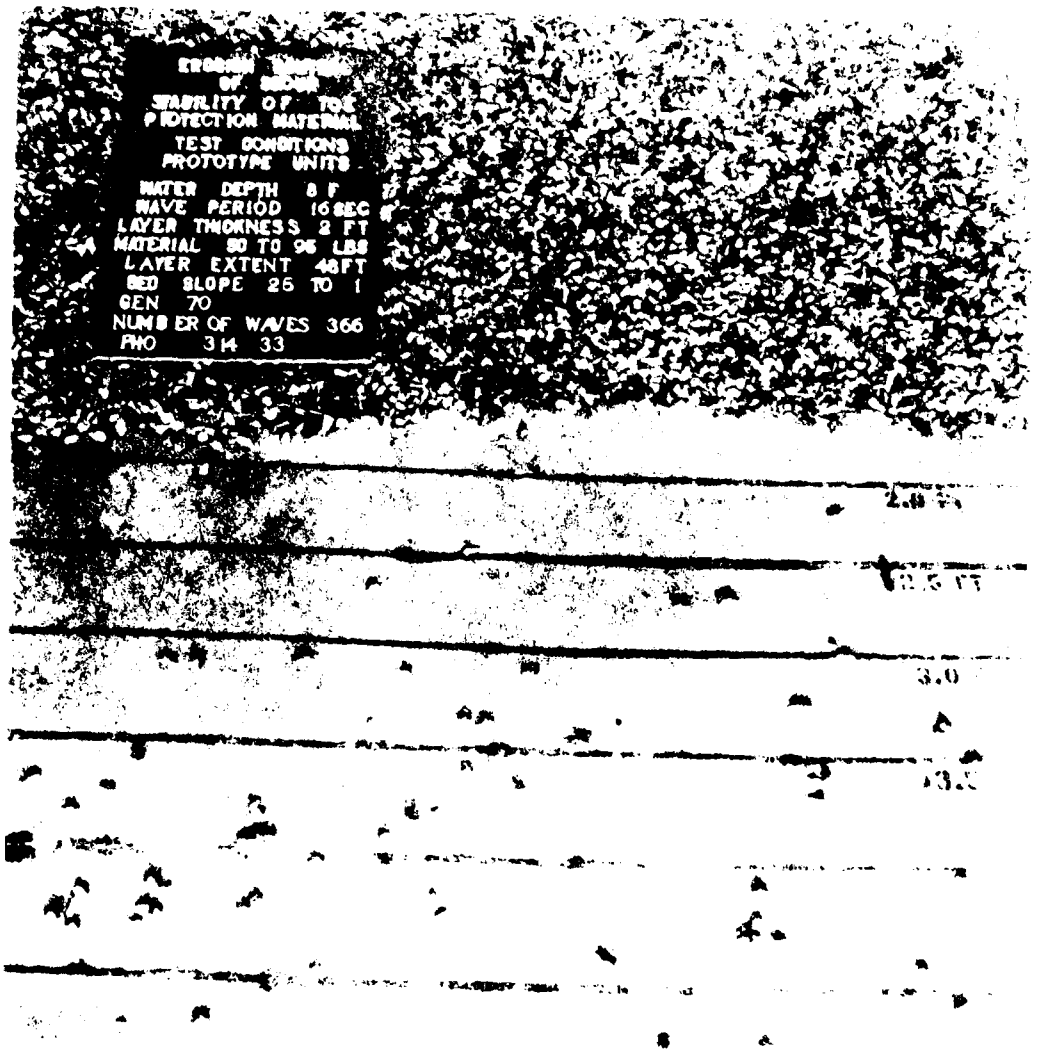

Photo A39. Material 50 to 95 lb prototype (WUL = 72 lb prototype); initial layer extent, 7.0 ft model = 112 ft prototype; number of waves 366; bed slope 1V on 25H; layer thickness 2 ft prototype; water depth 16 ft prototype; wave period 16 sec prototype; maximum wave height 23.2 ft prototype

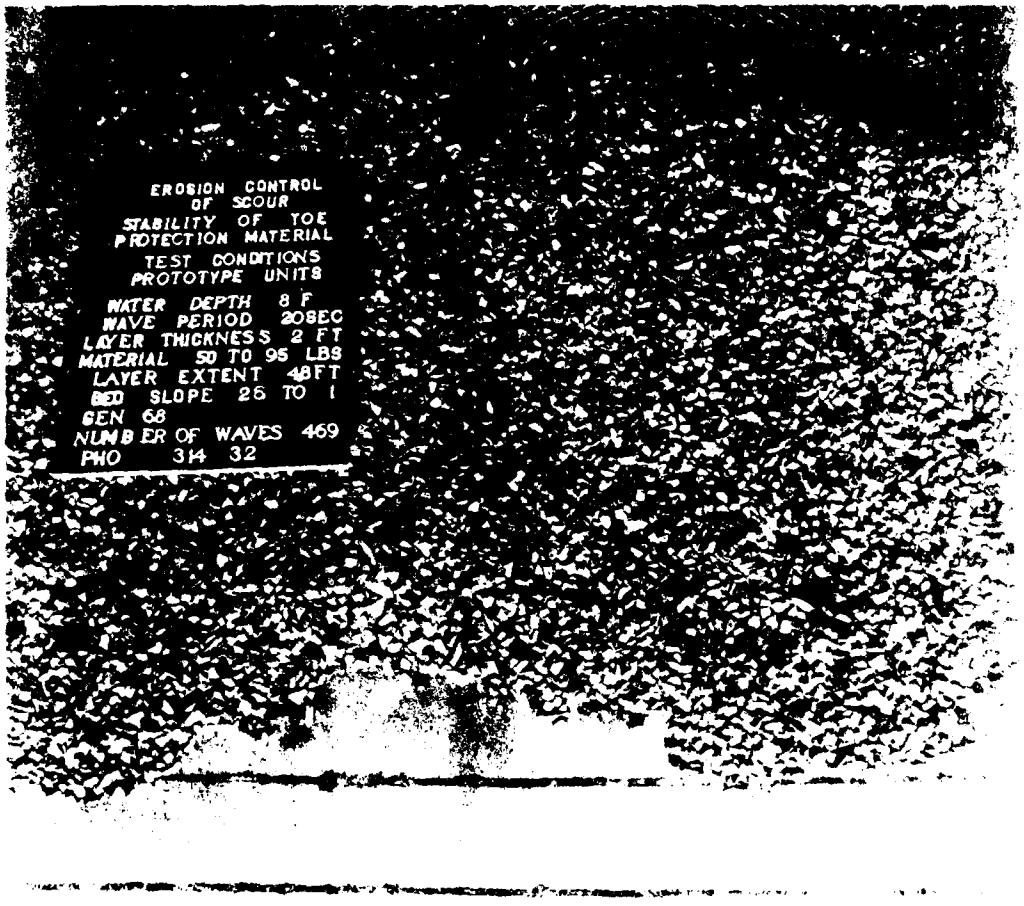

Photo A40. Material 50 to 95 lb prototype (WUL = 72 lb prototype); initial layer extent, 7.0 ft model = 112 ft prototype; number of waves 469; bed slope 1V on 25H; layer thickness 2 ft prototype; water depth 16 ft prototype; wave period 20 sec prototype; maximum wave height 17.9 ft prototype

Photo A41. Material 95 to 165 lb prototype (W_{50} = 130 lb prototype); initial layer extent, 3.0 ft model = 48 ft prototype; number of waves 0; bed slope 1V on 25H; layer thickness 2 ft prototype

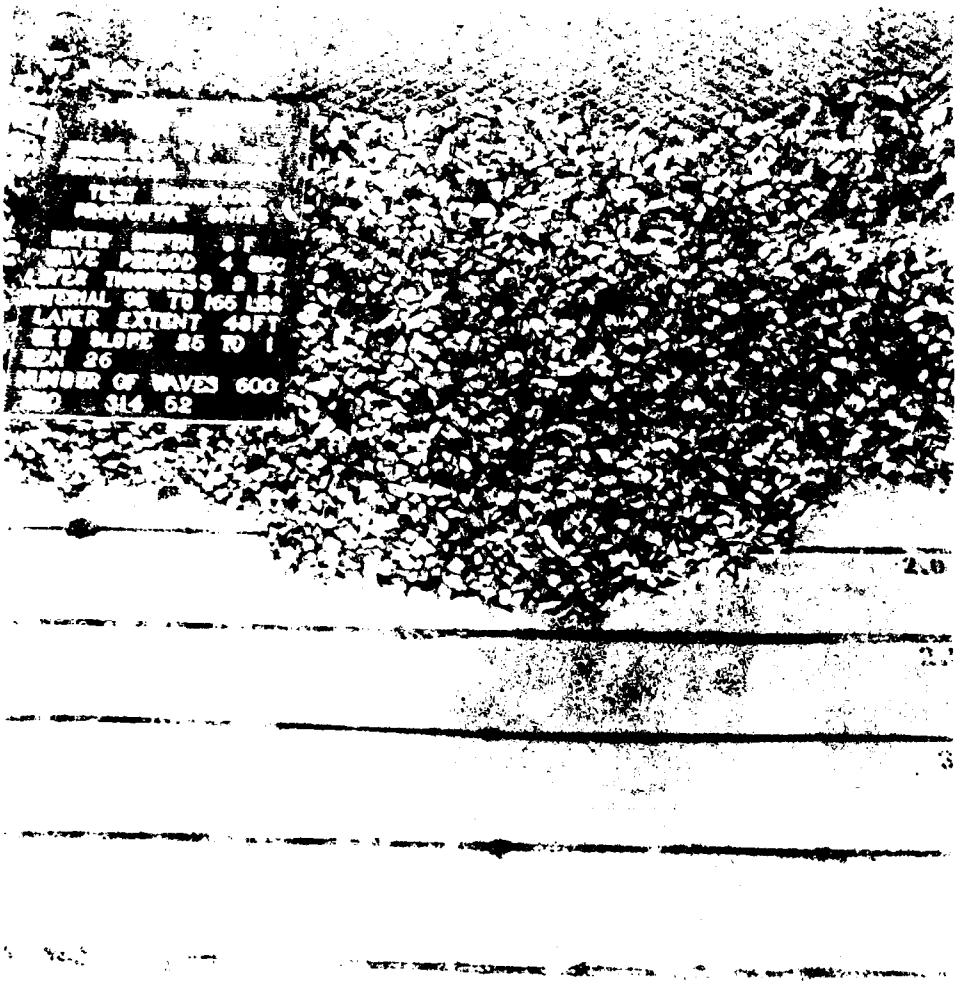

Photo A42. Material 95 to 165 lb prototype (WUL = 130 lb prototype); initial layer extent, 3.0 ft model = 48 ft prototype; number of waves 600; bed slope 1V on 25H; layer thickness 2 ft prototype; water depth 8 ft prototype; wave period 16 sec prototype; maximum wave height 12.8 ft prototype

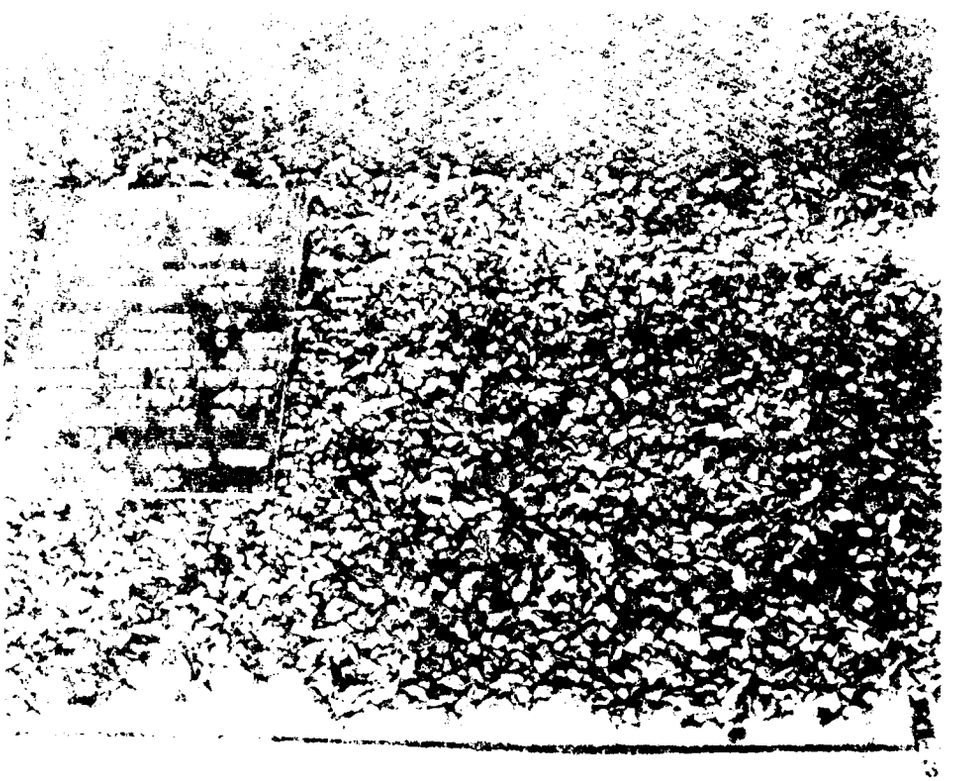

Photo A43. Material 95 to 165 lb prototype (WUL = 130 lb prototype); initial layer extent, 3.0 ft model = 48 ft prototype; number of waves 500; bed slope IV on 25ff; layer thickness 2 ft prototype; water depth 8 ft prototype; wave period 20 sec prototype; maximum wave height 10.9 ft prototype

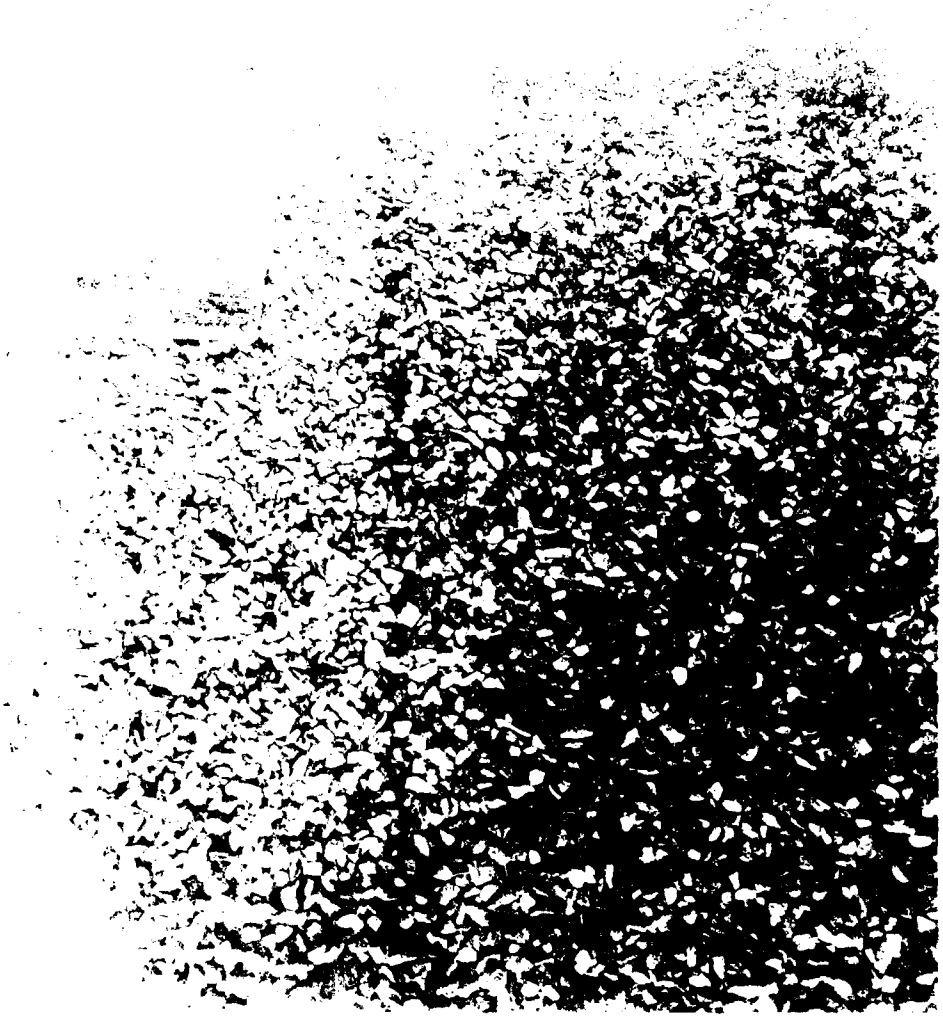

Photo A44. Material 95 to 165 lb prototype (W_{UL} = 130 lb prototype); initial layer extent, 5.0 ft model = 80 ft prototype; number of waves 0; bed slope 1V on 25H; layer thickness 2 ft prototype

Photo A45. Material 95 to 165 lb prototype $(W_{50}$ [illegible] for lb prototype, [illegible] layer extent, 5.0 ft model = 80 ft prototype; [illegible] waves [illegible] for slope 1V on 2SH; layer thickness 2 ft prototype; water depth [illegible] wave period 16 sec prototype; maximum wave height [illegible]

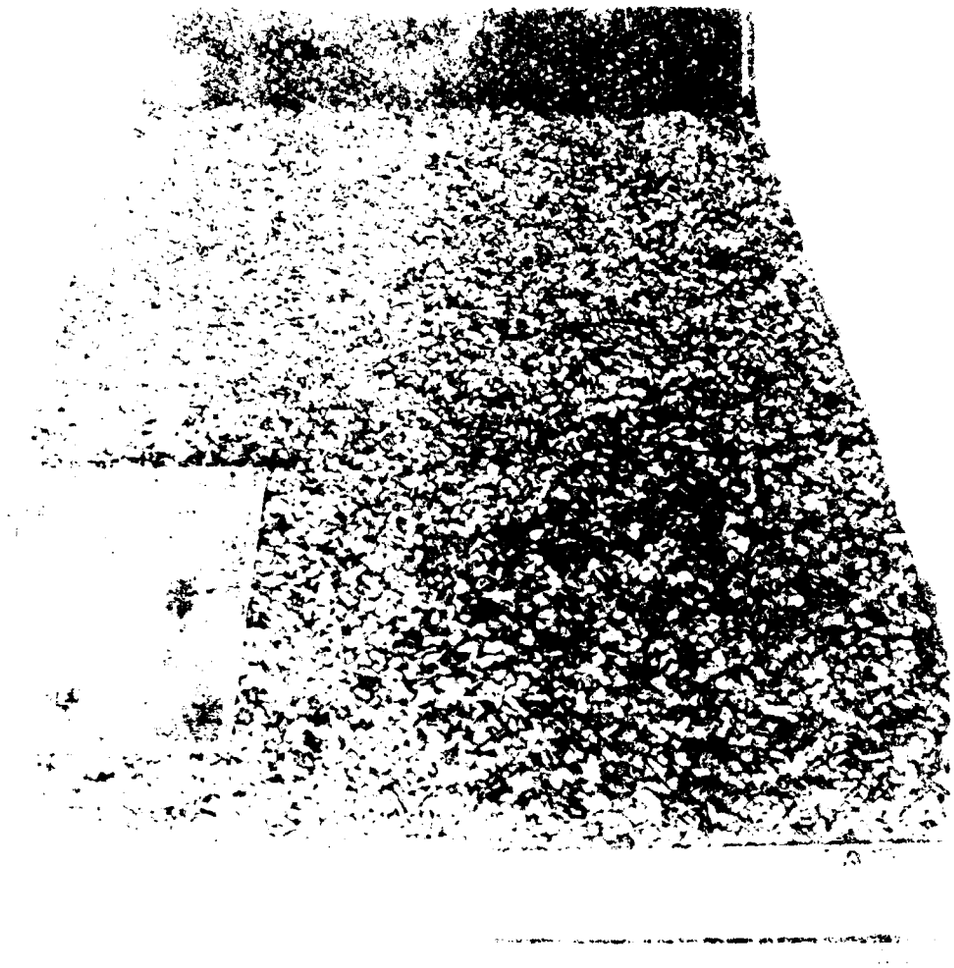

Photo A46. Material 95 to 165 lb prototype (W_{50} = 130 lb prototype); *initial* layer extent, 7.0 ft model = 112 ft prototype; number of waves 0; bed slope 1V on 25H; layer thickness 2 ft prototype

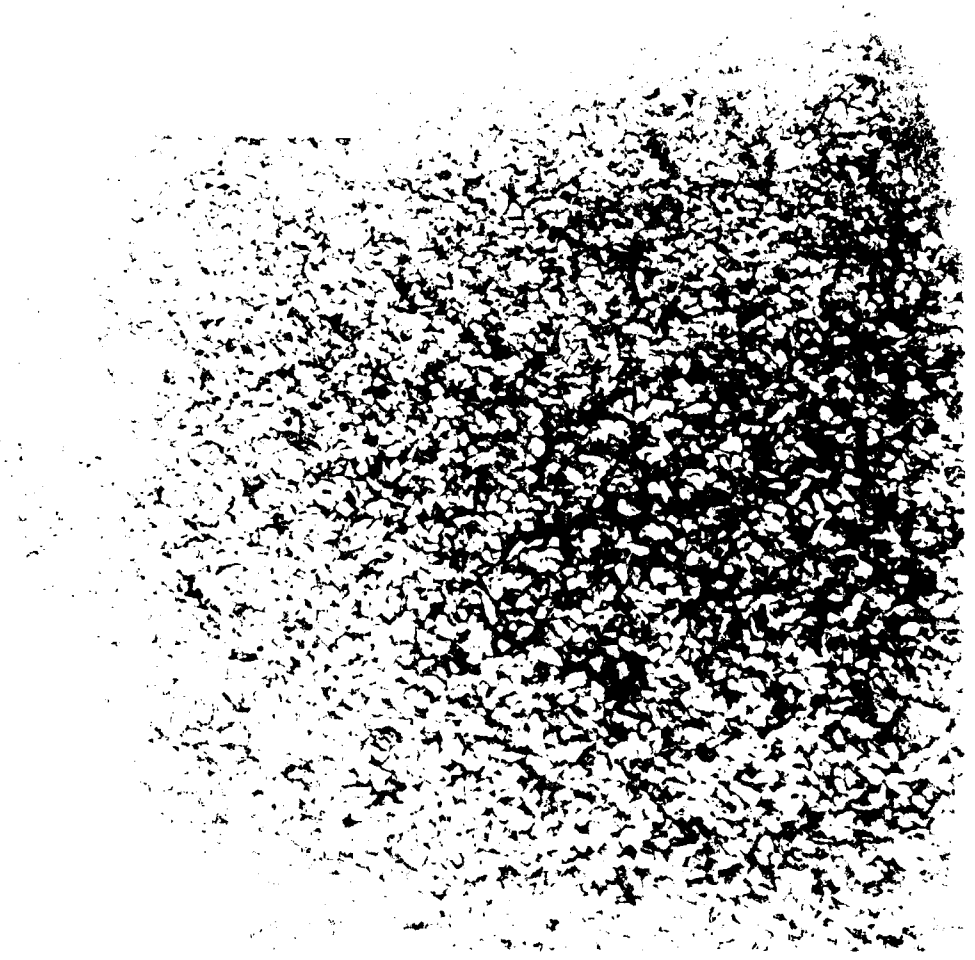

Photo A47. Material 95 to 165 lb prototype (WUL = 130 lb prototype); initial layer extent, 7.0 ft model = 112 ft prototype; number of waves 800; bed slope 1V on 2SH; layer thickness 2 ft prototype; water depth 8 ft prototype; wave period 16 sec prototype; maximum wave height 12.8 ft prototype

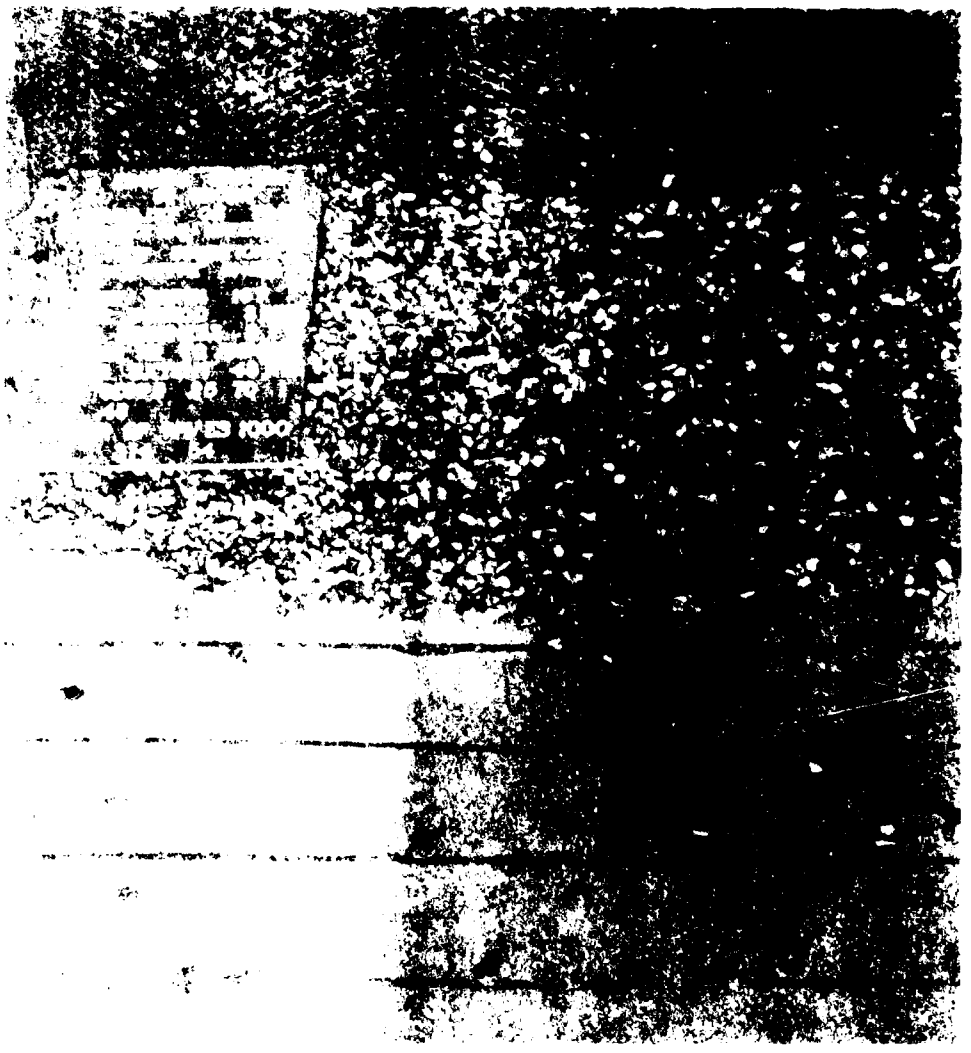

Photo A48 Material 9½ to 165 lb prototype (WUL = 130 lb prototype); initial layer extent, 3.0 ft model = 48 ft prototype; number of waves 1,000; bed slope 1V on 2½H; layer thickness 2 ft prototype; water depth 16 ft prototype; wave period 12 sec prototype; maximum wave height 17.8 ft prototype

Photo A49. Material 95 to 165 lb prototype (Wt = 130 lb prototype); initial layer extent, 3.0 ft model = 48 ft prototype; number of waves 147; bed slope 1V on 25H; layer thickness 2 ft prototype; water depth 16 ft prototype; wave period 16 sec prototype; maximum wave height 23.5 ft prototype

Photo A50. Material 95 to 165 lb prototype (WUL = 130 lb prototype); initial layer extent, 3.0 ft model = 48 ft prototype; number of waves 315; bed slope 1V on 25H; layer thickness 2 ft prototype; water depth 16 ft prototype; wave period 20 sec prototype; maximum wave height 17.9 ft prototype

Photo A51. Material 95 to 165 lb prototype (WUL = 130 lb prototype); initial layer extent, 5.0 ft model = 80 ft prototype; number of waves 175; bed slope 1V on 25H; layer thickness 2 ft prototype; water depth 16 ft prototype; wave period 16 sec prototype; maximum wave height 23.2 ft prototype

Photo A52. Material 95 to 165 lb prototype (WUL = 130 lb prototype); initial layer extent, 5.0 ft model = 80 ft prototype; number of waves 399; bed slope 1V on 25H; layer thickness 2 ft prototype; water depth 16 ft prototype; wave period 20 sec prototype; maximum wave height 17.9 ft prototype

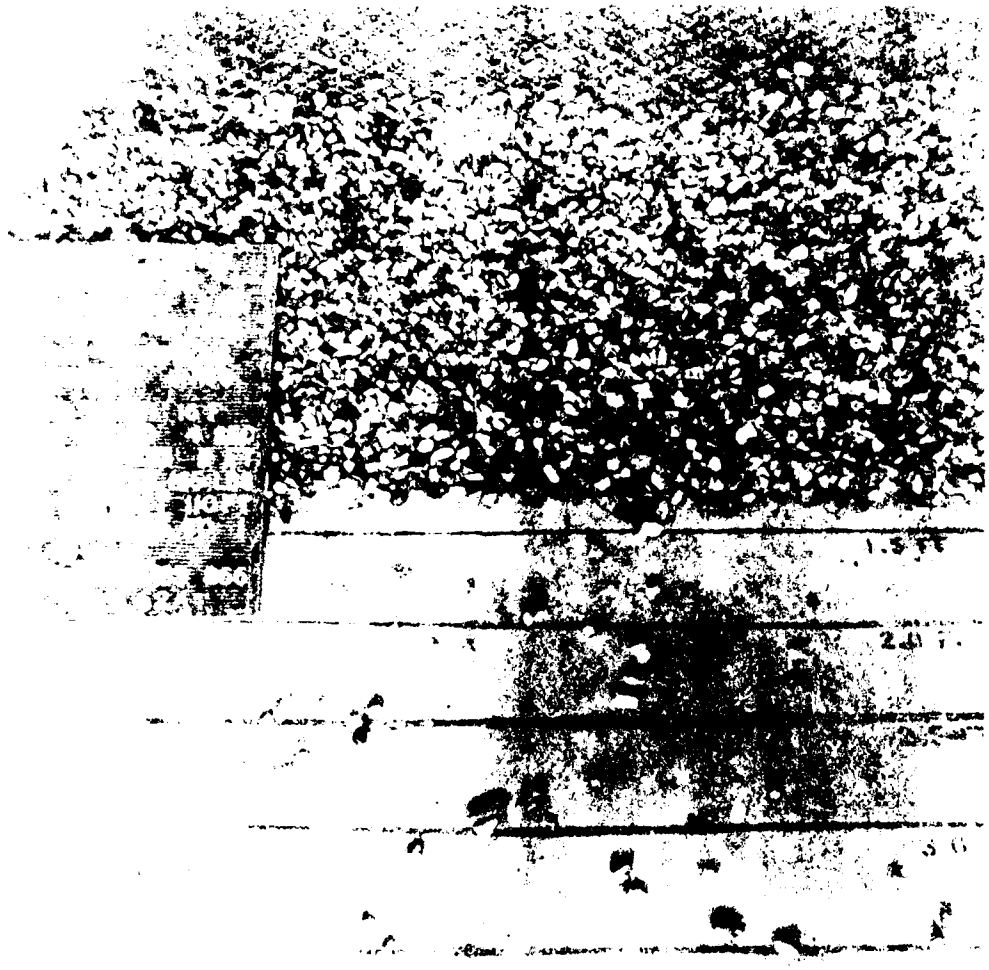

Photo A53. Material 95 to 165 lb prototype (WUL = 130 lb prototype); initial layer extent, 7.0 ft model = 112 ft prototype; number of waves 366; bed slope 1V on 25H; layer thickness 2 ft prototype; water depth 16 ft prototype; wave period 16 sec prototype; maximum wave height 23.2 ft prototype

Photo A54. Material 95 to 165 lb prototype (WUL = 130 lb prototype); initial layer extent, 7.0 ft model = 112 ft prototype; number of waves 480; bed slope 1V on 25H; layer thickness 2 ft prototype; water depth 16 ft prototype; wave period 20 sec prototype; maximum wave height 17.9 ft prototype

Photo A55. Material 165 to 260 lb prototype (WUL = 212 lb prototype); initial layer extent, 3.0 ft model = 48 ft prototype; number of waves 500; bed slope 1V on 25H; layer thickness 2 ft prototype; water depth 8 ft prototype; wave period 16 sec prototype; maximum wave height 12.8 ft prototype

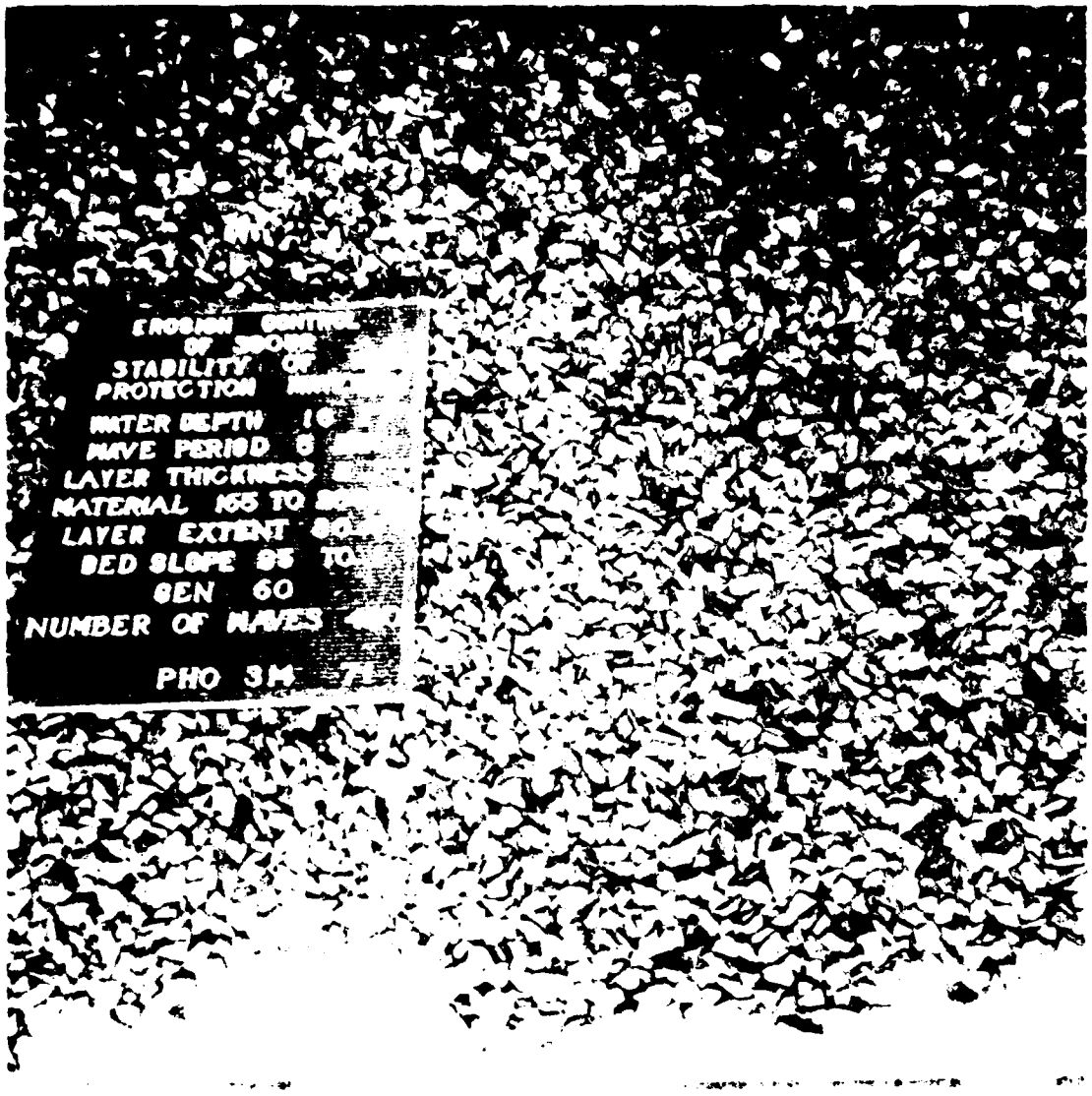

Photo A56. Material 165 to 260 lb prototype (WUL = 212 lb prototype); initial layer extent, 5.0 ft model = 80 ft prototype; number of waves 420; bed slope 1V on 25H; layer thickness 2 ft prototype; water depth 16 ft prototype; wave period 20 sec prototype; maximum wave height 17.9 ft prototype

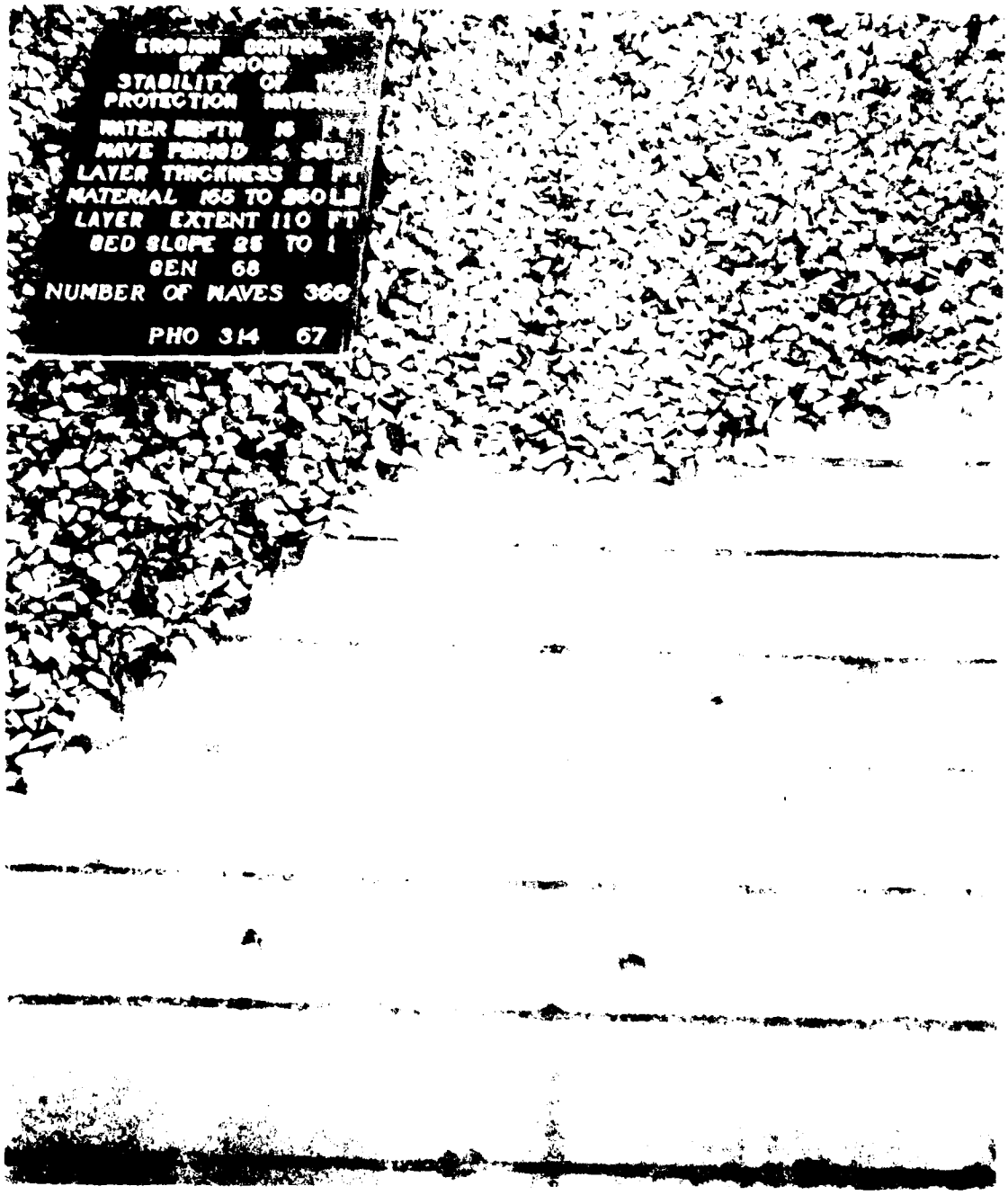

Photo A57. Material 165 to 260 lb prototype (WUL = 212 lb prototype); initial layer extent, 7.0 ft model = 112 ft prototype; number of waves 366; bed slope 1V on 25H; layer thickness 2 ft prototype; water depth 15 ft prototype; wave period 16 sec prototype; maximum wave height 23.2 ft prototype

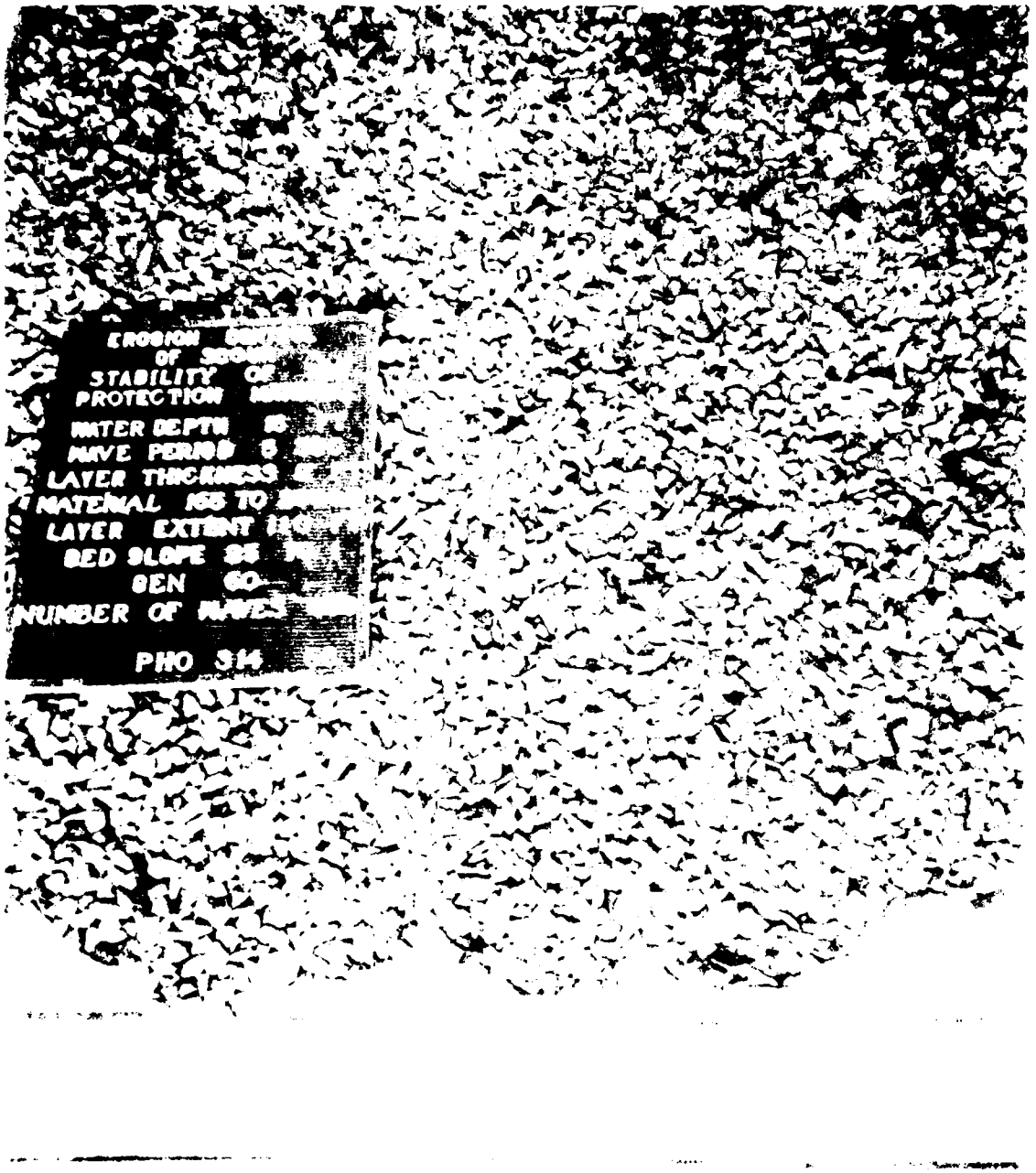

Photo A58. Material 165 to 260 lb prototype (WUL = 212 lb prototype); initial layer extent, 7.0 ft model = 112 ft prototype; number of waves 500; bed slope 1V on 25H; layer thickness 2 ft prototype; water depth 16 ft prototype; wave period 20 sec prototype; maximum wave height 17.9 ft prototype

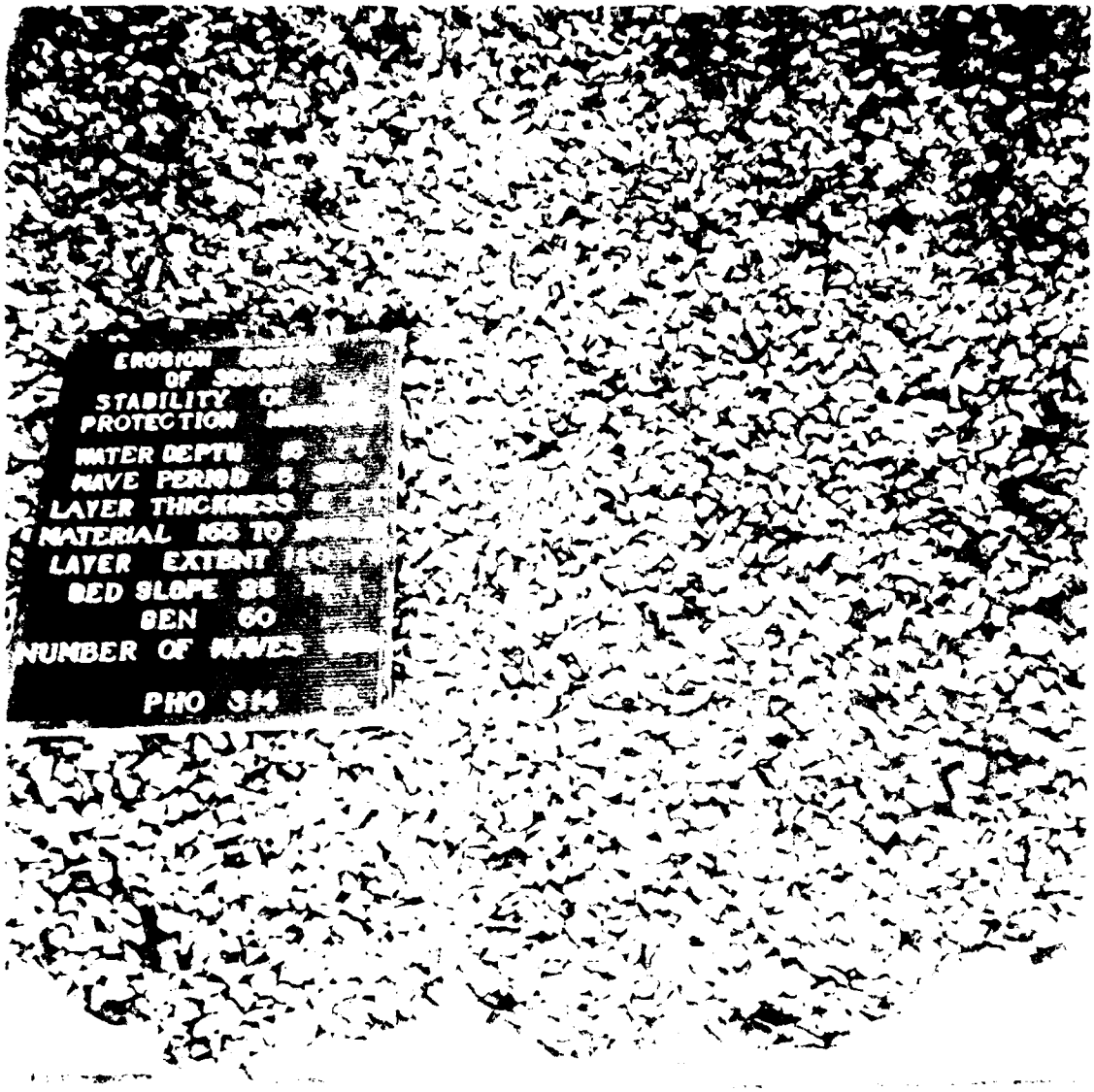

Photo A58. Material 165 to 260 lb prototype (WUL = 212 lb prototype); initial layer extent, 7.0 ft model = 112 ft prototype; number of waves 500; bed slope 1V on 25H; layer thickness 2 ft prototype; water depth 16 ft prototype; wave period 20 sec prototype; maximum wave height 17.9 ft prototype

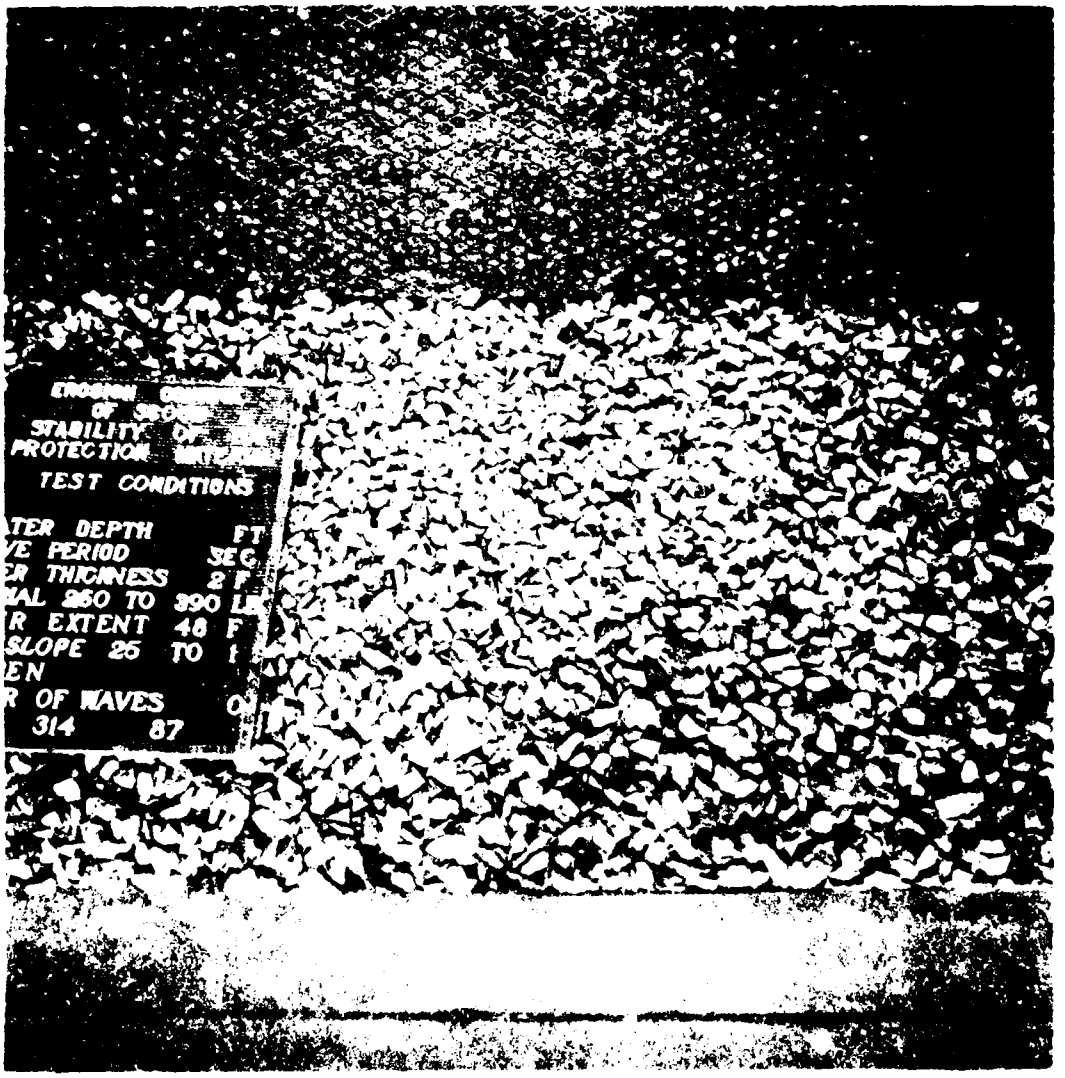

Photo A59. Material 260 to 390 lb prototype (WUL = 325 lb prototype); initial layer extent, 3.0 ft model = 48 ft prototype; number of waves 0; bed slope 1V on 2.5H; layer thickness 2 ft prototype

Photo A60. Material 260 to 390 lb prototy (WUL = 325 lb prototype); initial layer extent, 3.0 ft model = 48 ft prototype; number of waves 500; bed slope IV on 25H; layer thickness 2 ft prototype; water depth 8 ft prototype; wave period 16 sec prototype; maximum wave height 12.8 ft prototype

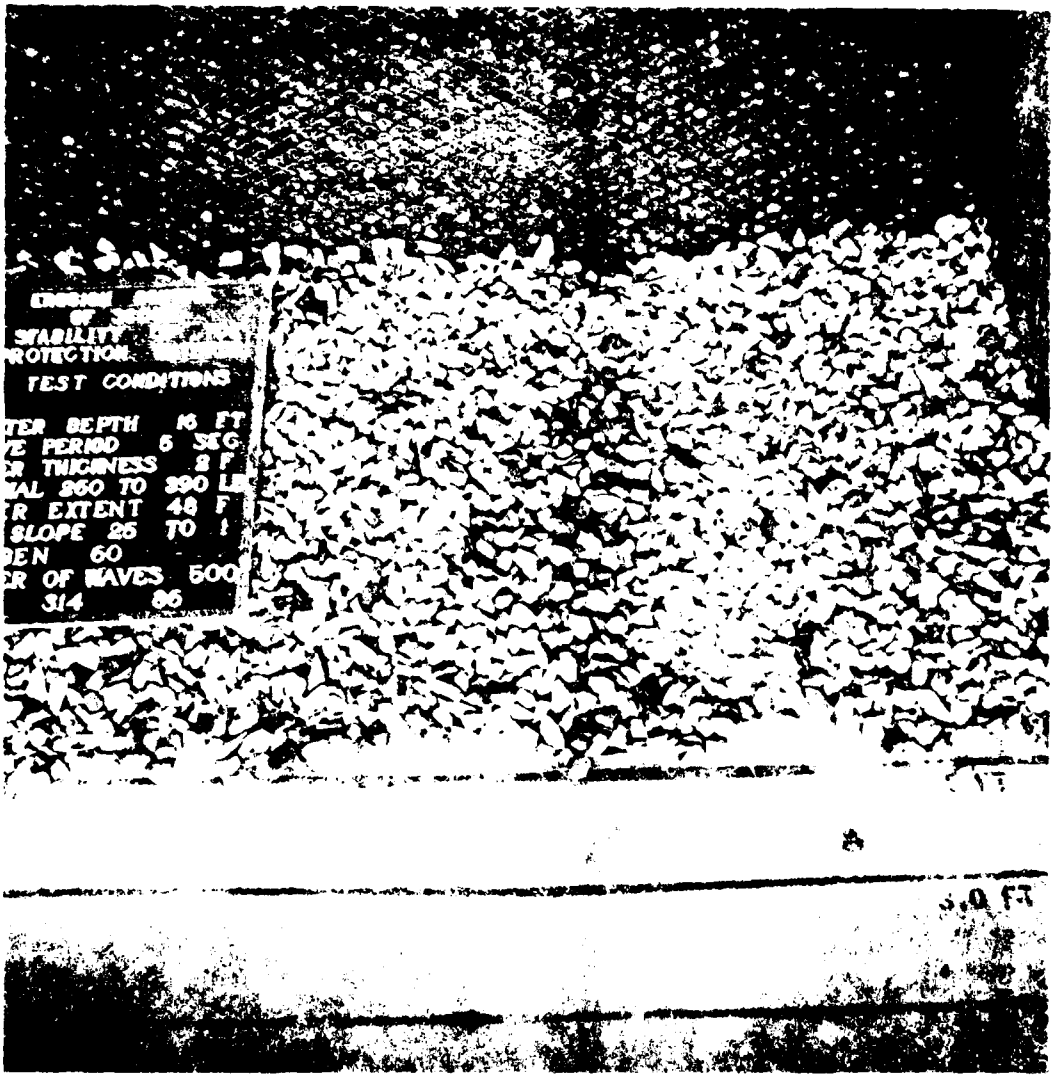

Photo A61. Material 260 to 390 lb prototype (WUL = 325 lb prototype); initial layer extent, 3.0 ft model = 38 ft prototype; number of waves 500; bed slope 1V on 25H; layer thickness 2 ft prototype; water depth 16 ft prototype; wave period 20 sec prototype; maximum wave height 17.9 ft prototype

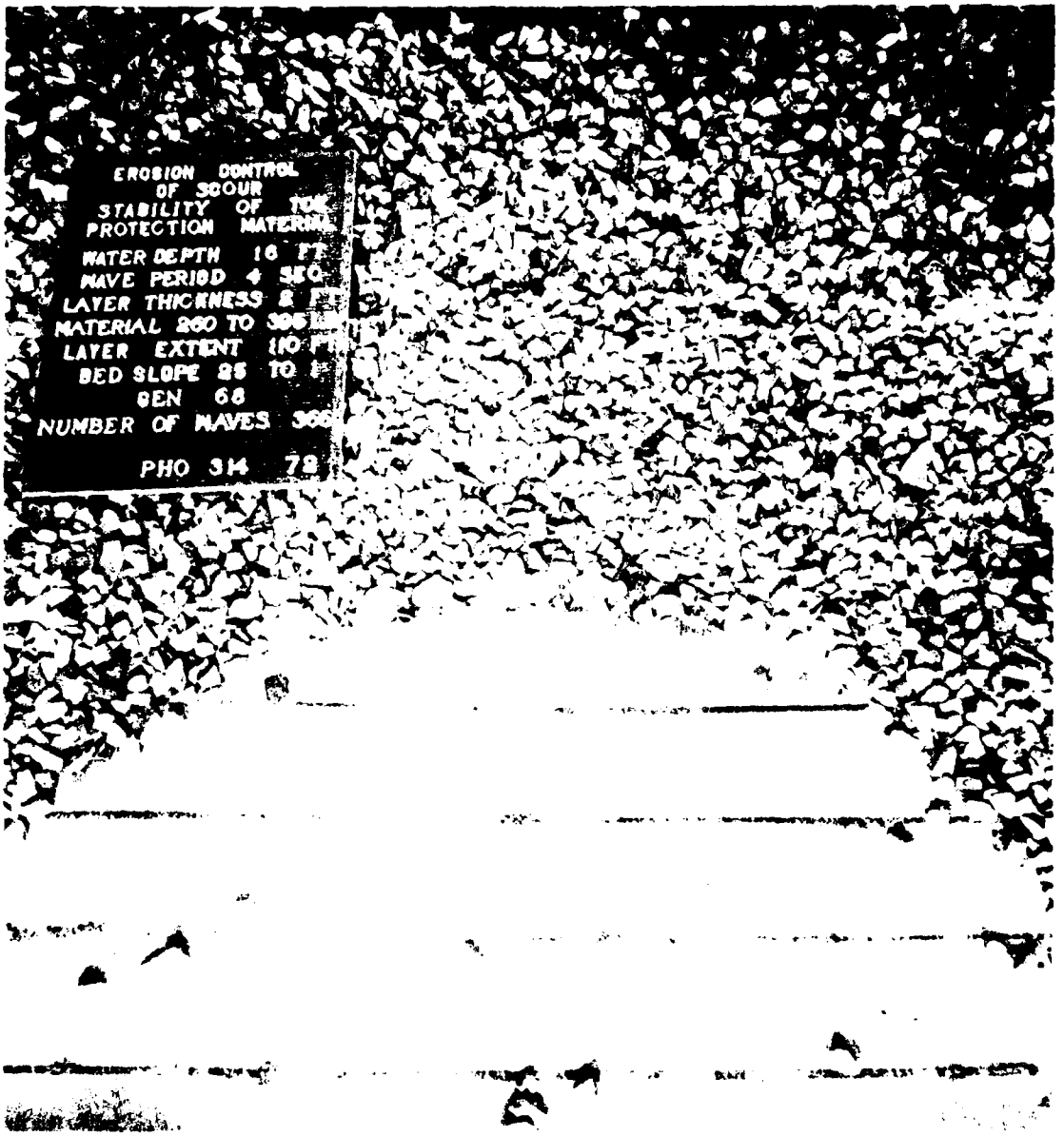

Photo A62. Material 260 to 390 lb prototype (WUL = 325 lb prototype); initial layer extent, 7.0 ft model = 112 ft prototype; number of waves 366; bed slope 1V on 25H; layer thickness 2 ft prototype; water depth 16 ft prototype; wave period 16 sec prototype; maximum wave height 23.2 ft prototype

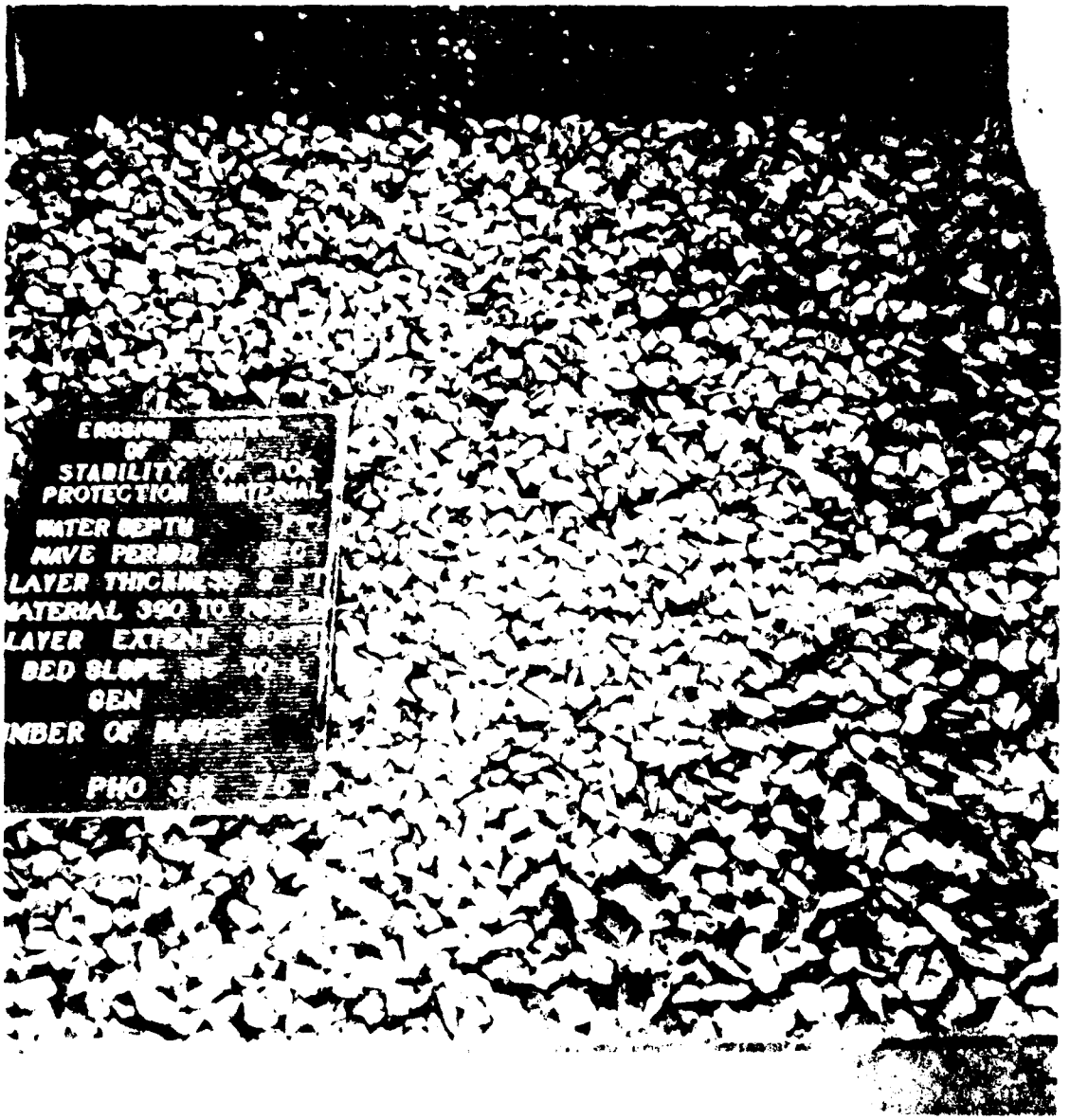

Photo A63. Material 390 to 765 lb prototype (WUL = 577 lb prototype); initial layer extent, 5.0 ft model = 80 ft prototype; number of waves 0; bed slope 1V on 25H; layer thickness 2 ft prototype

Photo A64. Material 390 to 765 lb prototype (WUL = 577 lb prototype); initial layer extent, 5.0 ft model = 80 ft prototype; number of waves 500; bed slope 1V on 25H; layer thickness 2 ft prototype; water depth 16 ft prototype; wave period 20 sec prototype; maximum wave height 17.9 ft prototype

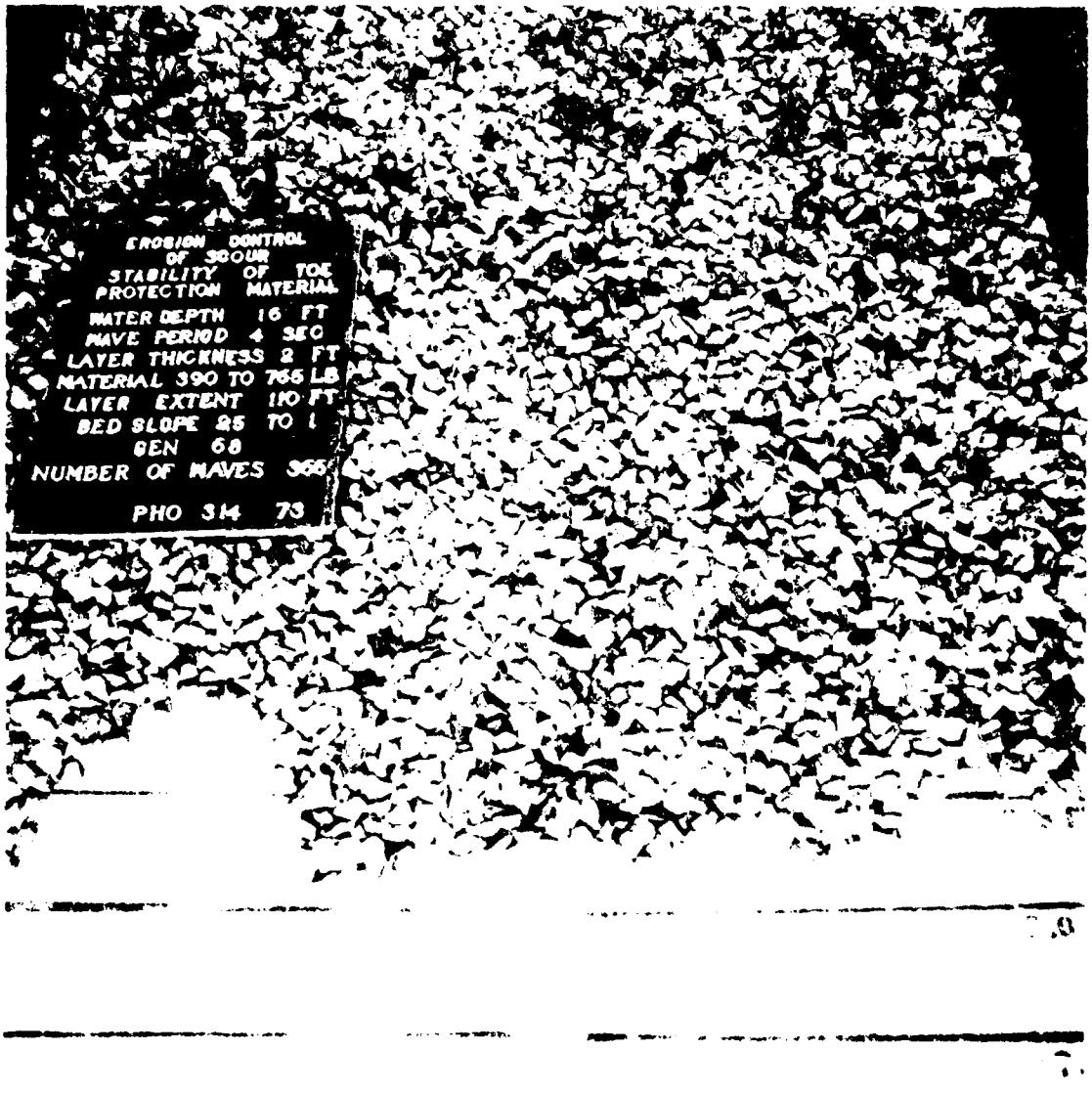

Photo A65. Material 390 to 765 lb prototype (WUL = 577 lb prototype), initial layer extent, 7.0 ft model = 112 ft prototype; number of waves 366; bed slope 1V on 25H; layer thickness 2 ft prototype; water depth 16 ft prototype; wave period 16 sec prototype; maximum wave height 23.2 ft prototype

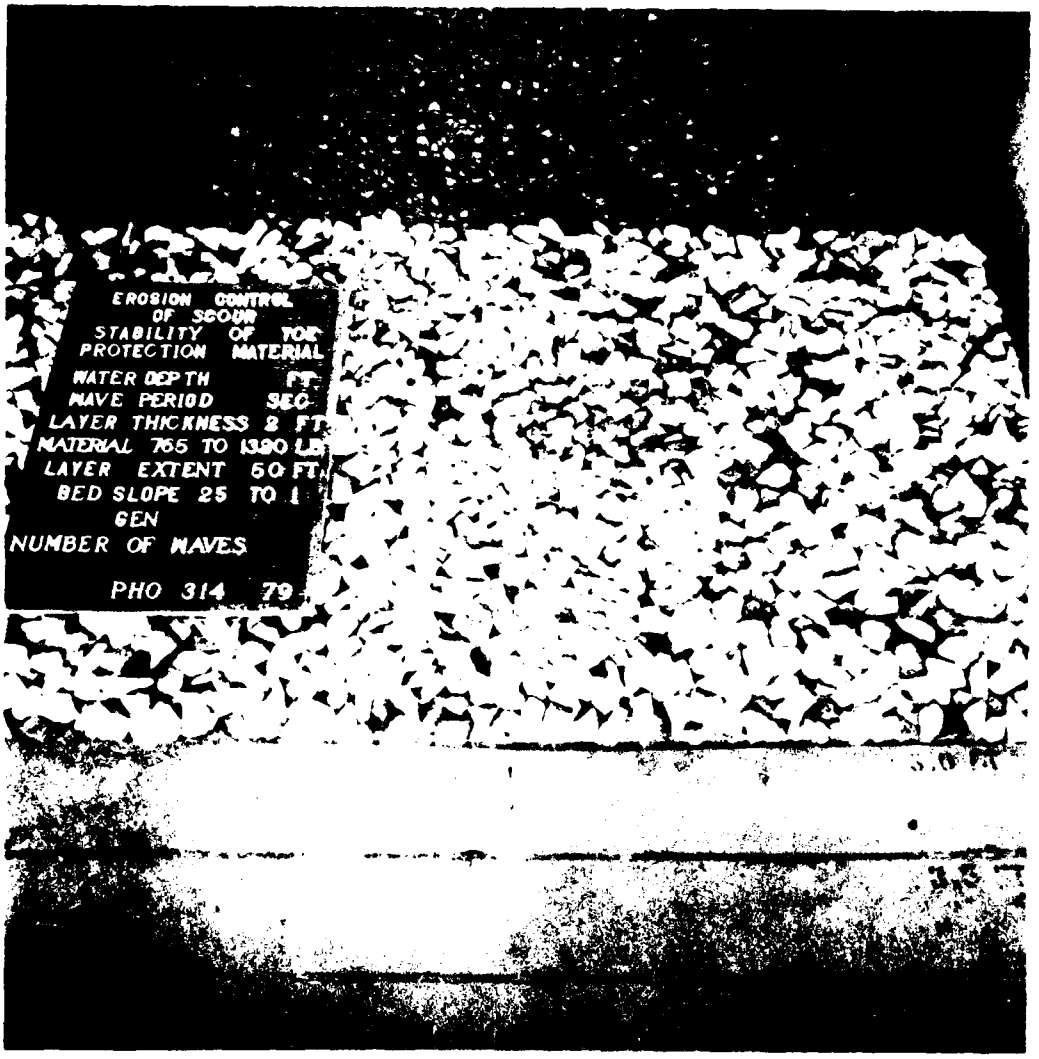

Photo A66. Material 765 to 1,320 lb prototype (WUL = 1,042 lb prototype); initial layer extent, 3.0 ft model = 48 ft prototype; number of waves 0; bed slope 1V on 25H; layer thickness 2 ft prototype

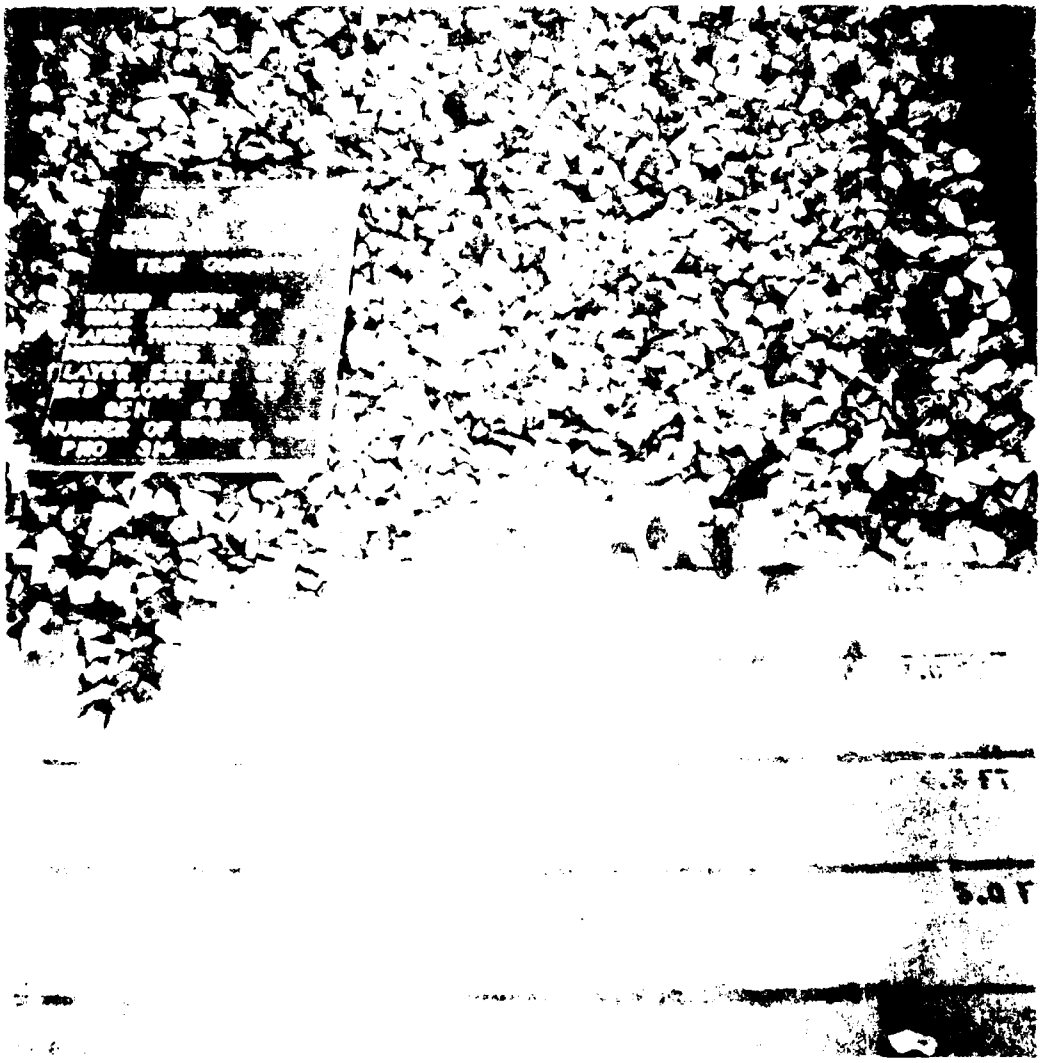

Photo A67. Material 765 to 1,320 lb prototype (WUL = 1,042 lb prototype); initial layer extent, 5.0 ft model = 80 ft prototype; number of waves 300; bed slope 1V on 25H; layer thickness 2 ft prototype; water depth 16 ft prototype; wave period 16 sec prototype; maximum wave height 23.2 ft prototype

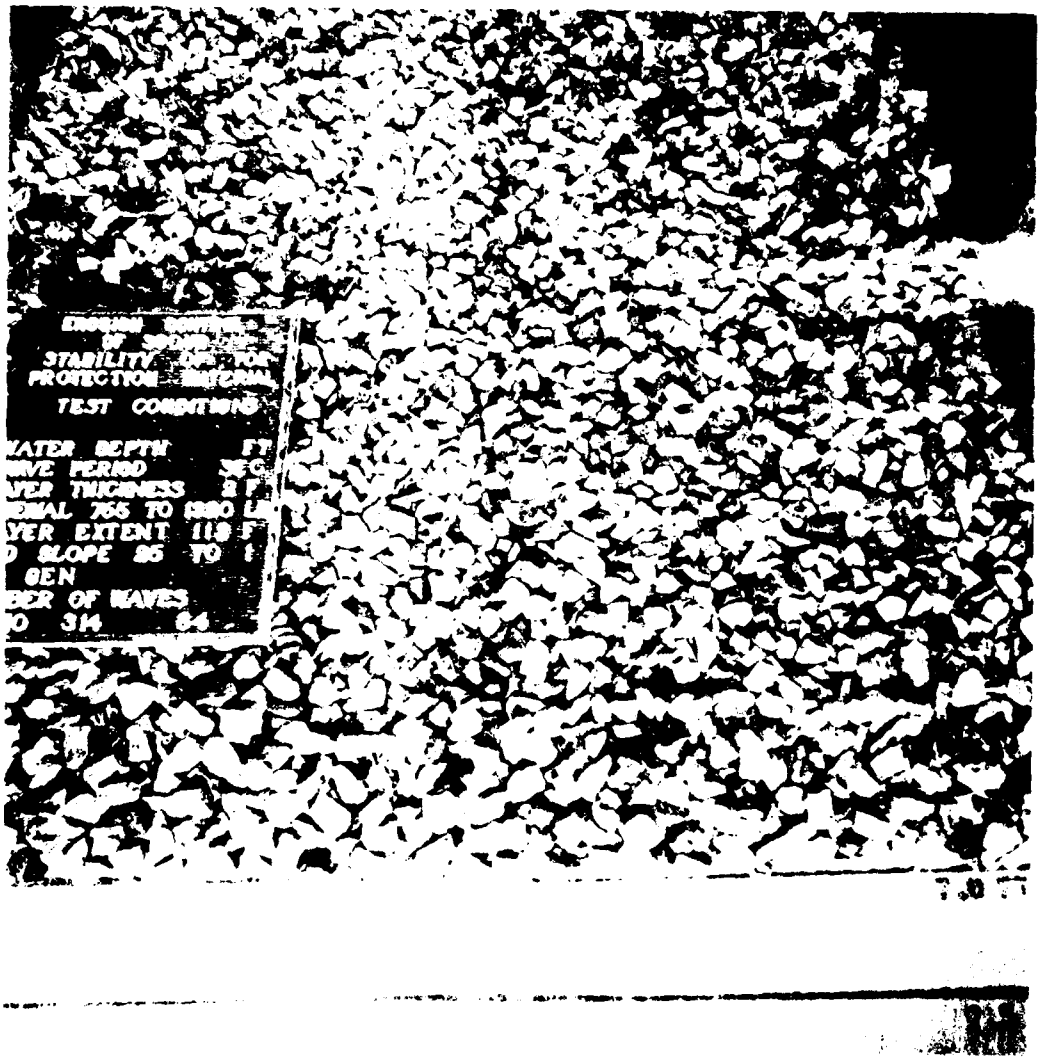

Photo A68. Material 765 to 1,320 lb prototype (WUL = 1,042 lb prototype) initial layer extent, 7.0 ft model = 112 ft prototype; number of waves 0; bed slope 1V on 25H; layer thickness 2 ft prototype

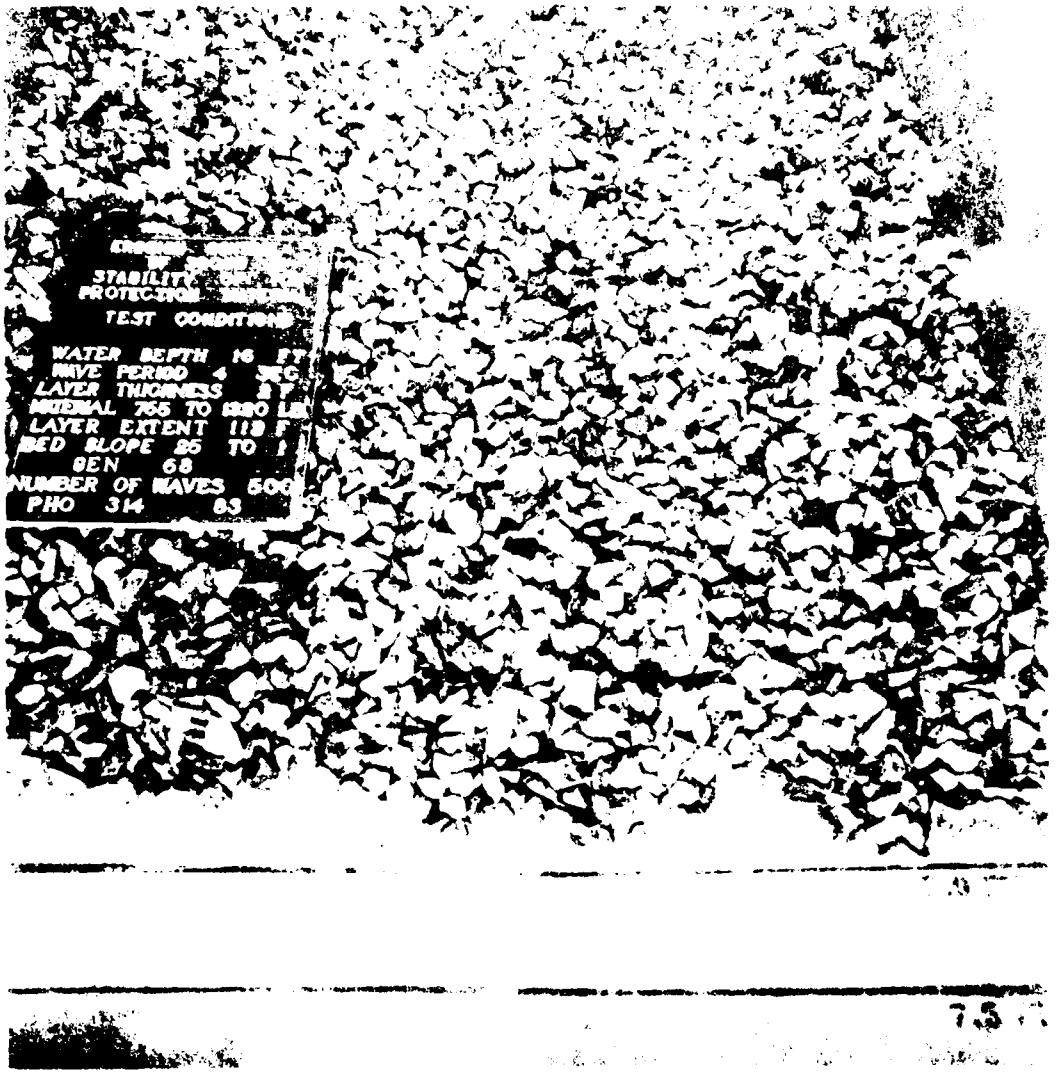

Photo A69. Material 765 to 1,320 lb prototype (WUL = 1,042 lb prototype); initial layer extent, 7.0 ft model = 112 ft prototype; number of waves 500; bed slope 1V on 25H; layer thickness 2 ft prototype; water depth 16 ft prototype; wave period 16 sec prototype; maximum wave height [illegible] ft prototype

APPENDIX B: MATERIAL LOCATION AFTER N WAVES

MATERIAL LOCATION AFTER N WAVES

Still-Water Depth, ft
Model: 0.5
Prototype: 8.0

Layer Thickness, ft
Model: 0.125
Prototype: 2.0

Layer Extent, ft
Model: 3
Prototype: 48

Material Size, in.
Model: 3/8 - 1/2
Prototype: 6 - 8

Material Weight, lb
Model: 0.005 - 0.012
Prototype: 20 - 50

Wave Period, sec
Model: 3
Prototype: 12

Bed Slope: 1V on 25H

Maximum Breaker Wave Height, ft
Model: 0.70
Prototype: 11.2

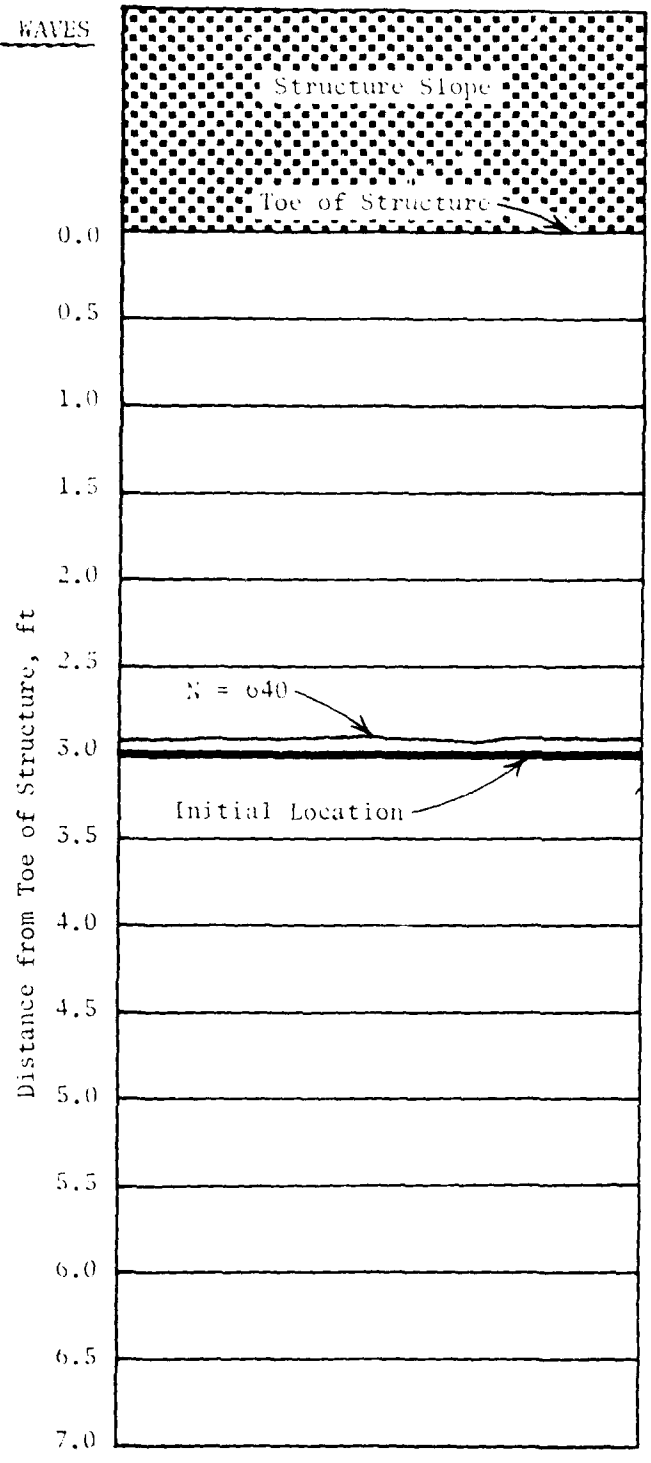

MATERIAL LOCATION AFTER N WAVES

Still-Water Depth, ft
Model: 0.5
Prototype: 8.0

Layer Thickness, ft
Model: 0.125
Prototype: 2.0

Layer Extent, ft
Model: 3
Prototype: 48

Material Size, in.
Model: 3/8 - 1/2
Prototype: 6 - 8

Material Weight, lb
Model: 0.005 - 0.012
Prototype: 20 - 50

Wave Period, sec
Model: 4
Prototype: 16

Bed Slope: 1V on 25H

Maximum Breaker Wave Height, ft
Model: 0.80
Prototype: 12.8

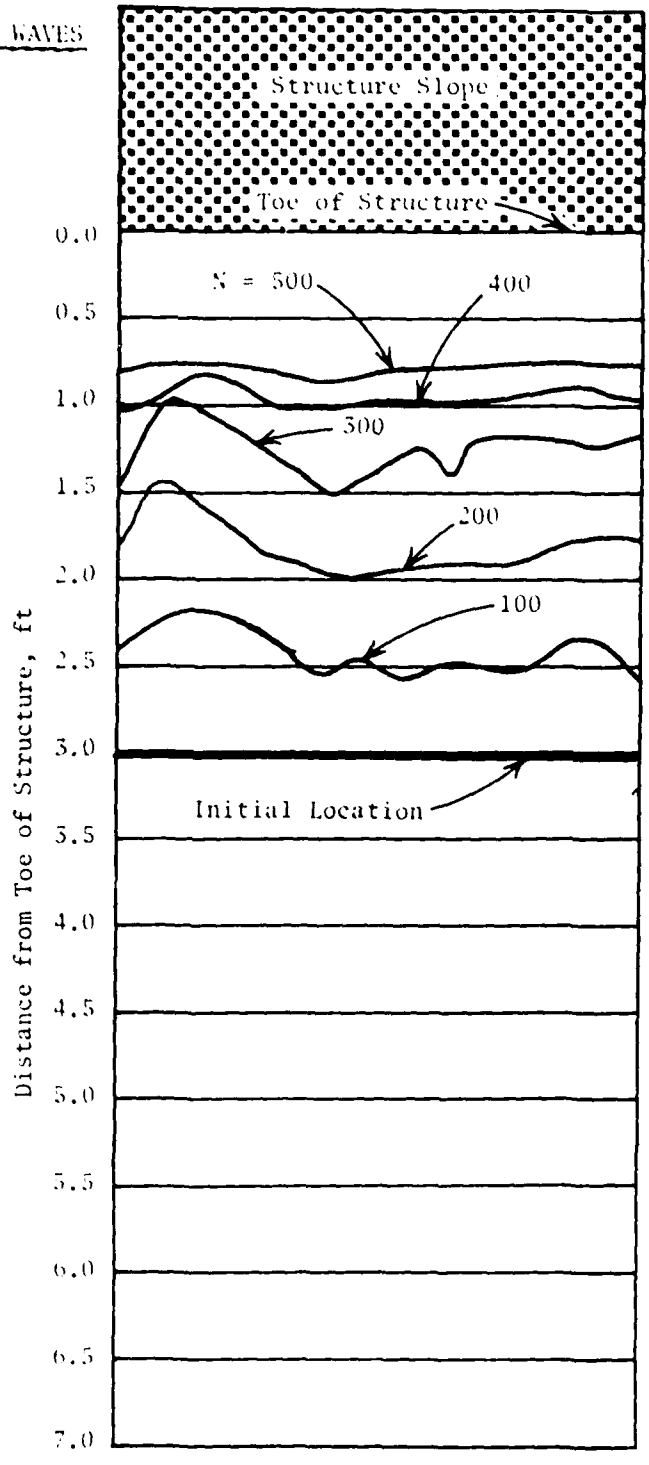

MATERIAL LOCATION AFTER N WAVES

Still-Water Depth, ft
Model: 0.5
Prototype: 8.0

Layer Thickness, ft
Model: 0.125
Prototype: 2.0

Layer Extent, ft
Model: 3
Prototype: 48

Material Size, in.
Model: 3/8 - 1/2
Prototype: 6 - 8

Material Weight, lb
Model: 0.005 - 0.012
Prototype: 20 - 50

Wave Period, sec
Model: 5
Prototype: 20

Bed Slope: 1V on 25H

Maximum Breaker Wave Height, ft
Model: 0.68
Prototype: 10.9

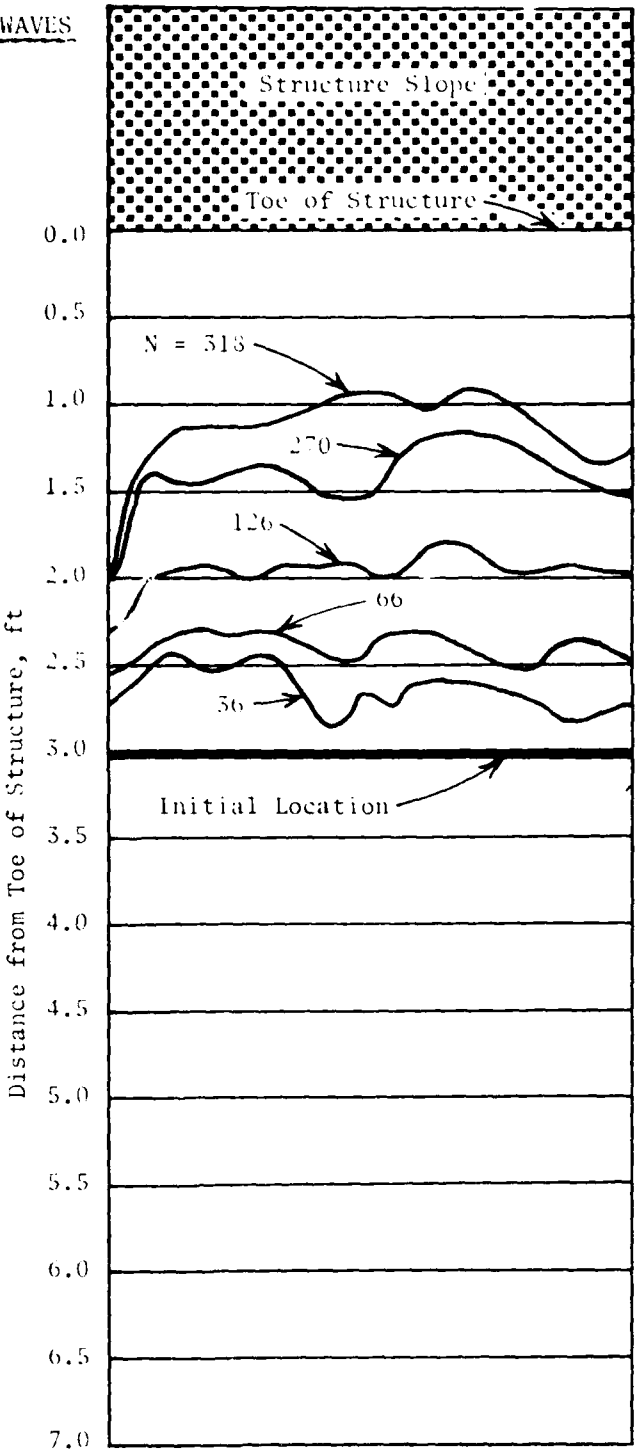

MATERIAL LOCATION AFTER N WAVES

Still-Water Depth, ft
Model: 0.5
Prototype: 8.0

Layer Thickness, ft
Model: 0.125
Prototype: 2.0

Layer Extent, ft
Model: 5
Prototype: 80

Material Size, in.
Model: 3/8 - 1/2
Prototype: 6 - 8

Material Weight, lb
Model: 0.005 - 0.012
Prototype: 20 - 50

Wave Period, sec
Model: 3
Prototype: 12

Bed Slope: 1V on 25H

Maximum Breaker Wave Height, ft
Model: 0.70
Prototype: 11.2

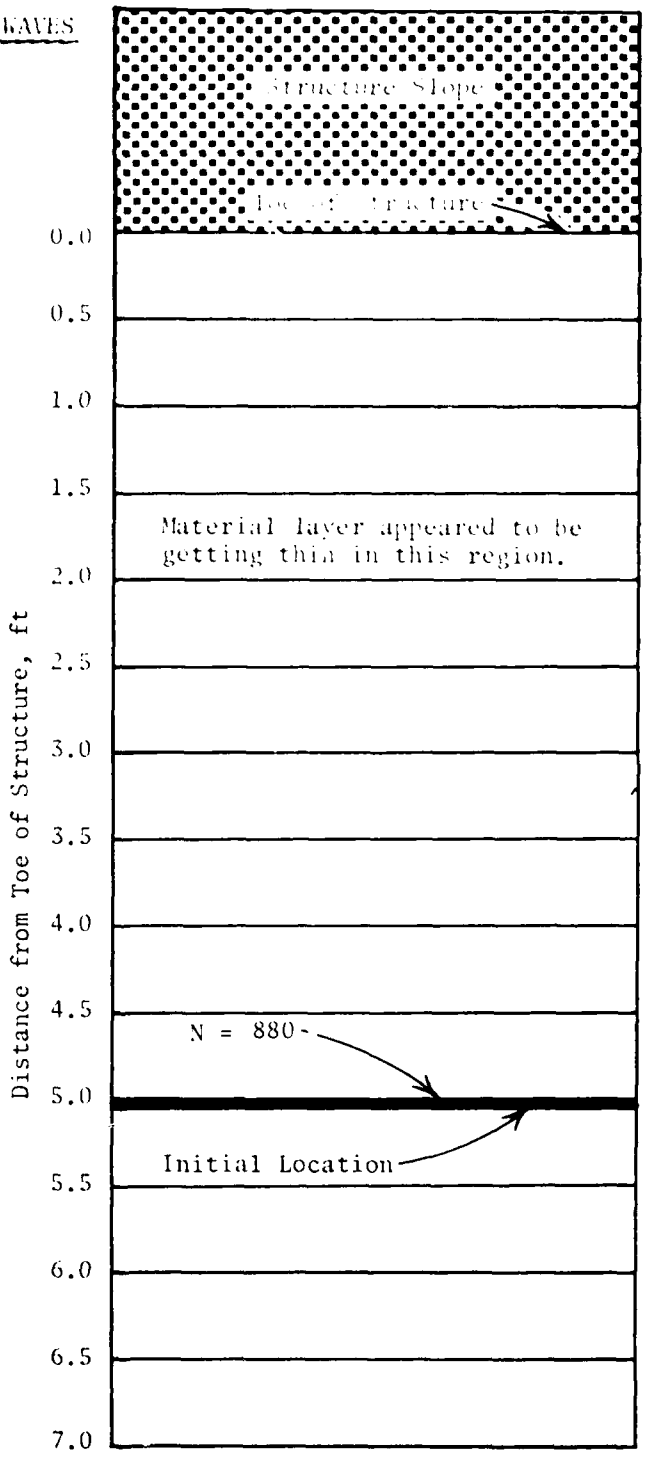

MATERIAL LOCATION AFTER N WAVES

Still-Water Depth, ft
Model: 0.5
Prototype: 8.0

Layer Thickness, ft
Model: 0.125
Prototype: 2.0

Layer Extent, ft
Model: 5
Prototype: 80

Material Size, in.
Model: 3/8 - 1/2
Prototype: 6 - 8

Material Weight, lb
Model: 0.005 - 0.012
Prototype: 20 - 50

Wave Period, sec
Model: 4
Prototype: 16

Bed Slope: 1V on 25H

Maximum Breaker Wave Height, ft
Model: 0.80
Prototype: 12.8

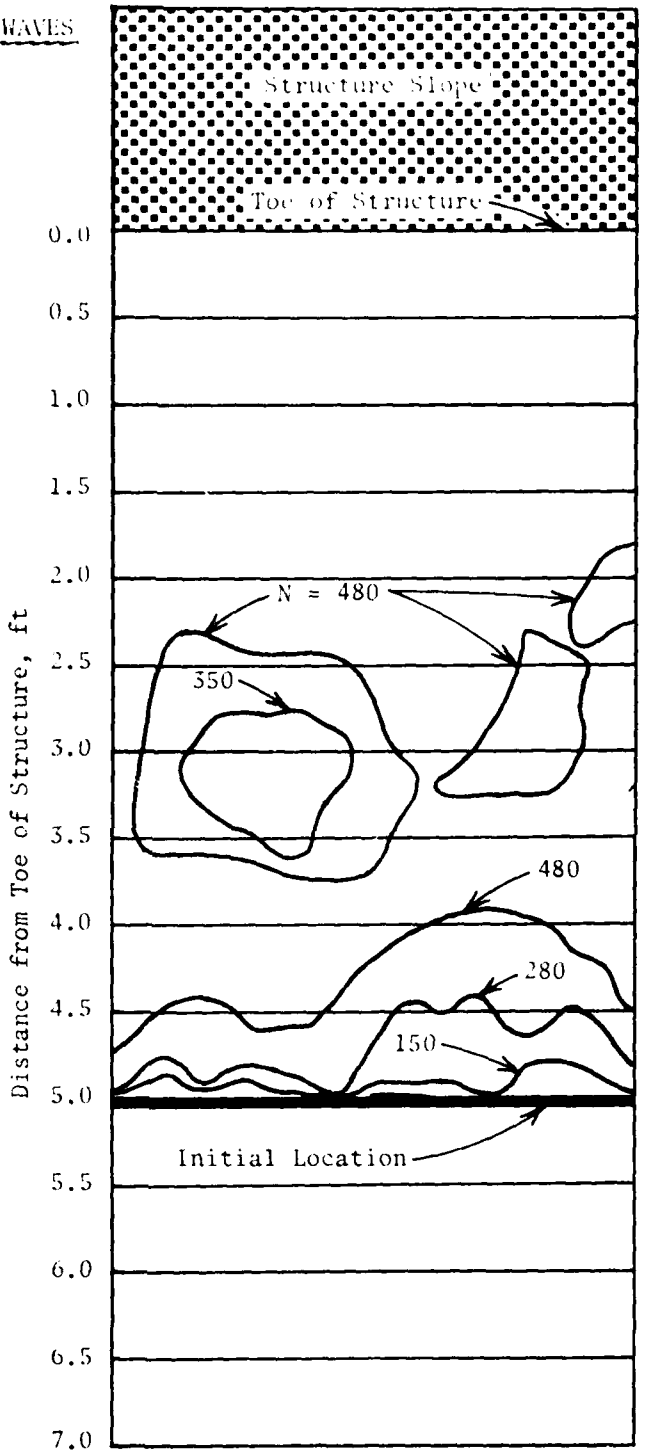

MATERIAL LOCATION AFTER N WAVES

Still-Water Depth, ft
Model: 0.5
Prototype: 8.0

Layer Thickness, ft
Model: 0.125
Prototype: 2.0

Layer Extent, ft
Model: 5
Prototype: 80

Material Size, in.
Model: 3/8 - 1/2
Prototype: 6 - 8

Material Weight, lb
Model: 0.005 - 0.012
Prototype: 20 - 50

Wave Period, sec
Model: 5
Prototype: 20

Bed Slope: 1V on 25H

Maximum Breaker Wave Height, ft
Model: 0.68
Prototype: 10.9

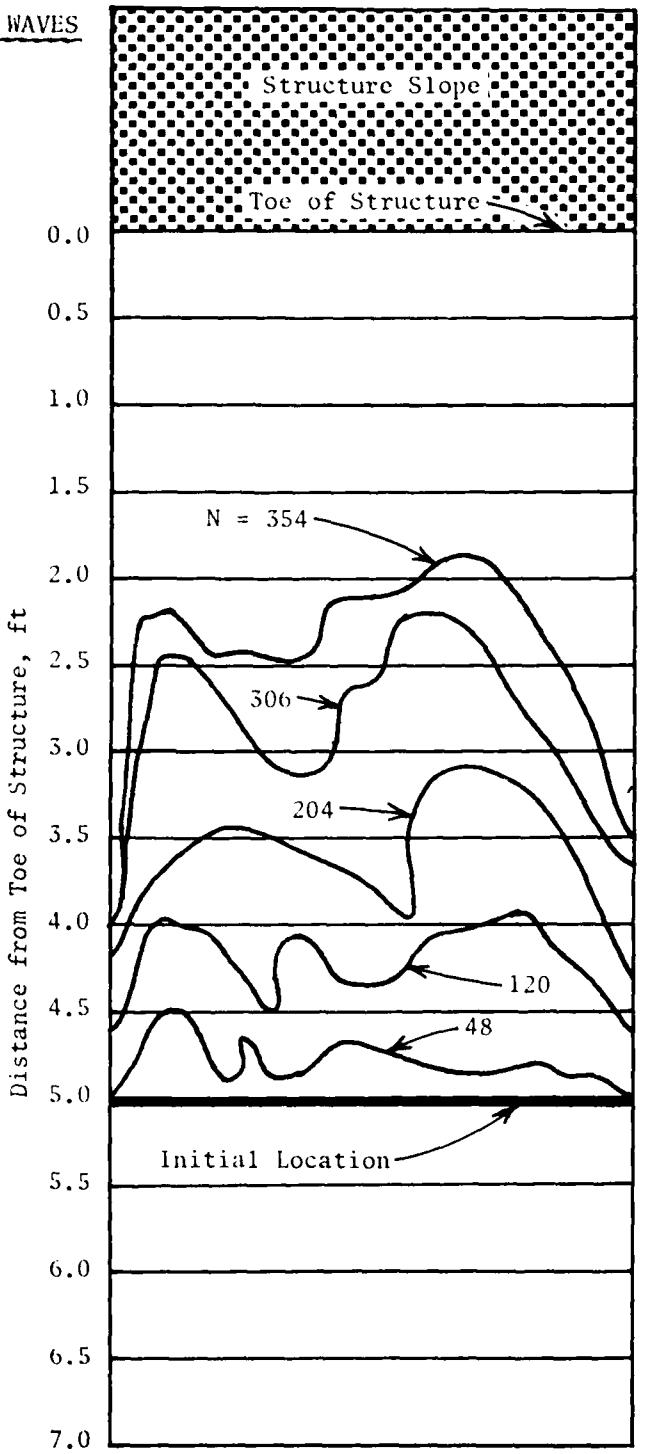

MATERIAL LOCATION AFTER N WAVES

Still-Water Depth, ft
Model: 0.5
Prototype: 8.0

Layer Thickness, ft
Model: 0.125
Prototype: 2.0

Layer Extent, ft
Model: 7
Prototype: 112

Material Size, in.
Model: 3/8 - 1/2
Prototype: 6 - 8

Material Weight, lb
Model: 0.005 - 0.012
Prototype: 20 - 50

Wave Period, sec
Model: 4
Prototype: 16

Bed Slope: 1V on 25H

Maximum Breaker Wave Height, ft
Model: 0.80
Prototype: 12.8

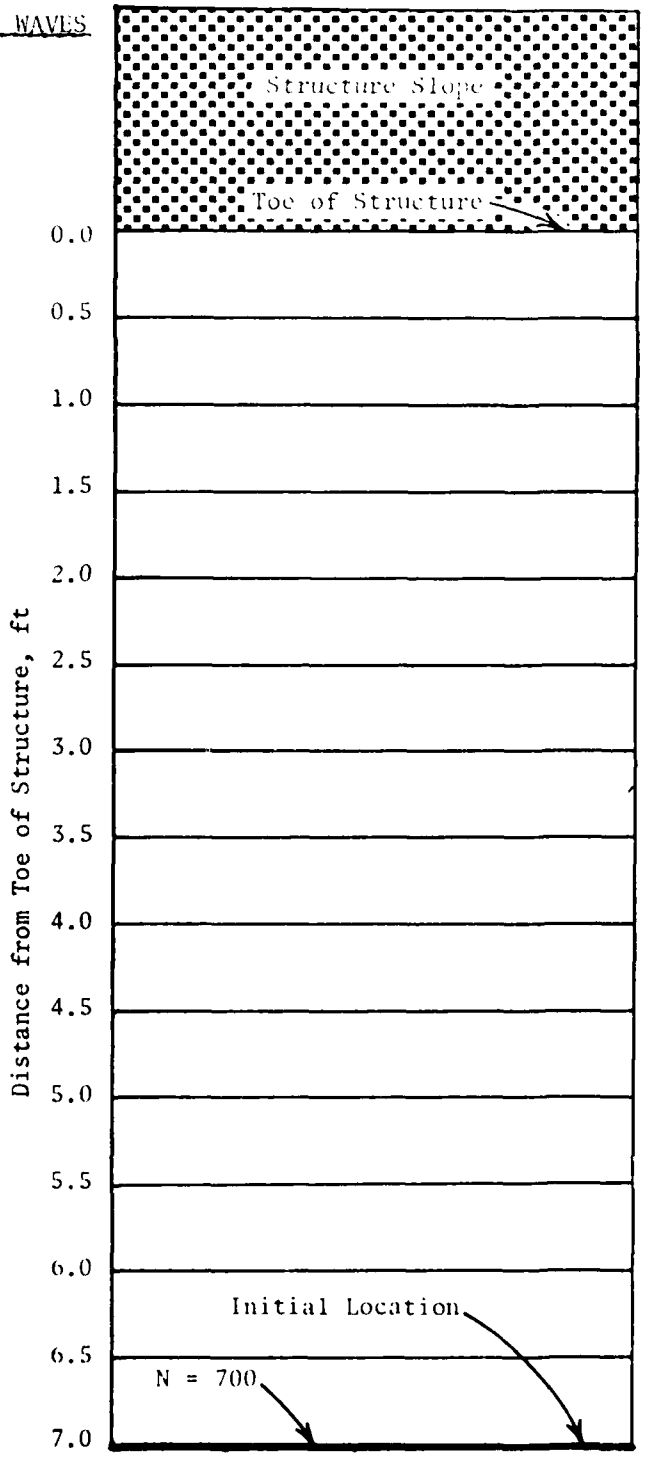

MATERIAL LOCATION AFTER N WAVES

Still-Water Depth, ft
Model: 0.5
Prototype: 8.0

Layer Thickness, ft
Model: 0.125
Prototype: 2.0

Layer Extent, ft
Model: 7
Prototype: 112

Material Size, in.
Model: 3/8 - 1/2
Prototype: 6 - 8

Material Weight, lb
Model: 0.005 - 0.012
Prototype: 20 - 50

Wave Period, sec
Model: 5
Prototype: 20

Bed Slope: 1V on 25H

Maximum Breaker Wave Height, ft
Model: 0.68
Prototype: 10.9

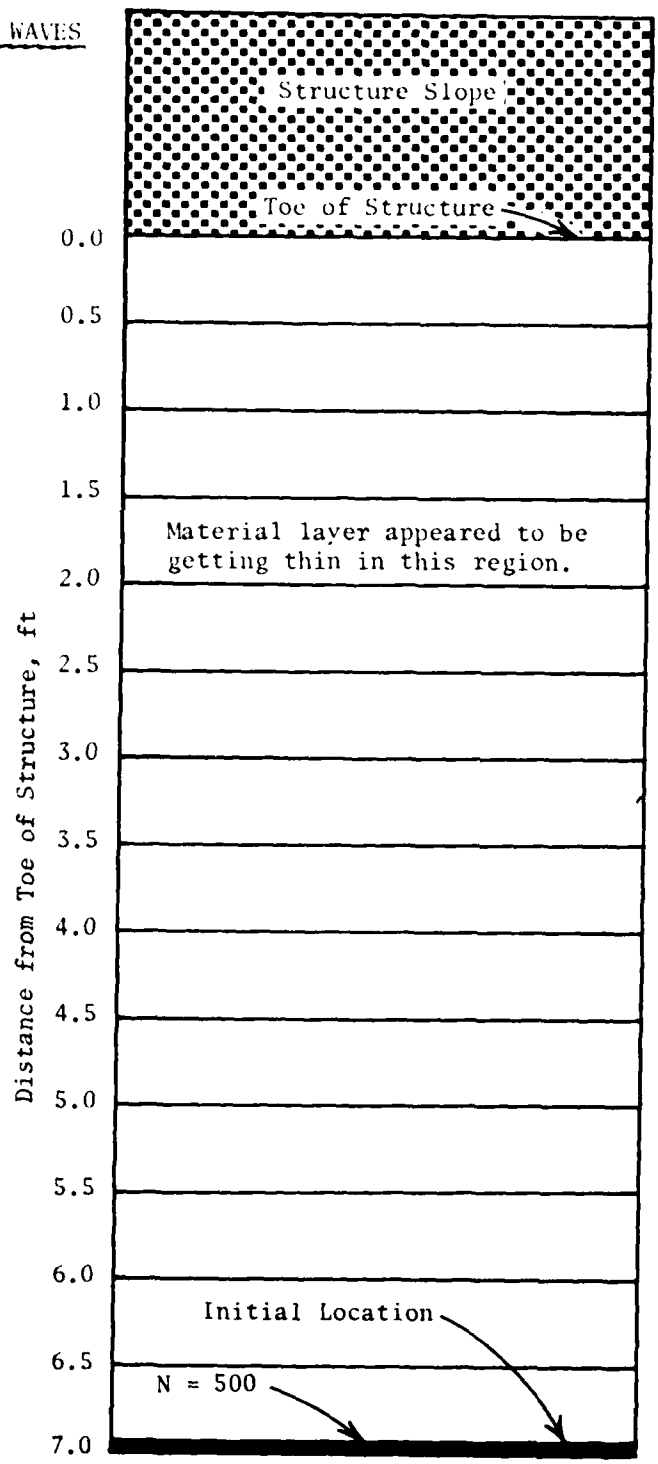

MATERIAL LOCATION AFTER N WAVES

Still-Water Depth, ft
Model: 1.0
Prototype: 16.0

Layer Thickness, ft
Model: 0.125
Prototype: 2.0

Layer Extent, ft
Model: 3
Prototype: 48

Material Size, in.
Model: 3/8 - 1/2
Prototype: 6 - 8

Material Weight, lb
Model: 0.005 - 0.012
Prototype: 20 - 50

Wave Period, sec
Model: 2
Prototype: 8

Bed Slope: 1V on 25H

Maximum Breaker Wave Height, ft
Model: 1.09
Prototype: 17.4

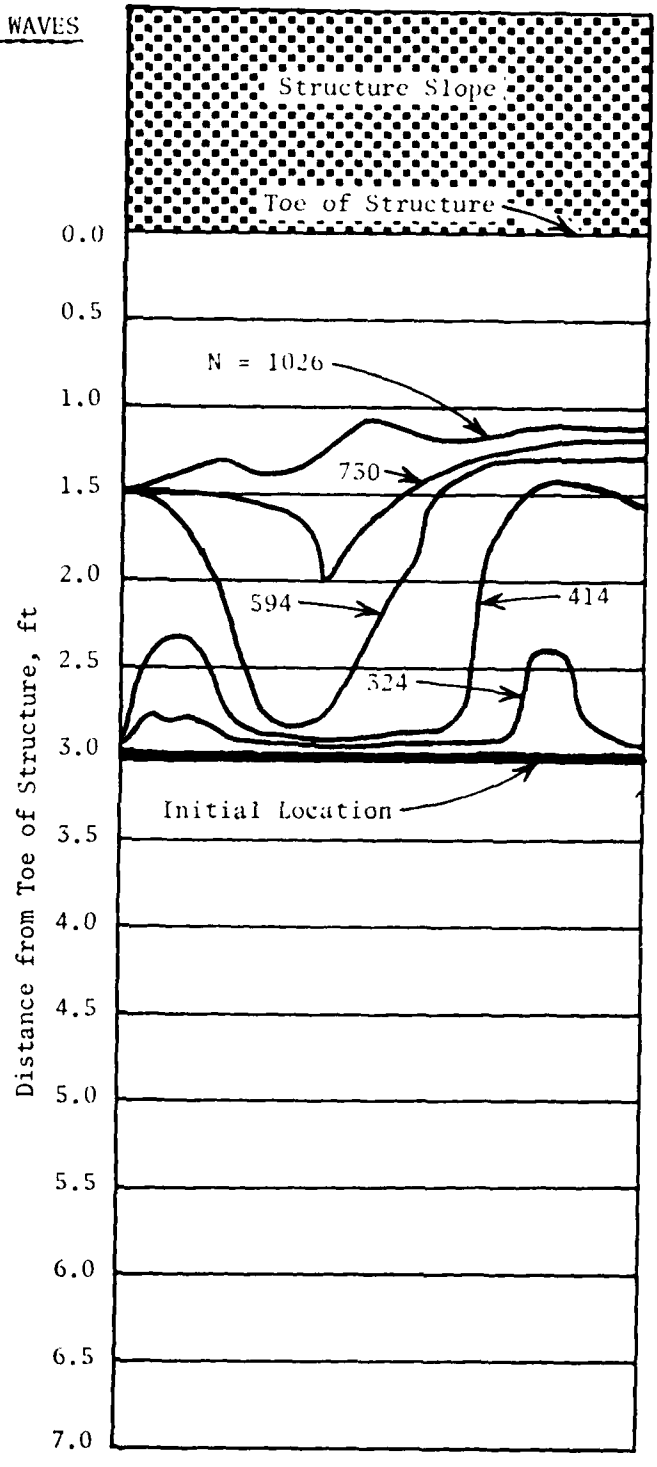

MATERIAL LOCATION AFTER N WAVES

Still-Water Depth, ft
Model: 1.0
Prototype: 16.0

Layer Thickness, ft
Model: 0.125
Prototype: 2.0

Layer Extent, ft
Model: 3
Prototype: 48

Material Size, in.
Model: 3/8 - 1/2
Prototype: 6 - 8

Material Weight, lb
Model: 0.005 - 0.012
Prototype: 20 - 50

Wave Period, sec
Model: 3
Prototype: 12

Bed Slope: 1V on 25H

Maximum Breaker Wave Height, ft
Model: 1.11
Prototype: 17.8

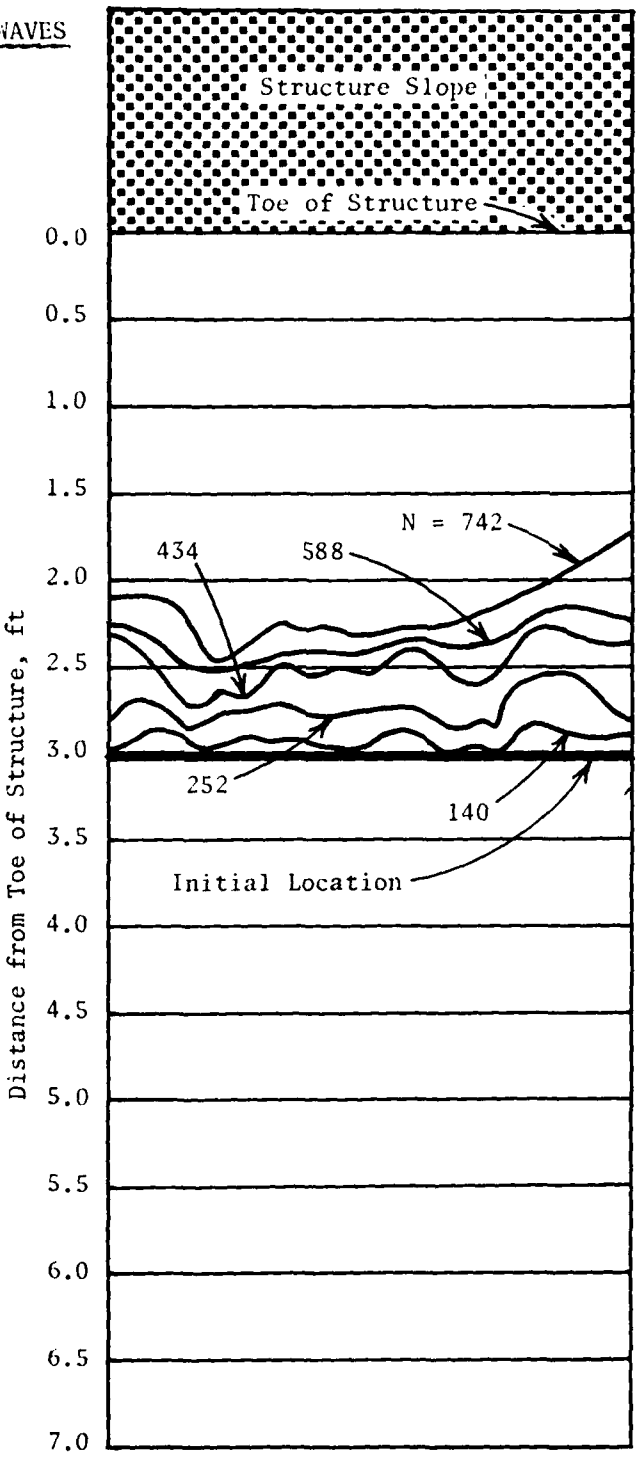

MATERIAL LOCATION AFTER N WAVES

Still-Water Depth, ft

Model: 1.0

Prototype: 16.0

Layer Thickness, ft

Model: 0.125

Prototype: 2.0

Layer Extent, ft

Model: 3

Prototype: 48

Material Size, in.

Model: 3/8 - 1/2

Prototype: 6 - 8

Material Weight, lb

Model: 0.005 - 0.012

Prototype: 20 - 50

Wave Period, sec

Model: 4

Prototype: 16

Bed Slope: 1V on 25H

Maximum Breaker Wave Height, ft

Model: 1.45

Prototype: 23.2

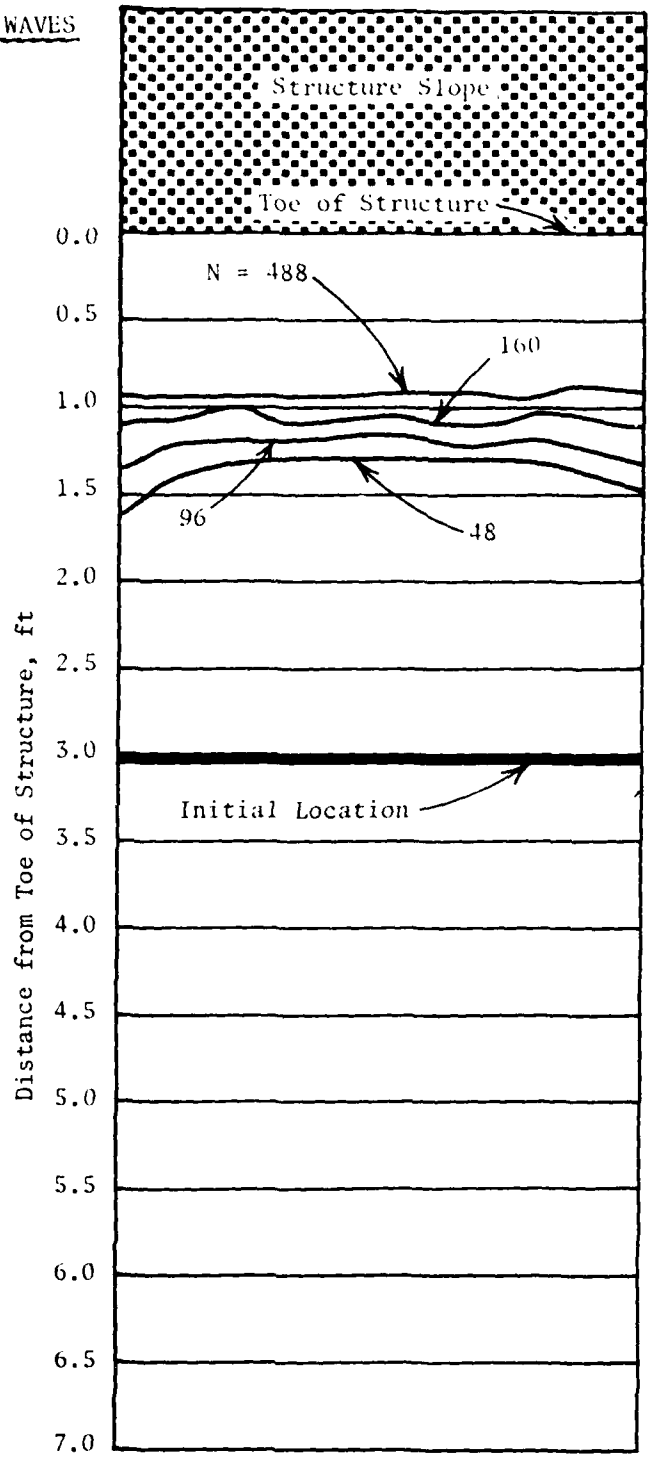

MATERIAL LOCATION AFTER N WAVES

Still-Water Depth, ft
Model: 1.0
Prototype: 16.0

Layer Thickness, ft
Model: 0.125
Prototype: 2.0

Layer Extent, ft
Model: 3
Prototype: 48

Material Size, in.
Model: 3/8 - 1/2
Prototype: 6 - 8

Material Weight, lb
Model: 0.005 - 0.012
Prototype: 20 - 50

Wave Period, sec
Model: 5
Prototype: 20

Bed Slope: 1V on 25H

Maximum Breaker Wave Height, ft
Model: 1.12
Prototype: 17.9

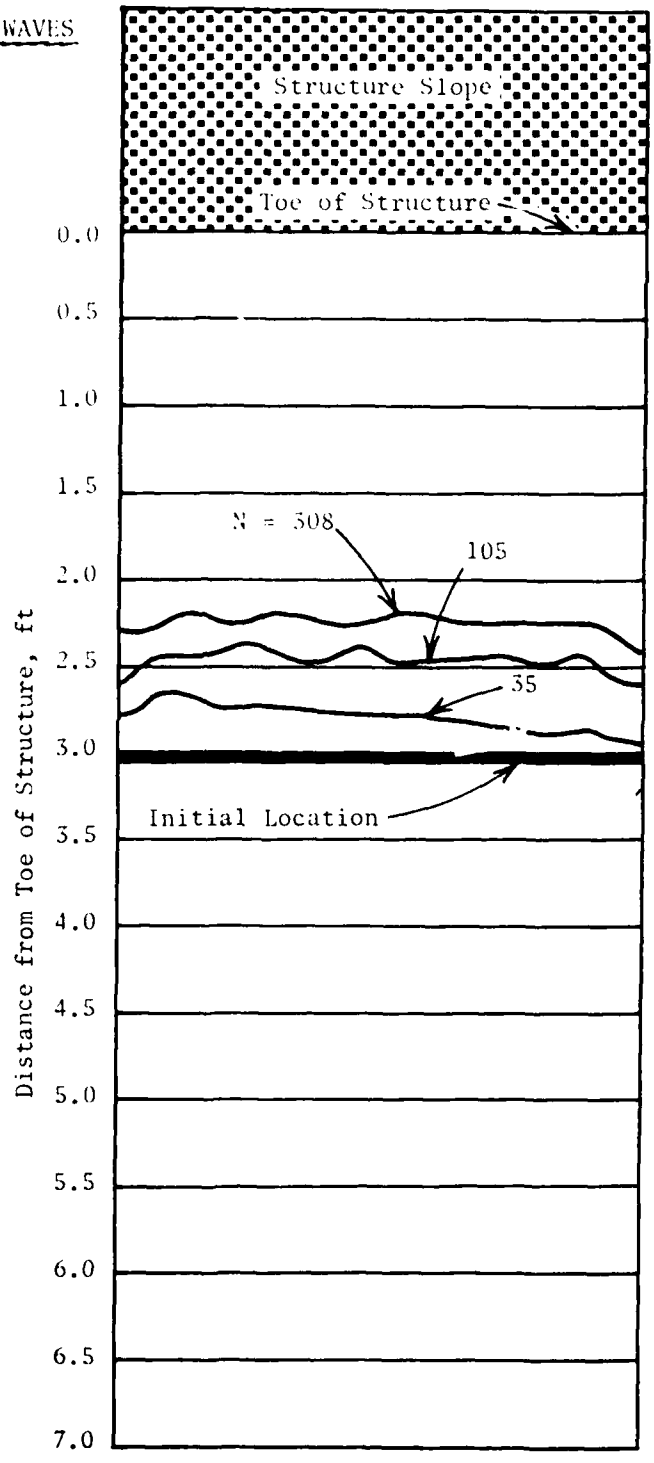

MATERIAL LOCATION AFTER N WAVES

Still-Water Depth, ft

Model: 1.0

Prototype: 16.0

Layer Thickness, ft

Model: 0.125

Prototype: 2.0

Layer Extent, ft

Model: 5

Prototype: 80

Material Size, in.

Model: 3/8 - 1/2

Prototype: 6 - 8

Material Weight, lb

Model: 0.005 - 0.012

Prototype: 20 - 50

Wave Period, sec

Model: 2

Prototype: 8

Bed Slope: 1V on 25H

Maximum Breaker Wave Height, ft

Model: 1.09

Prototype: 17.4

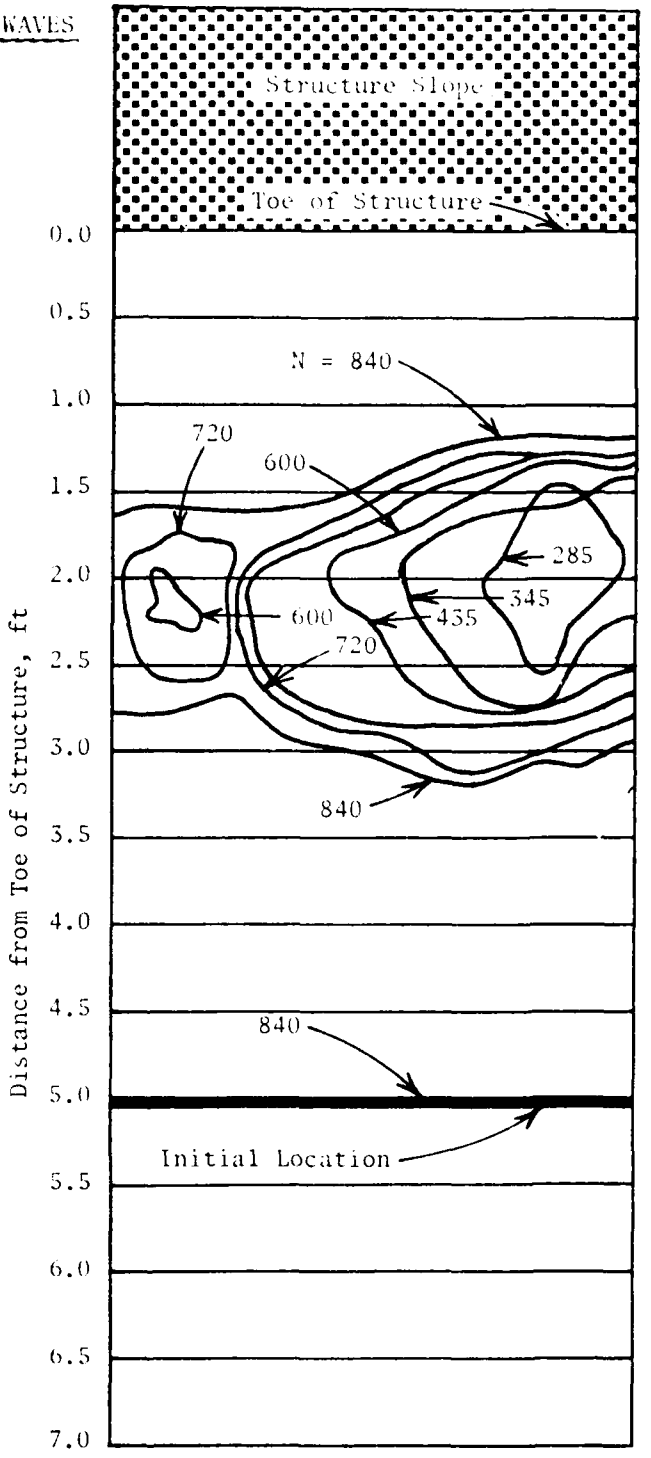

MATERIAL LOCATION AFTER N WAVES

Still-Water Depth, ft
Model: 1.0
Prototype: 16.0

Layer Thickness, ft
Model: 0.125
Prototype: 2.0

Layer Extent, ft
Model: 5
Prototype: 80

Material Size, in.
Model: 3/8 - 1/2
Prototype: 6 - 8

Material Weight, lb
Model: 0.005 - 0.012
Prototype: 20 - 50

Wave Period, sec
Model: 3
Prototype: 12

Bed Slope: 1V on 25H

Maximum Breaker Wave Height, ft
Model: 1.11
Prototype: 17.8

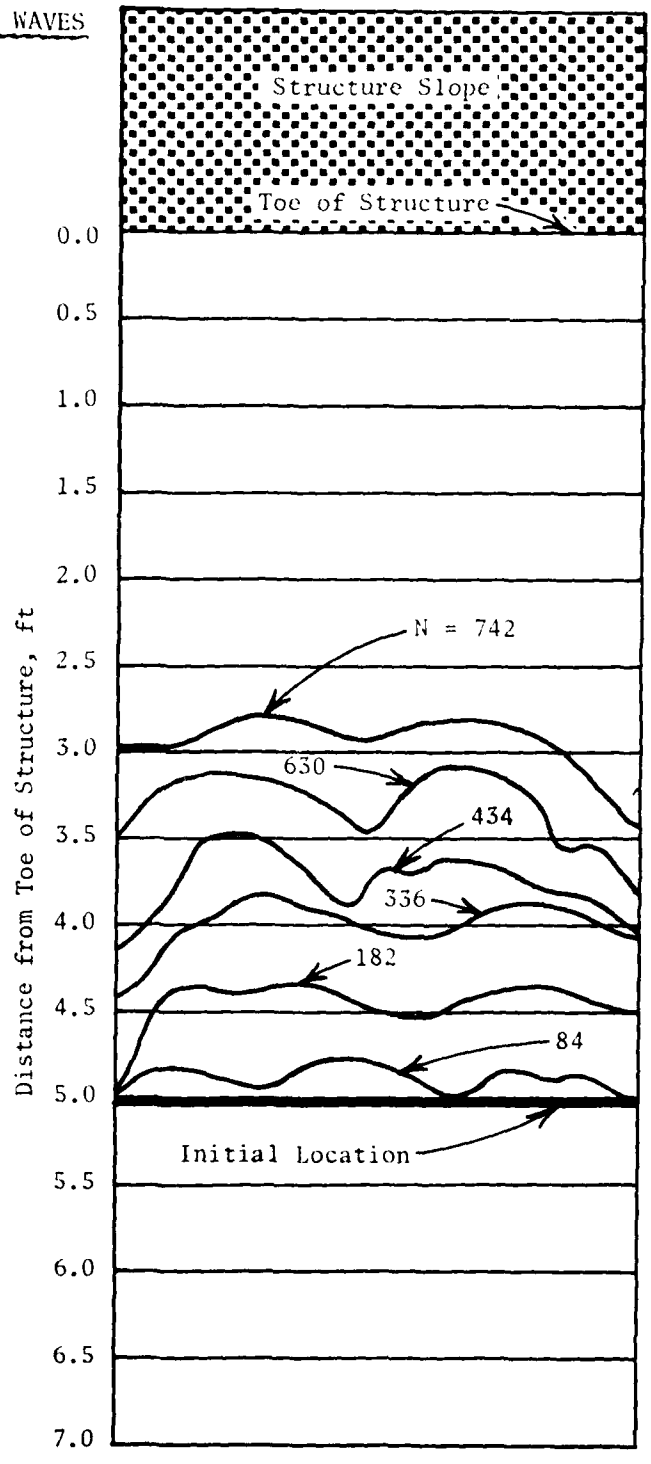

MATERIAL LOCATION AFTER N WAVES

Still-Water Depth, ft
Model: 1.0
Prototype: 16.0

Layer Thickness, ft
Model: 0.125
Prototype: 2.0

Layer Extent, ft
Model: 5
Prototype: 80

Material Size, in.
Model: 3/8 - 1/2
Prototype: 6 - 8

Material Weight, lb
Model: 0.005 - 0.012
Prototype: 20 - 30

Wave Period, sec
Model: 4
Prototype: 16

Bed Slope: 1V on 25H

Maximum Breaker Wave Height, ft
Model: 1.45
Prototype: 23.2

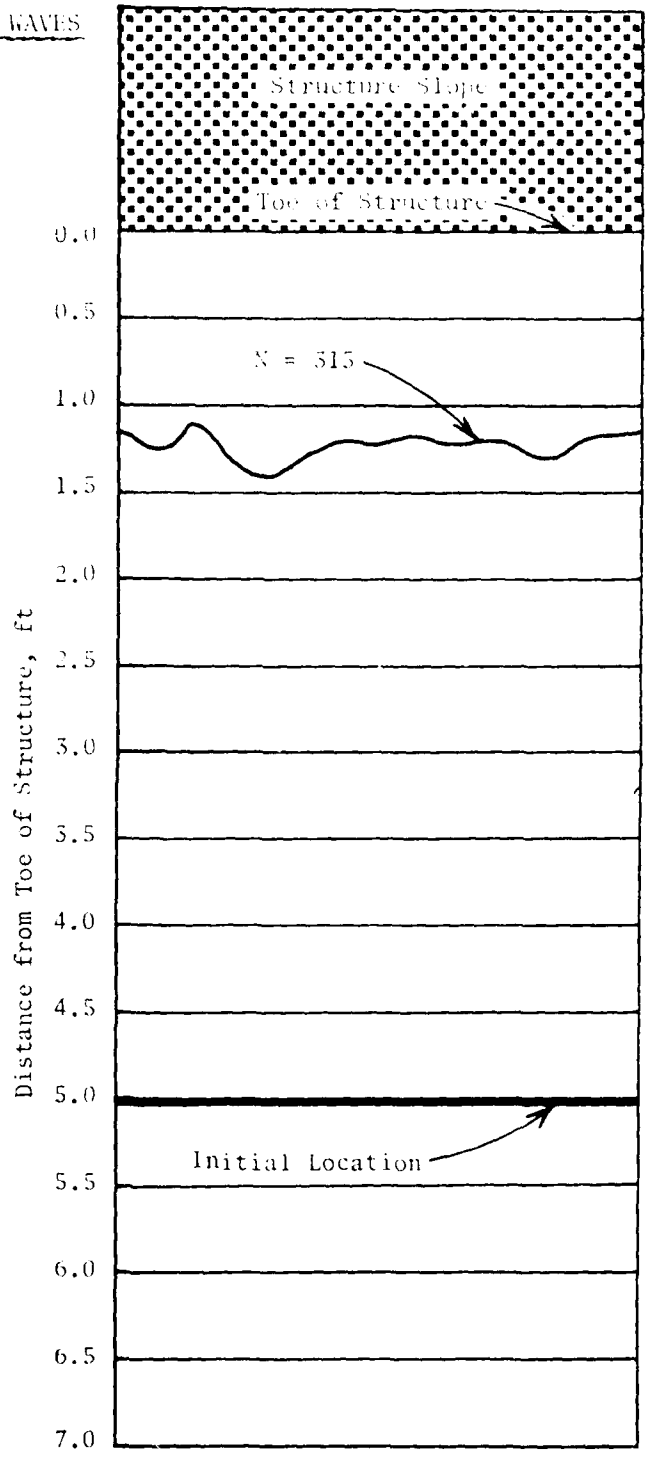

MATERIAL LOCATION AFTER N WAVES

Still-Water Depth, ft
Model: 1.0
Prototype: 16.0

Layer Thickness, ft
Model: 0.125
Prototype: 2.0

Layer Extent, ft
Model: 5
Prototype: 80

Material Size, in.
Model: 3/8 - 1/2
Prototype: 6 - 8

Material Weight, lb
Model: 0.005 - 0.012
Prototype: 20 - 60

Wave Period, sec
Model: 5
Prototype: 20

Bed Slope: 1V on 25H

Maximum Breaker Wave Height, ft
Model: 1.12
Prototype: 17.9

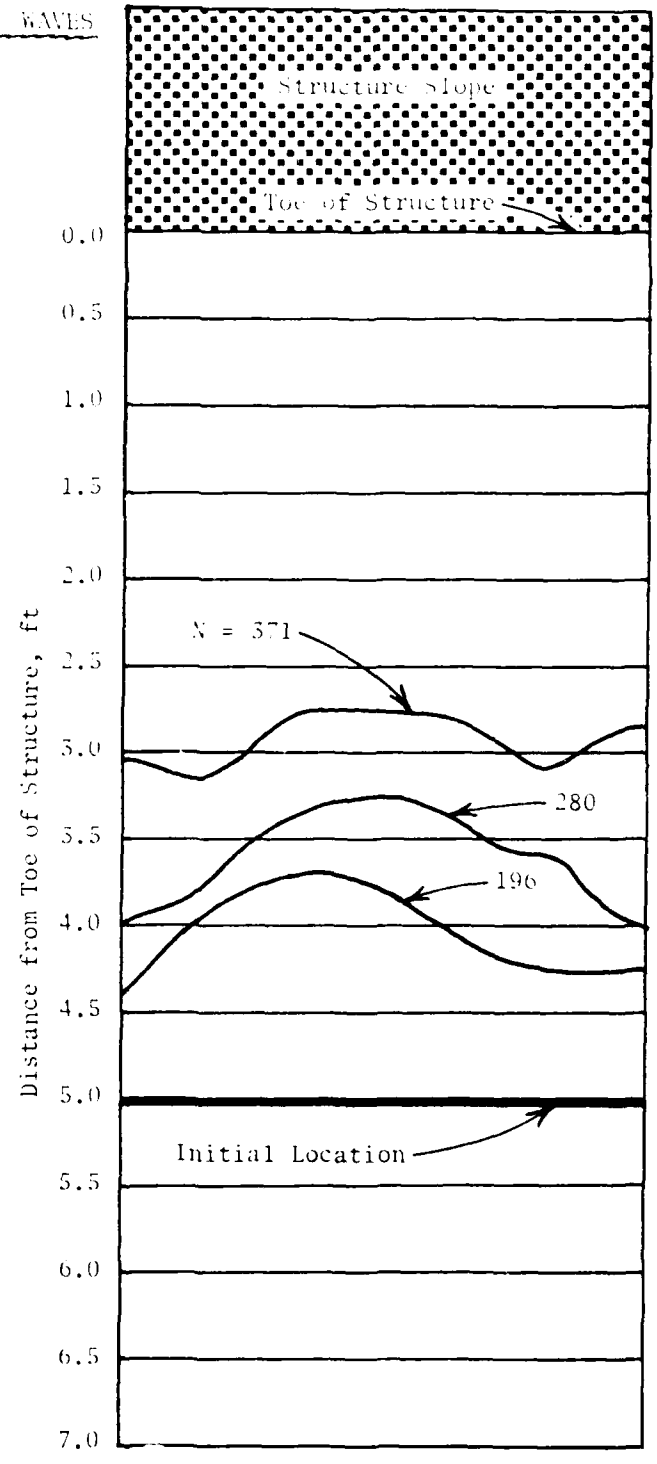

MATERIAL LOCATION AFTER N WAVES

Still-Water Depth, ft
Model: 1.0
Prototype: 16.0

Layer Thickness, ft
Model: 0.125
Prototype: 2.0

Layer Extent, ft
Model: 7
Prototype: 112

Material Size, in.
Model: 3/8 - 1/2
Prototype: 6 - 8

Material Weight, lb
Model: 0.005 - 0.012
Prototype: 20 - 50

Wave Period, sec
Model: 2
Prototype: 8

Bed Slope: 1V on 25H

Maximum Breaker Wave Height, ft
Model: 1.09
Prototype: 17.4

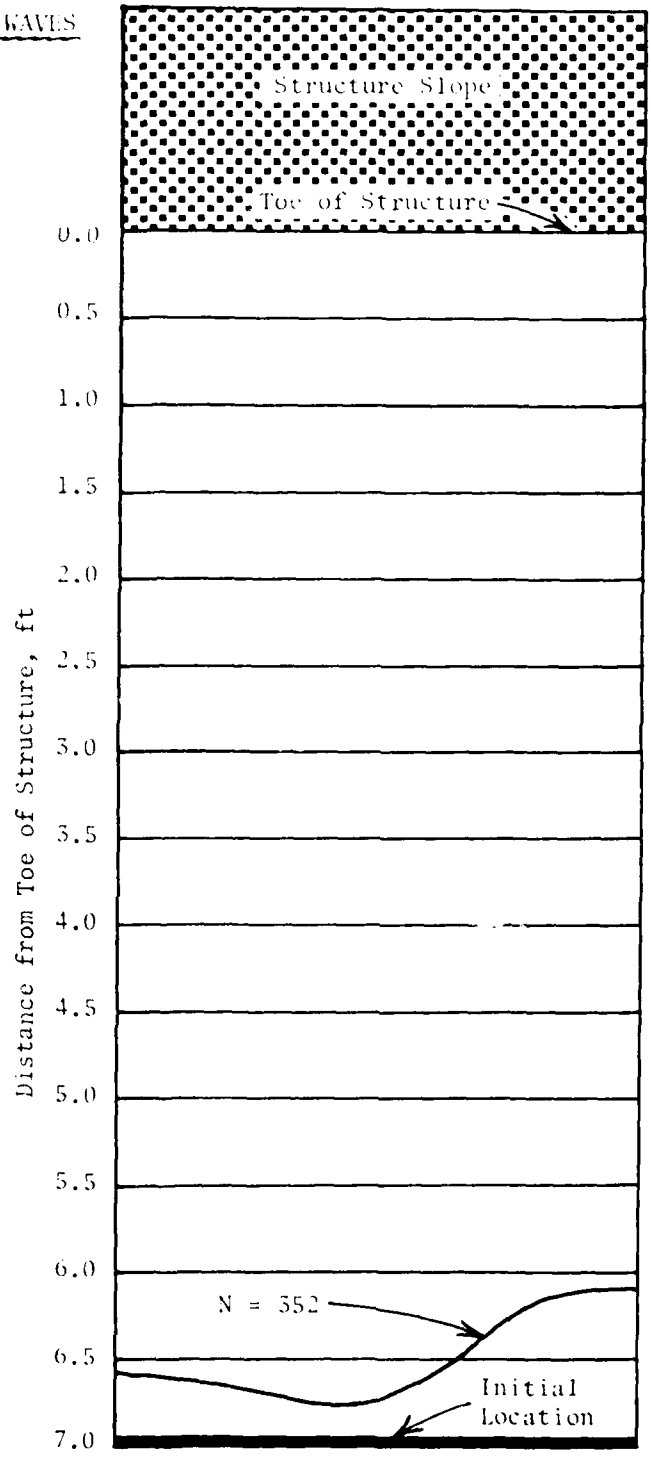

MATERIAL LOCATION AFTER N WAVES

Still-Water Depth, ft
Model: 1.0
Prototype: 16.0

Layer Thickness, ft
Model: 0.125
Prototype: 2.0

Layer Extent, ft
Model: 7
Prototype: 112

Material Size, in.
Model: 3/8 - 1/2
Prototype: 6 - 8

Material Weight, lb
Model: 0.005 - 0.012
Prototype: 20 - 50

Wave Period, sec
Model: 3
Prototype: 12

Bed Slope: 1V on 25H

Maximum Breaker Wave Height, ft
Model: 1.11
Prototype: 17.8

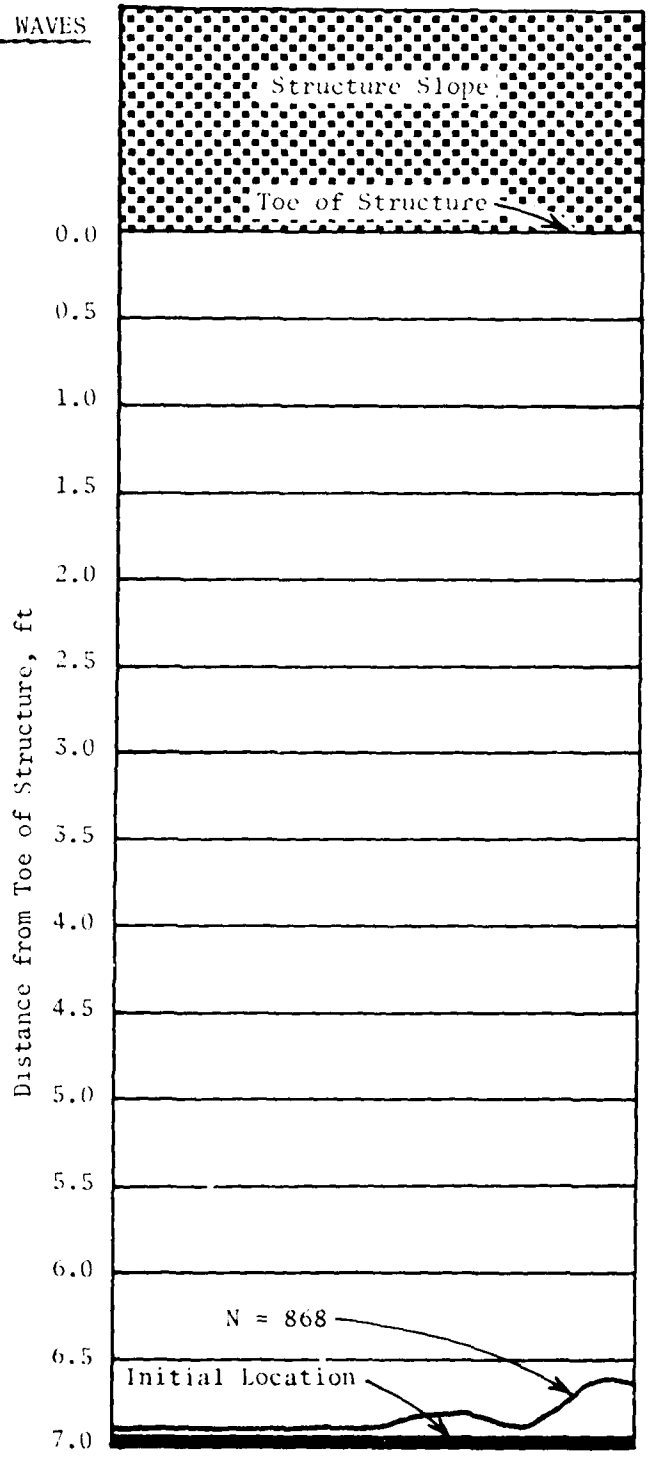

MATERIAL LOCATION AFTER N WAVES

Still-Water Depth, ft
Model: 1.0
Prototype: 16.0

Layer Thickness, ft
Model: 0.125
Prototype: 2.0

Layer Extent, ft
Model: 7
Prototype: 112

Material Size, in.
Model: 3/8 - 1/2
Prototype: 6 - 8

Material Weight, lb
Model: 0.005 - 0.012
Prototype: 20 - 50

Wave Period, sec
Model: 4
Prototype: 16

Bed Slope: 1V on 25H

Maximum Breaker Wave Height, ft
Model: 1.45
Prototype: 23.2

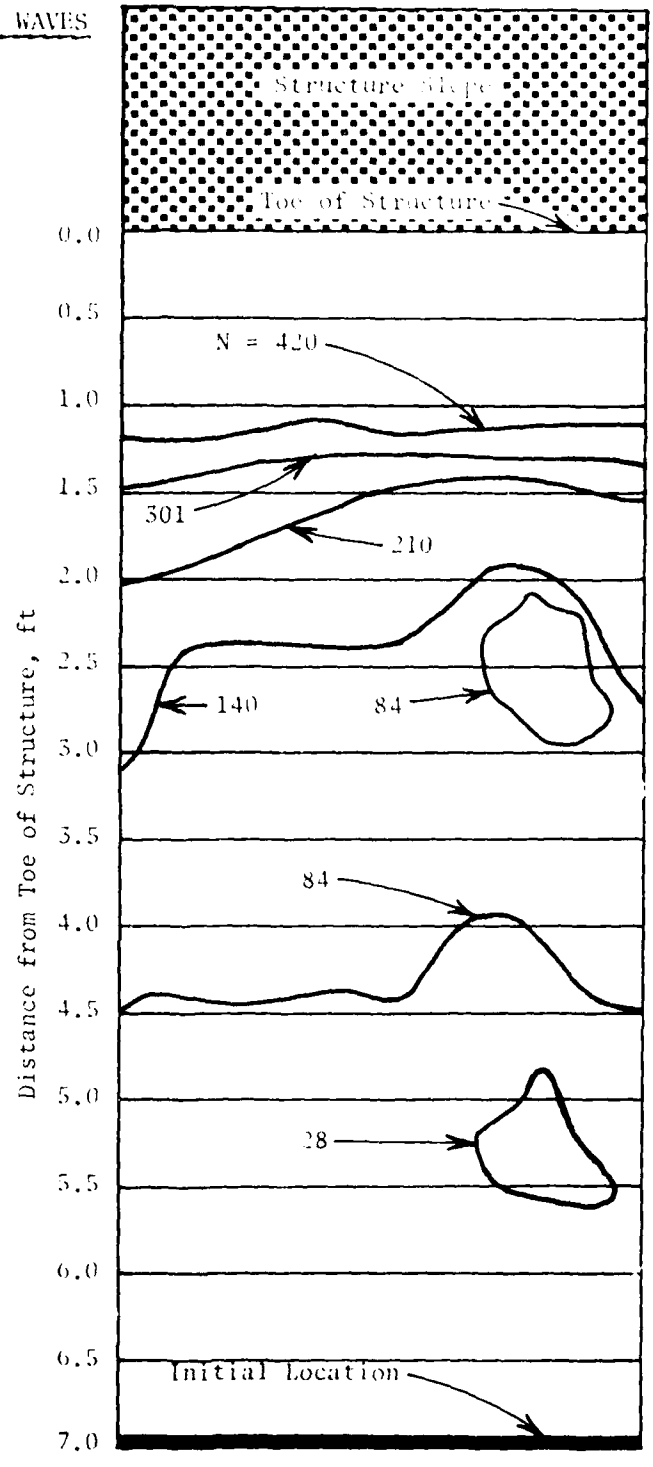

MATERIAL LOCATION AFTER N WAVES

Still-Water Depth, ft
Model: 1.0
Prototype: 16.0

Layer Thickness, ft
Model: 0.125
Prototype: 2.0

Layer Extent, ft
Model: 7
Prototype: 112

Material Size, in.
Model: 3/8 - 1/2
Prototype: 6 - 8

Material Weight, lb
Model: 0.005 -0.012
Prototype: 20 - 50

Wave Period, sec
Model: 5
Prototype: 20

Bed Slope: 1V on 25H

Maximum Breaker Wave Height, ft
Model: 1.12
Prototype: 17.9

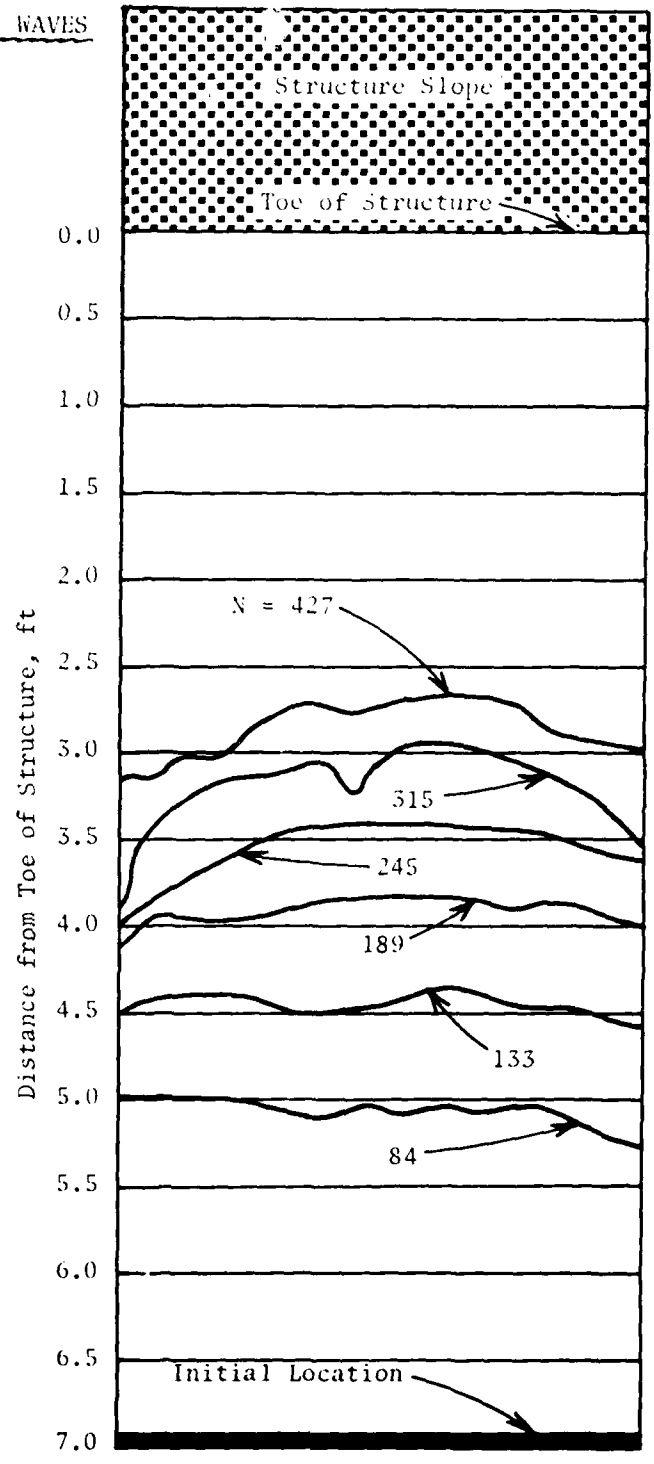

MATERIAL LOCATION AFTER N WAVES

Still-Water Depth, ft
Model: 0.5
Prototype: 8.0

Layer Thickness, ft
Model: 0.125
Prototype: 2.0

Layer Extent, ft
Model: 3
Prototype: 48

Material Size, in.
Model: 1/2 - 5/8
Prototype: 8 - 10

Material Weight, lb
Model: 0.012 - 0.025
Prototype: 50 - 95

Wave Period, sec
Model: 4
Prototype: 16

Bed Slope: 1V on 25H

Maximum Breaker Wave Height, ft
Model: 0.80
Prototype: 12.8

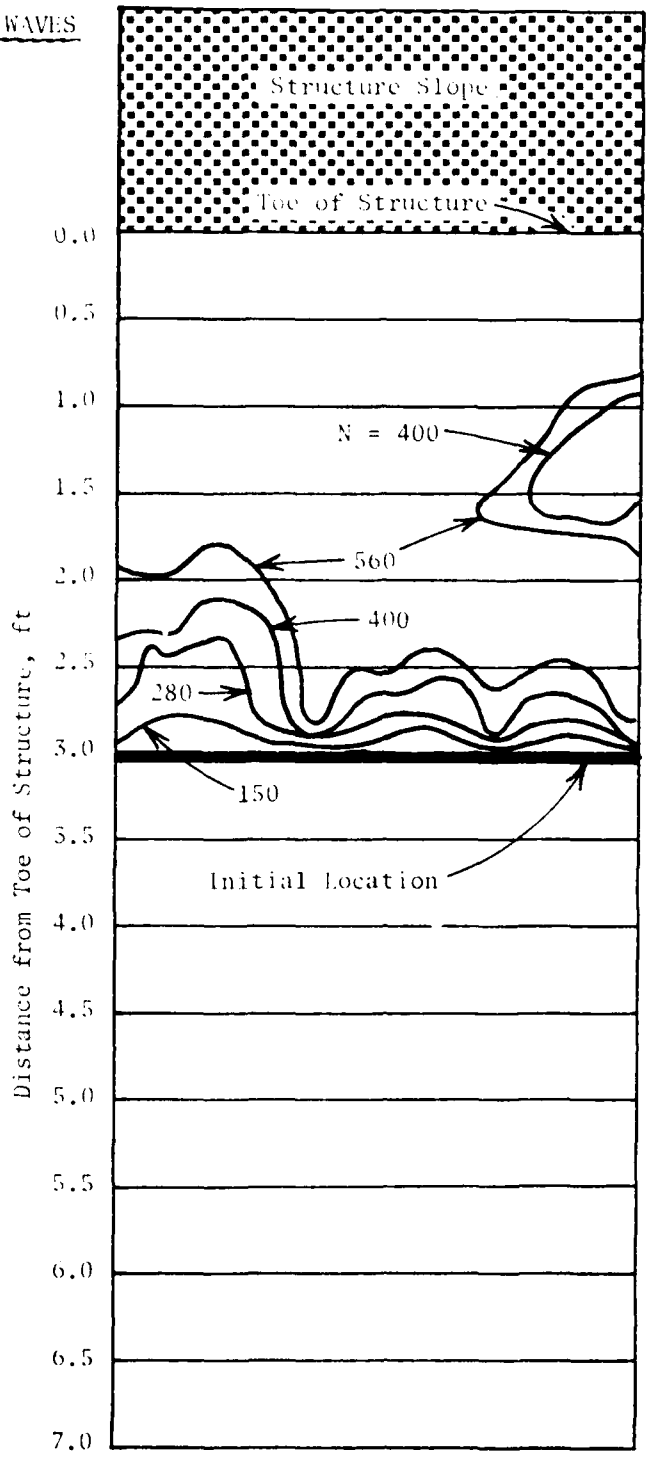

MATERIAL LOCATION AFTER N WAVES

Still-Water Depth, ft
Model: 0.5
Prototype: 8.0

Layer Thickness, ft
Model: 0.125
Prototype: 2.0

Layer Extent, ft
Model: 3
Prototype: 48

Material Size, in.
Model: 1/2 - 5/8
Prototype: 8 - 10

Material Weight, lb
Model: 0.012 - 0.023
Prototype: 50 - 95

Wave Period, sec
Model: 5
Prototype: 20

Bed Slope: 1V on 25H

Maximum Breaker Wave Height, ft
Model: 0.68
Prototype: 10.9

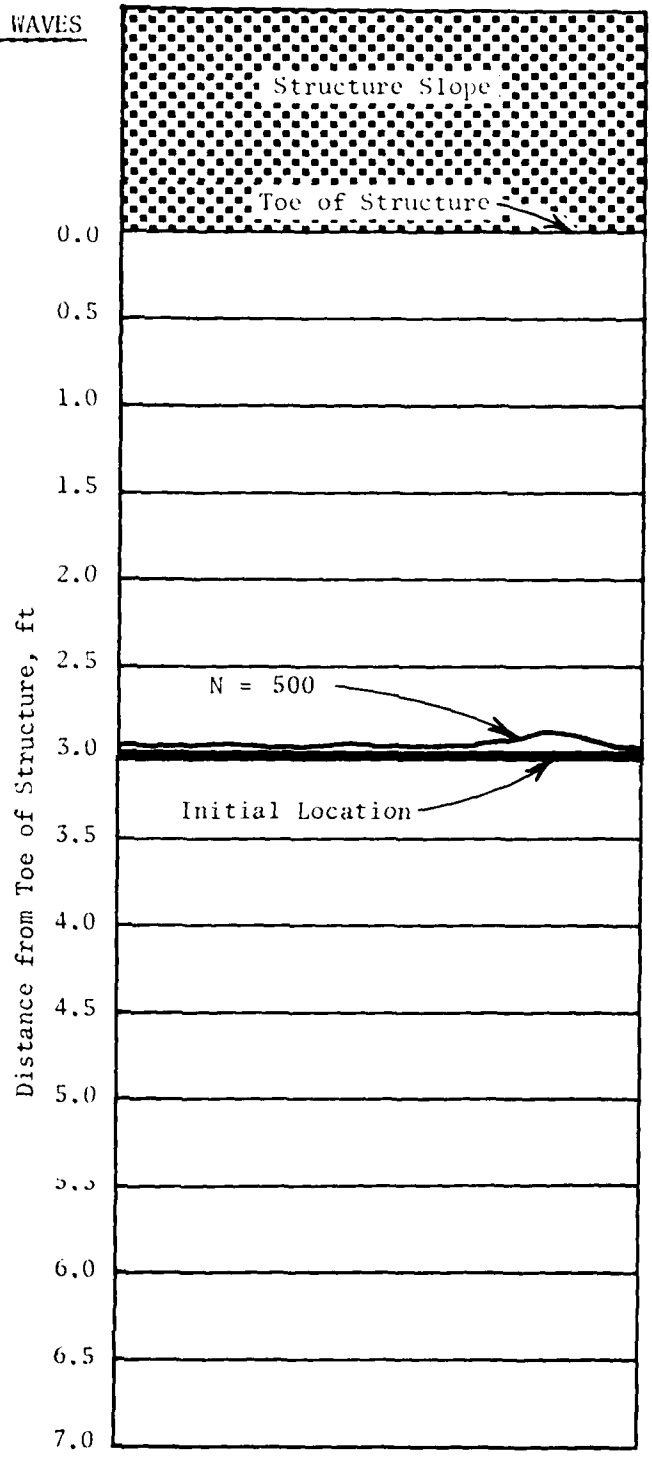

MATERIAL LOCATION AFTER N WAVES

Still-Water Depth, ft
Model: 0.5
Prototype: 8.0

Layer Thickness, ft
Model: 0.125
Prototype: 2.0

Layer Extent, ft
Model: 5
Prototype: 80

Material Size, in.
Model: 1/2 - 5/8
Prototype: 8 - 10

Material Weight, lb
Model: 0.012 - 0.025
Prototype: 50 - 95

Wave Period, sec
Model: 4
Prototype: 16

Bed Slope: 1V on 25H

Maximum Breaker Wave Height, ft
Model: 0.80
Prototype: 12.8

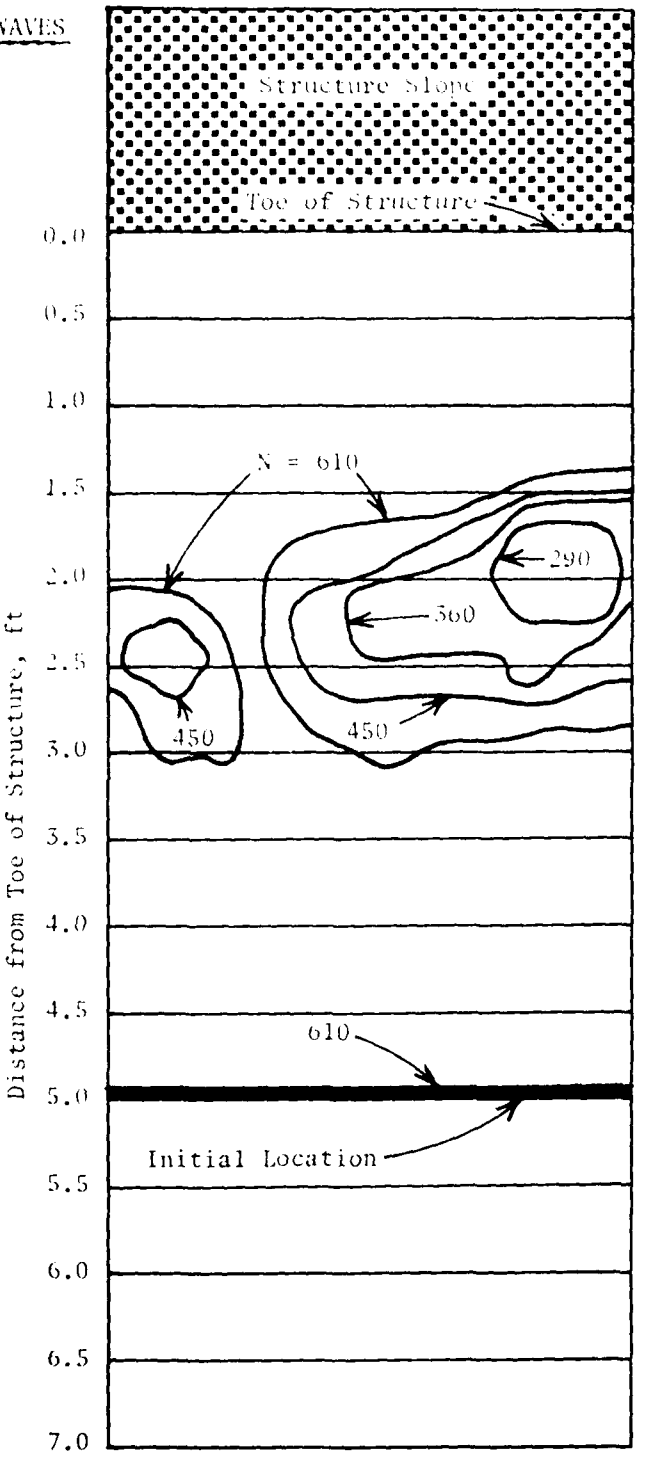

MATERIAL LOCATION AFTER N WAVES

Still-Water Depth, ft
Model: 0.5
Prototype: 8.0

Layer Thickness, ft
Model: 0.125
Prototype: 2.0

Layer Extent, ft
Model: 5
Prototype: 80

Material Size, in.
Model: 1/2 - 5/8
Prototype: 8 - 10

Material Weight, lb
Model: 0.012 - 0.023
Prototype: 50 - 95

Wave Period, sec
Model: 5
Prototype: 20

Bed Slope: 1V on 25H

Maximum Breaker Wave Height, ft
Model: 0.68
Prototype: 10.9

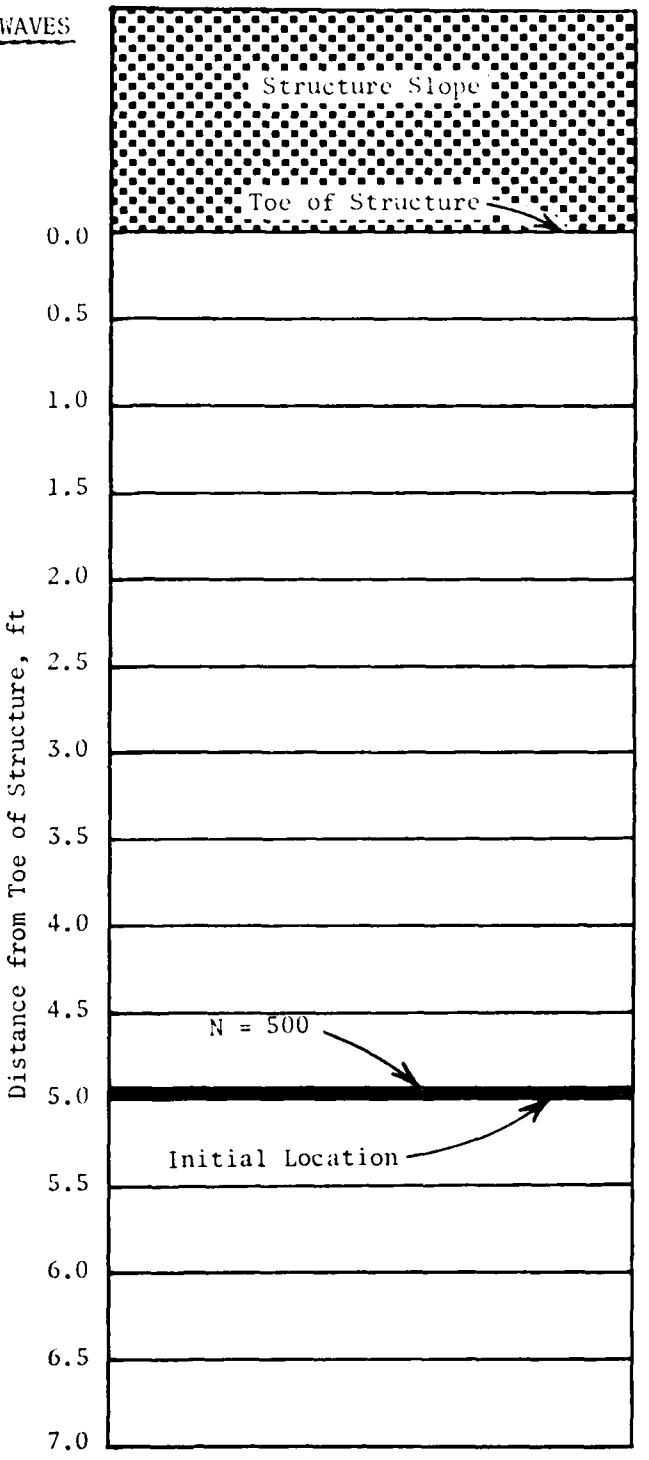

MATERIAL LOCATION AFTER N WAVES

Still-Water Depth, ft
Model: 0.5
Prototype: 8.0

Layer Thickness, ft
Model: 0.125
Prototype: 2.0

Layer Extent, ft
Model: 7
Prototype: 112

Material Size, in.
Model: 1/2 - 5/8
Prototype: 8 - 10

Material Weight, lb
Model: 0.012 - 0.025
Prototype: 50 - 95

Wave Period, sec
Model: 4
Prototype: 16

Bed Slope: 1V on 25H

Maximum Breaker Wave Height, ft
Model: 0.80
Prototype: 12.8

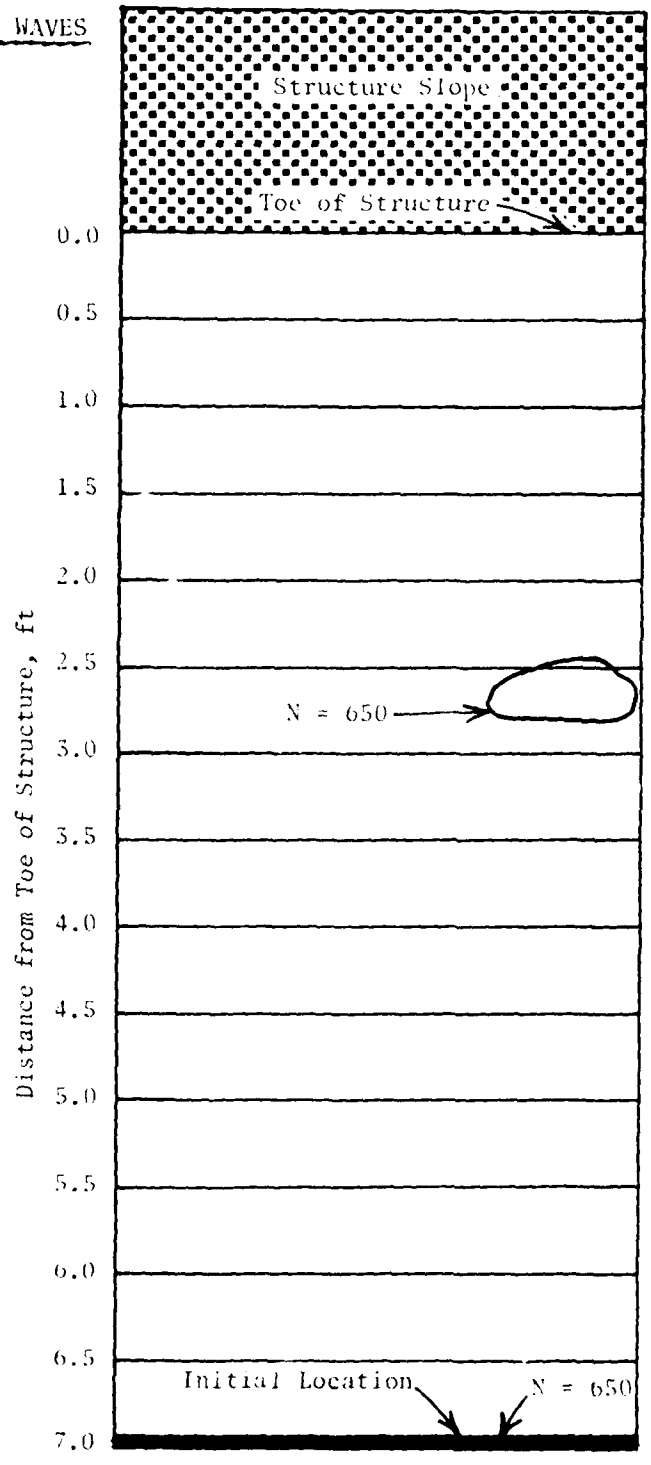

MATERIAL LOCATION AFTER N WAVES

Still-Water Depth, ft
Model: 0.5
Prototype: 8.0

Layer Thickness, ft
Model: 0.125
Prototype: 2.0

Layer Extent, ft
Model: 7
Prototype: 112

Material Size, in.
Model: 1/2 - 5/8
Prototype: 8 - 10

Material Weight, lb
Model: 0.012 - 0.023
Prototype: 50 - 95

Wave Period, sec
Model: 5
Prototype: 20

Bed Slope: 1V on 25H

Maximum Breaker Wave Height, ft
Model: 0.68
Prototype: 10.9

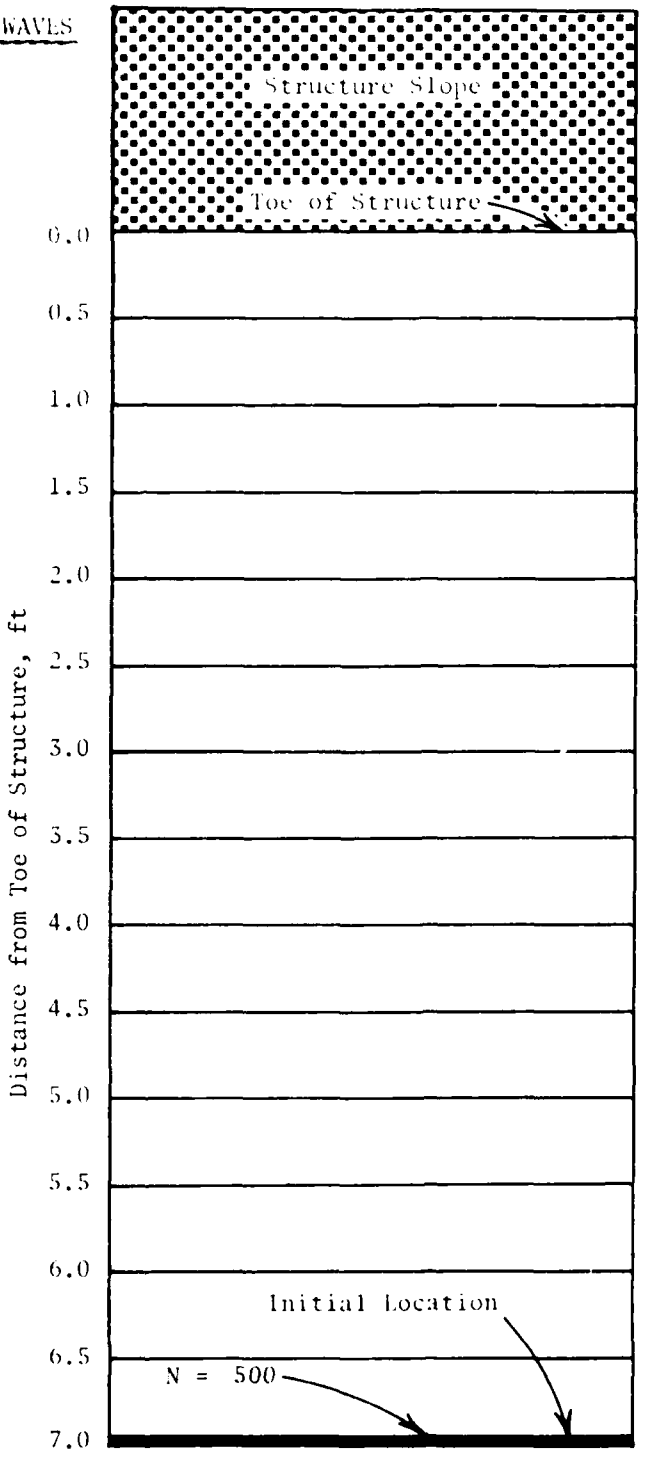

MATERIAL LOCATION AFTER N WAVES

Still-Water Depth, ft

Model: 1.0

Prototype: 16.0

Layer Thickness, ft

Model: 0.125

Prototype: 2.0

Layer Extent, ft

Model: 3

Prototype: 48

Material Size, in.

Model: 1.2 - 3.8

Prototype: 8 - 10

Material Weight, lb

Model: 0.012 - 0.025

Prototype: 50 - 95

Wave Period, sec

Model: 2

Prototype: 8

Bed Slope: 1V on 25H

Maximum Breaker Wave Height, ft

Model: 1.09

Prototype: 17.4

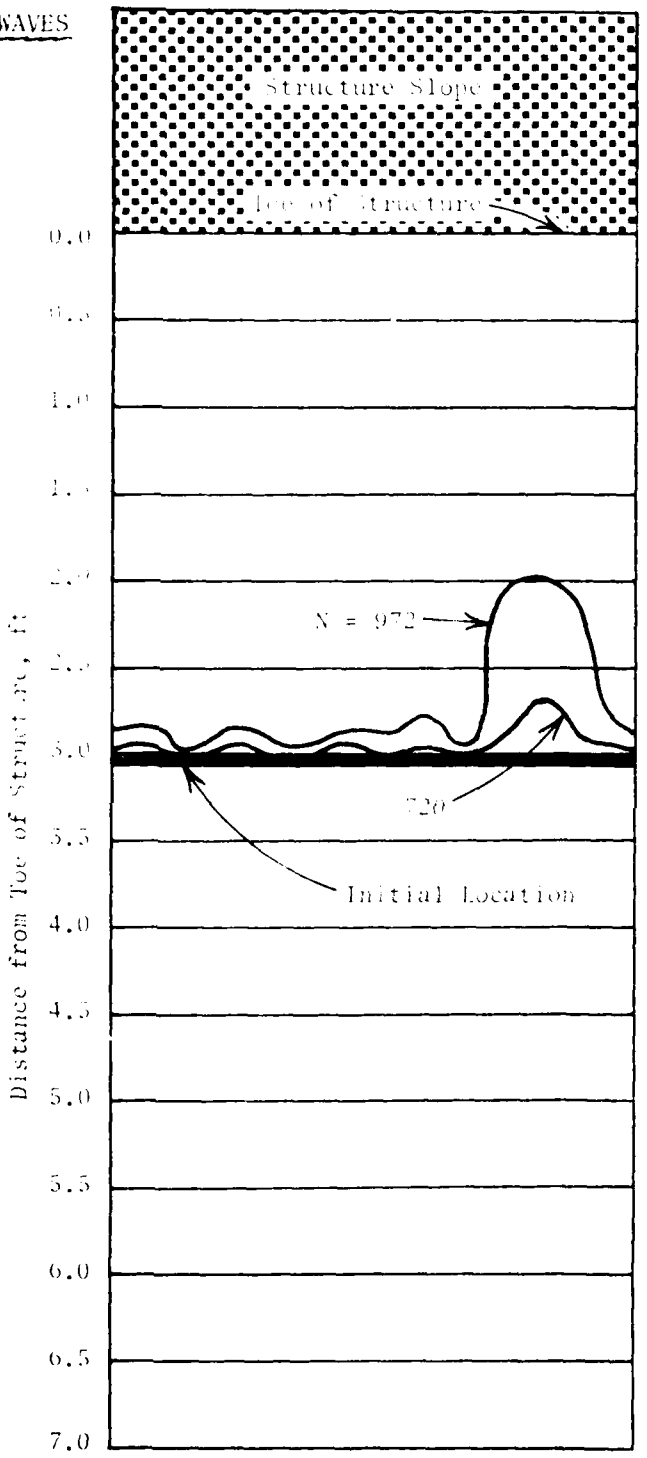

MATERIAL LOCATION AFTER N WAVES

Still-Water Depth, ft
Model: 1.0
Prototype: 16.0

Layer Thickness, ft
Model: 0.125
Prototype: 2.0

Layer Extent, ft
Model: 3
Prototype: 48

Material Size, in.
Model: 1/2 - 5/8
Prototype: 8 - 10

Material Weight, lb
Model: 0.012 - 0.023
Prototype: 50 - 95

Wave Period, sec
Model: 3
Prototype: 12

Bed Slope: 1V on 25H

Maximum Breaker Wave Height, ft
Model: 1.11
Prototype: 17.8

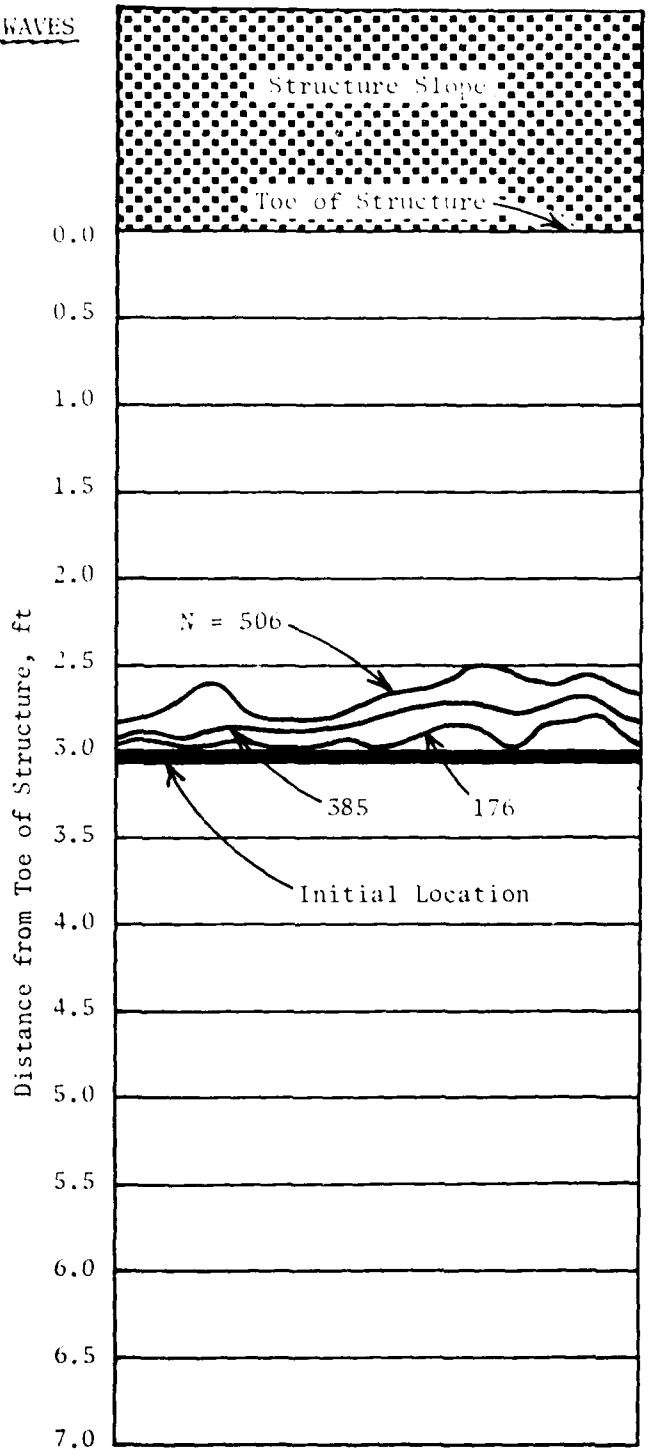

MATERIAL LOCATION AFTER N WAVES

Still-Water Depth, ft
Model: 1.0
Prototype: 16.0

Layer Thickness, ft
Model: 0.125
Prototype: 2.0

Layer Extent, ft
Model: 3
Prototype: 48

Material Size, in.
Model: 1/2 - 5/8
Prototype: 8 - 10

Material Weight, lb
Model: 0.012 - 0.025
Prototype: 50 - 95

Wave Period, sec
Model: 4
Prototype: 16

Bed Slope: 1V on 25H

Maximum Breaker Wave Height, ft
Model: 1.45
Prototype: 23.2

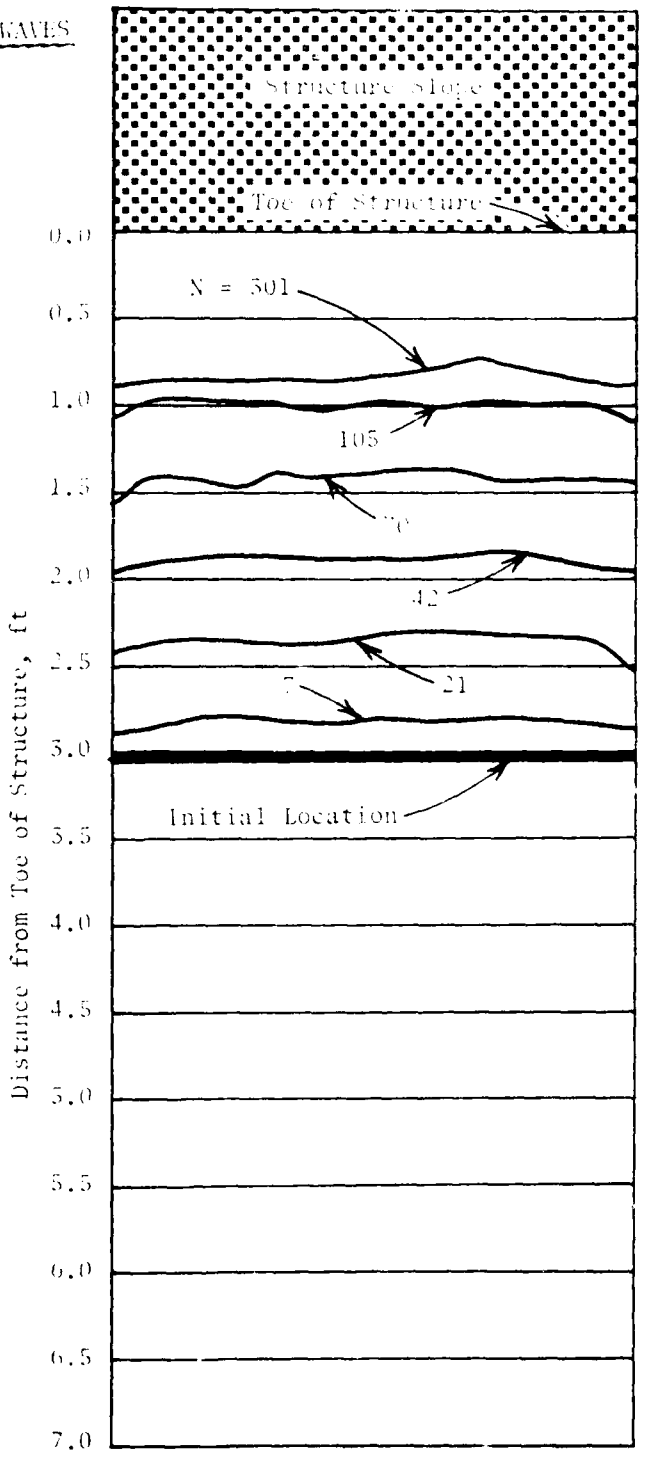

MATERIAL LOCATION AFTER N WAVES

Still-Water Depth, ft
Model: 1.0
Prototype: 16.0

Layer Thickness, ft
Model: 0.125
Prototype: 2.0

Layer Extent, ft
Model: 5
Prototype: 48

Material Size, in.
Model: 1/2 - 5/8
Prototype: 8 - 10

Material Weight, lb
Model: 0.012 - 0.025
Prototype: 50 - 95

Wave Period, sec
Model: 5
Prototype: 20

Bed Slope: 1V on 25H

Maximum Breaker Wave Height, ft
Model: 1.12
Prototype: 17.9

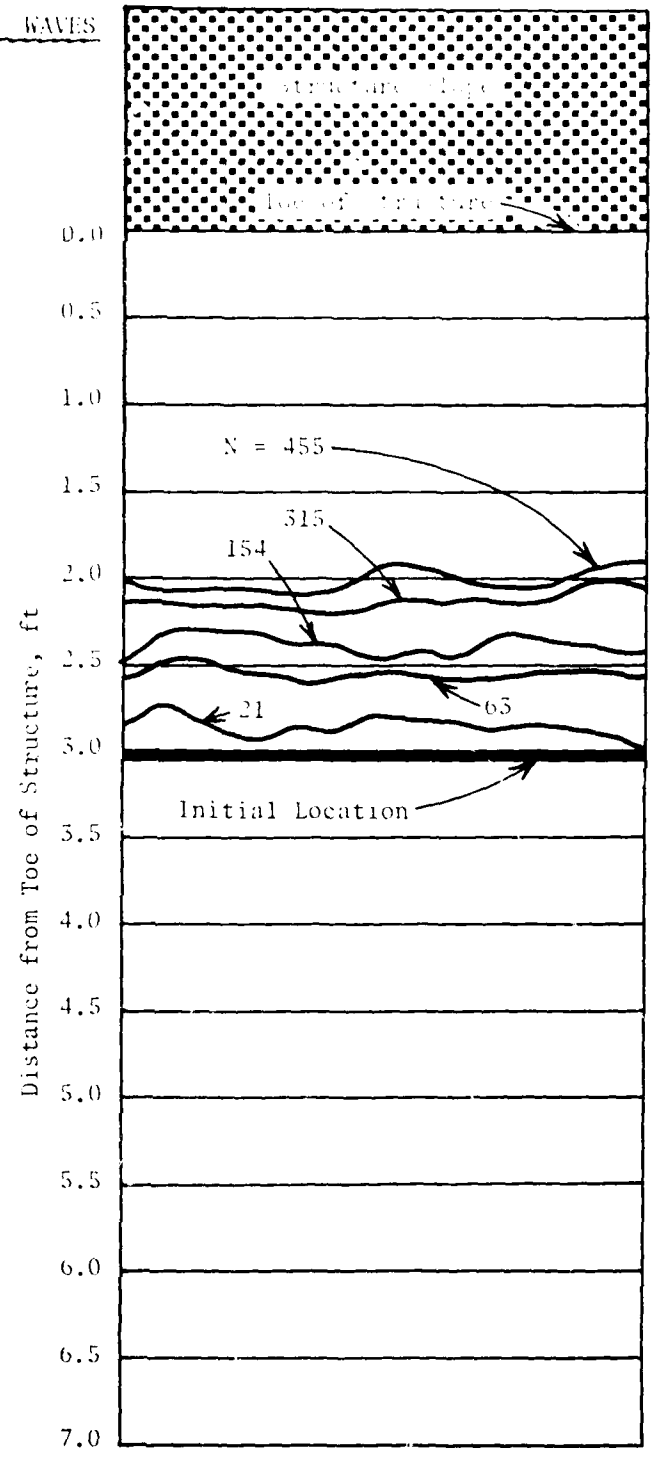

MATERIAL LOCATION AFTER N WAVES

Still-Water Depth, ft
Model: 1.0
Prototype: 10.0

Layer Thickness, ft
Model: 0.125
Prototype: 1.0

Layer Extent, ft
Model: 5
Prototype: 50

Material Size, in.
Model: 1/2 - 3/8
Prototype: 8 - 10

Material Weight, lb
Model: 0.012 - 0.025
Prototype: 50 - 95

Wave Period, sec
Model: 2
Prototype: 8

Bed Slope: 1V on 25H

Maximum Breaker Wave Height, ft
Model: 1.09
Prototype: 17.4

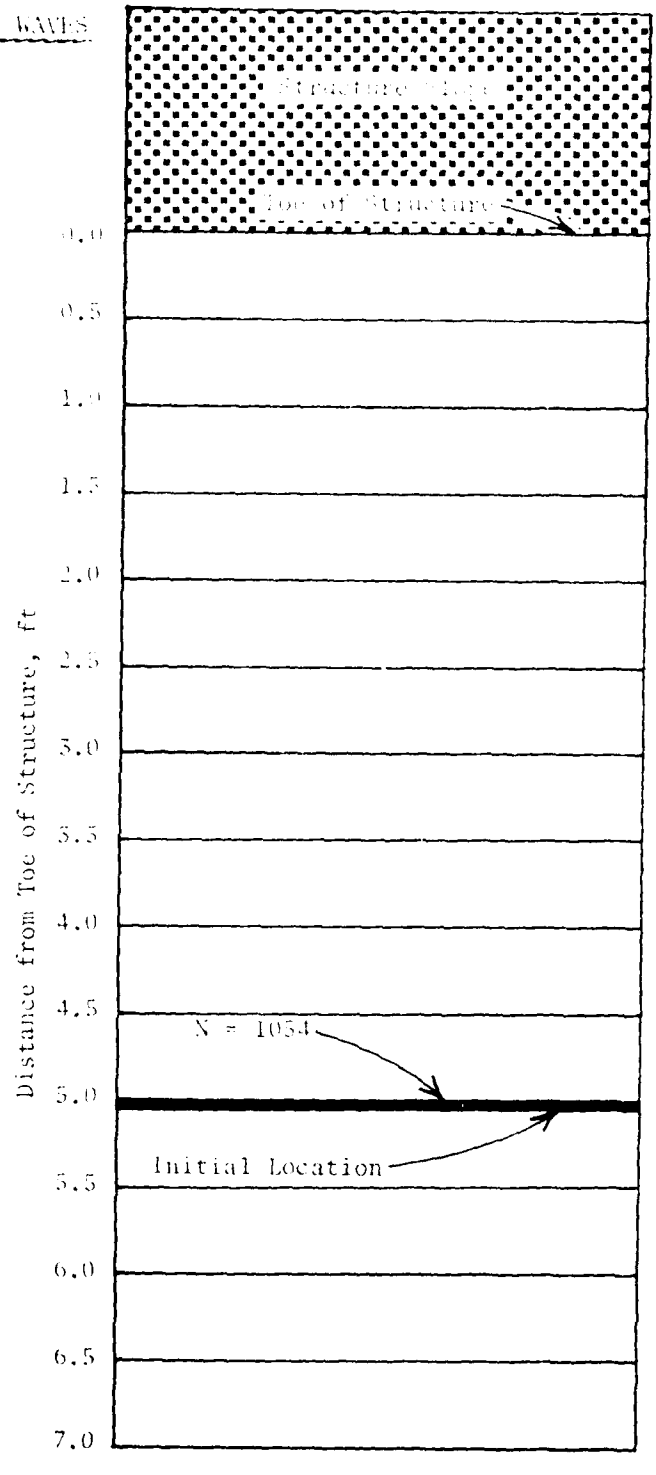

MATERIAL LOCATION AFTER N WAVES

Still-Water Depth, ft
Model: 1.0
Prototype: 16.0

Layer Thickness, ft
Model: 0.125
Prototype: 2.0

Layer Extent, ft
Model: 5
Prototype: 80

Material Size, in.
Model: 1/2 - 5/8
Prototype: 8 - 10

Material Weight, lb
Model: 0.012 - 0.025
Prototype: 50 - 95

Wave Period, sec
Model: 3
Prototype: 12

Bed Slope: 1V on 25H

Maximum Breaker Wave Height, ft
Model: 1.11
Prototype: 17.8

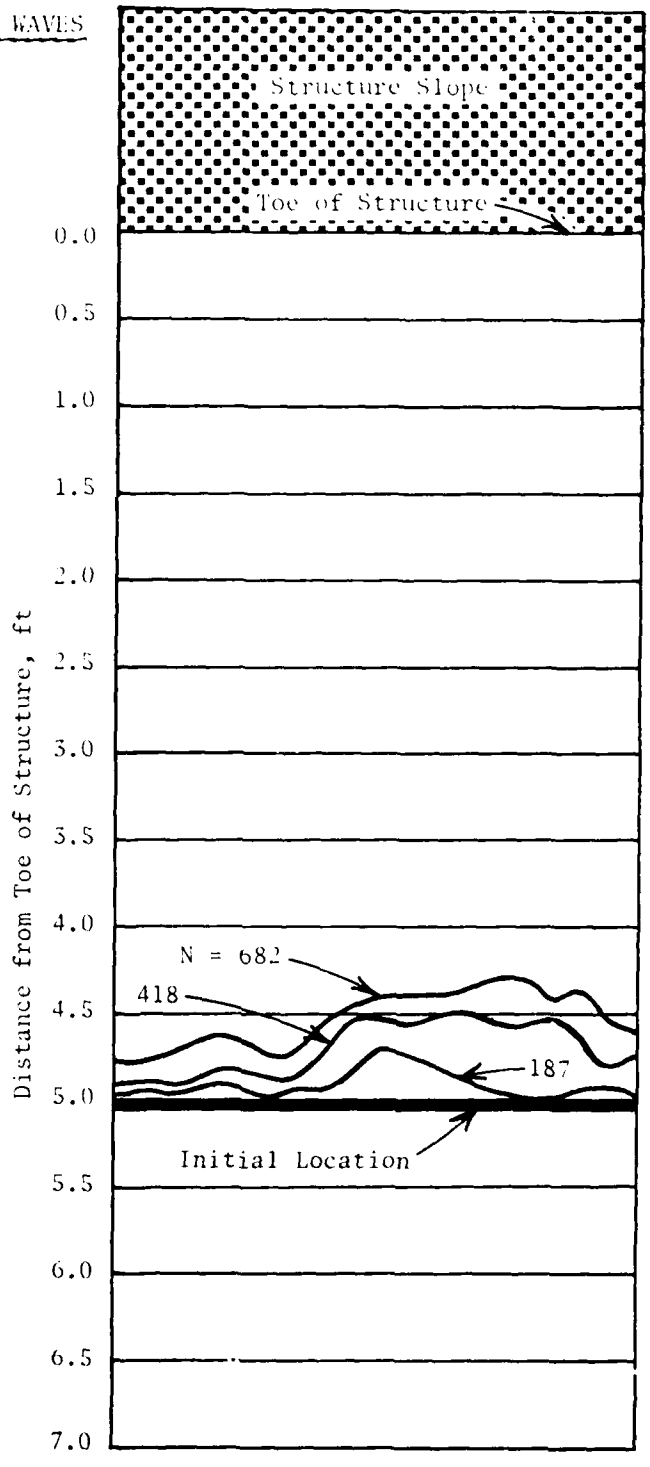

MATERIAL LOCATION AFTER N WAVES

Still-Water Depth, ft
Model: 1.0
Prototype: 16.0

Layer Thickness, ft
Model: 0.125
Prototype: 2.0

Layer Extent, ft
Model: 5
Prototype: 80

Material Size, in.
Model: 1/2 - 5/8
Prototype: 8 - 10

Material Weight, lb
Model: 0.012 - 0.025
Prototype: 50 - 95

Wave Period, sec
Model: 4
Prototype: 16

Bed Slope: 1V on 25H

Maximum Breaker Wave Height, ft
Model: 1.45
Prototype: 23.2

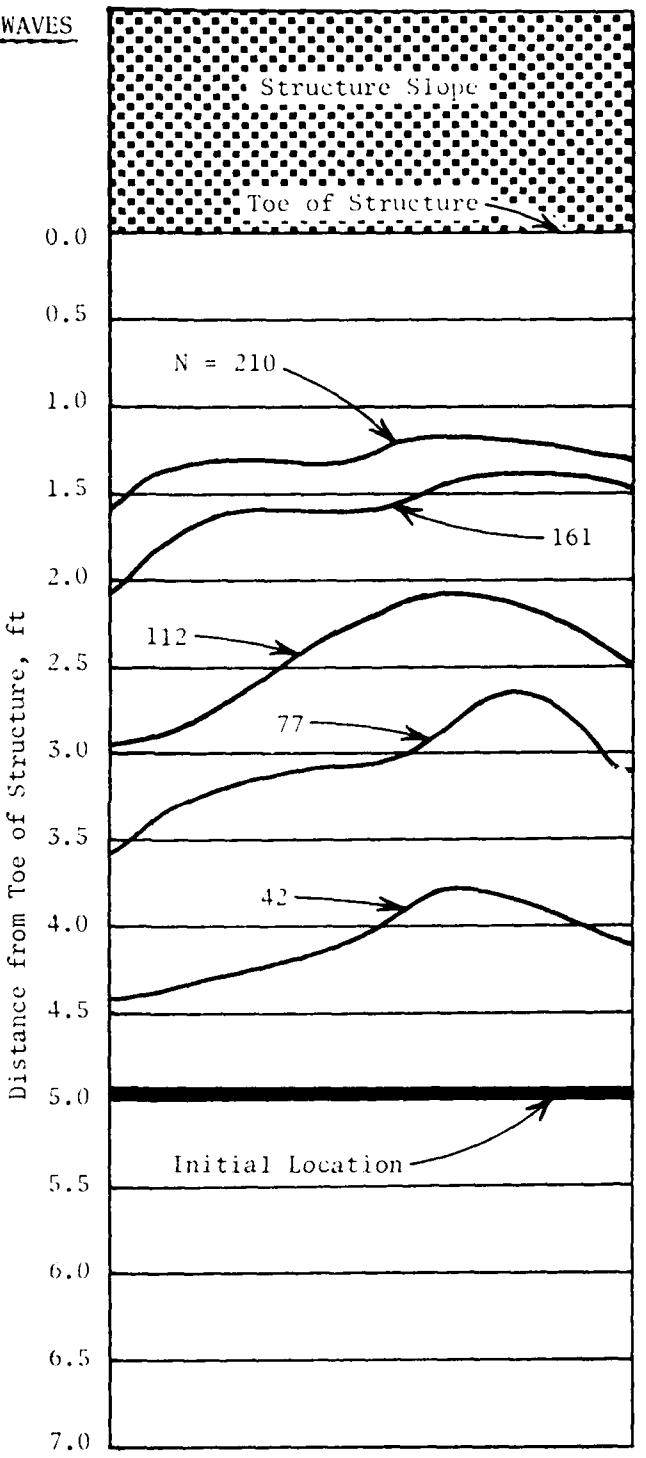

MATERIAL LOCATION AFTER N WAVES

Still-Water Depth, ft

Model: 1.0

Prototype: 16.0

Layer Thickness, ft

Model: 0.125

Prototype: 2.0

Layer Extent, ft

Model: 5

Prototype: 80

Material Size, in.

Model: 1/2 - 5/8

Prototype: 8 - 10

Material Weight, lb

Model: 0.012 - 0.023

Prototype: 50 - 95

Wave Period, sec

Model: 5

Prototype: 20

Bed Slope: 1V on 25H

Maximum Breaker Wave Height, ft

Model: 1.12

Prototype: 17.9

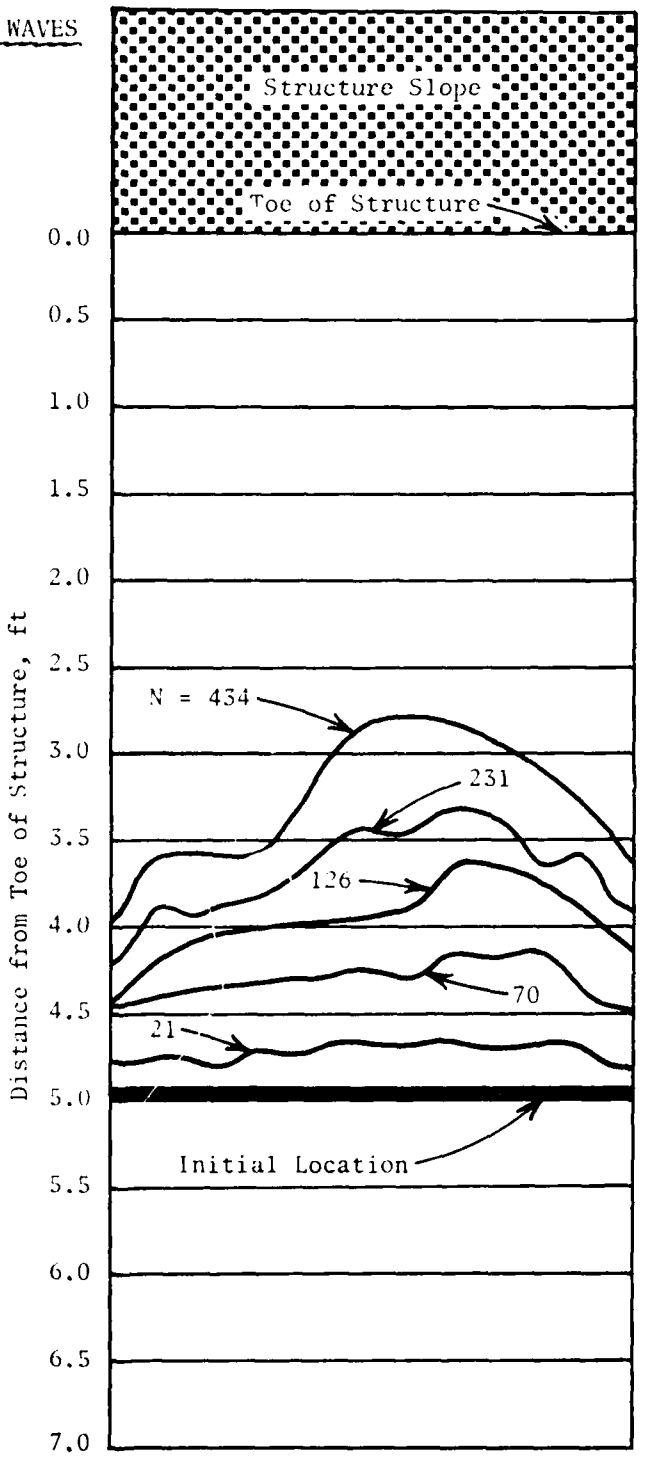

MATERIAL LOCATION AFTER N WAVES

Still-Water Depth, ft
Model: 1.0
Prototype: 16.0

Layer Thickness, ft
Model: 0.125
Prototype: 2.0

Layer Extent, ft
Model: 7
Prototype: 112

Material Size, in.
Model: 1/2 - 5/8
Prototype: 8 - 10

Material Weight, lb
Model: 0.012 - 0.025
Prototype: 50 - 95

Wave Period, sec
Model: 2
Prototype: 8

Bed Slope: 1V on 25H

Maximum Breaker Wave Height, ft
Model: 1.09
Prototype: 17.4

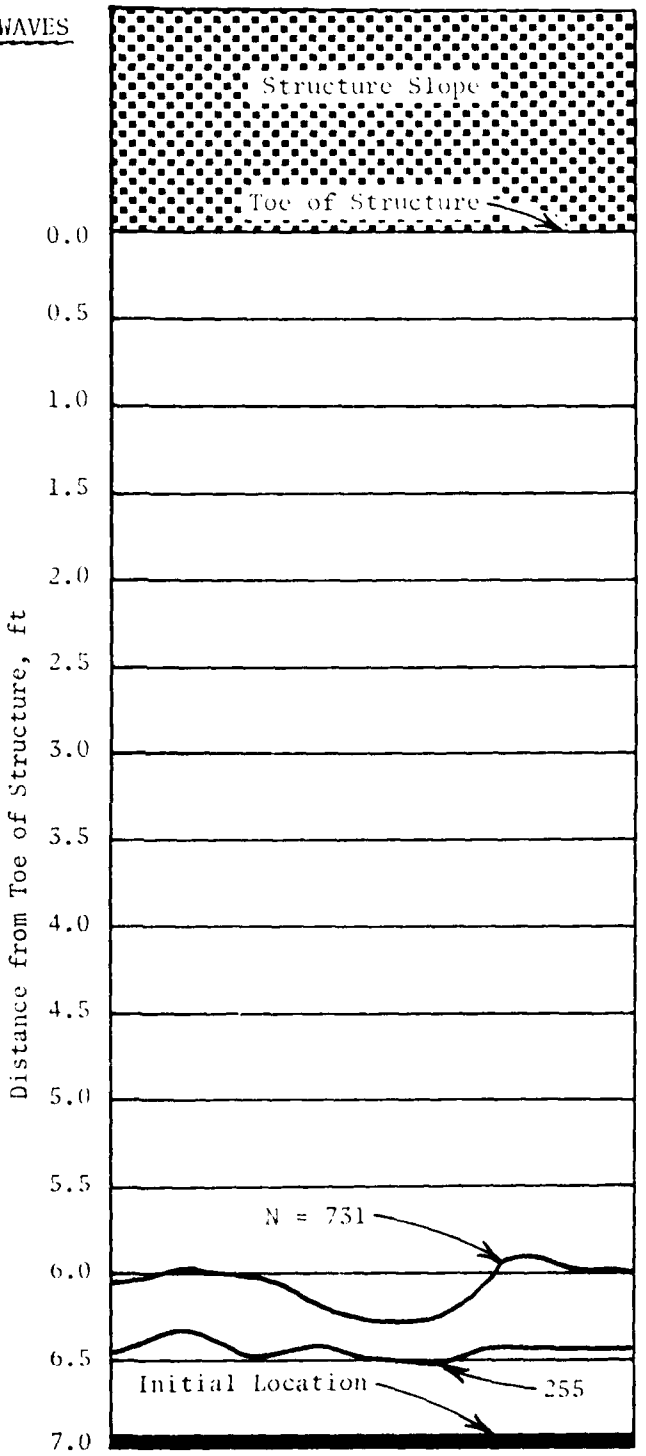

MATERIAL LOCATION AFTER N WAVES

Still-Water Depth, ft

Model: 1.0

Prototype: 16.0

Layer Thickness, ft

Model: 0.125

Prototype: 2.0

Layer Extent, ft

Model: 7

Prototype: 112

Material Size, in.

Model: 1/2 - 5/8

Prototype: 8 - 10

Material Weight, lb

Model: 0.012 - 0.023

Prototype: 50 - 95

Wave Period, sec

Model: 3

Prototype: 12

Bed Slope: 1V on 25H

Maximum Breaker Wave Height, ft

Model: 1.11

Prototype: 17.8

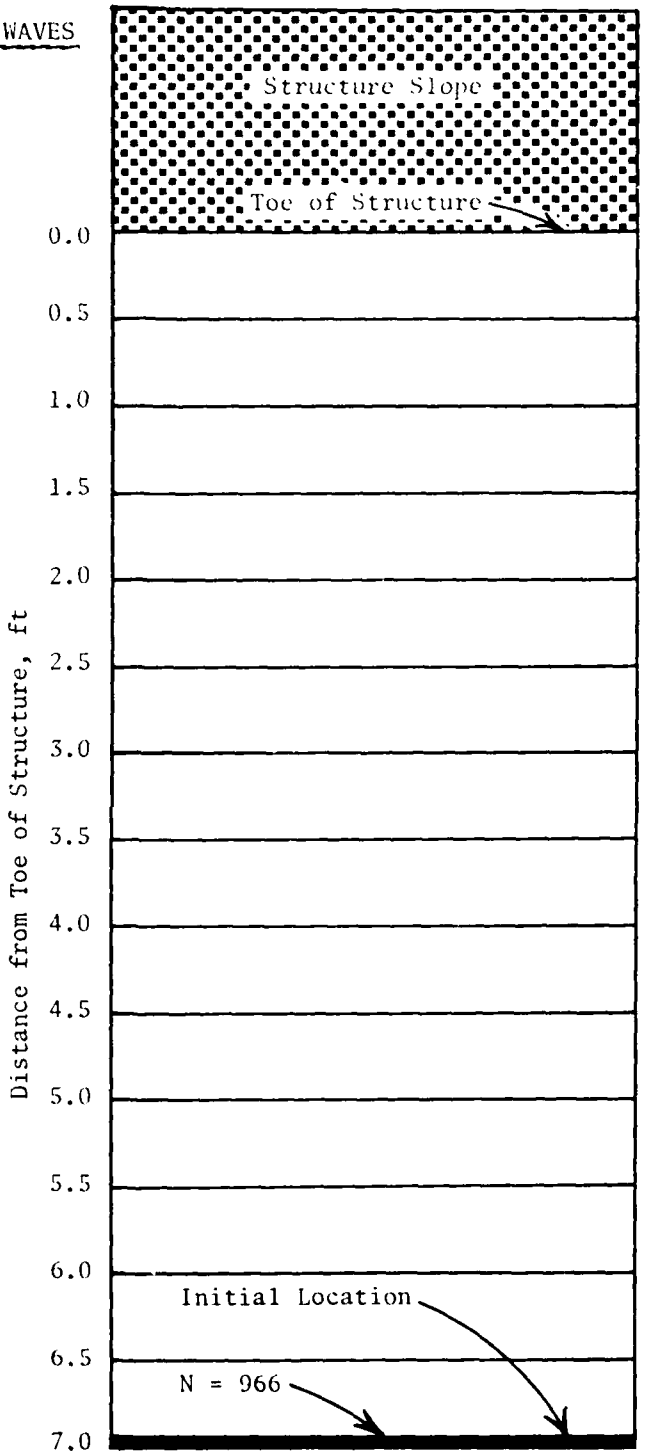

MATERIAL LOCATION AFTER N WAVES

Still-Water Depth, ft

Model: 1.0

Prototype: 16.0

Layer Thickness, ft

Model: 0.125

Prototype: 2.0

Layer Extent, ft

Model: 7

Prototype: 112

Material Size, in.

Model: 1/2 - 5/8

Prototype: 8 - 10

Material Weight, lb

Model: 0.012 - 0.023

Prototype: 50 - 95

Wave Period, sec

Model: 4

Prototype: 16

Bed Slope: 1V on 25H

Maximum Breaker Wave Height, ft

Model: 1.45

Prototype: 23.2

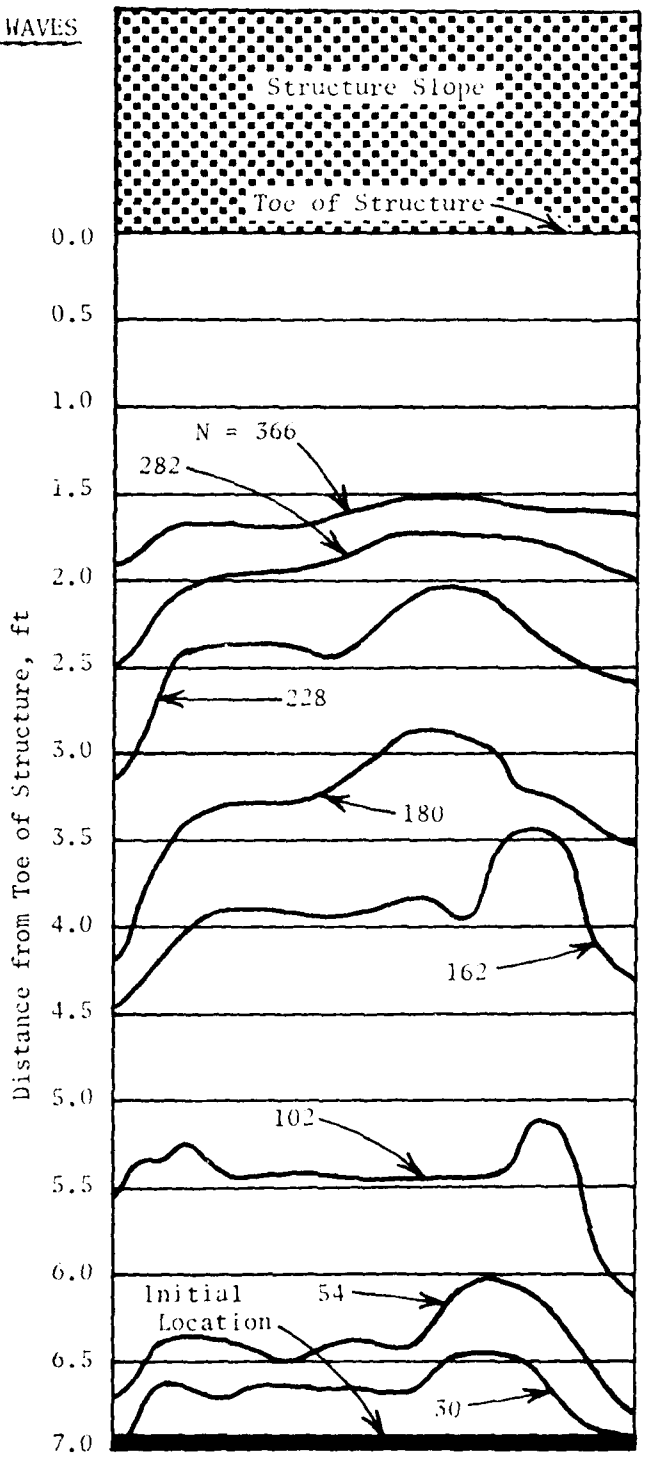

MATERIAL LOCATION AFTER N WAVES

Still-Water Depth, ft
Model: 1.0
Prototype: 16.0

Layer Thickness, ft
Model: 0.125
Prototype: 2.0

Layer Extent, ft
Model: 7
Prototype: 112

Material Size, in.
Model: 1/2 - 5/8
Prototype: 8 - 10

Material Weight, lb
Model: 0.012 - 0.023
Prototype: 50 - 95

Wave Period, sec
Model: 5
Prototype: 20

Bed Slope: 1V on 25H

Maximum Breaker Wave Height, ft
Model: 1.12
Prototype: 17.9

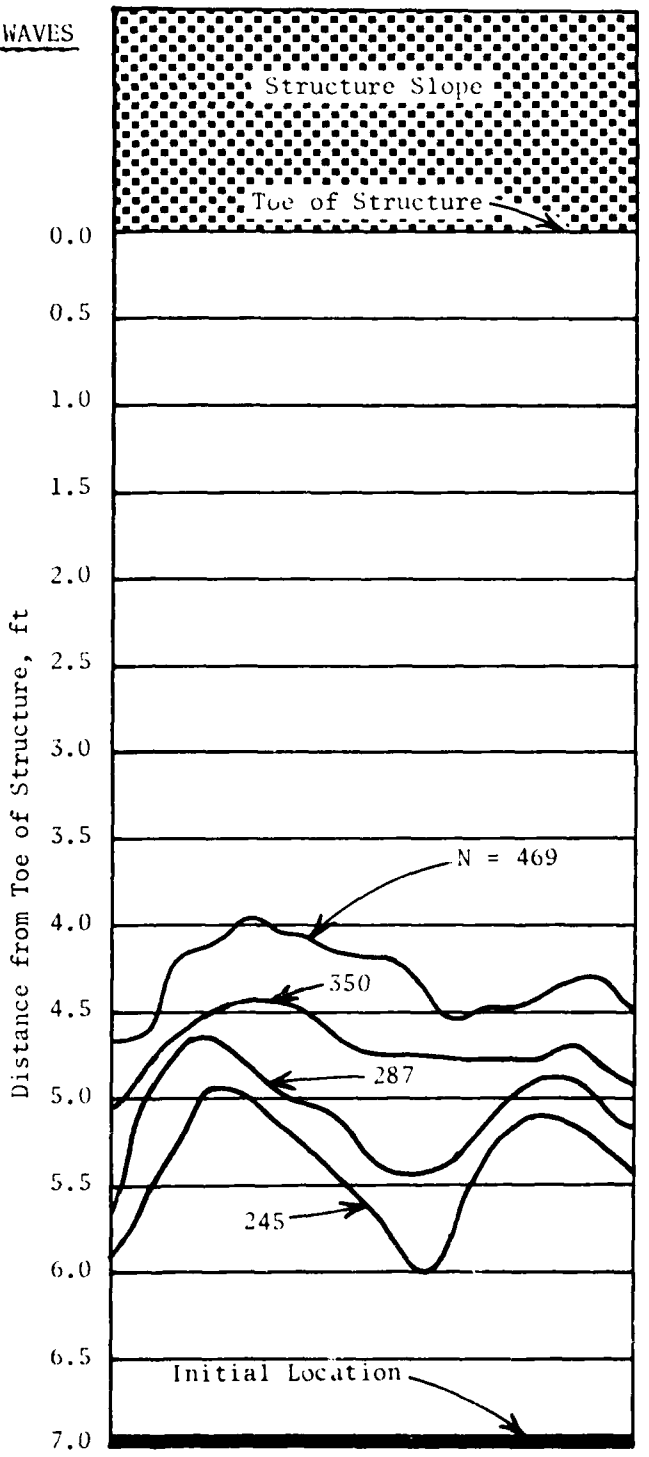

MATERIAL LOCATION AFTER N WAVES

Still-Water Depth, ft
Model: 0.5
Prototype: 8.0

Layer Thickness, ft
Model: 0.125
Prototype: 2.0

Layer Extent, ft
Model: 3
Prototype: 48

Material Size, in.
Model: 5/8 - 3/4
Prototype: 10 - 12

Material Weight, lb
Model: 0.023 - 0.040
Prototype: 95 - 165

Wave Period, sec
Model: 4
Prototype: 16

Bed Slope: 1V on 25H

Maximum Breaker Wave Height, ft
Model: 0.80
Prototype: 12.8

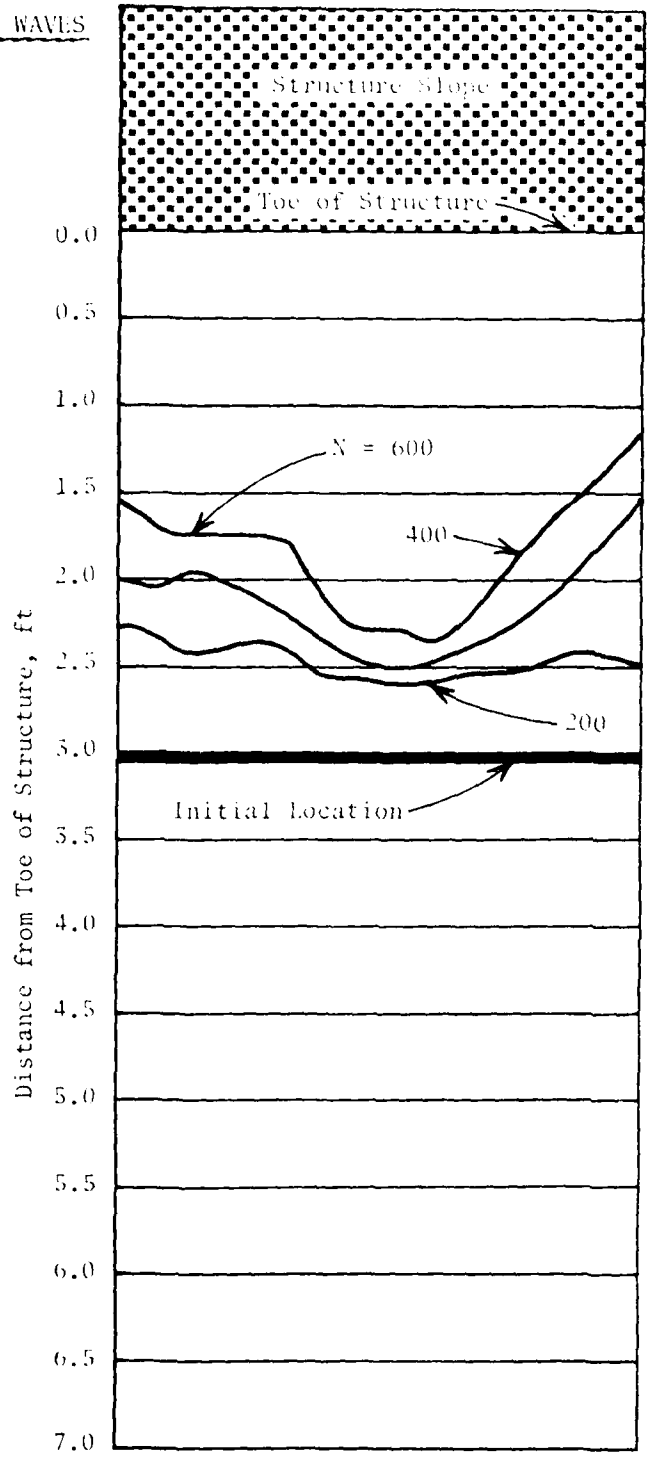

MATERIAL LOCATION AFTER N WAVES

Still-Water Depth, ft
Model: 0.5
Prototype: 8.0

Layer Thickness, ft
Model: 0.125
Prototype: 2.0

Layer Extent, ft
Model: 3
Prototype: 48

Material Size, in.
Model: 5/8 - 3/4
Prototype: 10 - 12

Material Weight, lb
Model: 0.023 - 0.040
Prototype: 95 - 165

Wave Period, sec
Model: 5
Prototype: 20

Bed Slope: 1V on 25H

Maximum Breaker Wave Height, ft
Model: 0.68
Prototype: 10.9

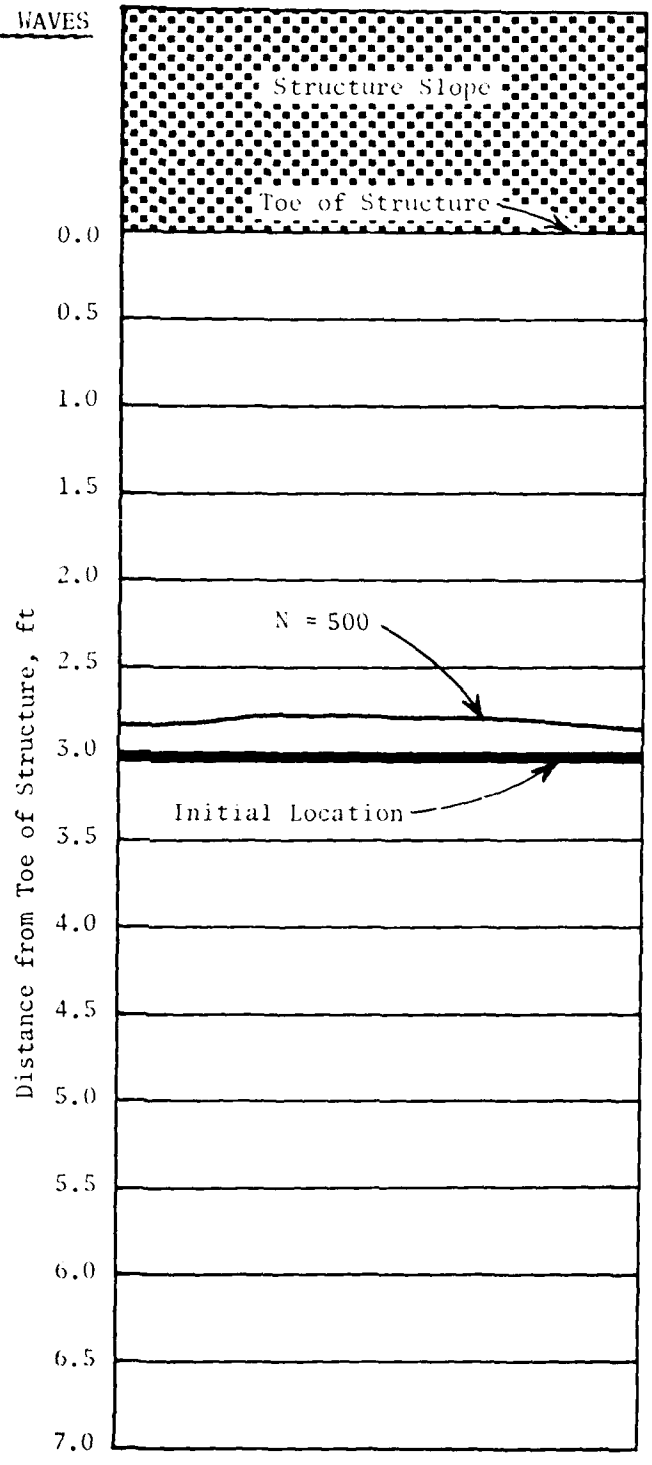

MATERIAL LOCATION AFTER N WAVES

Still-Water Depth, ft
Model: 0.5
Prototype: 8.0

Layer Thickness, ft
Model: 0.125
Prototype: 2.0

Layer Extent, ft
Model: 5
Prototype: 80

Material Size, in.
Model: 5/8 - 3/4
Prototype: 10 - 12

Material Weight, lb
Model: 0.023 - 0.040
Prototype: 95 - 165

Wave Period, sec
Model: 4
Prototype: 16

Bed Slope: 1V on 25H

Maximum Breaker Wave Height, ft
Model: 0.80
Prototype: 12.8

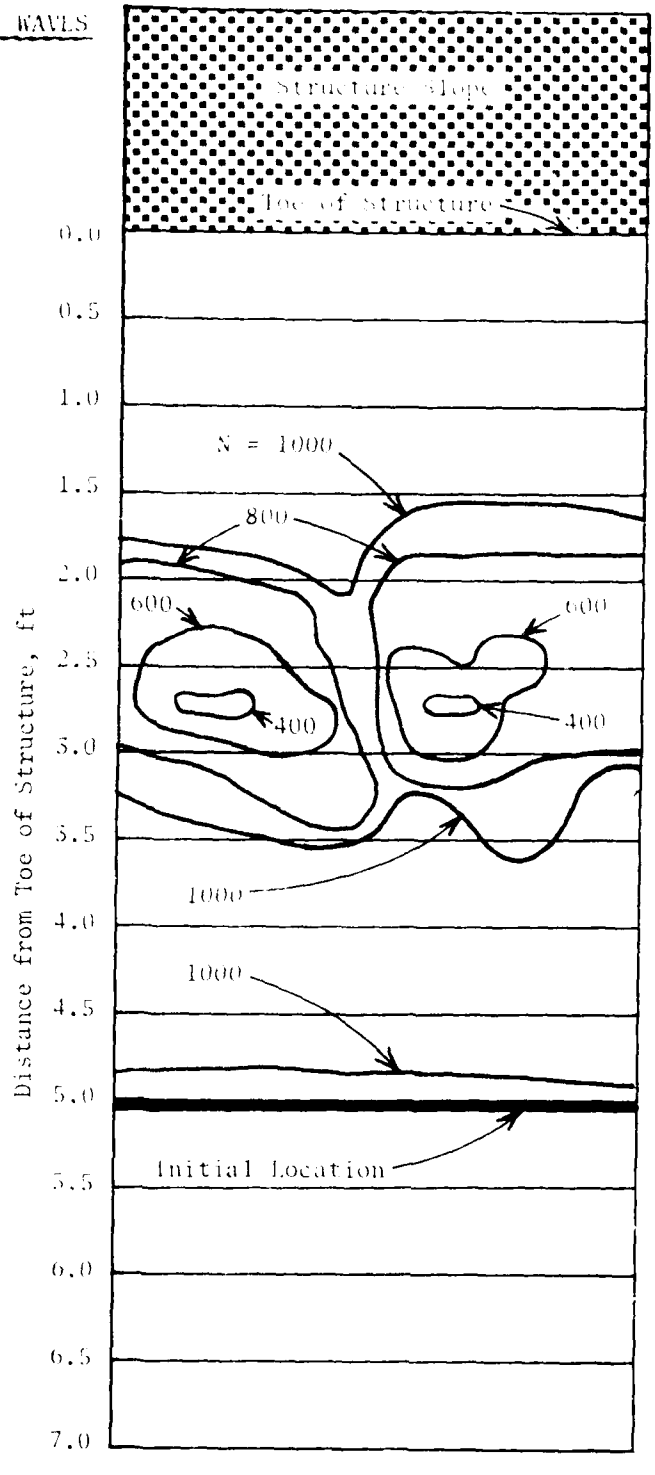

MATERIAL LOCATION AFTER N WAVES

Still-Water Depth, ft

Model: 0.5

Prototype: 8.0

Layer Thickness, ft

Model: 0.125

Prototype: 2.0

Layer Extent, ft

Model: 7

Prototype: 112

Material Size, in.

Model: 5/8 - 3/4

Prototype: 10 - 12

Material Weight, lb

Model: 0.023 - 0.040

Prototype: 95 - 165

Wave Period, sec

Model: 4

Prototype: 16

Bed Slope: 1V on 25H

Maximum Breaker Wave Height, ft

Model: 0.80

Prototype: 12.8

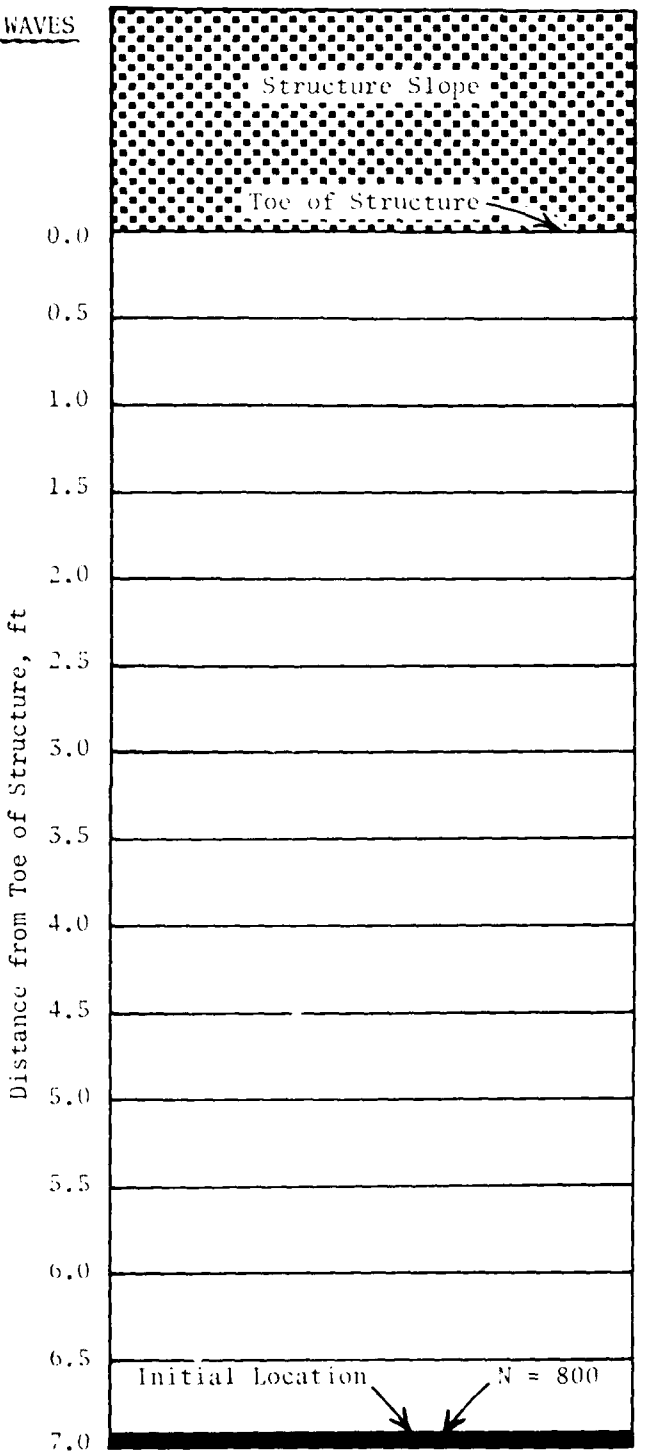

MATERIAL LOCATION AFTER N WAVES

Still-Water Depth, ft

Model: 1.0

Prototype: 16.0

Layer Thickness, ft

Model: 0.125

Prototype: 2.0

Layer Extent, ft

Model: 5

Prototype: 48

Material Size, in.

Model: 3/8 - 3/4

Prototype: 10 - 12

Material Weight, lb

Model: 0.025 - 0.040

Prototype: 95 - 165

Wave Period, sec

Model: 3

Prototype: 12

Bed Slope: 1V on 20H

Maximum Breaker Wave Height, ft

Model: 1.11

Prototype: 17.8

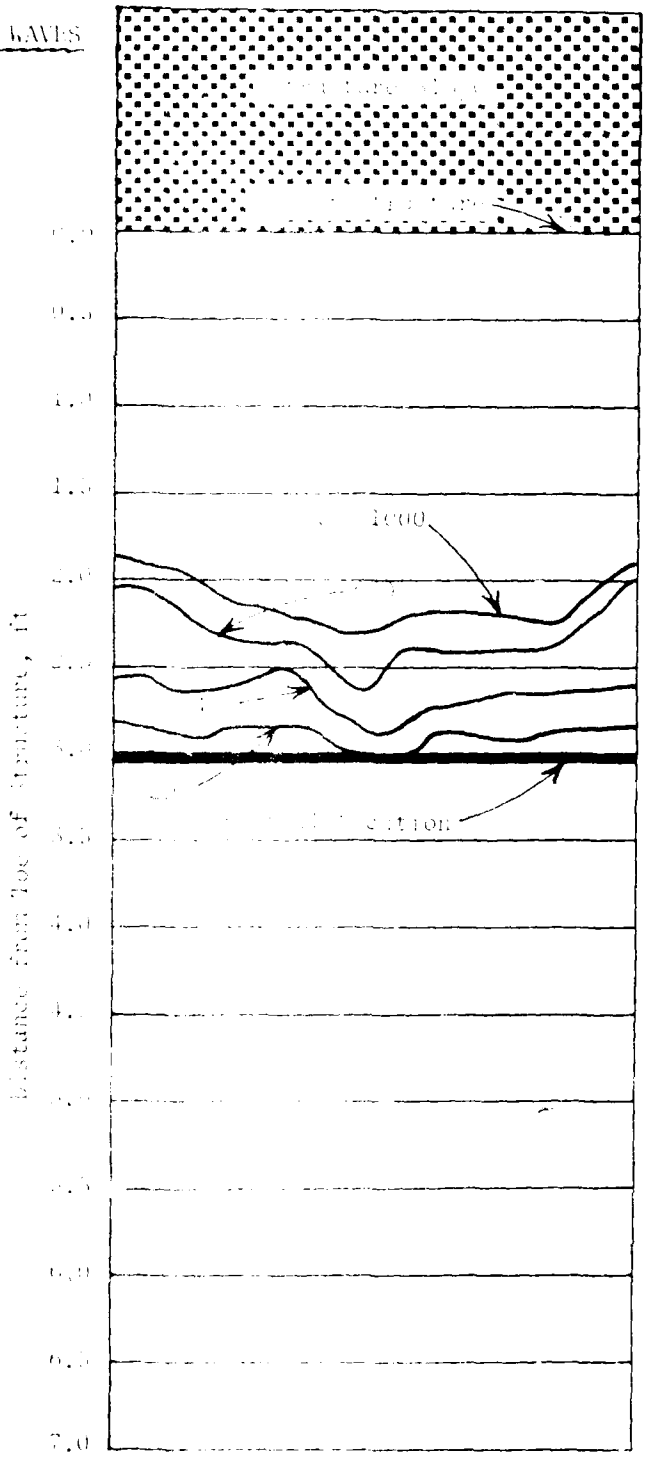

AD-A135 945 EROSION CONTROL OF SCOUR DURING CONSTRUCTION REPORT 4 3/3
STABILITY OF UNDERL..(U) ARMY ENGINEER WATERWAYS
EXPERIMENT STATION VICKSBURG MS HYDRA..
UNCLASSIFIED L Z HALES ET AL. JUN 83 WES/TR/HL-80-3-4 F/G 8/3 NL

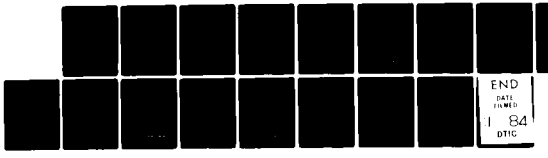

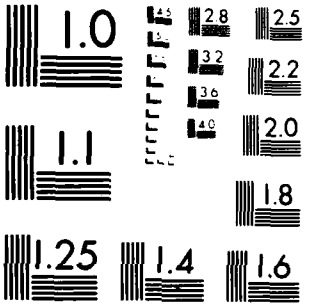

MATERIAL LOCATION AFTER N WAVES

Still-Water Depth, ft
Model: 1.0
Prototype: 16.0

Layer Thickness, ft
Model: 0.125
Prototype: 2.0

Layer Extent, ft
Model: 3
Prototype: 48

Material Size, in.
Model: 5/8 - 3/4
Prototype: 10 - 12

Material Weight, lb
Model: 0.023 - 0.040
Prototype: 95 - 165

Wave Period, sec
Model: 4
Prototype: 16

Bed Slope: 1V on 25H

Maximum Breaker Wave Height, ft
Model: 1.45
Prototype: 23.2

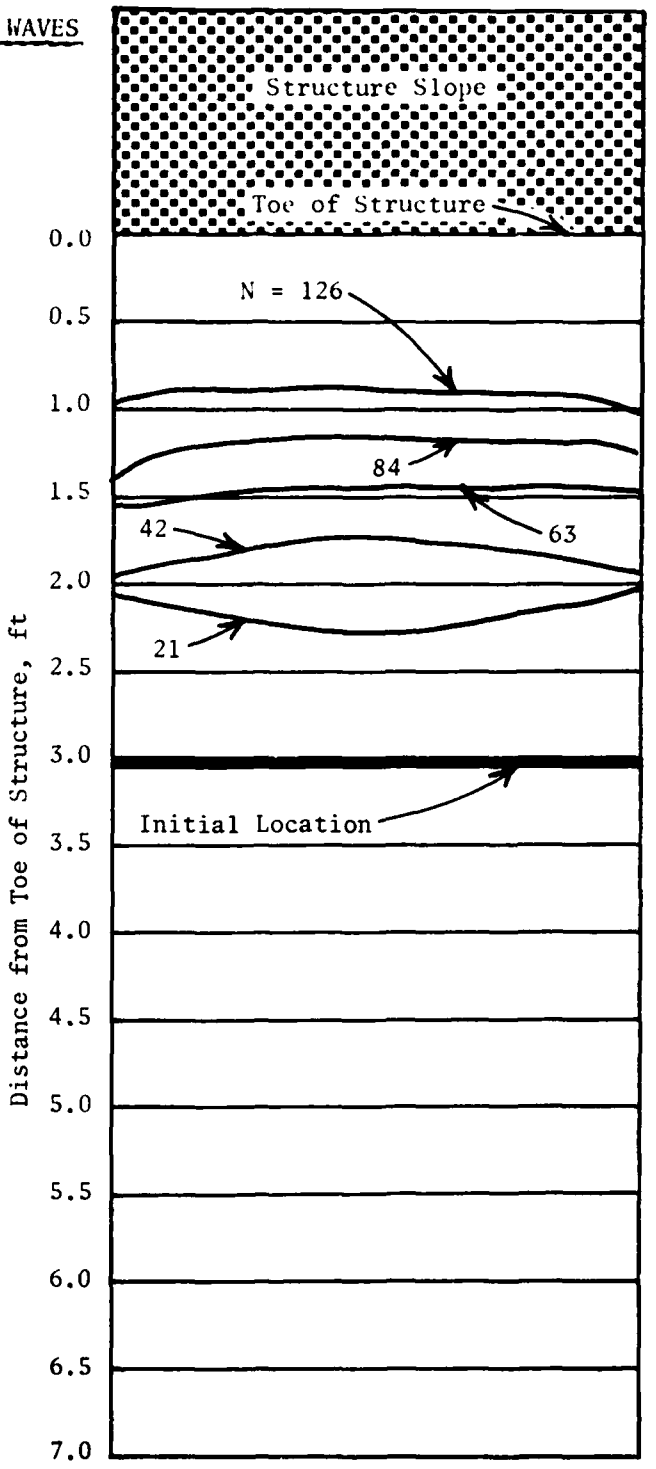

MATERIAL LOCATION AFTER N WAVES

Still-Water Depth, ft
Model: 1.0
Prototype: 16.0

Layer Thickness, ft
Model: 0.125
Prototype: 2.0

Layer Extent, ft
Model: 3
Prototype: 48

Material Size, in.
Model: 5/8 - 3/4
Prototype: 10 - 12

Material Weight, lb
Model: 0.023 - 0.040
Prototype: 95 - 165

Wave Period, sec
Model: 5
Prototype: 20

Bed Slope: 1V on 25H

Maximum Breaker Wave Height, ft
Model: 1.12
Prototype: 17.9

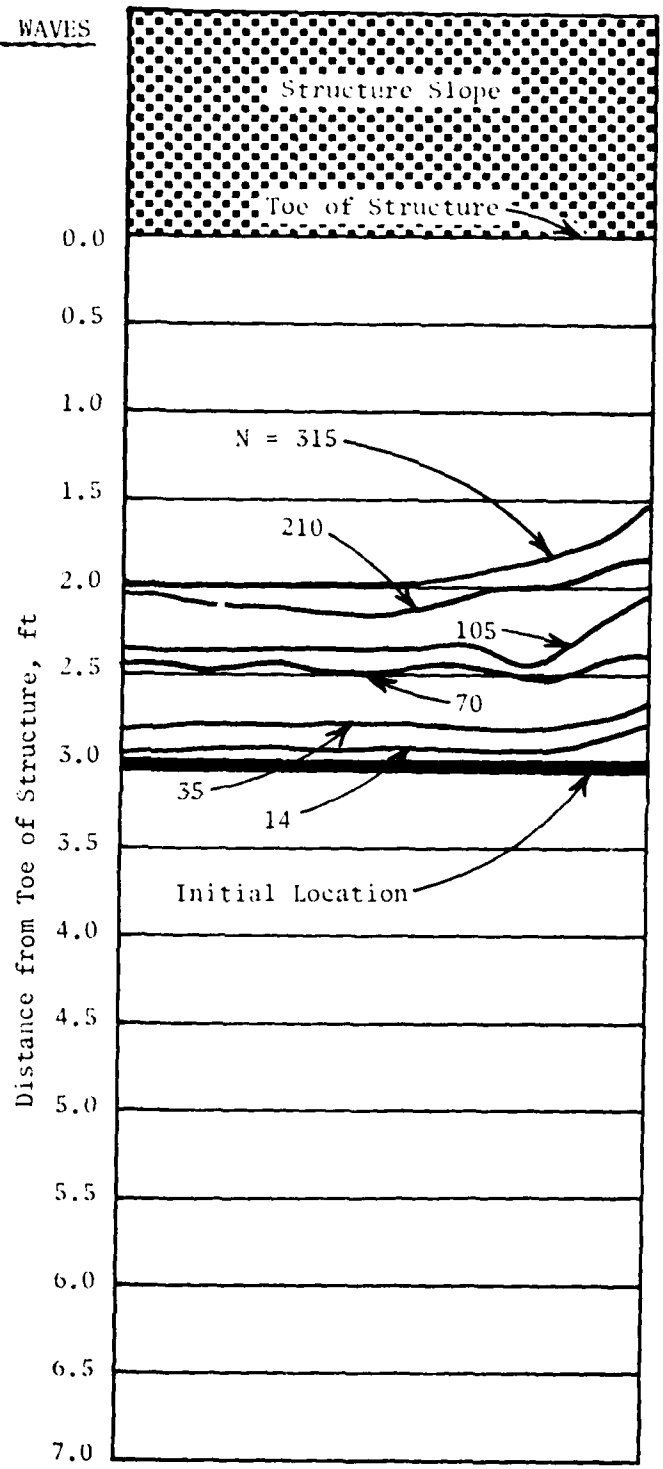

MATERIAL LOCATION AFTER N WAVES

Still-Water Depth, ft
Model: 1.0
Prototype: 16.0

Layer Thickness, ft
Model: 0.125
Prototype: 2.0

Layer Extent, ft
Model: 5
Prototype: 80

Material Size, in.
Model: 5/8 - 3/4
Prototype: 10 - 12

Material Weight, lb
Model: 0.023 - 0.040
Prototype: 95 - 165

Wave Period, sec
Model: 4
Prototype: 16

Bed Slope: 1V on 25H

Maximum Breaker Wave Height, ft
Model: 1.45
Prototype: 23.2

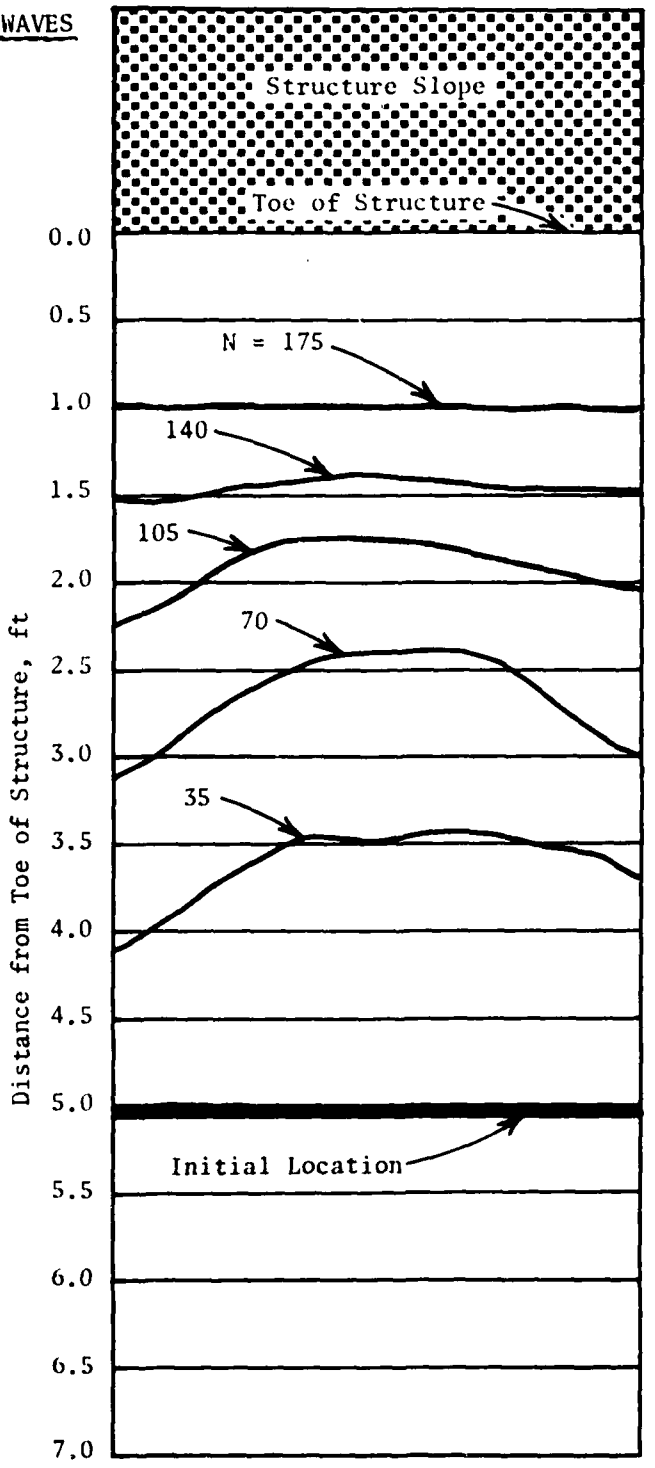

MATERIAL LOCATION AFTER N WAVES

Still-Water Depth, ft
Model: 1.0
Prototype: 16.0

Layer Thickness, ft
Model: 0.125
Prototype: 2.0

Layer Extent, ft
Model: 5
Prototype: 80

Material Size, in.
Model: 5/8 - 3/4
Prototype: 10 - 12

Material Weight, lb
Model: 0.023 - 0.040
Prototype: 95 - 165

Wave Period, sec
Model: 5
Prototype: 20

Bed Slope: 1V on 25H

Maximum Breaker Wave Height, ft
Model: 1.12
Prototype: 17.9

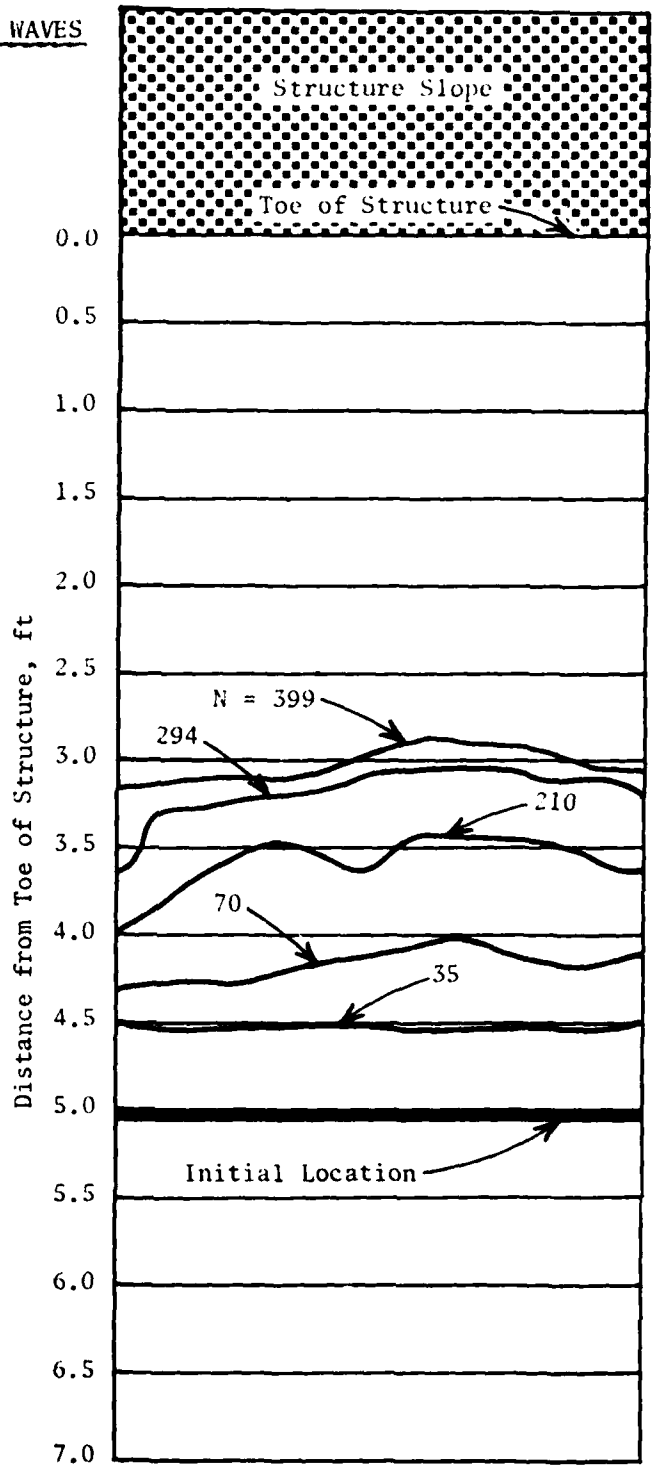

MATERIAL LOCATION AFTER N WAVES

Still-Water Depth, ft
Model: 1.0
Prototype: 16.0

Layer Thickness, ft
Model: 0.125
Prototype: 2.0

Layer Extent, ft
Model: 7
Prototype: 112

Material Size, in.
Model: 5/8 - 3/4
Prototype: 10 - 12

Material Weight, lb
Model: 0.023 - 0.040
Prototype: 95 - 165

Wave Period, sec
Model: 4
Prototype: 16

Bed Slope: 1V on 25H

Maximum Breaker Wave Height, ft
Model: 1.45
Prototype: 23.2

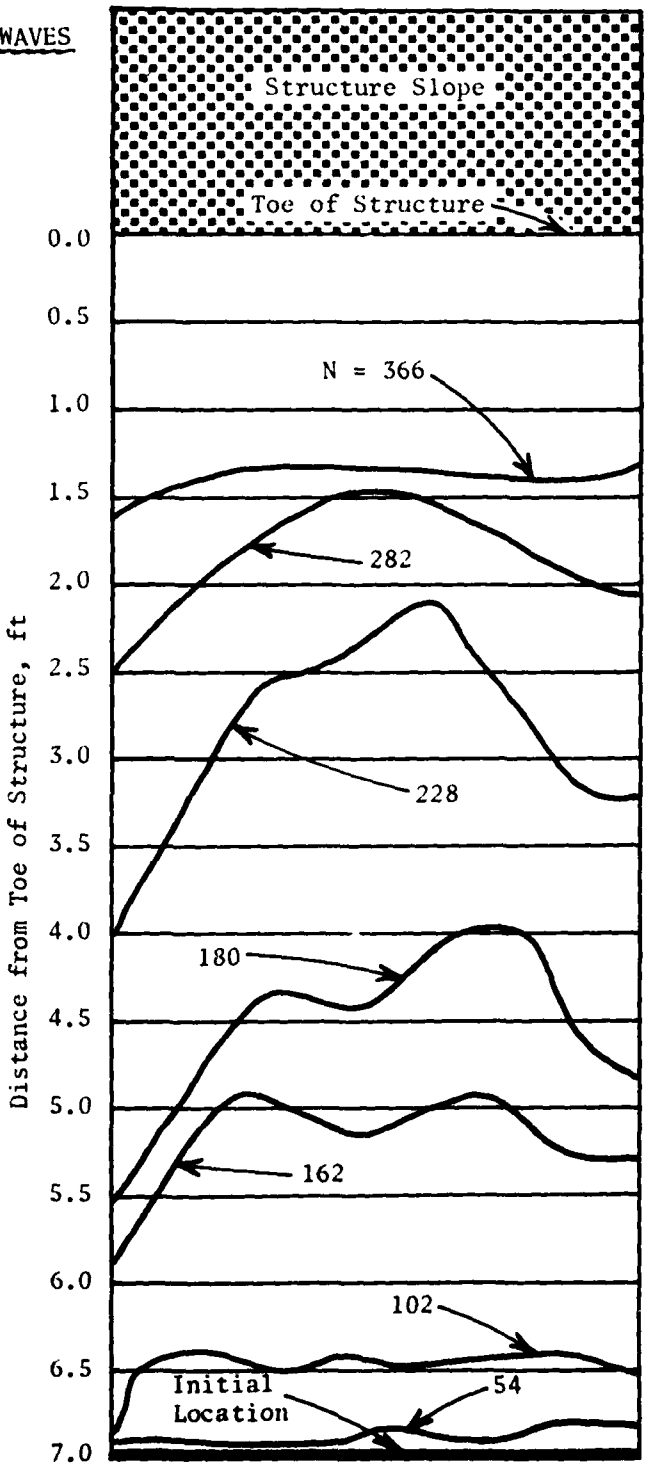

MATERIAL LOCATION AFTER N WAVES

Still-Water Depth, ft
Model: 1.0
Prototype: 16.0

Layer Thickness, ft
Model: 0.125
Prototype: 2.0

Layer Extent, ft
Model: 7
Prototype: 112

Material Size, in.
Model: 5/8 - 3/4
Prototype: 10 - 12

Material Weight, lb
Model: 0.023 - 0.040
Prototype: 95 - 165

Wave Period, sec
Model: 5
Prototype: 20

Bed Slope: 1V on 25H

Maximum Breaker Wave Height, ft
Model: 1.12
Prototype: 17.9

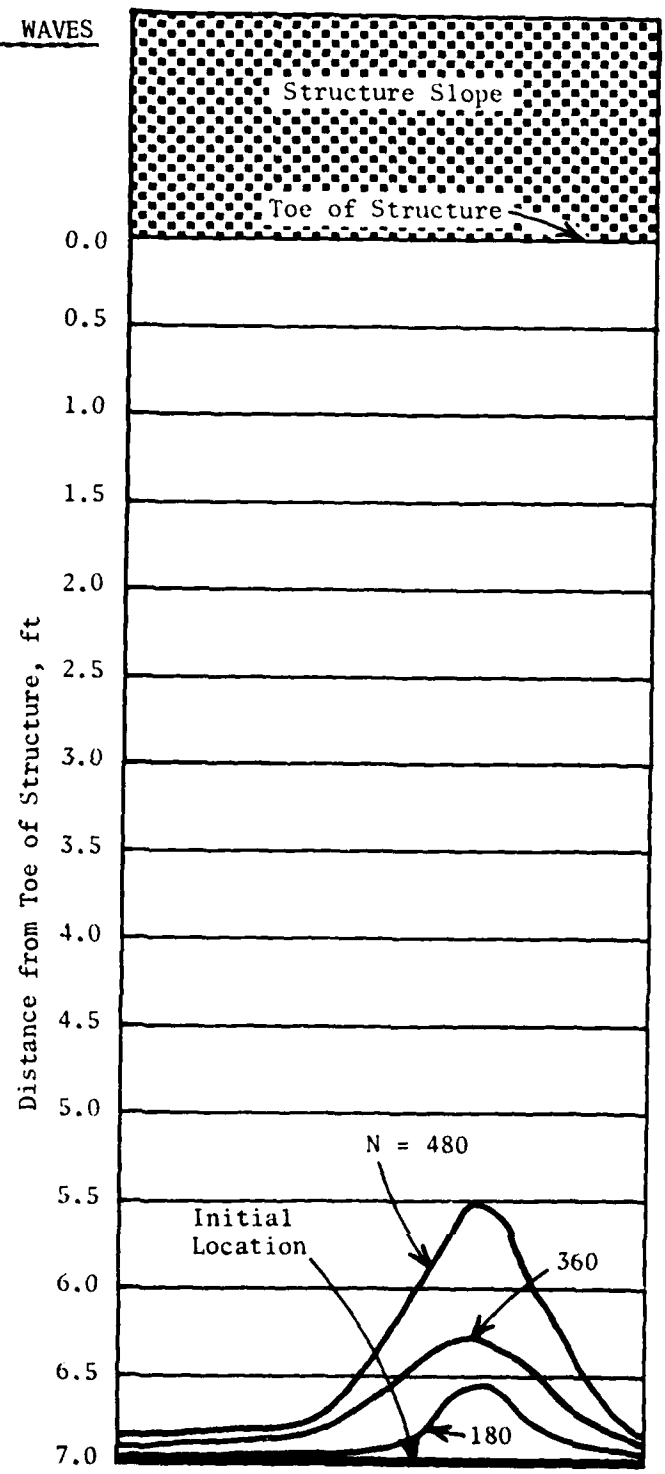

MATERIAL LOCATION AFTER N WAVES

Still-Water Depth, ft
Model: 0.5
Prototype: 8.0

Layer Thickness, ft
Model: 0.125
Prototype: 2.0

Layer Extent, ft
Model: 3
Prototype: 48

Material Size, in.
Model: 3/4 - 7/8
Prototype: 12 - 14

Material Weight, lb
Model: 0.040 - 0.064
Prototype: 165 - 260

Wave Period, sec
Model: 4
Prototype: 16

Bed Slope: 1V on 25H

Maximum Breaker Wave Height, ft
Model: 0.80
Prototype: 12.8

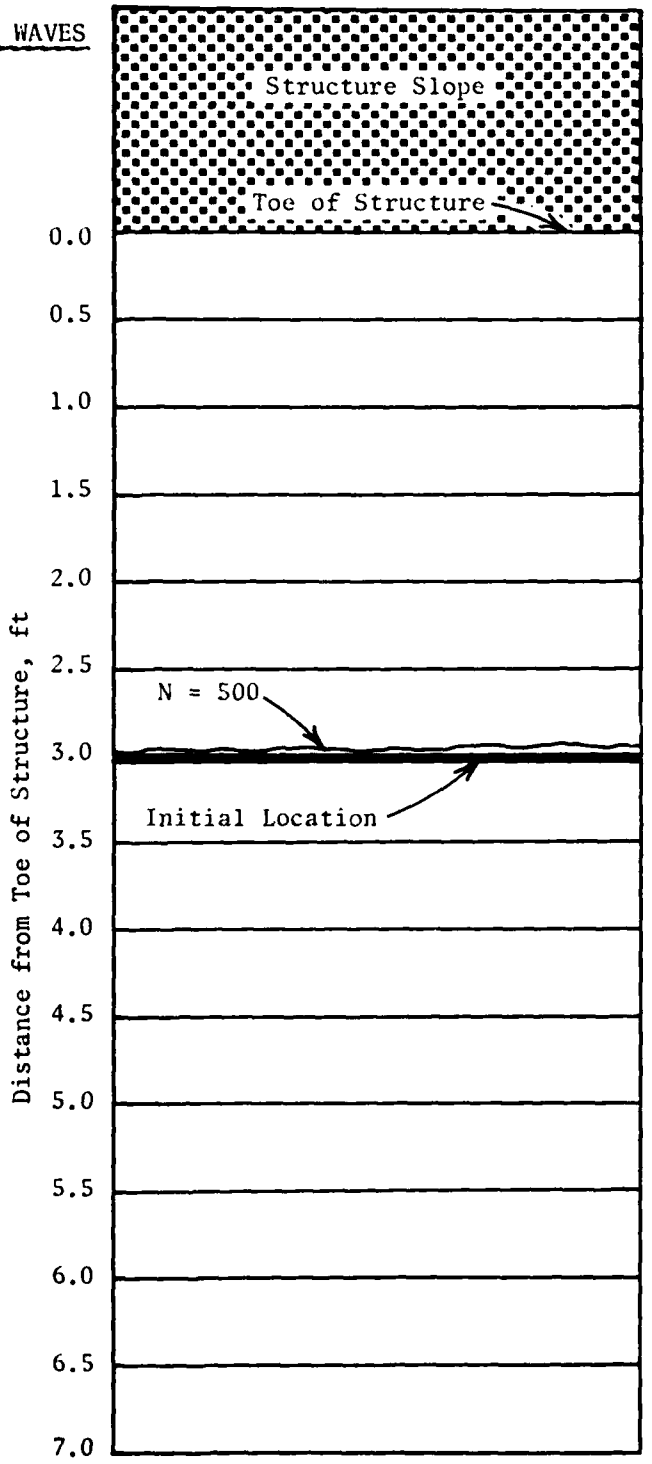

MATERIAL LOCATION AFTER N WAVES

Still-Water Depth, ft
Model: 1.0
Prototype: 16.0

Layer Thickness, ft
Model: 0.125
Prototype: 2.0

Layer Extent, ft
Model: 5
Prototype: 80

Material Size, in.
Model: 3/4 - 7/8
Prototype: 12 - 14

Material Weight, lb
Model: 0.040 - 0.064
Prototype: 165 - 260

Wave Period, sec
Model: 5
Prototype: 20

Bed Slope: 1V on 25H

Maximum Breaker Wave Height, ft
Model: 1.12
Prototype: 17.9

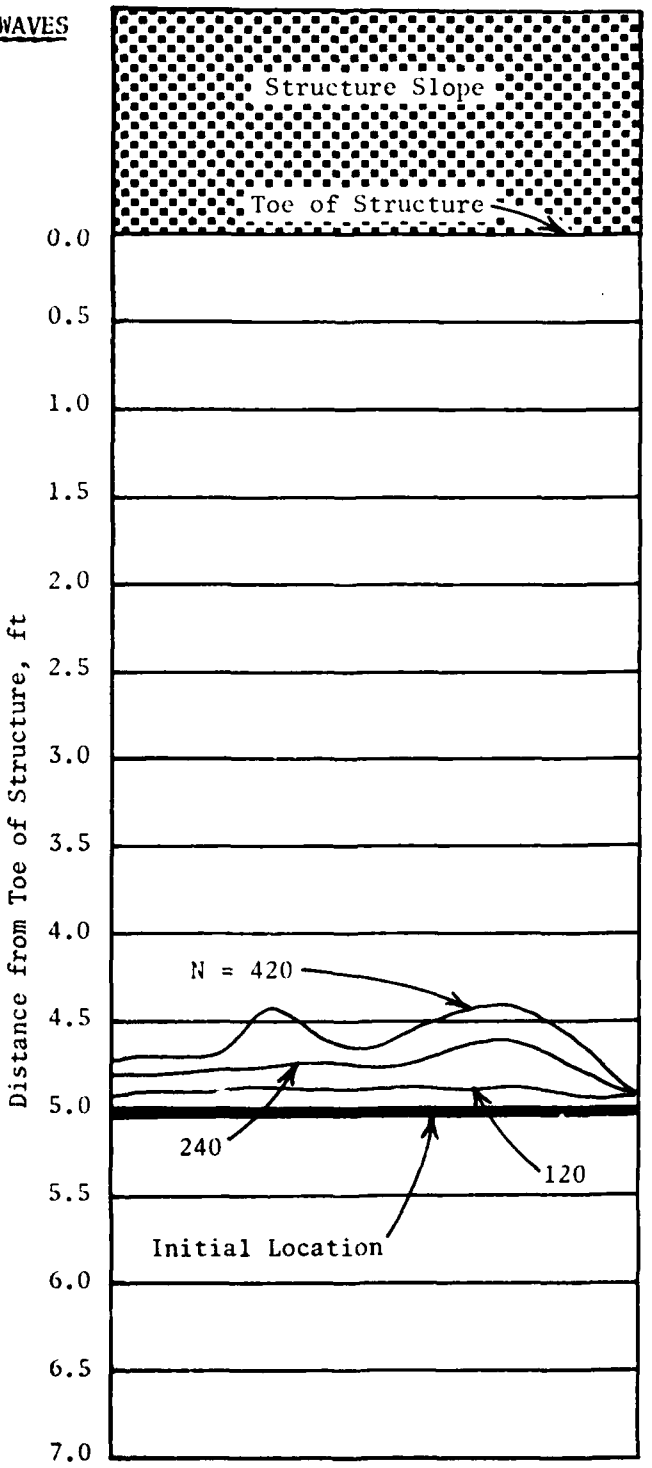

MATERIAL LOCATION AFTER N WAVES

Still-Water Depth, ft
Model: 1.0
Prototype: 16.0

Layer Thickness, ft
Model: 0.125
Prototype: 2.0

Layer Extent, ft
Model: 7
Prototype: 112

Material Size, in.
Model: 3/4 - 7/8
Prototype: 12 - 14

Material Weight, lb
Model: 0.040 - 0.064
Prototype: 165 - 260

Wave Period, sec
Model: 4
Prototype: 16

Bed Slope: 1V on 25H

Maximum Breaker Wave Height, ft
Model: 1.45
Prototype: 23.2

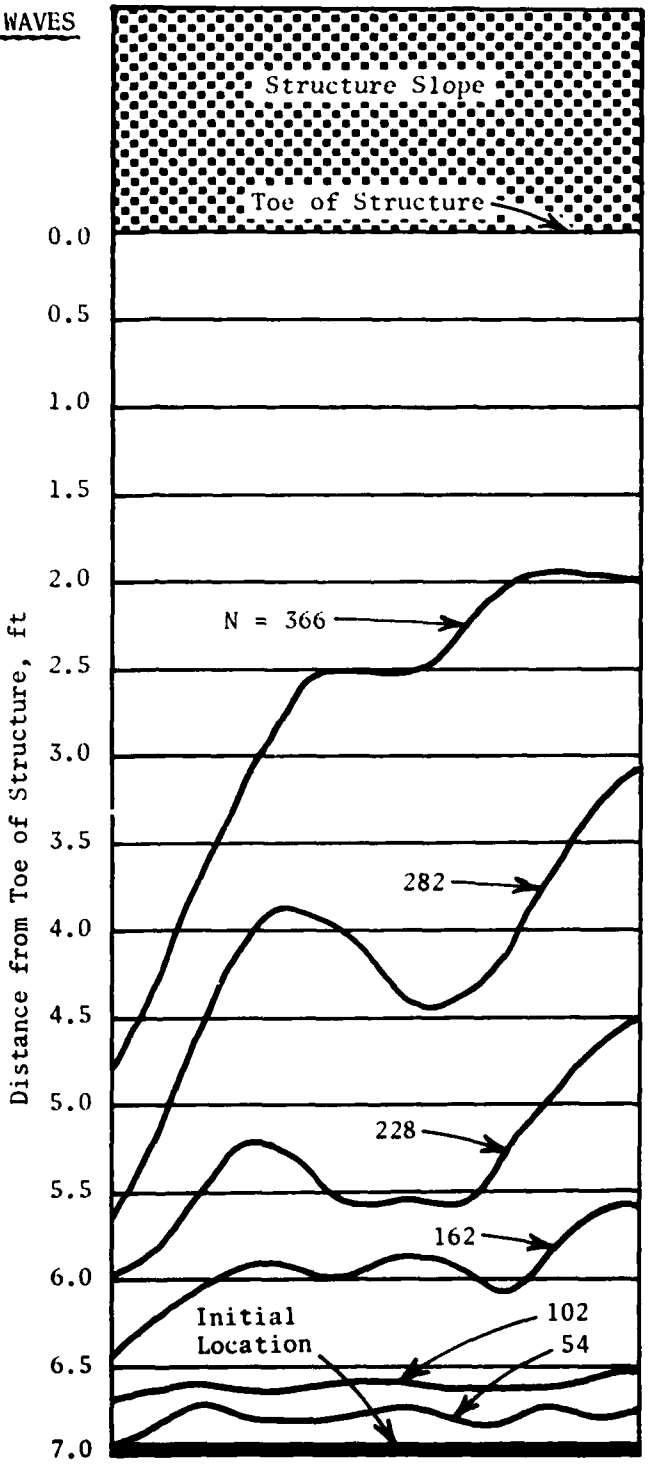

MATERIAL LOCATION AFTER N WAVES

Still-Water Depth, ft
Model: 1.0
Prototype: 16.0

Layer Thickness, ft
Model: 0.125
Prototype: 2.0

Layer Extent, ft
Model: 7
Prototype: 112

Material Size, in.
Model: 3/4 - 7/8
Prototype: 12 - 14

Material Weight, lb
Model: 0.040 - 0.064
Prototype: 165 - 260

Wave Period, sec
Model: 5
Prototype: 20

Bed Slope: 1V on 25H

Maximum Breaker Wave Height, ft
Model: 1.12
Prototype: 17.9

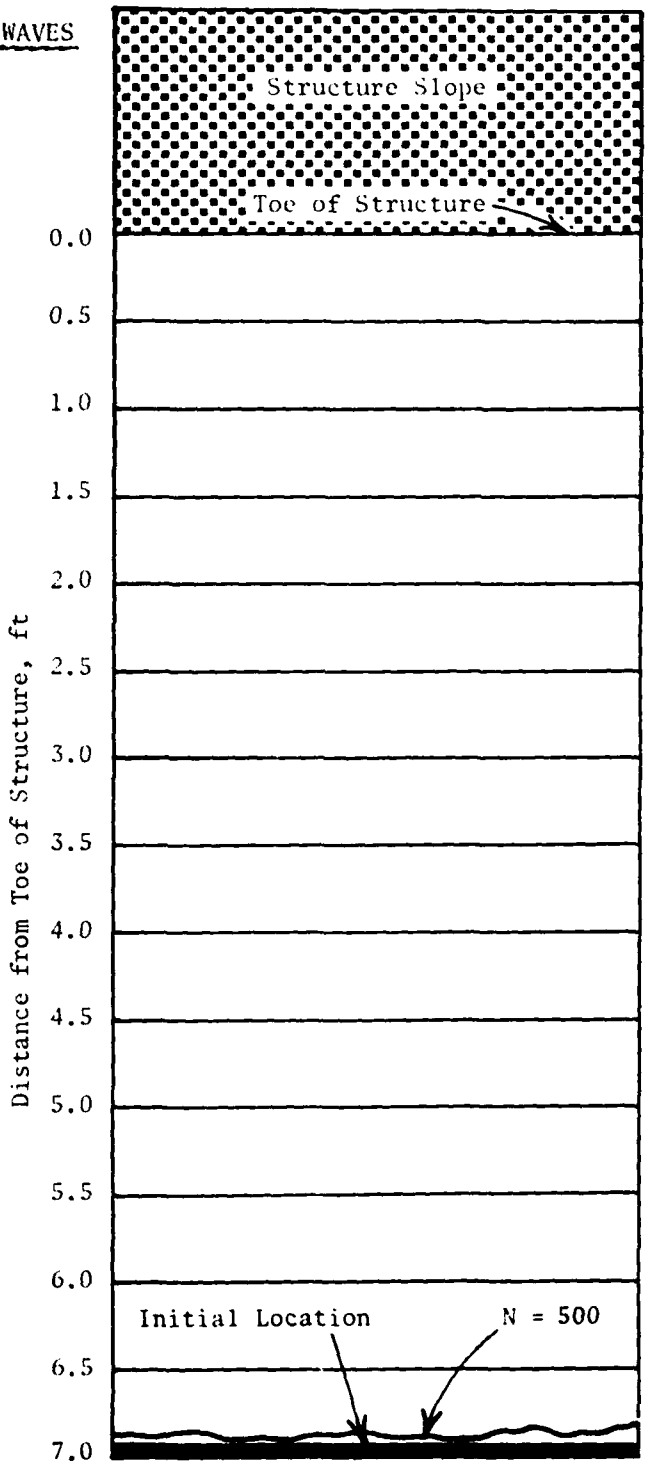

MATERIAL MOVEMENT AFTER N WAVES

Still-Water Depth, ft
Model: 0.5
Prototype: 8.0

Layer Thickness, ft
Model: 0.125
Prototype: 2.0

Layer Extent, ft
Model: 3
Prototype: 48

Material Size, in.
Model: 7/8 - 1.0
Prototype: 14 - 16

Material Weight, lb
Model: 0.064 - 0.095
Prototype: 390 - 765

Wave Period, sec
Model: 4
Prototype: 16

Bed Slope: 1V on 25H

Maximum Breaker Wave Height, ft
Model: 0.80
Prototype: 12.8

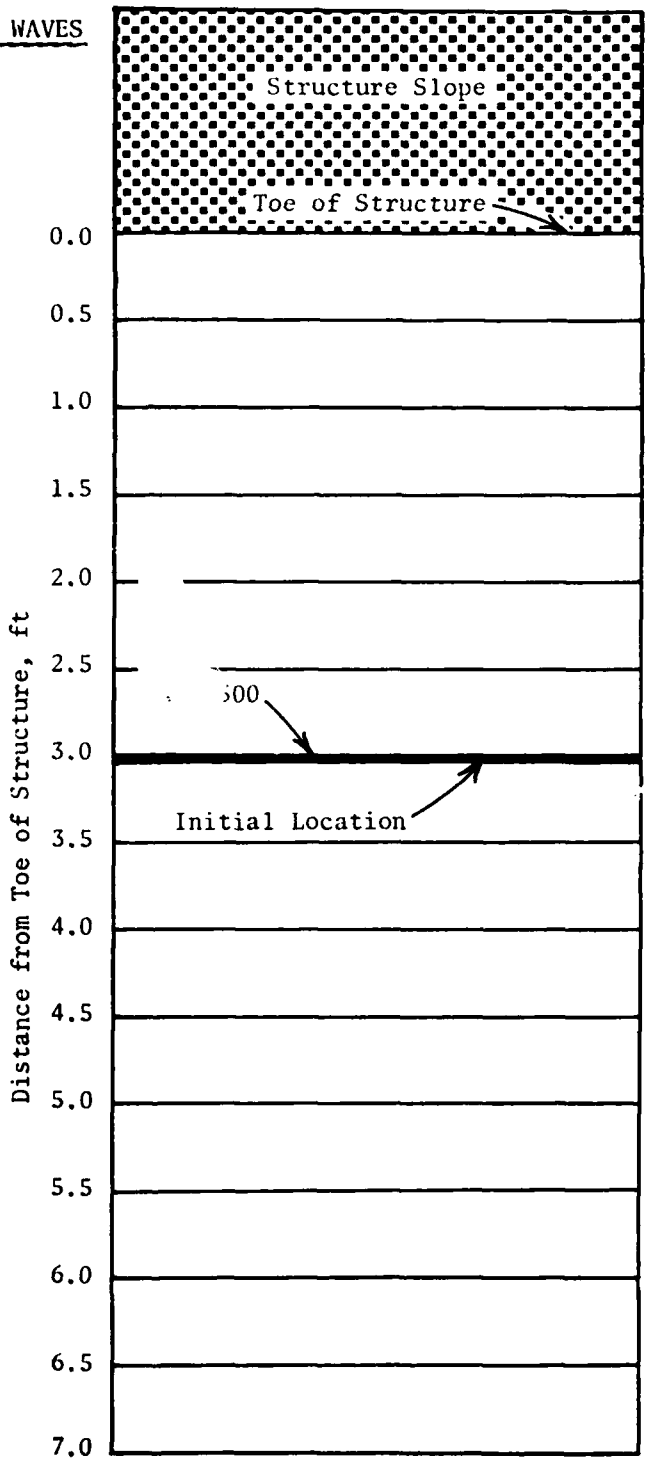

MATERIAL LOCATION AFTER N WAVES

Still-Water Depth, ft
Model: 1.0
Prototype: 16.0

Layer Thickness, ft
Model: 0.12
Prototype: 2.0

Layer Extent, ft
Model: 3
Prototype: 48

Material Size, in.
Model: 7/8 - 1.0
Prototype: 14 - 16

Material Weight, lb
Model: 0.064 - 0.095
Prototype: 390 - 765

Wave Period, sec
Model: 5
Prototype: 20

Bed Slope: 1V on 25H

Maximum Breaker Wave Height, ft
Model: 1.12
Prototype: 17.9

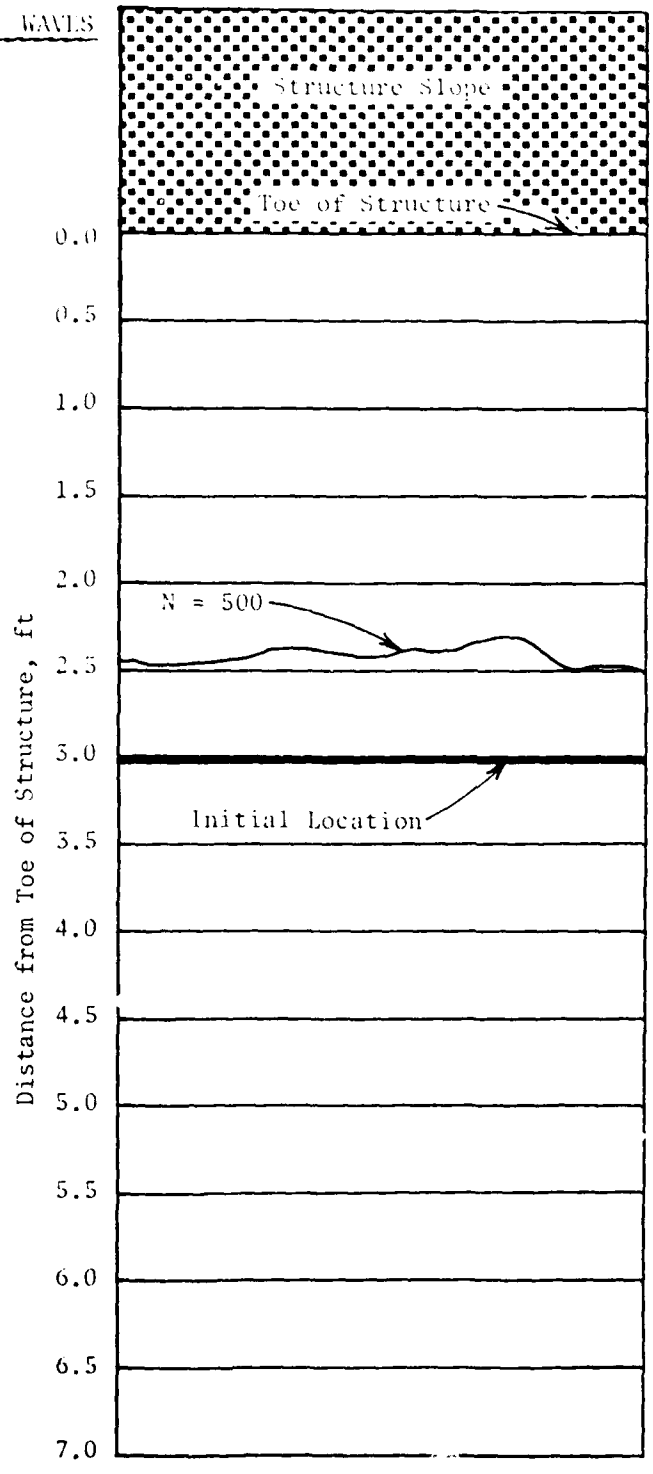

MATERIAL LOCATION AFTER N WAVES

Still-Water Depth, ft
Model: 1.0
Prototype: 16.0

Layer Thickness, ft
Model: 0.125
Prototype: 2.0

Layer Extent, ft
Model: 7
Prototype: 112

Material Size, in.
Model: 7/8 - 1.0
Prototype: 14 - 16

Material Weight, lb
Model: 0.064 - 0.095
Prototype: 390 - 765

Wave Period, sec
Model: 4
Prototype: 16

Bed Slope: 1V on 25H

Maximum Breaker Wave Height, ft
Model: 1.45
Prototype: 23.2

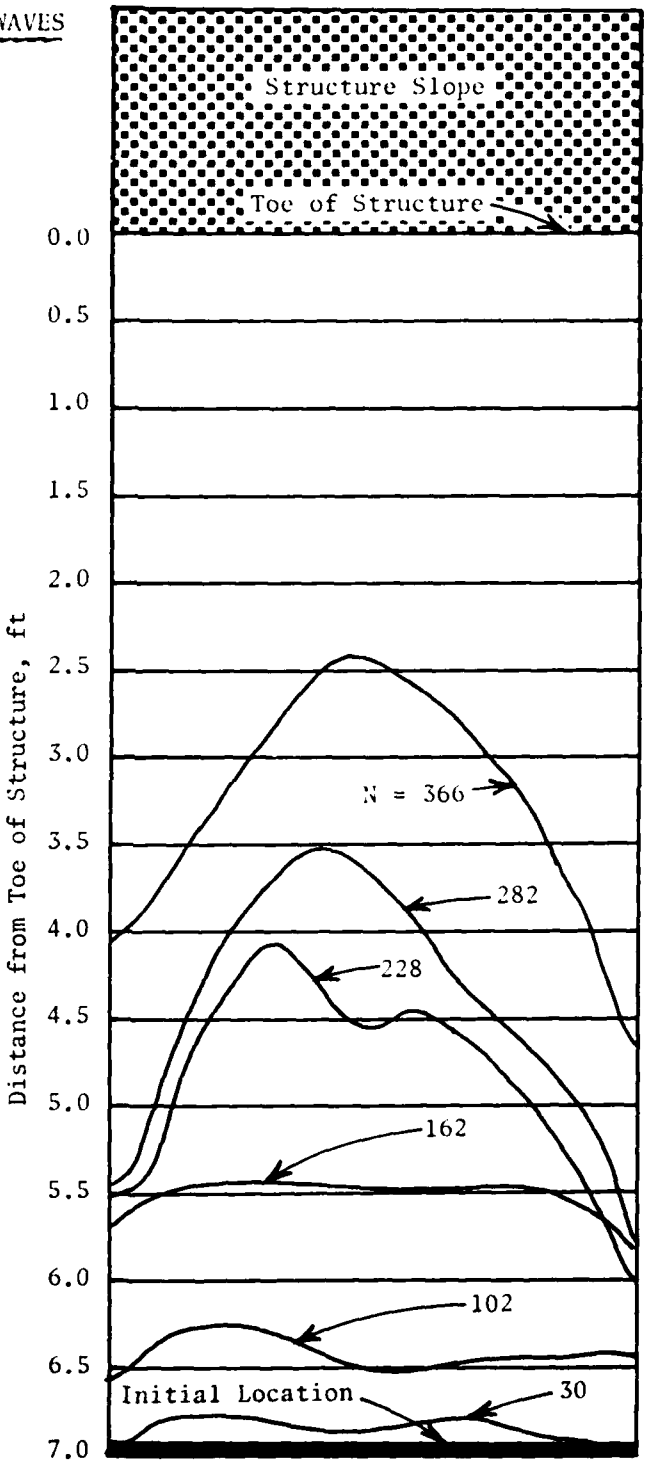

MATERIAL LOCATION AFTER N WAVES

Still-Water Depth, ft
Model: 1.0
Prototype: 16.0

Layer Thickness, ft
Model: 0.125
Prototype: 2.0

Layer Extent, ft
Model: 5
Prototype: 80

Material Size, in.
Model: 1 - 1-1/4
Prototype: 16 - 20

Material Weight, lb
Model: 0.095 - 0.186
Prototype: 390 - 765

Wave Period, sec
Model: 5
Prototype: 20

Bed Slope: 1V on 25H

Maximum Breaker Wave Height, ft
Model: 1.12
Prototype: 17.9

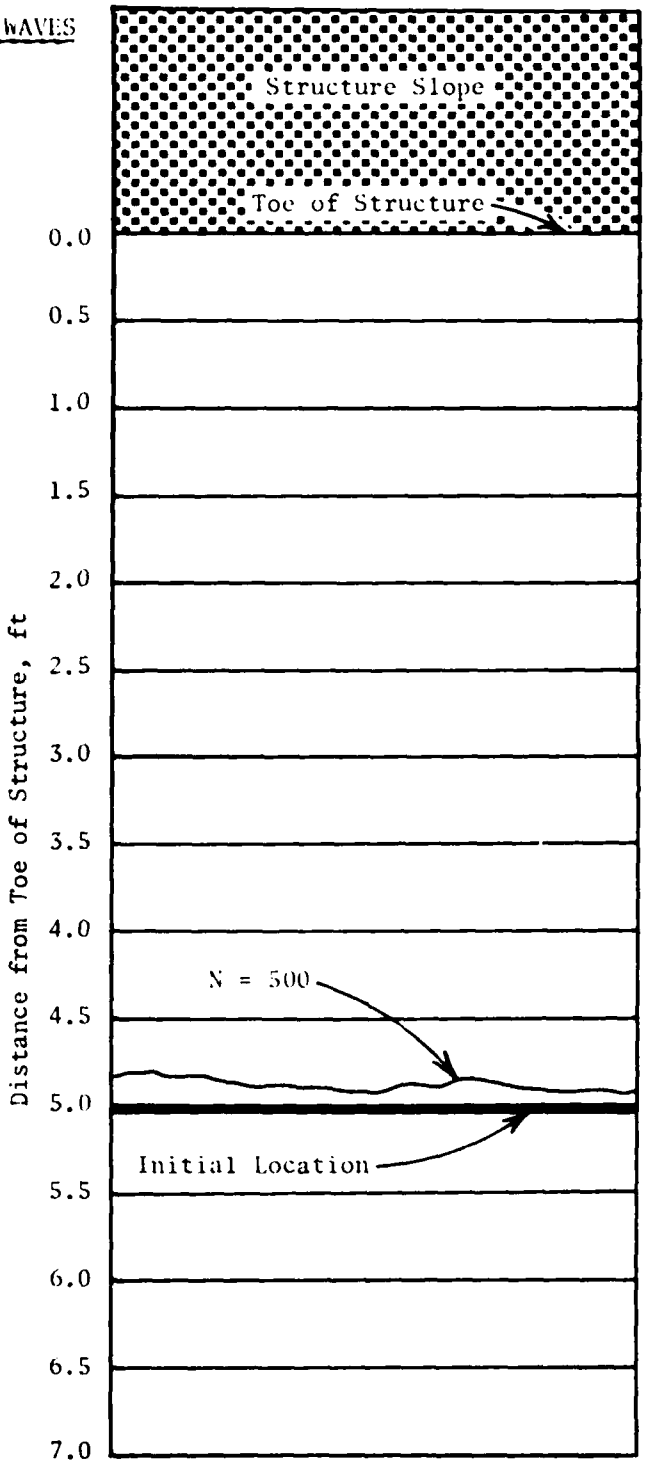

MATERIAL LOCATION AFTER N WAVES

Still-Water Depth, ft

Model: 1.0

Prototype: 16.0

Layer Thickness, ft

Model: 0.125

Prototype: 2.0

Layer Extent, ft

Model: 7

Prototype: 112

Material Size, in.

Model: 1 - 1-1/4

Prototype: 16 - 20

Material Weight, lb

Model: 0.095 - 0.186

Prototype: 390 - 765

Wave Period, sec

Model: 4

Prototype: 16

Bed Slope: 1V on 25H

Maximum Breaker Wave Height, ft

Model: 1.45

Prototype: 23.2

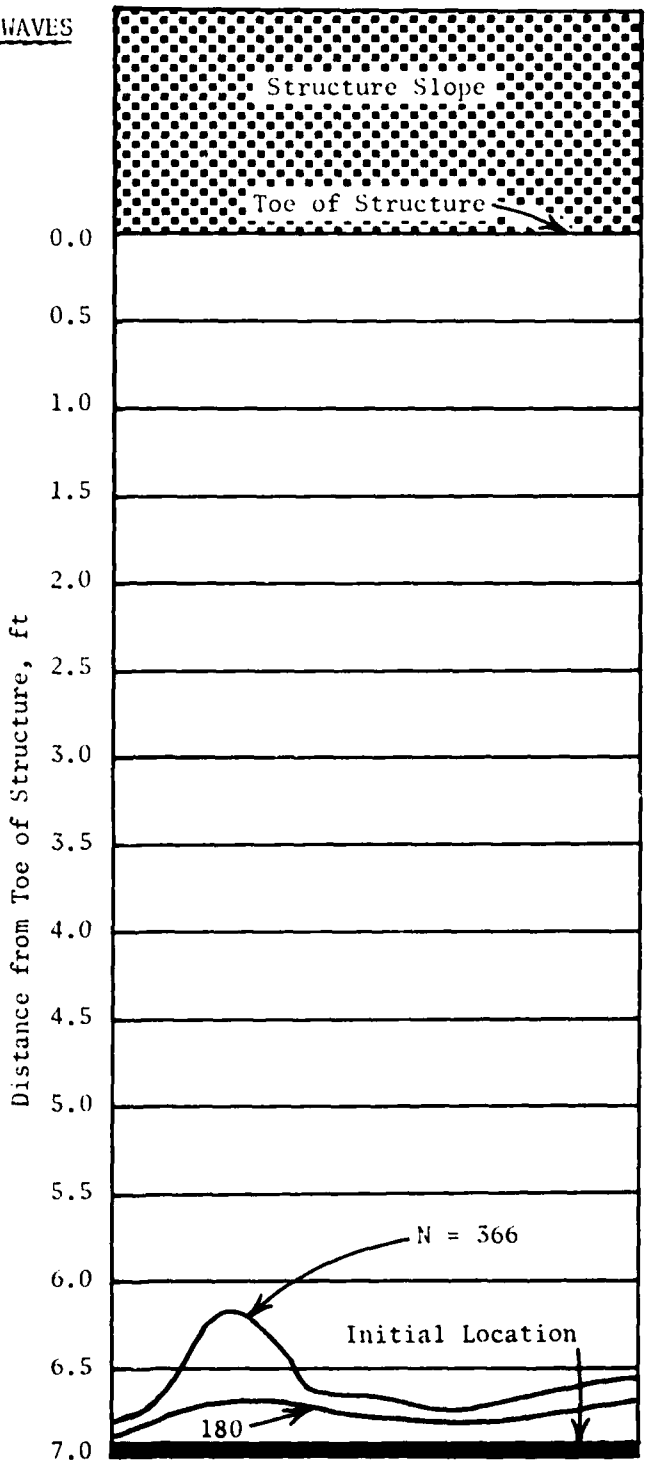

MATERIAL LOCATION AFTER N WAVES

Still-Water Depth, ft
Model: 1.0
Prototype: 16.0

Layer Thickness, ft
Model: 0.125
Prototype: 2.0

Layer Extent, ft
Model: 5
Prototype: 80

Material Size, in.
Model: 1-1/4 - 1-1/2
Prototype: 20 - 24

Material Weight, lb
Model: 0.186 - 0.322
Prototype: 765 - 1320

Wave Period, sec
Model: 4
Prototype: 16

Bed Slope: 1V on 25H

Maximum Breaker Wave Height, ft
Model: 1.45
Prototype: 23.2

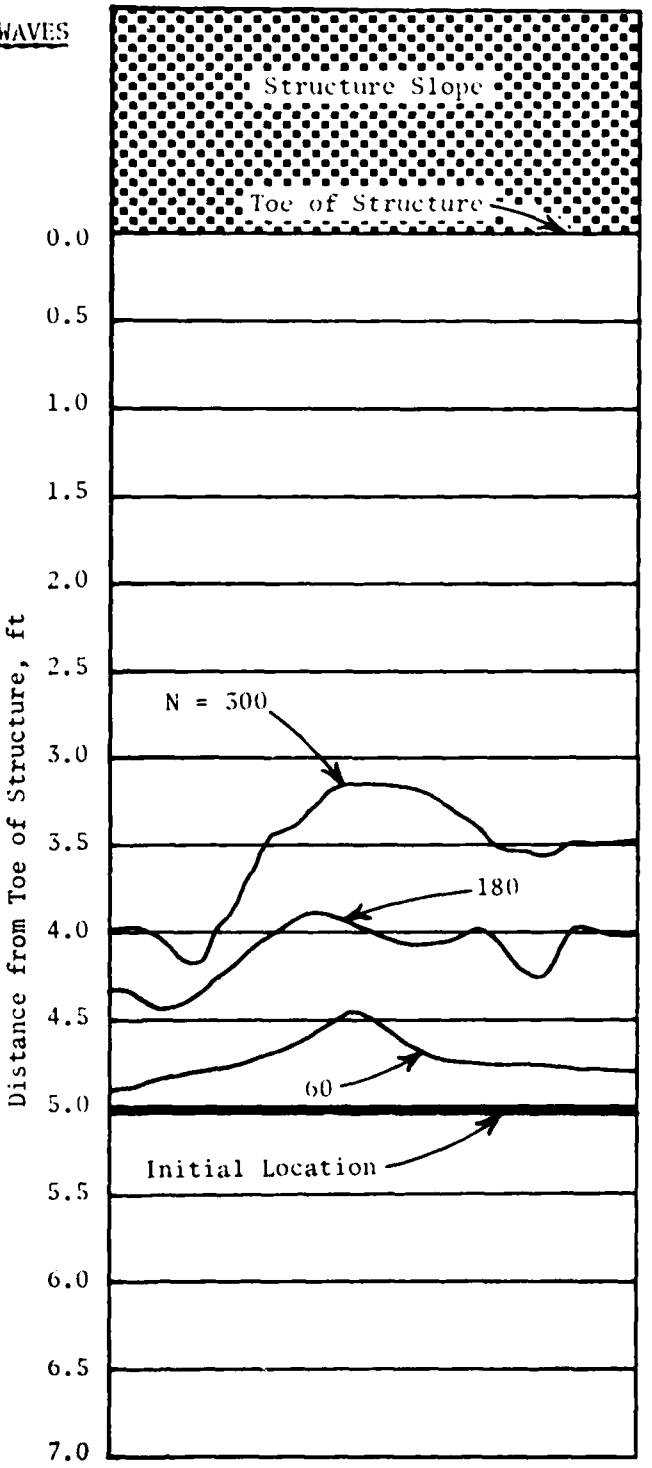

MATERIAL LOCATION AFTER N WAVES

Still-Water Depth, ft
Model: 1.0
Prototype: 16.0

Layer Thickness, ft
Model: 0.125
Prototype: 2.0

Layer Extent, ft
Model: 7
Prototype: 112

Material Size, in.
Model: 1-1/4 - 1-1/2
Prototype: 20 - 24

Material Weight, lb
Model: 0.186 - 0.322
Prototype: 765 - 1320

Wave Period, sec
Model: 4
Prototype: 16

Bed Slope: 1V on 25H

Maximum Breaker Wave Height, ft
Model: 1.45
Prototype: 23.2

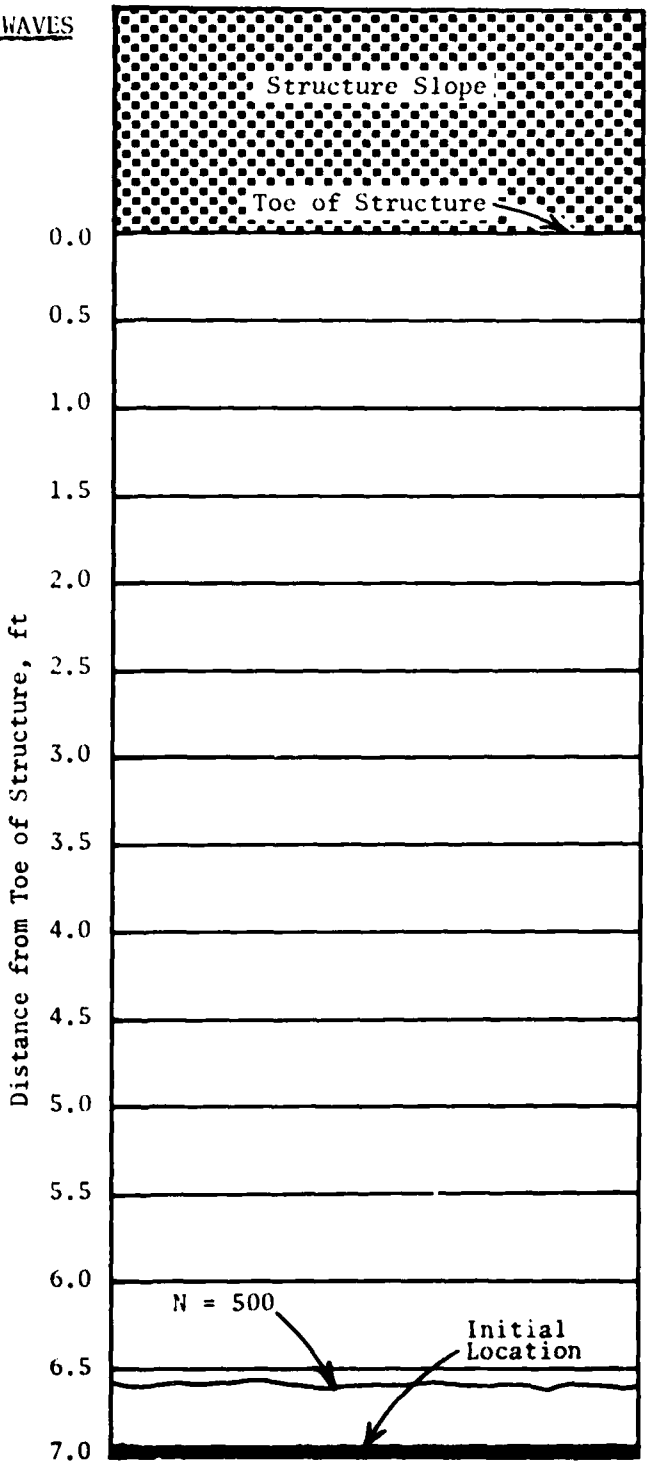

APPENDIX C: NOTATION

a	Wave amplitude within a porous structure, ft
a_i	Amplitude of incident wave, ft
a_t	Amplitude of transmitted wave, ft
A	Surface area, ft^2
C	Wave celerity, ft/sec
C_m	Keulegan model numerical multiplier, dimensionless
C_p	Keulegan prototype numerical multiplier, dimensionless
d	Undisturbed average still-water depth, ft
d_b	Bed particle diameter, ft
d_m	Model rock size, ft
d_p	Prototype rock size, ft
d_{50}	Fifty percent finer of a material by weight, dimensionless
D	Hudson damage parameter, dimensionless
D_m	Effective model stone dimension, ft
D_p	Effective prototype stone dimension, ft
e	Base of system of natural logarithms, 2.71828, dimensionless
g	Gravitational constant, 32.174 ft/sec^2
H	Wave height, ft
H_b	Maximum breaking wave height, ft
H_B	Iribarren breaking wave height, m
H_s	Significant wave height, average of highest one-third of waves, ft
H_{10}	Average of highest 10 percent of waves, ft
k	Wave number, $2\pi/\lambda$, 1/ft
k_Δ	Rubble-mound armor unit layer coefficient, dimensionless
K	Model scaling coefficient, dimensionless
K_B	Iribarren breakwater coefficient, kg/m^3
K_D	Rubble-mound structure armor unit stability coefficient, dimensionless
K_F	Naheer solitary wave friction coefficient, dimensionless
K_K	Keulegan model scaling coefficient, dimensionless
K_L	LeMéhauté model scaling coefficient, dimensionless
L	Underlayer material extent, ft
L_m	Model representative length, ft
L_p	Prototype representative length, ft
M	Keulegan rubble-mound parameter
n	Number of quarrystone or concrete armor units in thickness comprising the cover layer, dimensionless

N_r	Required number of armor units for a given surface area of rubble-mound structure, dimensionless
N_s	Stability number, dimensionless
P	Average porosity of cover layer or core section, percent
P_m	Porosity of model structure core material, percent
P_p	Porosity of prototype structure core material, percent
S_r	Specific gravity of rock or concrete unit relative to water ($S_r = \omega_r/\omega_w$), dimensionless
S_{cr}	Iribarren specific weight of cap rock metric tons per cubic meter
T	Wave period, sec
W	Weight of an individual armor stone in rubble-mound structure, lb
W_R	Iribarren cover-stone weight, kg
W_s	Structure width, ft
W_{UL}	Weight of representative individual stone in underlayer material section, lb
x	Arbitrary horizontal location, ft
y	Arbitrary vertical location, ft
α	Keulegan dissipation coefficient, dimensionless
ΔH	Height of incident wave, ft
ΔL	Average width of core material section, ft
θ	Angle of rubble-mound structure slope with horizontal, deg
κ	Darcy's or engineer's coefficient of permeability, ft/sec
λ	Wavelength, ft
ν	Fluid kinematic viscosity, ft^2/sec
π	3.14159, dimensionless
ρ_s	Density of bed particles, $lb\text{-}sec^2/ft^4$
ρ_w	Density of water, $lb\text{-}sec^2/ft^4$
τ_{max}	Maximum shear stress, lb/ft^2
ω_r	Unit weight of rock, lb/ft^3
ω_w	Unit weight of water, lb/ft^3

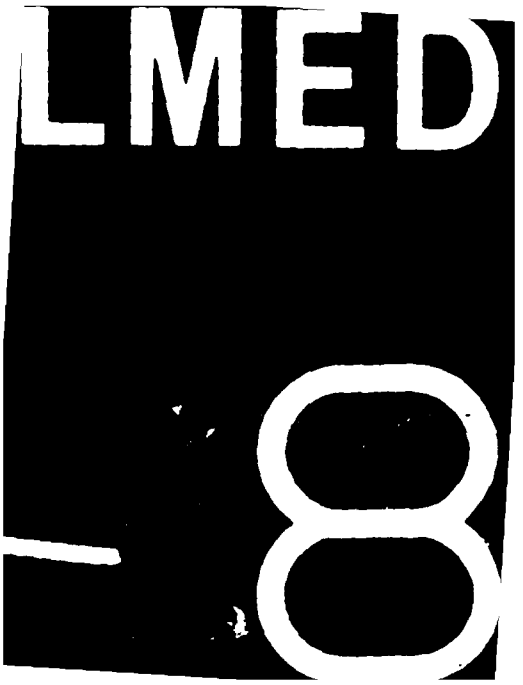
LMED
8